This is to certify that the

dissertation entitled

THE QUADRUPOLE MOMENTS OF THE FIRST AND SECOND ROW HOMONUCLEAR DIATOMICS AND THE SPECTROSCOPIC PROPERTIES OF METAL LITHIDES

presented by

Daniel B. Lawson

has been accepted towards fulfillment
of the requirements for

Ph.D. degree in Chemistry

James F. Harrison
Major professor

Date 10/21/97

THE QUADRUPOLE MOMENTS OF THE FIRST AND SECOND ROW HOMONUCLEAR DIATOMICS

AND

THE SPECTROSCOPIC PROPERTIES OF METAL LITHIDES

By

Daniel B. Lawson

A DISSERTATION

Submitted to
Michigan State University
in partial fulfillment of the requirements
for the degree of

DOCTOR OF PHILOSOPHY

Department of Chemistry

1997

ABSTRACT

PART I. ON THE DISTANCE DEPENDENCE OF THE QUADRUPOLE MOMENTS OF THE FIRST AND SECOND ROW HOMONUCLEAR DIATOMICS

PART II. THE ELECTRONIC STRUCTURE OF AlLi, ScLi, TiLi, VLi, CrLi, CuLi AND THEIR POSITIVE IONS

By

Daniel B. Lawson

In Part I of this thesis, we estimate the complete basis set limits for the Hartree-Fock, MP2, CASSCF, and CASSCF + 1 + 2 wavefunctions for the first and second row homonuclear diatomics and calculate the molecular quadrupole moment as a function of bond length. Our recommended values for (v = 0, J = 0), compare favorably to the current experimental values and previous high-level calculations. To aid in the analysis of the relationship between the molecule's electronic structure and quadrupole moment, we introduce the concept of a quadrupole moment density that permits one to write the molecular quadrupole moment as a sum of the separated atoms quadrupole and a purely molecular contribution. The quadrupole density provides a (reference state dependent) means of determining the contribution to Θ from various regions in the molecule and gives considerable insight into the relationship between the electron density and the magnitude and sign of Θ, and it allows a detailed assessment of the contribution of electron correlation to Θ.

In Part II, we begin with a study of the ground and low-lying excited states of the transition-metal lithides ScLi, TiLi, VLi, CrLi, and CuLi and their mono-positive ions, and report bond energies, bond lengths, and vibrational frequencies, calculated

using MRCI and ACPF techniques. The ground states of ScLi ($^3\Delta$) and TiLi ($^4\Phi$) trace their lineage to the ground s^2d^n configuration of the transition element and are weakly bound. The ground states of CrLi ($^6\Sigma^+$) and CuLi ($^1\Sigma^+$) trace their lineage to the ground sd^{n+1} configurations and are more strongly bound. VLi ($^5\Delta$) traces its lineage to the excited sd^4 configuration and is strongly bound, relative to this asymptote. The positive ions $ScLi^+$ ($^2\Delta$), $TiLi^+$ ($^3\Phi$), VLi^+ ($^4\Delta$), and $CrLi^+$ ($^7\Sigma^+$) are more strongly bound than their neutral precursors, while $CuLi^+$ ($^2\Sigma^+$) is more weakly bound than its neutral precursor. In general, the structure of those transition-metal lithides that dissociate to the s^2d^n asymptote are very sensitive to electron correlation, while those that dissociate to an sd^{n+1} asymptote are less sensitive. The bonding in the positive ions is primarily ionic. And, in the last chapter of Part II, the ground state ($^1\Sigma^+$) and several low lying excited states (including the $^1\Sigma^-$, $^3\Sigma^-$, $^1\Pi$, and $^3\Pi$) of LiAl are characterized by MCSCF, MRCI, and ACPF techniques using a large correlation consistent basis set.

To my wife, Jeanne

Acknowledgments

I would like to take this opportunity to thank Dr. James F. Harrison for his unending support and guidance during the work that led to this thesis. I am indeed grateful to him both as a mentor and friend. I would also like to thank my guidance committee, Dr. Ned Jackson, Dr. Gary Blanchard, and Dr. Katherine Hunt. I would like to acknowledge the faculty and staff of Michigan State University's Department of Chemistry. Special thanks to Paul Reed and Dr. Tom Atkinson for maintaining the departmental computers along with answering my many questions. I would like to thank the many friends that I have acquired at Michigan State University, especially those of the Harrison and Hunt research groups. Without their contributions and support, I certainly would not have completed my studies.

Finally, I would like to thank my entire family. They were helpful, supportive, and inspirational throughout my years in graduate school.

TABLE OF CONTENTS

LIST OF TABLES

CHAPTER 4

CHAPTER 5

CHAPTER 6

LIST OF FIGURES

CHAPTER 4

CHAPTER 5

KEYS TO SYMBOLS AND ABBREVIATIONS

Symbols

Θ	Quadrupole Moment
Θ_σ	Sigma component of the molecular quadrupole
Θ_{mol}^{σ}	Sigma component of the molecular quadrupole moment referenced to its asymptotic atomic contribution.
Θ_π	Pi component of the molecular quadrupole
Θ_{mol}^{π}	Pi component of the molecular quadrupole moment referenced to its asymptotic atomic contribution.
q_{zz}	Field Gradient
a_0	Atomic Units of Length
e/a_0^2	Atomic Units of Energy
ea_0^2	Atomic Units of Quadrupole Moment
e	Atomic Units of Quadrupole Moment Second Derivative
ea_0	Atomic Units of Quadrupole Moment First Derivative
e/a_0^3	Atomic Units of Field Gradient

Abbreviations

ACPF	Averaged Coupled Pair Functional
CASSCF	Complete Active Space Self Consistent Field
CASSCF+1+2	Complete Active Space Self Consistent Field Singles and Doubles Configuration Interaction
CBS	Complete Basis Limit
CISD	Single and Double Configuration Interaction
CSF	Configuration State Functions
EEL	Exchange Energy Loss
MP2	Second Order Möller-Plesset Perturbation
MCSCF	Multi-Configuration Self Consistent Field
MRCI	Multi-Reference Singles and Doubles Configuration Interaction
RHF/UHF	Restricted/Unrestricted Hartree-Fock
ROHF	Restricted Open Shell Hartree-Fock
R_{opt}	Optimal Model Separation
R_{exp}	Experimental Separation

CHAPTER 1

Introduction

A. Introduction

The purpose of Part I of this thesis is to discuss the calculation and interpretation of the quadrupole moments of the first and second row homonuclear diatomics, and their distance dependence. The primary interest is in developing a qualitative understanding of the relationship between a molecule's quadrupole moment and electronic structure, and, in order to do so reliably, we have explored the sensitivity of the calculated quadrupole moment to basis sets as well as electron correlation. Using Self-Consistent Field (SCF), Multi-Configurational Self-Consistent Field (MCSCF/CASSCF), Möller-Plesset Second Order Perturbation (MP2), and Multireference Configuration Interaction (MRCI/CASSCF+1+2), we calculate quadrupole moments, as a function of internuclear separation, for a sequence of basis sets obtained from the Dunning Augmented Correlation Consistent basis sets by deleting g and higher symmetries.

The goal is to provide accurate calculated quadrupole moments of the first and second row homonuclear diatomics, an interpretation of the magnitude and sign of the quadrupole moment, the effects of correlation, and the distance dependence of the quadrupole moment.

The work in Part I divided into three chapters. Chapter II is a description of the distance dependence of the quadrupole moment for H_2, N_2, O_2, and F_2. The next chapter is a discussion of the quadrupole moments and distance dependence of P_2, S_2, and Cl_2, and a comparison with their first row conjugates. In the fourth chapter of this work we discuss and compare the quadrupole moment and distance dependence of H_2, Li_2, and Na_2.

Appendix A outlines the quadrupole moment as a molecular property by giving a derivation of the multipole moments, and a description of how multipole moments are determined. Appendix B contains the basis sets used in these calculations. Appendix C contains the dissociation energy, quadrupole moment and field gradient as function of internuclear separation. Appendix D gives complete tables of the Homonuclear Diatomics for which calculations were done, but may not have been discussed.

In part II of this thesis, we describe the calculations of the excited states and positive ions of certain metal lithides. Chapter V describes the ground and low-lying excited states of the transition-metal lithides ScLi, TiLi, VLi, CrLi, and CuLi and their mono-positive ions, and report bond energies, bond lengths, and vibrational frequencies. Chapter VI includes the ground and excited states of AlLi and its positive ions.

CHAPTER 2

On the Distance Dependence and Spatial Distribution of the Molecular Quadrupole Moments of H_2, N_2, O_2, and F_2

A. Introduction

We first discuss the quadrupole moments of the titled molecules at the calculated equilibrium separations and compare these with experiment and previous calculations. Then, we examine the quadrupole moment functions (variation of the quadrupole moment with the internuclear separation), using MCSCF and MRCI techniques. Finally, we develop an interpretation of the molecular quadrupole moment as the sum of atomic contributions associated with the free (non-interacting) atoms and a molecular contribution that depends on the shift in the electron density due to molecule formation (the deformation density). Using the deformation density, we define a quadrupole density whose integral is the molecular contribution to the molecular quadrupole moment. The distance dependence of the quadrupole moment, the differing contributions to Θ from various regions of the charge distribution, and the role of electron correlation in determining Θ are analyzed in terms of the quadrupole density.

B. Discussion

Let's look, first, at the H_2 results. Figure 1 shows the graphical representation of the quadrupole data in Table C-1 of Appendix C. Several characteristics are evident. First, the convergence to the CBS limit is only monotonic after the aug-cc-pvdz basis and, accordingly, we use the last three basis sets to extrapolate to the CBS limit. Within these three basis sets, increasing the flexibility of the basis decreases, as does increasing the level of correlation. The aug-cc-pv5z basis set results are close to the CBS limit for each model wavefunction.

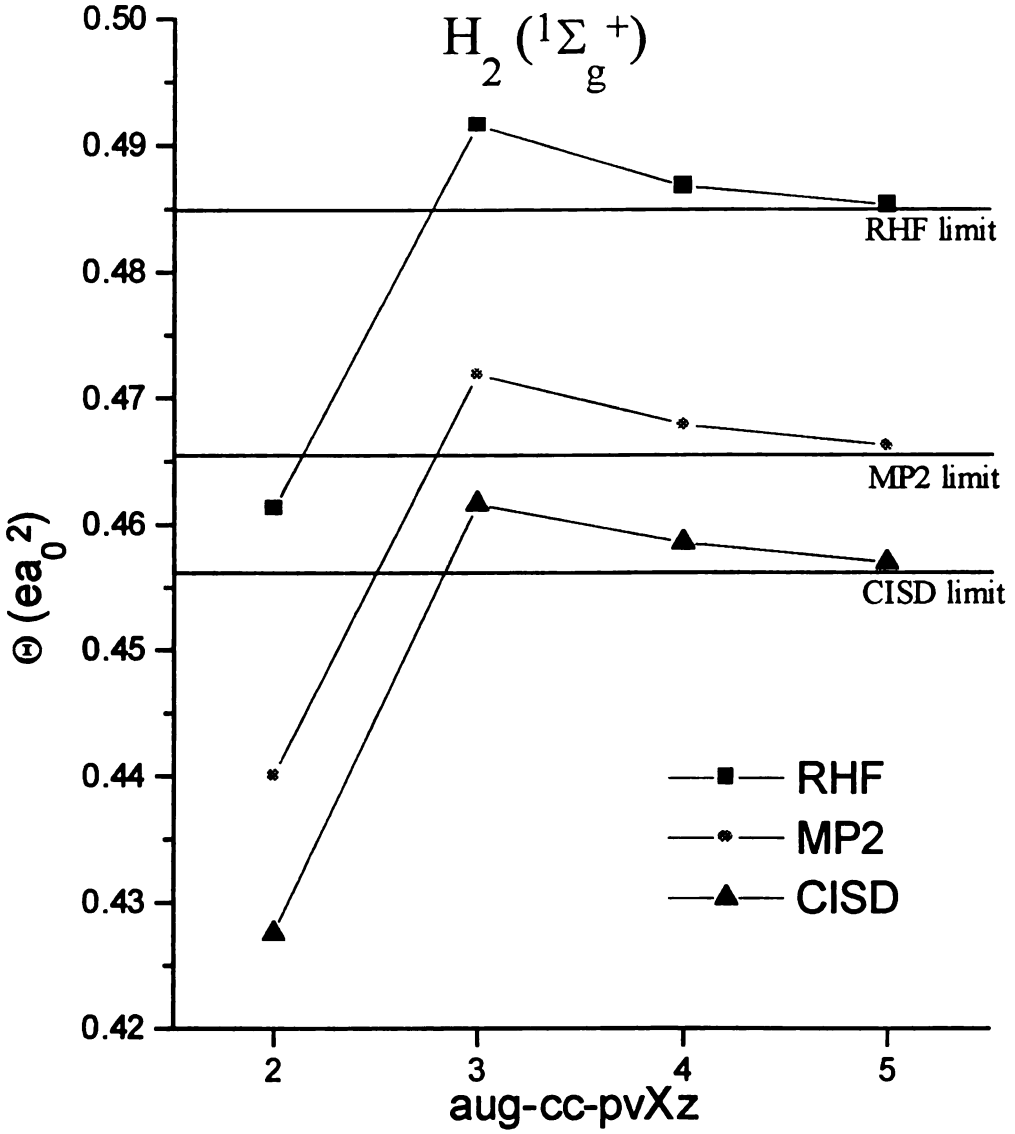

Figure 1. Model dependence of Θ for H_2 as a function of basis set.

Note that the CBS-CISD limit predicts an equilibrium bond length R_{opt} = 1.4010 a_0 and a dissociation energy De = 4.740 ev in excellent agreement with the experimental values[1] 1.4011 a_0 and 4.749 ev. Our CBS-CISD value of Θ is + 0.455 ea_0^2 and agrees with the essentially exact theoretical result[2] of + 0.457 ea_0^2. The experimental value for Θ, + 0.460 ± 0.021 ea_0^2, is an indirect value assembled from the magnetic susceptibility anisotropy and the molecular g value, assuming a vibrationless H_2.[2-4] As such, it agrees well with our CBS-CISD estimate of the vibrationless Θ, + 0.455 ea_0^2. Buckingham and Cordle[5] have estimated the vibrational (v = 0, J = 1) value to be 0.4853 ea_0^2. Figure 2 shows the variation of Θ with R for the SCF and CISD wavefunctions, using the aug-cc-pvqz basis. These data were fit to a quadratic function of the form

$$\Theta(R) = \Theta(R_{opt}) + \left(\frac{d\Theta}{dR}\right)_{opt}(R - R_{opt}) + \left(\frac{d^2\Theta}{dR^2}\right)_{opt}\frac{(R - R_{opt})^2}{2} \qquad (3)$$

and the parameters are reported in Table 2-1. These data are useful in correcting our calculated values to other bond lengths for comparison with previous calculations. Additionally, they allow us to estimate the vibrational dependence of Θ, using the formula[5,6]

$$\Theta_v = \Theta_{opt} + \frac{B_e}{\omega_e}\left[3\left(1 + \frac{\alpha_e\omega_e}{6B_e^2}\right)R_{opt}\left(\frac{d\Theta}{dR}\right)_{R_{opt}} + R_{opt}^2\left(\frac{d^2\Theta}{dR^2}\right)_{R_{opt}}\right]\left(v + \frac{1}{2}\right) \qquad (4)$$

and experimental values[1] for the spectroscopic parameters α_e, ω_e, and B_e. Using Equation 3 and our R_{opt} for the HF and CISD wavefunctions, we corrected Θ to the

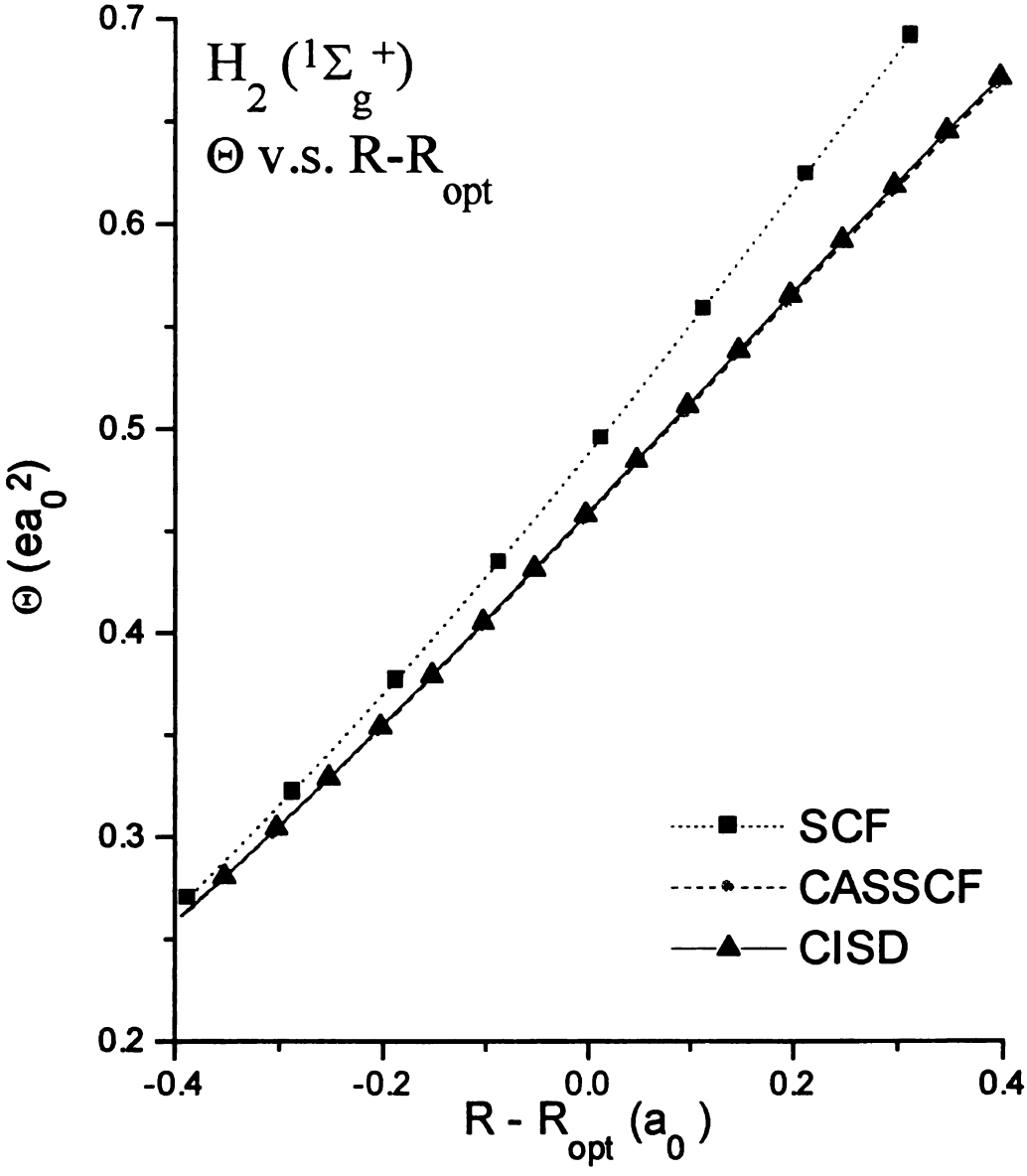

Figure 2. Distance dependence of Θ for H_2 calculated with various models using the aug-cc-pv5z basis.

Table 2-1. Equilibrium value of the first and second derivatives of the molecular quadrupole moment function for H_2, N_2, O_2, and F_2, calculated with various wavefunctions.

Molecule	Wavefunction	$R_{opt}(a_0)$	$\left(\frac{d\Theta}{dR}\right)_{R_{opt}}(ea_0)$	$\left(\frac{d^2\Theta}{dR^2}\right)_{R_{opt}}(e)$
H_2	SCF	1.3865	0.6064	0.2622
H_2	CISD	1.4022	0.5174	0.1028
N_2	SCF	2.0133	1.4017	0.5594
N_2	MCSCF	2.0825	0.9481	0.0548
N_2	MRCI	2.0806	0.9593	0.0892
O_2	ROSCF	2.1747	1.4797	−0.0744
O_2	MCSCF	2.2939	1.3720	−0.1998
O_2	MRCI	2.2864	1.4738	−0.2160
F_2	SCF	2.5071	1.1656	−0.6212
F_2	MCSCF	2.7632	1.1399	−0.9718
F_2	MRCI	2.6825	1.2134	−0.9142

experimental R_{exp} = 1.4011 a_0 at which most other calculations were done. Our HF result at R_{exp} is 0.4937 ea_0^2, in excellent agreement with the numerical HF result (0.4934 ea_0^2) of Larksonen, Pyykkö, and Sundholm.[7] Using (4) and the data in Table 2-1, we estimate the vibrational dependent CBS-CISD value of Θ to be

$$\Theta(H_2;v) = +0.455 + 0.051\left(v+\frac{1}{2}\right)$$

$\Theta(H_2; v = 0) = 0.481 ea_0^2$, which is in good agreement with the v = 0 Wolniewicz[8] value, 0.484 ea_0^2 and the v = 0, J = 1 value, 0.4853 ea_0^2, of Buckingham and Cordle.[5] There are a vast number of calculations[2,3,9-14] of Θ (H_2), and we collect, in Table 2-2, a representative collection of ab initio values for Θ (H_2), along with the experimental values and our CBS-HF and CBS-CISD results.

From Figure 2, we see that the slope of Θ (H_2) around R_{opt} is positive; and, as we will see, this is also true for N_2, O_2, and F_2. Accordingly, to the extent that the HF model limit for R_{opt} is less than R_{exp}, the HF model limit for Θ is always less than the HF value calculated at R_{exp}. Note that electron correlation decreases Θ relative to the HF value. Precisely how much depends on whether one compares the HF and correlated value at the experimental bond length or at the optimal bond length (R_{opt}) corresponding to each model. Since correlation corrections to the HF wavefunction are responsible for changing the predicted R_{opt}, measuring correlation effects relative to the experimental bond length obscures this important effect. For example, Θ (CISD) at the experimental bond length is 7.8 percent smaller than Θ (HF) at this bond length, while Θ (CISD) and Θ (HF) differ by 6.0 percent when each is referred to its model limit R_{opt}.

Our N_2 results are summarized in Table C-6 and Figure 3 and compared with selected calculations[12,15-25] and experiments[26,27] in Table 2-3. As with H_2, increasing the quality of the basis set within a model reduces the calculated Θ, and adding correlation decreases Θ, relative to the SCF values. Our CBS-HF limit is

Table 2-2. Selection of H_2 quadrupole moments.

$R(a_0)$	$\Theta(ea_0^2)$	Reference	Comment
1.4	0.493	11	Hartree Fock limit
1.4	0.4934224	7	Numerical HF
1.3863	0.4845	This Work	CBS-HF; R_{opt}
1.4016	0.4937	This Work	CBS-HF; Exp. R_{exp}
1.4	0.457	9	essentially exact wavefunction
1.401	0.437	12	numerical DFT
1.40	0.4438	13	MP4 Sadlej[15] basis
1.40	0.4414	13	CISD Sadlej basis
1.3895	0.4649	This Work	CBS-MP2 R_{opt}
1.4016	0.4712	This Work	CBS-MP2 Exp. R_{exp}
1.4010	0.4552	This Work	CBS-CISD R_{opt}
vibrational average	0.516	This Work	CBS-HF; v = 0, J = 0
vibrational average	0.481	This Work	CBS-CISD; v = 0, J = 0
vibrational average	0.477	14	essentially exact wf-integrate radial wavefunction
experimental	0.460 ± 0.021	2	derived from exp. data - non-vibrating molecule
experimental	0.485	5	vibrational average of magnetic anisotropy and *g* factor; v = 0, J = 1

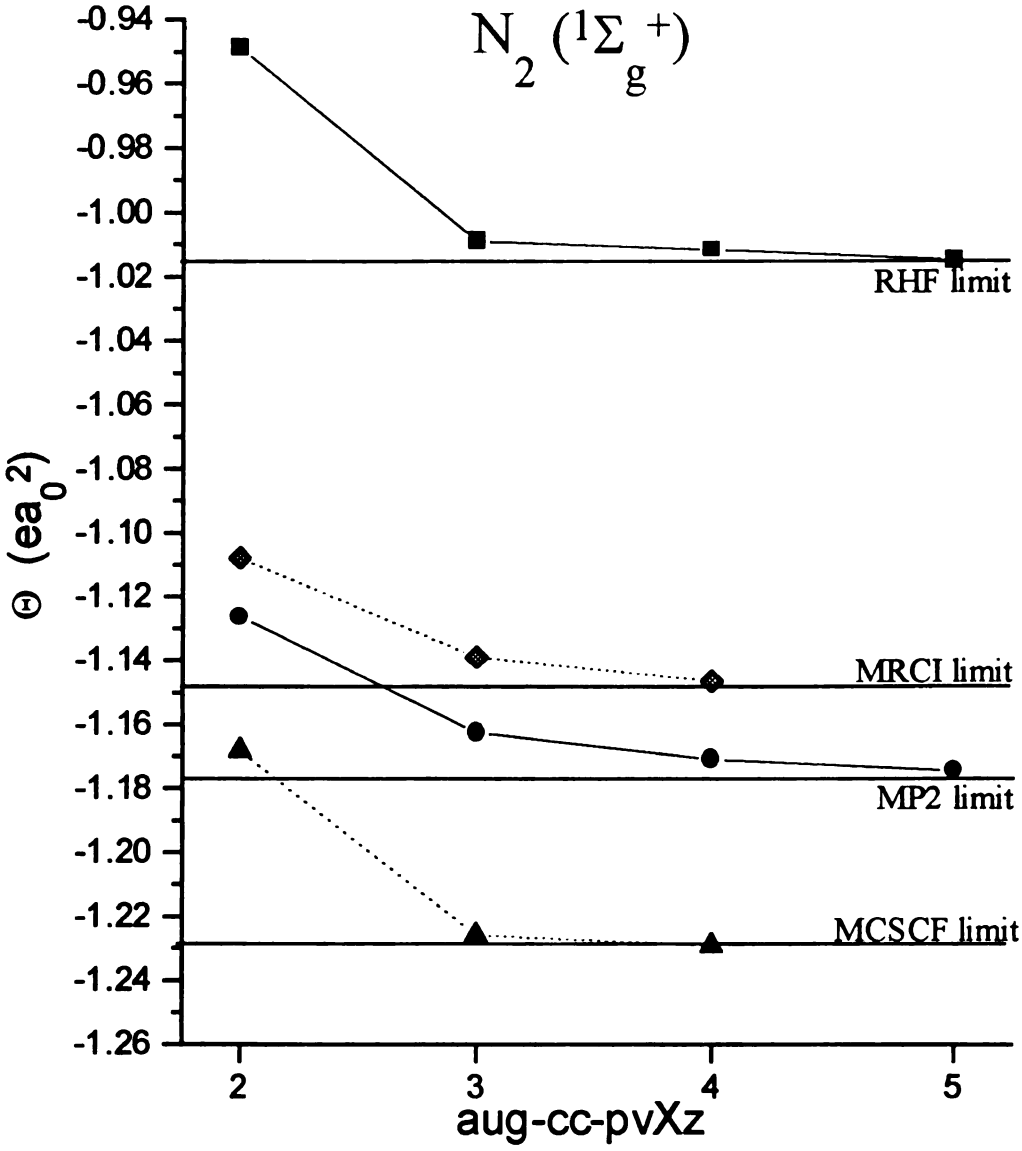

Figure 3. Model dependence of Θ for N_2 as a function of basis set.

Table 2-3. Selection of N_2 quadrupole moments.

R(a_0)	$\Theta(ea_0^2)$	Reference	Comment
2.07432	– 0.9310	15	numerical HF
2.068	– 0.9400	16,17	numerical HF
2.07432	– 0.9054	18	SCF large basis
2.07430	– 0.9285	19	SCF large basis
2.068	– 0.937	20	SCF
2.0133	– 1.0158	This Work	SCF at R_{opt}
2.07435	– 0.9306	This Work	CBS-SCF limit
2.075	– 1.137	12	numerical DFT
2.068	– 1.1426	21	numerical HFS
2.07430	– 1.1289	22	large basis set DFT
2.068	– 1.15	23	numerical HFS
2.07432	– 1.1131	18	SDQ-MPPT(4); 6s4p3d1f
2.07430	– 1.0905	19	MRSD-CI
2.068	– 1.154	20	MRSD-CI
2.068	– 1.16865	24	CCSD-Sadlej's[15] 5s4p2d basis
2.0856	– 1.1755	This Work	CBS-CASSCF; R_{opt}
2.0810	– 1.1270	This Work	CBS-CASSCF+1+2; R_{opt}
2.07432	– 1.1334	This Work	CBS-CASSCF+1+2; R_{exp}
vibrational average	– 1.118	This Work	CBS-CASSCF+1+2;v=0, J=0
vibrational average	– 1.1557	25	CCSD, v=0, J=0; Sadlej's 5s4p2d basis
experimental	– 1.09 ± 0.07	26	Optical Birefringence
experimental	– 1.05 ± 0.06	27	Optical Birefringence

-1.0158 ea_0^2 at R_{opt} of 2.0133 a_0 and – 0.9306 ea_0^2 at R = 2.07432 a_0, in excellent agreement with the numerical HF result[20] of – 0.9310 ea_0^2 at this bond length. The convergence of the MP2, MCSCF, and MRCI results all suggest that the aug-cc-pvqz basis produces a quadrupole moment that differs from the CBS limit by less than 0.2 %, suggesting that the individual CASSCF and CASSCF+1+2 values of – 1.1753 ea_0^2 and – 1.1247 ea_0^2 are near the model limit. The distance dependence of Θ around R_{opt} is shown in Figure 4 for the SCF, MCSCF, and MRCI models, using the aug-cc-pvqz basis. Note the similarity between the MCSCF and the MRCI Θ versus R curves. The SCF curve has significantly larger first and second derivatives, and these are in good agreement with calculations by Truhlar[28] and Maroules and Bishop.[29] Using the MRCI derivatives in Table 2-1, we estimate the vibrational dependence of the CBS-CASSCF+1+2 quadrupole moment as

$$\Theta(N_2; \mathrm{v}) = -1.1247 + 0.0137\left(\mathrm{v} + \frac{1}{2}\right)$$

and so our recommended vibrationally corrected quadrupole moment is $\Theta\ (N_2; \mathrm{v} = 0)$ $= -1.118\ ea_0^2$. This is in good agreement with the reported experimental quadrupole moments gathered in Table 2-3. The several experimental estimates of the quadrupole derivative available in the literature[33-36] average 0.95 ea_0, and these may be compared with our SCF, MCSCF, and MRCI results of 1.402 ea_0, 0.948 ea_0, and 0.959 ea_0. The SCF result is clearly much too large, while the correlated values agree with the average of the experimental values. The data are collected in Table 2-4. Note that the

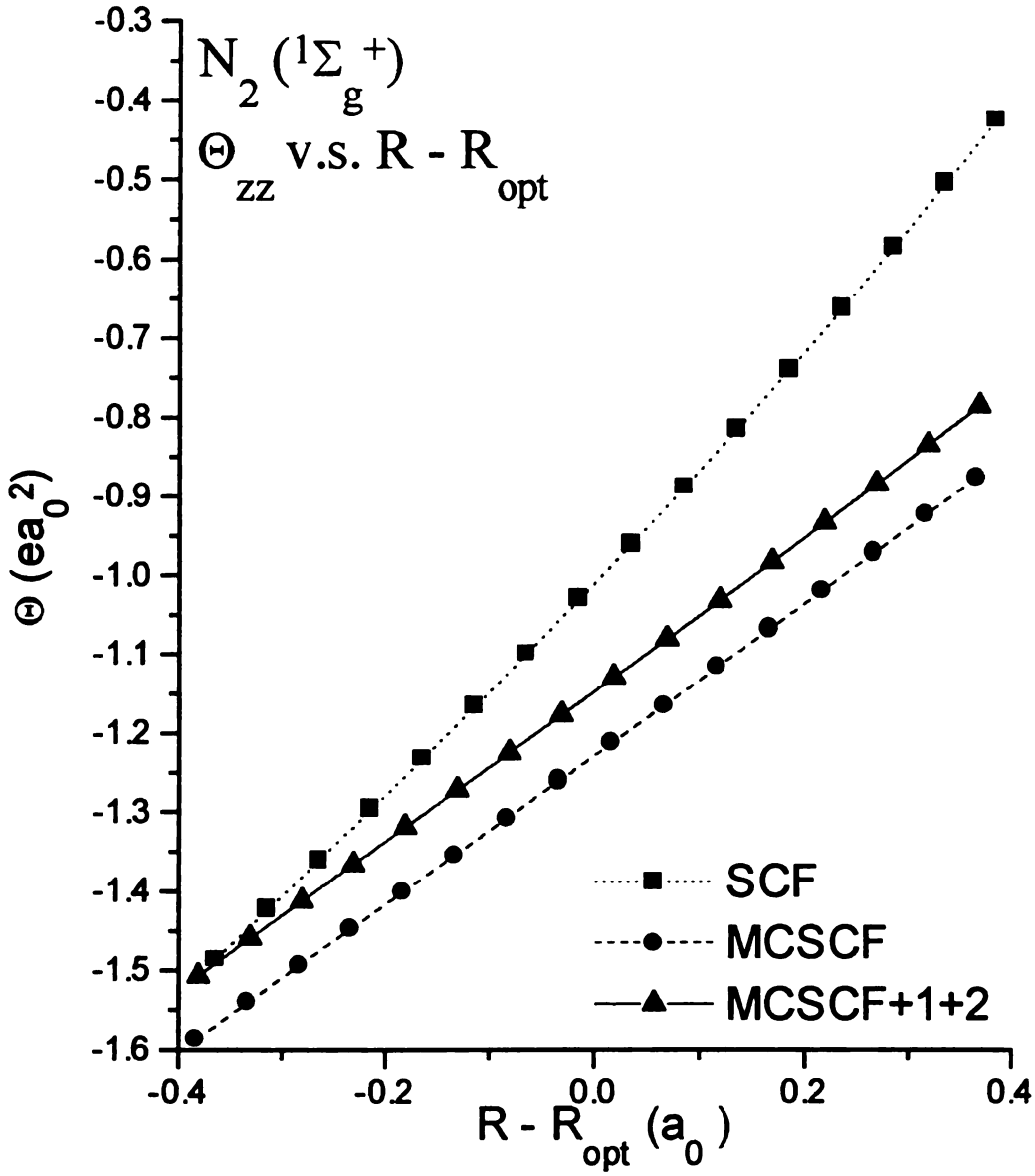

Figure 4. Distance dependence of Θ for N_2 calculated with various models using the aug-cc-pvqz basis.

significant reduction in dΘ/dR, when a correlated wavefunction is used, is implicit in the SCF vs GVB results reported by Cartwright and Dunning.[30]

Our O_2 results are summarized in Table C-7 and Figure 5. As with H_2 and N_2, increasing the quality of the basis set decreases the quadrupole moment. However, unlike H_2 and N_2, adding correlation increases the quadrupole moment (makes it less negative). The opposing effects of basis-set quality and correlation permits a limited correlation wavefunction with a small basis set to predict a quadrupole moment comparable with the CBS-MRCI limit. We have not found a reported Hartree Fock limit for Θ (O_2) with which to compare either our ROHF results $\left(R_{opt} = 2.1747\, a_0, \Theta = -0.4188\, ea_0^2\right)$ or our UHF results $\left(R_{opt} = 2.1885 a_0, \Theta = -0.3427\, ea_0^2\right)$. Our ROHF and UHF results at R = 2.28 a_0 are -0.264 ea_0^2 and –0.218 ea_0^2, respectively and are in reasonable agreement with a large basis SCF calculation, by Bundgen *et al.*,[20] at R = 2.2819 a_0 that predicts Θ = – 0.249 ea_0^2. There are two numerical HFS calculations of Θ, both at R = 2.28 a_0. The first, by Becke,[23] is an unrestricted calculation that predicts Θ = – 0.36 ea_0^2, while the second, by Laaksonen *et al.*,[21] is a spin-restricted calculation predicting Θ = –0.3885 ea_0^2.

Our CBS CASSCF and CASSCF+1+2 results are – 0.2885 ea_0^2 and – 0.2530 ea_0^2, respectively. It is fascinating that ROHF calculations at the experimental bond length predict a Θ (– 0.264 ea_0^2), which differs from our best correlated result

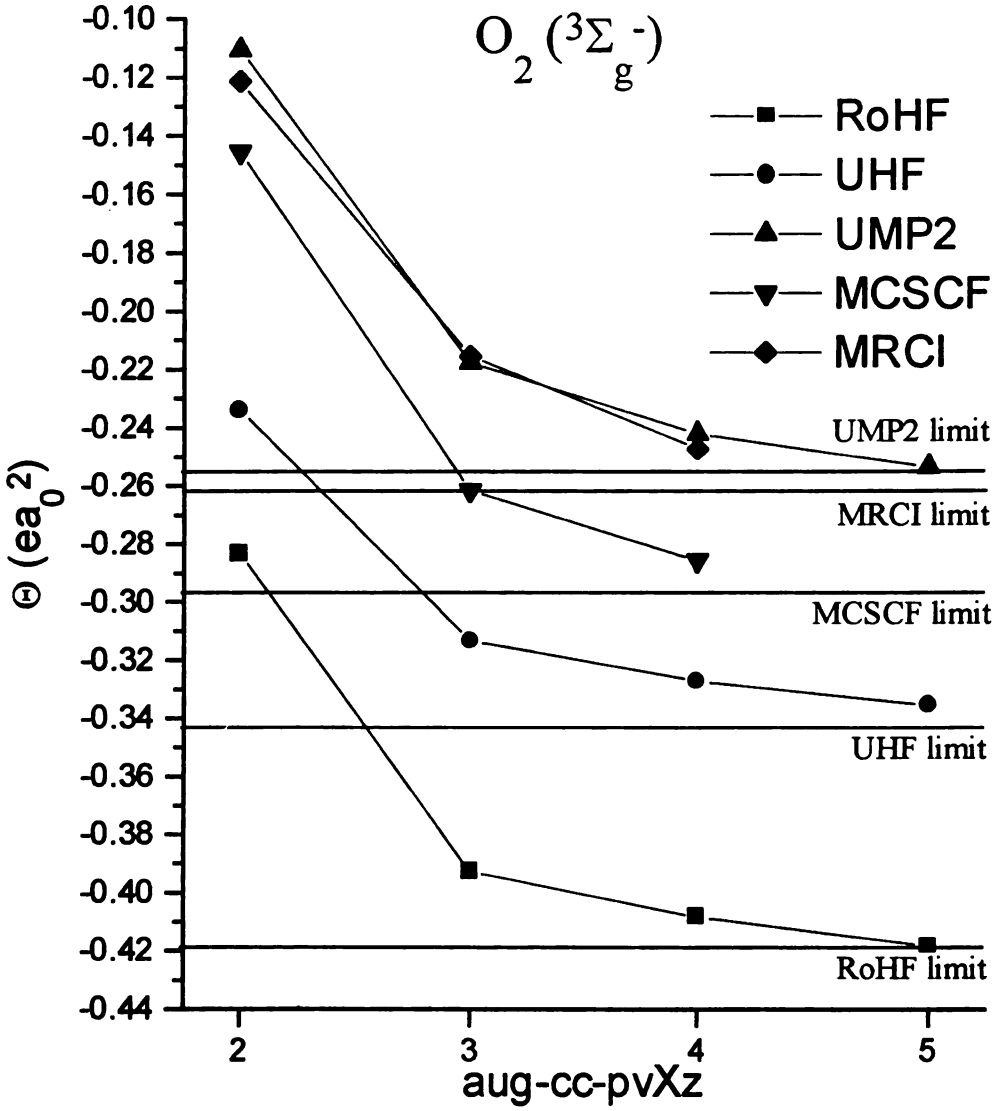

Figure 5. Model dependence of Θ for O_2 as a function of basis.

Table 2-4. Comparison of experimental and theoretical quadrupole-moment derivatives.

$(\partial\Theta/\partial R)_{R_e}(ea_0)$	Reference	Comment
+ 0.94	33	quadrupole absorption
+ 0.97	34	collision-induced
+ 0.95	35	collision-induced
+ 0.933±0.039	36	quadrupole absorption
0.959	This Work	MRCI aug-cc-pvqz; R_{opt}
0.948	This Work	MCSCF aug-cc-pvqz; R_{opt}
1.402	This Work	SCF aug-cc-pvqz; R_{opt}

(–0.253 ea_0^2) by only 4 percent. The reason for the insensitivity of Θ (O_2) to correlation effects is a consequence of the difference in the response of the σ and π electrons in O_2 to electron correlation and will be discussed after the quadrupole density is introduced. The distance dependence of Θ is shown in Figure 6. Unlike in N_2, the MCSCF and MRCI curves are not nearly as parallel as are the MRCI and SCF curves. The first and second derivatives of these curves are collected in Table 2-1.

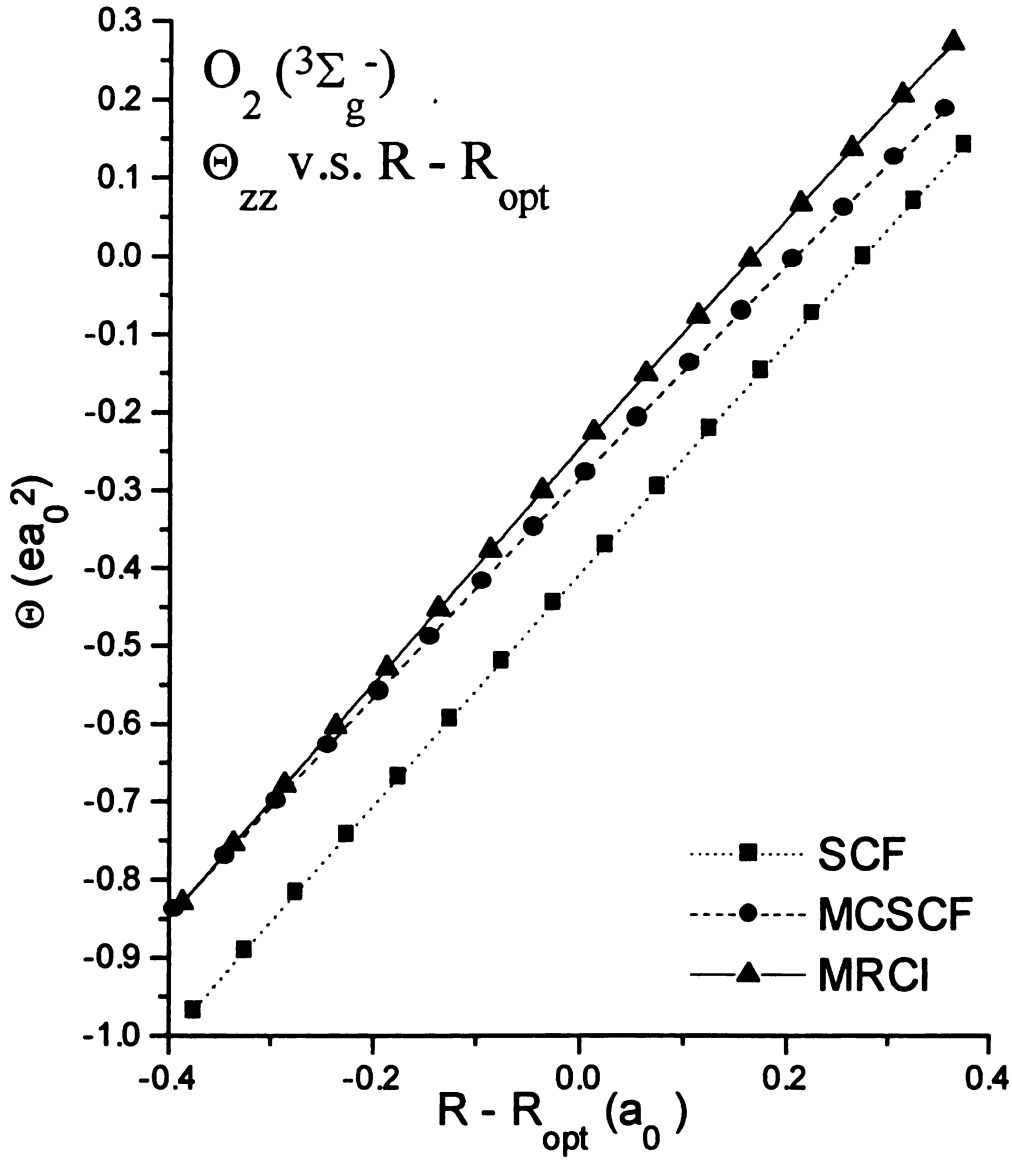

Figure 6. Distance dependence of Θ for O_2 calculated with various models using the aug-cc-pvqz basis.

Experimental data on O_2 is sparse. Buckingham *et al.*[37] report $-0.3 \pm 0.1\ ea_0^2$ from induced birefringence measurements, and Cohen and Birnbaum[32,37] report $|\Theta| = 0.25\ ea_0^2$ obtained from the interpretation of pressure-induced far-infrared spectra. These, and selected theoretical results, are shown in Table 2-5. Using the derivatives in Table 2-1, we estimate the vibrational correction to our CBS - CASSCF+1+2 result is

$$\Theta(O_2; v) = -0.2530 + 0.0257\left(v + \frac{1}{2}\right)$$

resulting in $\Theta(O_2, v = 0) = -0.2273\ ea_0^2$, which is in general agreement with the highly uncertain experimental values. The experimental estimate[33] of $(\partial\Theta/\partial R)_e$ for O_2, obtained from an analysis of the quadrupole absorption spectrum is + 1.6 ea_0 and is in reasonable agreement with our ROHF, MCSCF, and MRCI values of 1.8, 1.4, and 1.5 ea_0, respectively.

Our F_2 results are collected in Table C-8 and Figure 7. As with H_2, N_2, and O_2, the quadrupole moment decreases within a model with increasing quality of basis set and, as in O_2, electron correlation increases Θ. Our CBS-RHF limit is + 0.3081 ea_0^2 at R_{opt} = 2.5064 a_0 and + 0.501 ea_0^2 at R= 2.68 a_0. This latter value is in good agreement with the numerical Hartree-Fock result of McCullough,[17] + 0.505 ea_0^2, at R = 2.68 a_0. Our CBS-CASSCF+1+2 value of + 0.7131 ea_0^2 (R_{opt} = 2.6853 a_0) is in good agreement

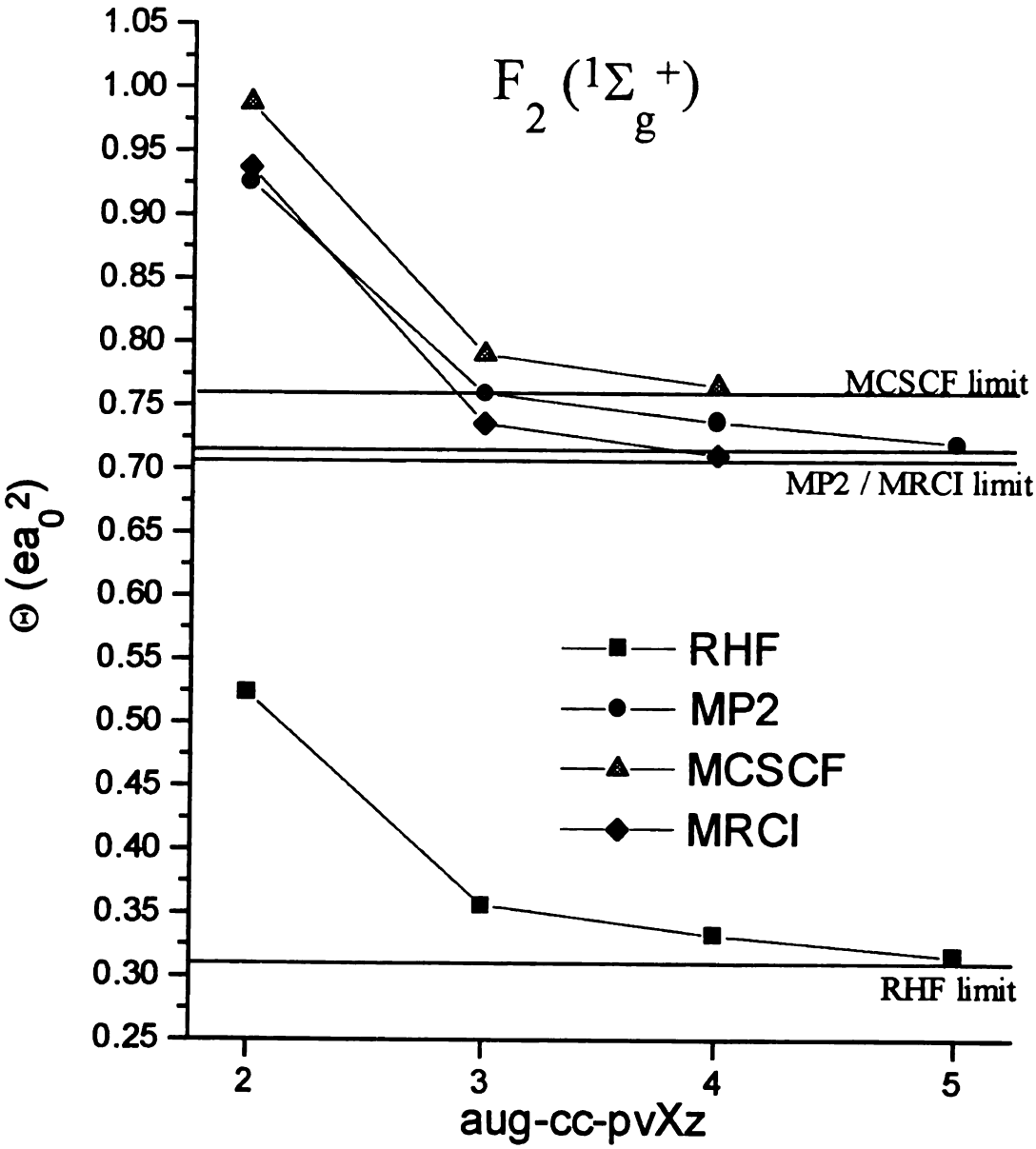

Figure 7. Model dependence of Θ for F_2 using various basis sets.

Table 2-5. Selection of O_2 quadrupole moments.

$R(a_0)$	$\Theta(ea_0^2)$	Reference	Comment
2.1747	– 0.4188	This Work	ROHF; R_{opt}
2.1885	– 0.3427	This Work	UHF; R_{opt}
2.28	– 0.2634	This Work	ROHF
2.28	– 0.188	20	SCF Sadlej[15] basis (5s3p2d)
2.28	– 0.249	20	SCF
2.2819	– 0.271	38	CI
2.282	– 0.356	12	numerical DFT (unrestricted)
2.28	– 0.3885	21	numerical HFS (α = 0.7)
2.28	– 0.36	23	numerical HFS (restricted)
2.2970	– 0.2885	This Work	CBS-CASSCF; R_{opt}
2.2873	– 0.2530	This Work	CBS-CASSCF+1+2; R_{opt}
vibrational average	– 0.240	This Work	CBS-CASSCF+1+2
experimental	|0.25|	32,37	pressure-induced, far-infrared spectrum
experimental	– 0.3 ± 0.1	31	Optical Birefringence

with the numerical HFS calculations of Laaksonen *et al.*,[21] 0.6911 ea_0^2 at R = 2.68 a_0, and those of Becke,[23] + 0.69 ea_0^2 also at R = 2.68 a_0. Our CBS limit at R = 2.68 a_0 is +0.7068 ea_0^2. The distance dependence of Θ (F_2) is shown in Figure 8. Correlation corrections effects more than double Θ (F_2), a much larger effect than in H_2, N_2, and O_2. As we will see subsequently, the correlation corrections to Θ, due to the σ and π electrons, are both in the same direction, and, rather than cancel as in O_2, they reinforce one another. Using the data in Table 2-1, we write the vibrational averaged Θ as

$$\Theta(F_2;\mathrm{v}) = +0.7131 + 0.0276\left(\mathrm{v}+\frac{1}{2}\right)$$

and, so, $\Theta(F_2;0) = +0.7269\ ea_0^2$. We collect the values of Θ from selected calculations in Table 2-6.

Table 2-6. Selection of F_2 quadrupole moments.

R(a_0)	$\Theta(ea_0^2)$	Reference	Comment
2.68	0.505	17	numerical HF
2.68	0.659	35	SCF
2.5064	0.3081	This Work	CBS-HF; R_{opt}
2.68	0.501	This Work	CBS-HF; R_{exp}
2.68	0.6911	17	numerical HFS (α = 0.7)
2.68	0.69	19	numerical HFS (α = 0.7)
2.6853	0.7131	This Work	CBS-CASSCF+1+2; R_{opt}
2.68	0.707	This Work	CBS-CASSCF+1+2; R_{exp}
vibrational average	0.727	This Work	CBS-CASSCF+1+2; v=0, J=0

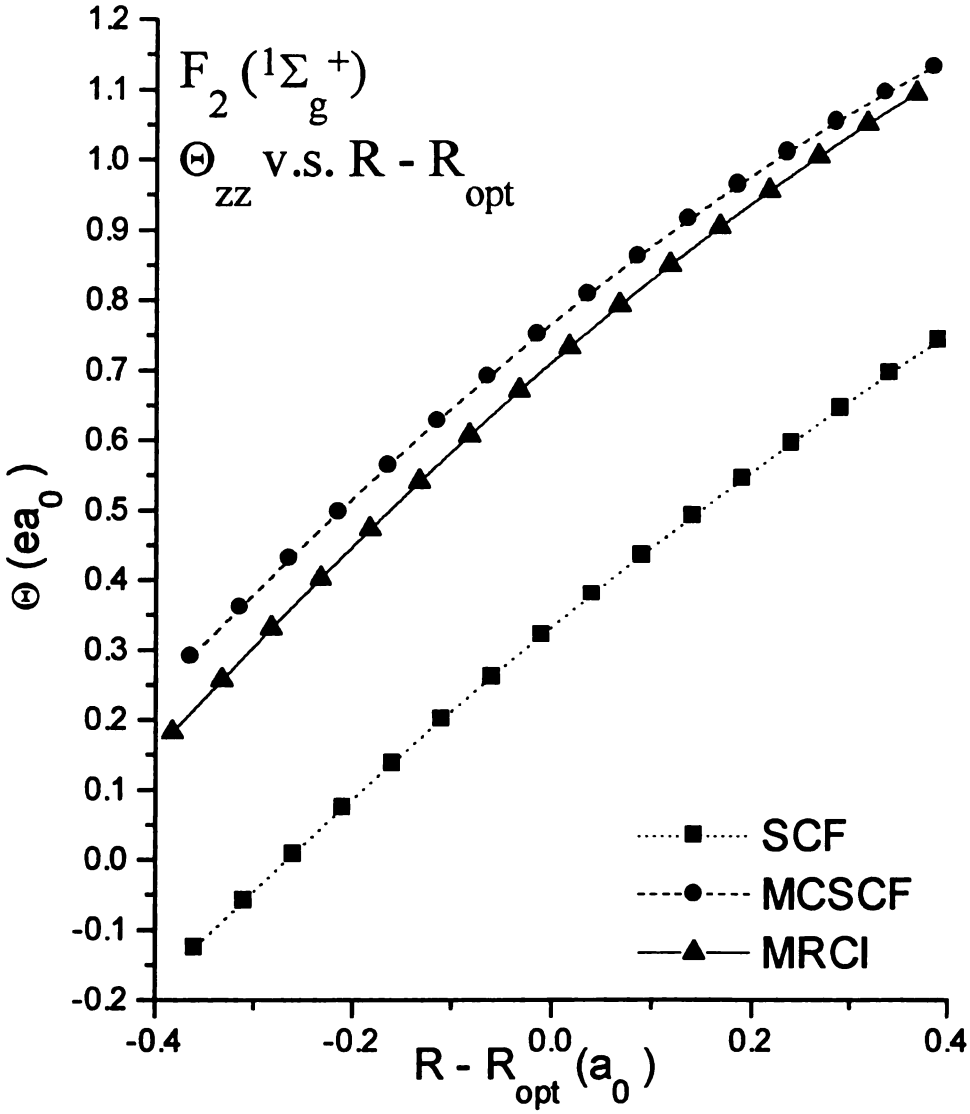

Figure 8. Distance dependence of Θ for F_2 calculated with various models using the aug-cc-pvqz basis.

There are no experimental measurements of Θ (F_2). We have collected the CASSCF+1+2 values of Θ along with the estimated CBS limit and vibrational corrections in Table 2-7.

Table 2-7. CASSCF+1+2 results for R_{opt} and Θ.

Molecule	aug-cc-pvqz		estimated complete basis set limit		
	$R_{opt}(a_0)$	$\Theta_{opt}(ea_0^2)$	$R_{opt}(a_0)$	$\Theta_{opt}(ea_0^2)$	vibration correction
H_2	1.4014	+ 0.4569	1.4009	+ 0.4552	+ 0.051 $(v + \frac{1}{2})$
N_2	2.0827	− 1.1247	2.0810	− 1.1270	+ 0.0137 $(v + \frac{1}{2})$
O_2	2.2907	− 0.2368	2.2873	− 0.2530	+ 0.0257 $(v + \frac{1}{2})$
F_2	2.6853	+ 0.7165	2.6853	+ 0.7131	+ 0.0276 $(v + \frac{1}{2})$

C. MP2 Results

It's apparent, from Figures 1, 3, 5, and 7, that MP2 is a significant improvement over the SCF model with little additional effort. We collect our MP2 results in Table 2-8 and compare them to the corresponding CBS CASSCF+1+2 results. The comparison is striking and suggests strongly that the corrections due to MP3 and MP4 cancel one another significantly as seen by Wolinski *et al.*[6] and Maroulis and Thakkar[14].

Table 2-8. Comparison of MP2 and CASSCF+1+2 results.

Molecule	MP2 (estimated CBS)		CASSCF+1+2 (estimated CBS)	
	$R_{opt}(a_0)$	$\Theta_{opt}\left(ea_0^2\right)$	$R_{opt}(a_0)$	$\Theta_{opt}\left(ea_0^2\right)$
H_2	1.3895	+ 0.4699	1.4009	+ 0.4552
N_2	2.0970	− 1.1751	2.0810	− 1.1270
O_2	2.3032	− 0.2546	2.2873	− 0.2530
F_2	2.6452	0.7178	2.6853	+ 0.7131

D. Hellmann-Feynman Theorem

When a perturbation on a Hamiltonian is the effect of an applied field of strength λ, the perturbed Hamiltonian can be written as

$$\hat{H} = \hat{H}^0 + \lambda\hat{O}$$

where $\hat{O}$ is for example, a dipole moment operator and H^0 is the full many-electron Hamiltonian for the unperturbed molecule. The Hellmann-Feynman theorem.[40,41,42] The Feynman is commonly written as,

$$\left(\frac{dE(\lambda)}{d\lambda}\right)_{\lambda=0} = \left\langle \Psi \middle| \hat{O} \middle| \Psi \right\rangle$$

where $\hat{O}$ is a one-electron operator of a given property that responds directly to the field and Ψ is the exact wavefunction. This equality is also true for certain approximate methods such as HF and MCSCF where all variables are variationally optimized within a given space. In the CI and MP wavefunctions, however, the configurational coefficients are variationally optimized, but the molecular orbital expansion coefficients are not so the equality is not assured.[42]

To assess the difference between $\langle\Psi|\hat{O}|\Psi\rangle$ and $(dE(\lambda)/d\lambda)_0$, calculations have been performed using both HF and MP2 methods to calculate the quadrupole moment of various diatomics. $\langle\Psi|\hat{O}|\Psi\rangle$ is determined as an expectation value (EV) while $(dE(\lambda)/d\lambda)_0$ is referred to as the point charge method (PC). Application of these techniques are described in Appendix A. As shown in Table 2-9 the MP2 wavefunction using an aug-cc-pvtz basis set brings the EV quadrupole moment to within 2% of the point PC quadrupole moment. The MP2 results can be compared to the HF

Table 2-9. Expectation Value Quadrupole moment and Point Charge Quadrupole Moment

	HF			MP2		
	E_{PC}	E_{EV}	%Diff.	E_{PC}	E_{EV}	%Diff.
$H_2(^1\Sigma_g^+)$	0.502	0.500	-0.34	0.478	0.476	-0.42
$N_2(^1\Sigma_g^+)$	-0.910	-0.920	-0.11	-1.171	-1.158	-1.11
$O_2(^3\Sigma_g^-)$	-0.160	-0.163	-1.85	-0.262	-0.264	0.76
$F_2(^1\Sigma_g^+)$	0.530	0.534	0.75	0.769	0.784	1.91

results also given in Table 2-9. With the exception of O_2, the difference in the HF-EV quadrupole moments and HF-PC quadrupole moments are smaller. Since the Hellmann-Feynman equality holds for HF wavefunctions, improving the 'completeness' of the basis sets should lessen the difference between EV quadrupole moments and the PC quadrupole moments for the other approximate wavefunctions and the results listed in Table 2-9 indicate this to be correct.

E. Quadrupole Moment Functions

We study the distance dependence of Θ (quadrupole-moment function), using the aug-cc-pvqz basis and the MCSCF and MRCI wavefunctions. The calculated potential energy curves for the molecules of interest are shown in Figure 9, and the calculated properties (R_e, D_e, ω_e) are very close to the CBS CASSCF+1+2 limits. These wavefunctions provide a reasonably accurate description of the molecule's electronic structure over a large range of internuclear distances, and we expect the calculated quadrupole-moment functions to be realistic.

The quadrupole moment functions for the four molecules of interest are shown in Figure 10, from which we see that H_2 is unique—having the only quadrupole-moment function that is everywhere positive. Θ for H_2 and N_2, is zero at large R because both molecules separate to atoms in S states. Θ, for F_2 and O_2, separates to the sum of the atomic quadrupole moments of the atoms. For F_2, the F atoms are in the $^2P_{m=0}$ (^2P_z) state, loosely corresponding to the configuration,

$$1s^2 2s^2 2p_x^2 2p_y^2 2p_z^1$$

with z labeling the internuclear axis. For O_2, the atoms are in the $^3P_{|M|=1}$ levels, which, in a real representation, corresponds to one atom in

$$1s^2 2s^2 2p_x^2 p_y^1 p_z^1$$

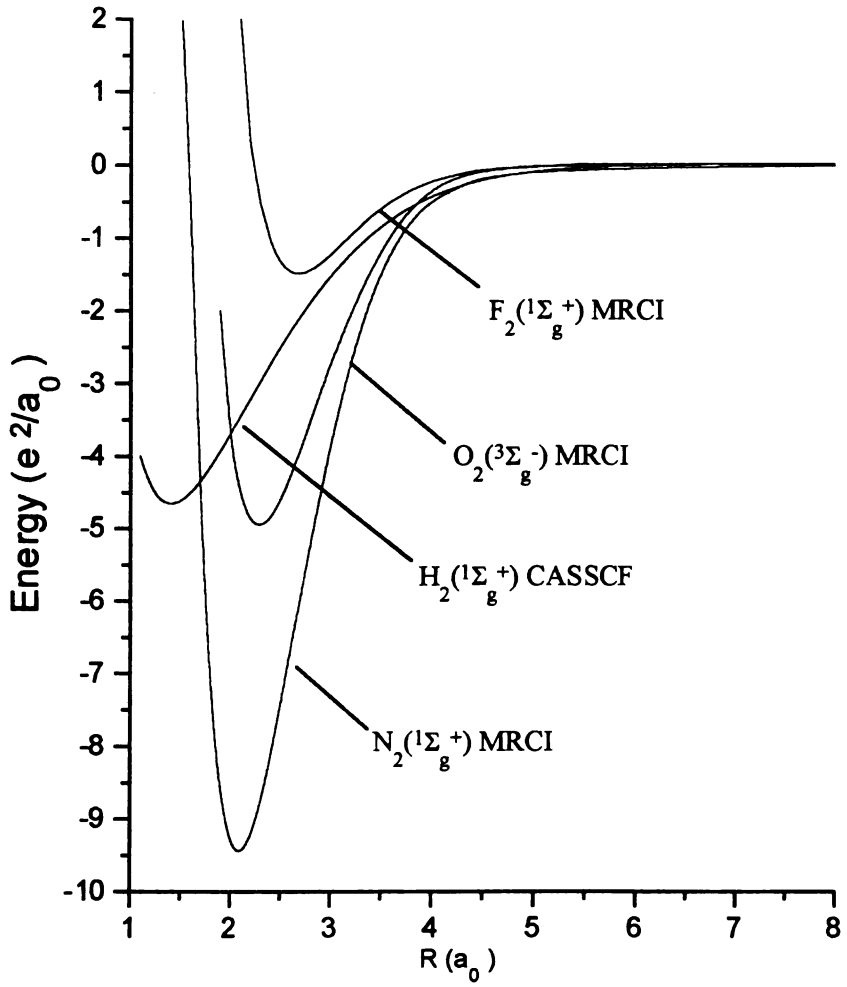

Figure 9. MRCI potential energy curves for N_2, O_2, and F_2 using the aug-cc-pvqz basis and a 10 CSF, CASSCF potential energy curve for H_2 using the aug-cc-pv5z basis.

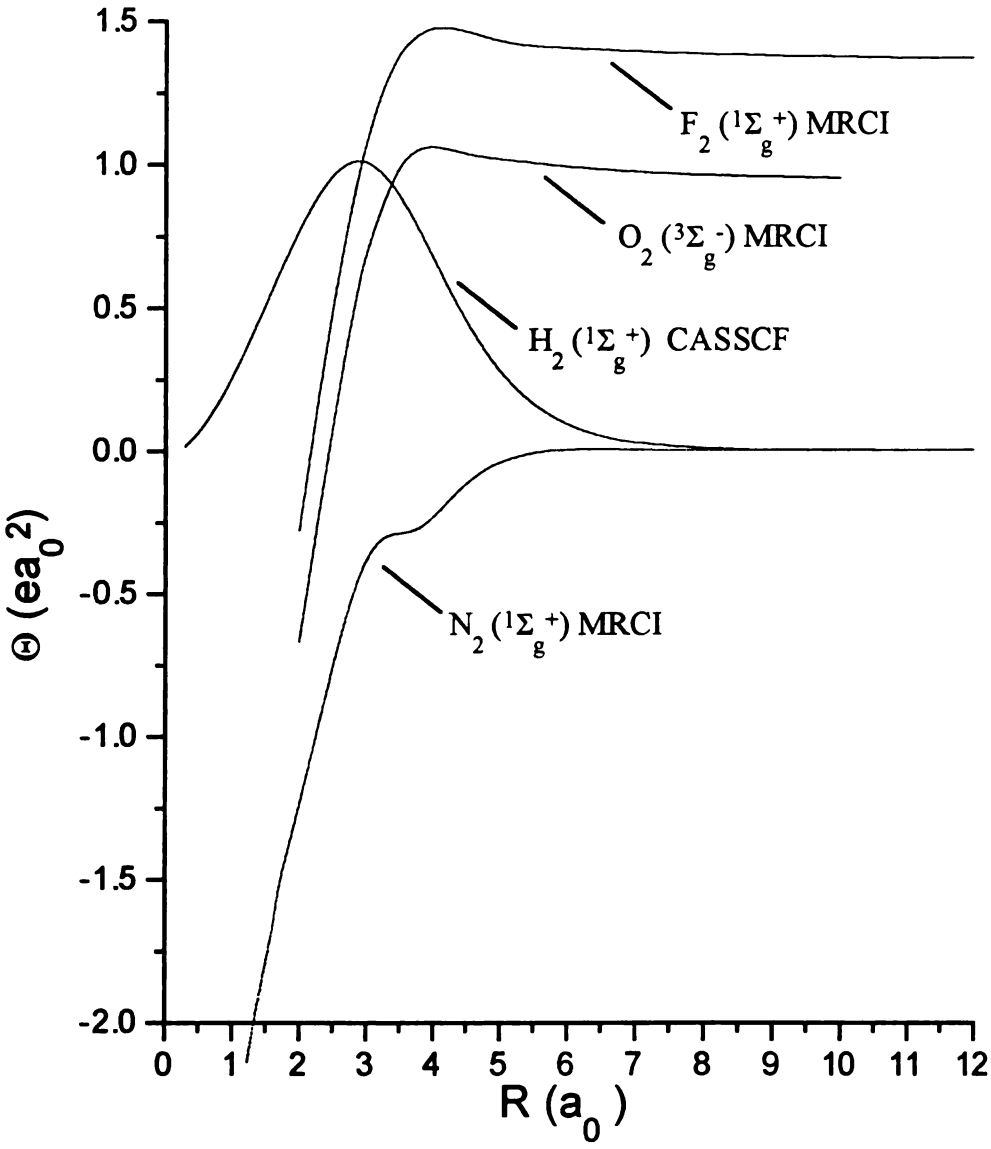

Figure 10. Molecular quadrupole moments of H_2, N_2, O_2, and F_2 as a function of bond length.

and one in

$$1s^2 2s^2 2p_x^1 2p_y^2 2p_z^1.$$

We will first consider N_2, O_2, and F_2, returning to H_2 latter. Let's first write the electron density at internuclear separation R as

$$n(\vec{r};R) = n_A^0(\vec{r}) + n_B^0(\vec{r}) + \delta n(\vec{r},R) \tag{5}$$

where n_A^0 and n_B^0 are the electron densities of the two non-interacting atoms placed at the appropriate nuclear positions. Note that δn is defined by this equation. As a practical matter, n_A^0 and n_B^0 are obtained from the natural orbitals of the MCSCF or MRCI wavefunctions at large values of R and translated, intact, to the internuclear separation of interest.

Using Equation 5, the quadrupole moment defined by Equation 1 can be rewritten as

$$\Theta(A_2;R) = 2\Theta^0(A) + \int \delta\Theta(\vec{r};R)dV \tag{6}$$

where $\Theta^0(A)$ is the quadrupole moment of the separated atom A in the diatomic A_2

$$\Theta^0(A) = -\frac{1}{2}\int n_A^0(\vec{r})\left(3z^2 - r^2\right)dV \tag{7}$$

and δΘ is the quadrupole-moment density

$$\delta\Theta = -\frac{1}{2}\delta n(\vec{r};R)\left(3z^2 - r^2\right). \tag{8}$$

Note that the nuclear contribution to $\Theta(A_2;R)$ is now implicit in $\delta n(\vec{r},R)$. Note, also, that $\Theta(A_2;R)$ is now written as the sum of a (constant) atomic contribution, $2\Theta^0(A)$ and a contribution Θ_{mol}, due to molecule formation

$$\Theta_{mol}(R) = \int \delta\Theta(\vec{r};R)dV \,. \tag{9}$$

Since we may easily partition δn into σ and π contributions,

$$\delta n = \delta n_{\sigma} + \delta n_{\pi}, \tag{10}$$

we may also write

$$\Theta(A_2;R) = \Theta_{\sigma}(A_2;R) + \Theta_{\pi}(A_2;R), \tag{11}$$

where

$$\Theta_{\sigma}(A_2;R) = 2\Theta_{\sigma}^{0}(A) + \int \delta\Theta_{\sigma}(\vec{r},R)dV, \tag{12}$$

with an analogous expression for $\Theta_{\pi}(A_2;R)$. The σ and π components of the quadrupole-moment curves for N_2, O_2, and F_2 are shown in Figure 11 for a MRCI wavefunction in an aug-cc-pvqz basis. Note that Θ_{σ} is always negative and Θ_{π} is always positive; and, while the sign of Θ depends on the relative magnitudes of these contributions, Θ usually decreases from its asymptotic value with decreasing R. The relative asymptotic values are easily understood, in terms of an orbital model. For example, the zz component of the atomic quadrupole moment of (oriented, m = 0) F is given by

$$\Theta\left(F;\,^2\mathrm{P}_z\right) = \Theta(2p_z) + 2\Theta\left(2p_y\right) + 2\Theta(2p_x)$$

where

$$\Theta(2p_{\alpha}) = -\frac{1}{2}\int (2p_{\alpha})^2\left(3z^2 - r^2\right)dV \,.$$

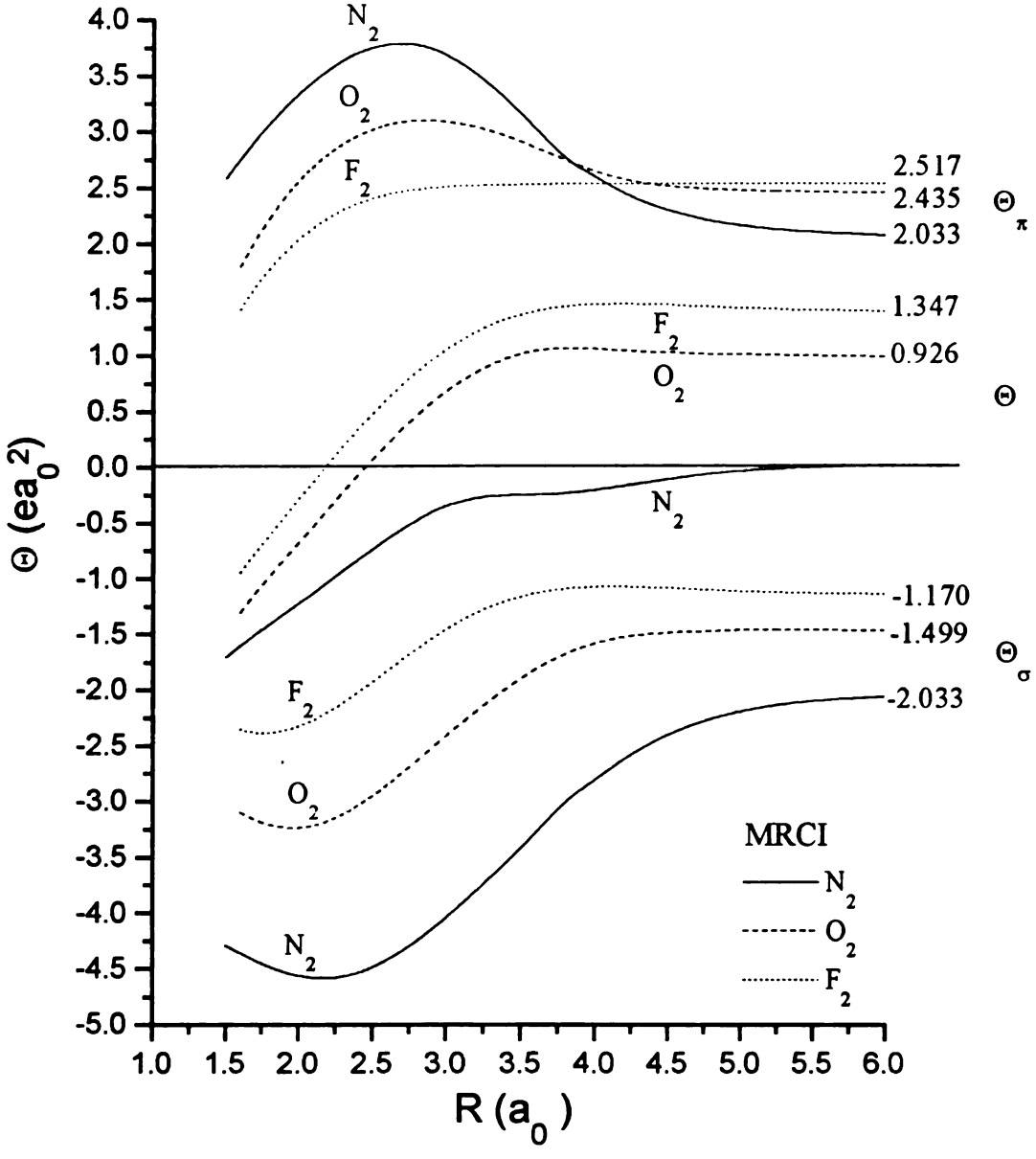

Figure 11. Distance dependence of the quadrupole moments of N_2, O_2, and F_2 partitioned into the Θ_σ and Θ_π components.

By symmetry

$$\Theta(2p_x) = \Theta(2p_y)$$

and $\Theta(2p_x) + \Theta(2p_y) + \Theta(2p_z) = 0$.

With z as the internuclear line,

$$\Theta_\pi(F) = 2\Theta(2p_x) + 2\Theta(2p_y) = -2\Theta(2p_z) \equiv -2\Theta_\sigma(F).$$

It's easy to show

$$\Theta(2p_z) = \Theta_\sigma(F) < 0,$$

so, in an orbital model where all $2p$ orbitals are radially equivalent,

$$\Theta_\pi(F) = -2\Theta_\sigma(F) > 0.$$

Our asymptotic values are

$$\Theta_\pi(F) = +2.517\ ea_0^2$$

$$\Theta_\sigma(F) = -1.170\ ea_0^2.$$

These are not precisely in the symmetry determined ratio because our wavefunction has D_{2h} symmetry and our correlated wavefunction results in asymptotic p functions that are not equivalent.

In a similar fashion, the O $\left({}^3P_{|M|=1}\right)$ quadrupole moment is given by

$$\Theta\left(O;\, {}^3P_{|M|=1}\right) = 2\Theta(2p_x) + \Theta(2p_y) + \Theta(2p_z)$$

$$\Theta_\pi(O) = 2\Theta(2p_x) + \Theta(2p_y)$$

$$\Theta_\sigma(O) = \Theta(2p_z)$$

$$\Theta_{\pi}(O) = 3\left(-\tfrac{1}{2}\Theta_{\sigma}(O)\right) = -3/2\,\Theta_{\sigma}(O).$$

Our asymptotic values are

$$\Theta_{\pi}(O) = +2.435\ ea_0^2$$

$$\Theta_{\sigma}(O) = -1.499\ ea_0^2$$

Differing from the simple orbital ratios for reasons described earlier.

If we reference each molecular quadrupole-moment function to its asymptotic atomic contribution, we obtain Figures 12-14, which are simply $\Theta_{mol}(R)$ and its component Θ_{mol}^{σ} and Θ_{mol}^{π}. Some insight into why Θ_{mol}^{σ} is always negative and Θ_{mol}^{π} is always positive may be obtained by examining $\delta\Theta_{\sigma}(\vec{r},R)$ and $\delta\Theta_{\pi}(\vec{r},R)$. Recall

$$\delta\Theta_{\sigma} = -\frac{1}{2}\delta n_{\sigma}(\vec{r},R)\left(3z^2 - r^2\right) = -\frac{1}{2}r^2\,\delta n_{\sigma}(\vec{r},R)\left(3\cos^2\theta - 1\right) \qquad (13)$$

where the origin is the molecular midpoint and θ is measured relative to the internuclear line as the polar axis. This equation relates electron shifts in the σ system, upon bond formation to the molecular contribution to the quadrupole moment. Note that the factor $-\frac{1}{2}\left(3\cos^2\theta - 1\right)$ partitions the molecular space into two regions, labeled N and P and shown in Figure 15. It is interesting to note that the parabolas delineating the Berlin[45] bonding and antibonding regions are asymptotically tangent to the nodal surfaces separating the N and P regions. In the conical regions labeled N, to the rear of the nuclei, the angular factor is negative, and, thus, a positive δn_{σ} in this region results in a negative contribution to Θ_{mol}^{σ}. In N_2, the σ bond involves a large sp hybridization, moving charge towards the midpoint of the molecule. Simultaneously, the opposite-

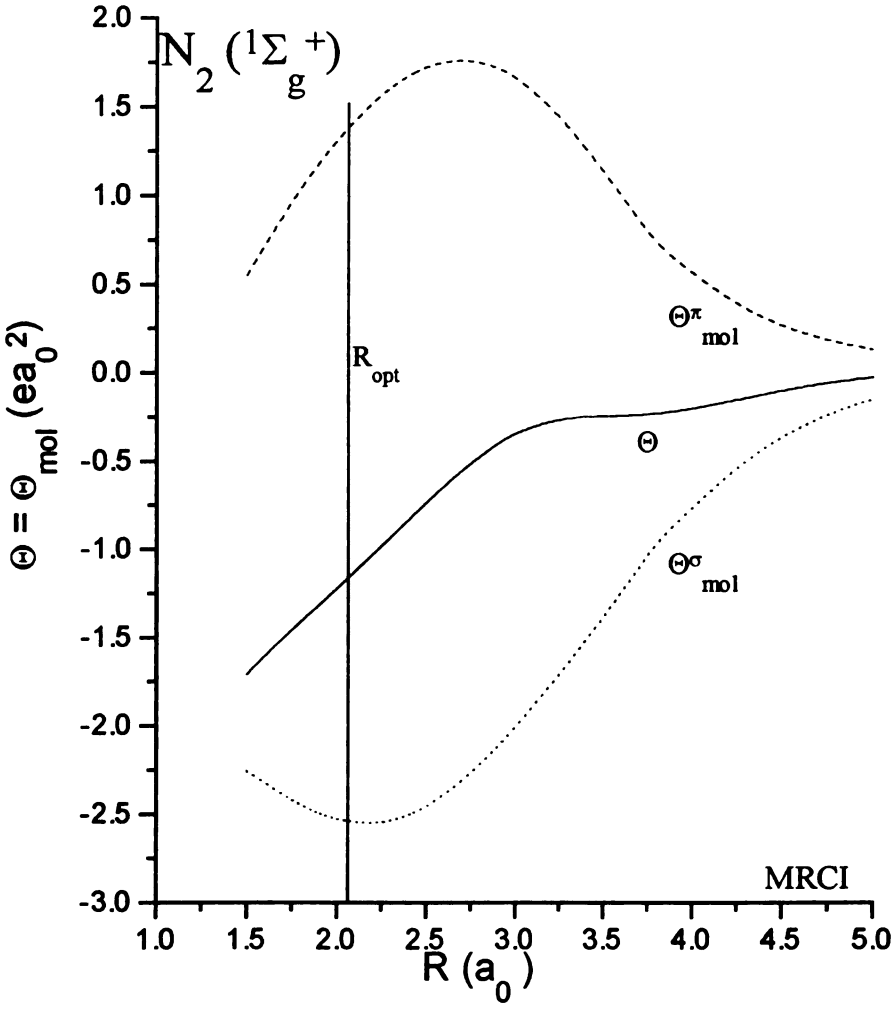

Figure 12. Distance dependence of the quadrupole moment of N_2 partitioned into its Θ^{σ}_{mol} and Θ^{π}_{mol} components.

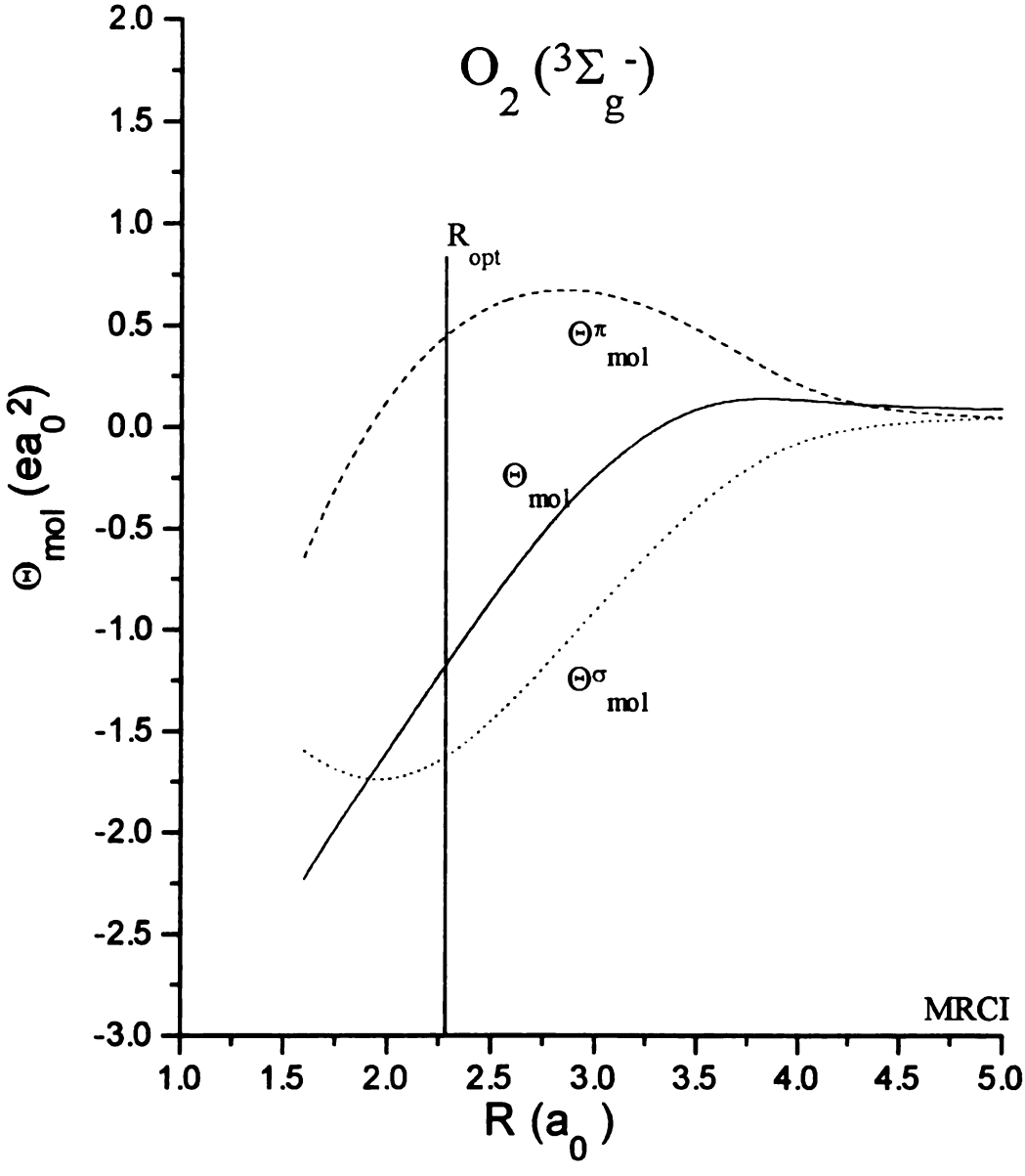

Figure 13. Distance dependence of Θ_{mol} for O_2 partitioned into its Θ^{σ}_{mol} and Θ^{π}_{mol} components.

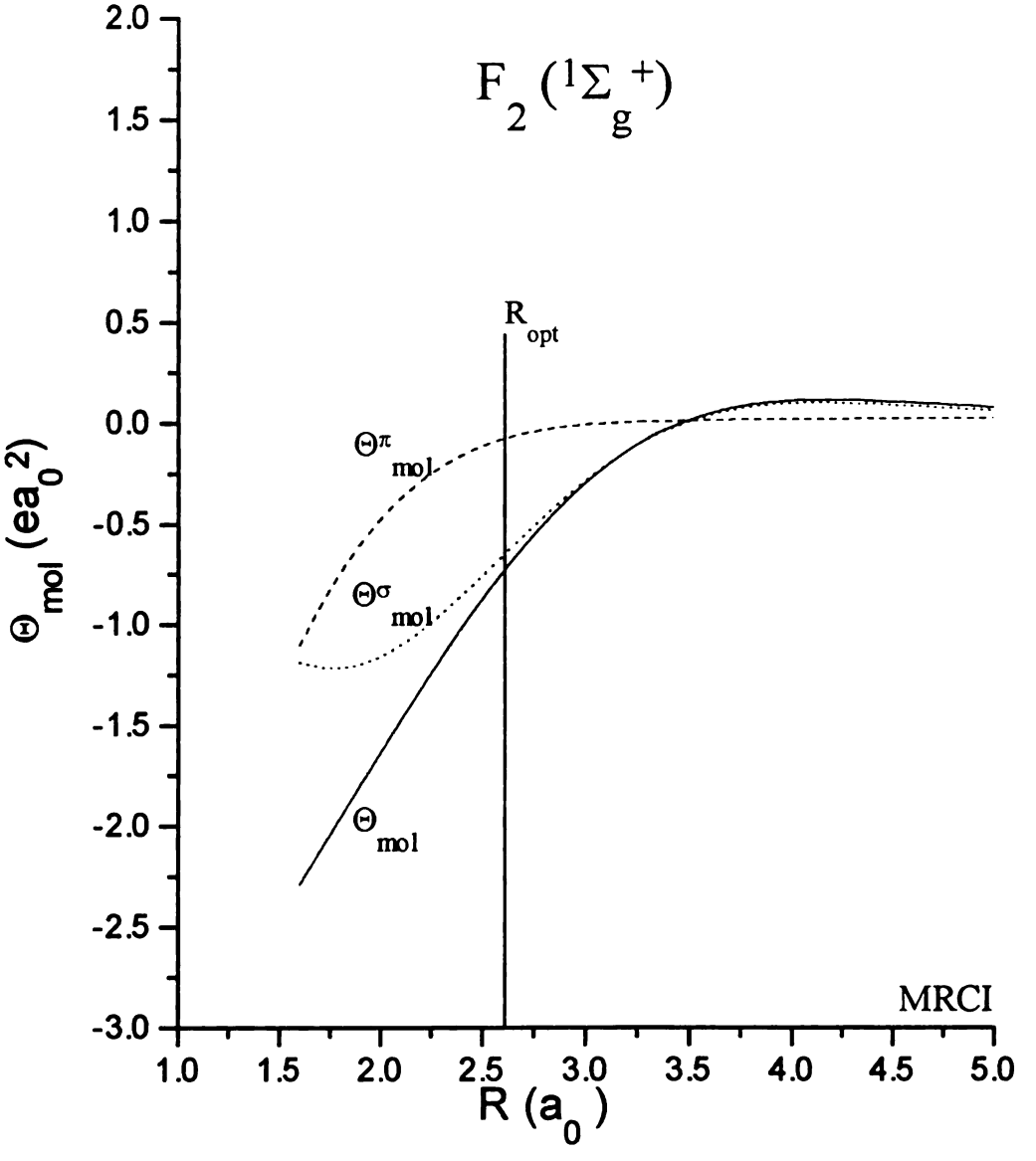

Figure 14. Distance dependence of Θ_{mol} for F_2 partitioned into its Θ^{σ}_{mol} and Θ^{π}_{mol} components.

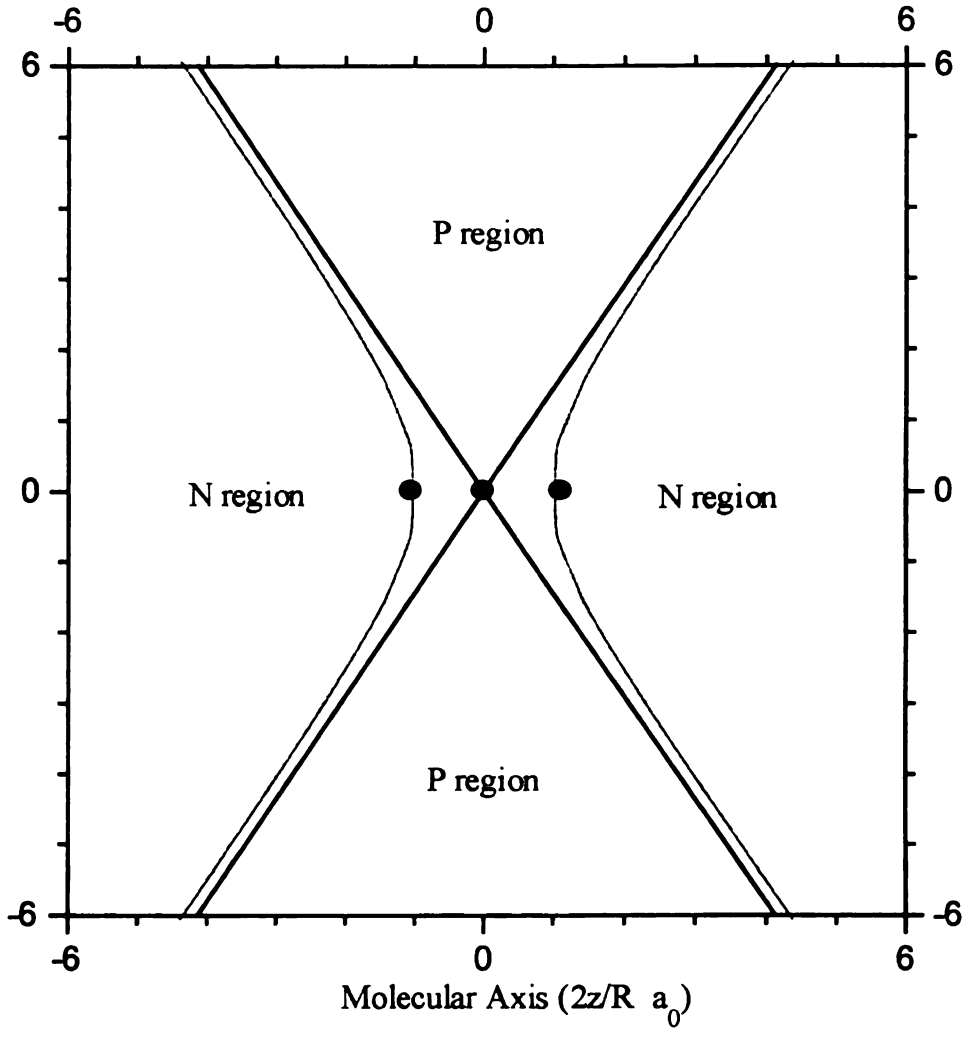

Figure 15. Quadrupole density nodes represented by solid lines. Berlin bonding and antibonding regions separated by parabolic curves.

phase sp hybrid pooches out to the rear of the nuclei contributing to a positive δn_σ and, therefore, a negative $\delta\Theta_\sigma$. Note that this effect is enhanced by the r^2 term in Equation 13, which weights heavily the farther reaches of δn_σ. Along with the σ bond in N_2, we, of course, have the π bond, which results in δn_π being positive in the region between the nuclei and above the molecular line; and, since $\delta\Theta_\pi = -\frac{1}{2}r^2\delta n_\pi\left(3\cos^2\theta - 1\right)$, this is precisely where the angular factor is positive, and, therefore, an accumulation of charge in the π system (positive δn_π) results in a positive value of $\delta\Theta_\pi$ and contributes toward a positive value of Θ^π_{mol}. These effects are vividly illustrated in Figure 16-18, which show δn, δn_σ, and δn_π and the associated $\delta\Theta$, $\delta\Theta_\sigma$, and $\delta\Theta_\pi$ densities for N_2. Note that the increase in charge density around the molecular midpoint contributes little to Θ_{mol}, as it is multiplied by r^2 (small in this region), and much cancellation results from the integration over $3\cos^2\theta - 1$. The situation with O_2 and F_2 differ only in degree. sp hybridization decreases in going from N_2 to O_2 to F_2, and this is reflected in a less negative value of Θ^σ_{mol} in O_2 and F_2, relative to N_2.

The π systems in O_2 and F_2 are qualitatively different from N_2's, and this is reflected in the Θ^π_{mol} curves shown in Figures 12-14. For O_2, δn_π is smaller than in N_2 and, thus, $\Theta^\pi_{mol}(O_2)$ is less positive. For F_2, δn_π is almost zero and $\Theta^\pi_{mol}(F_2)$ is small. These characteristics of O_2 and F_2 are illustrated by the contour plots in Figures 19-21 and 22-24. One striking feature of Θ^π_{mol} in N_2 and O_2 is the maximum (Figures 12 and

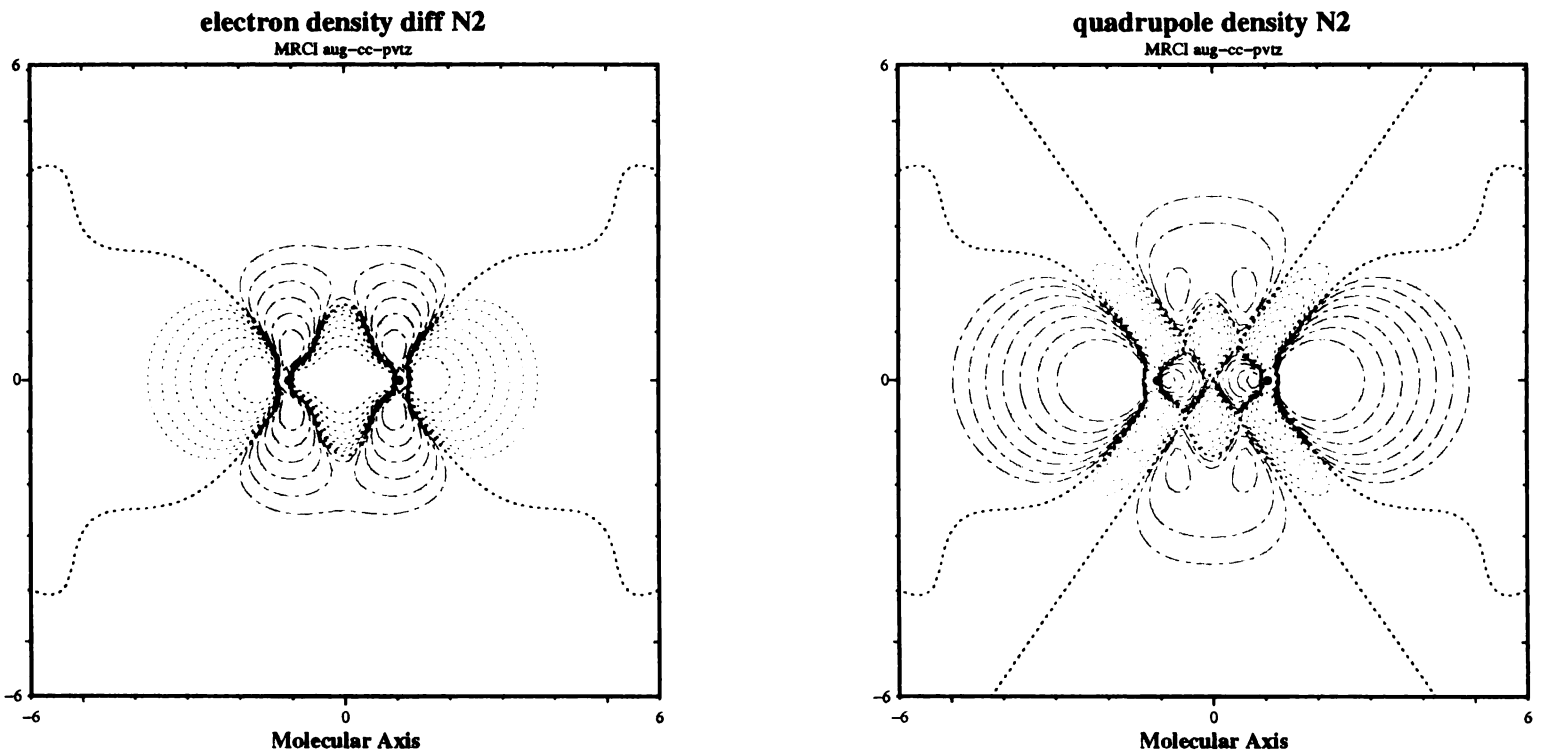

Figure 16. Electron-density difference and the associated quadrupole-density contours for N_2 at 2.1 a_0 calculated with the aug-cc-pvtz basis. The contour values are 2^N*10^{-3}(atomic units) with N = 0-6. The red contours are negative, the blue positive, and the nodes are in black.

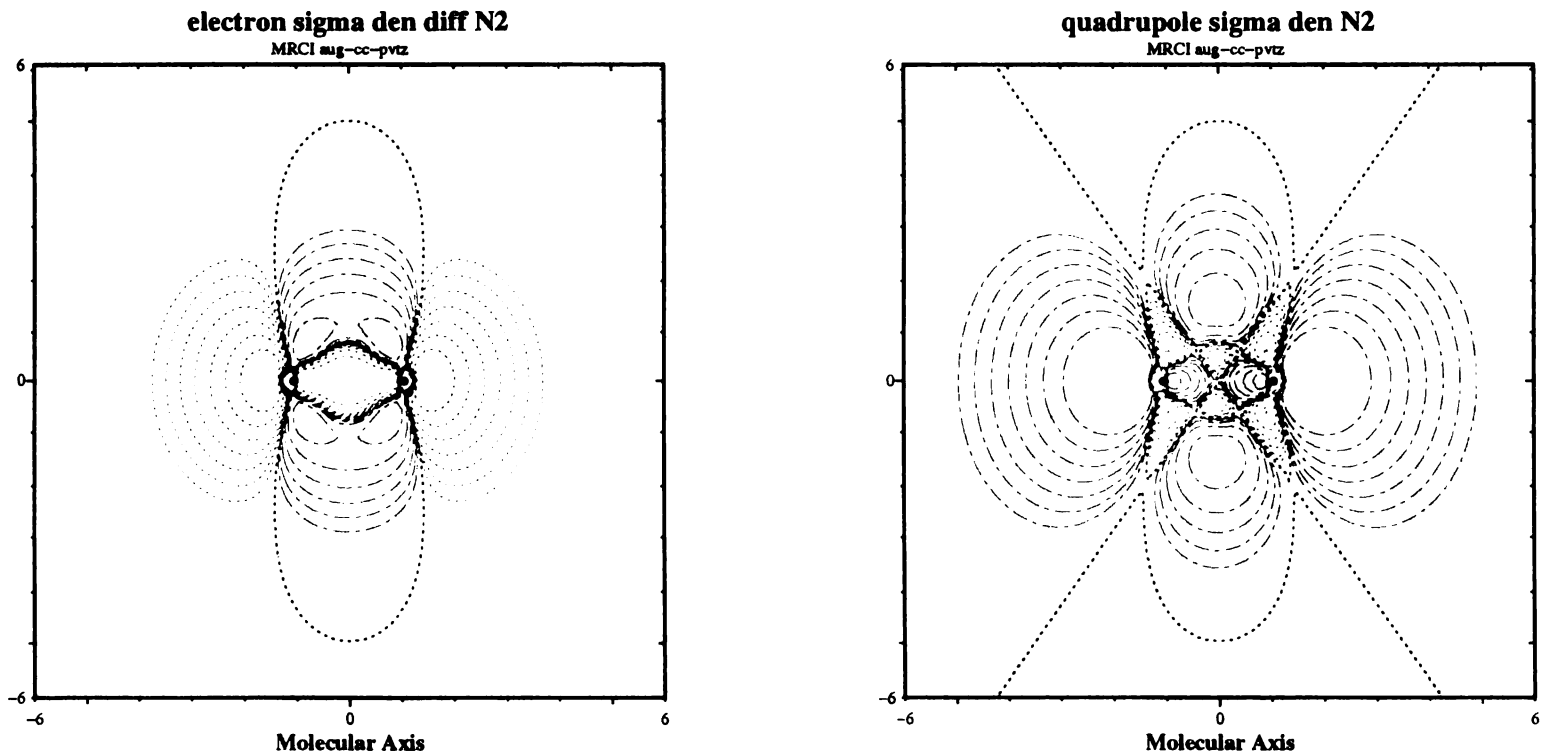

Figure 17. δn_σ and $\delta\Theta_\sigma$ for N_2 at 2.1 a_0 calculated with MRCI using the aug-cc-pvtz basis. Contours values and colors are same as in Figure 16.

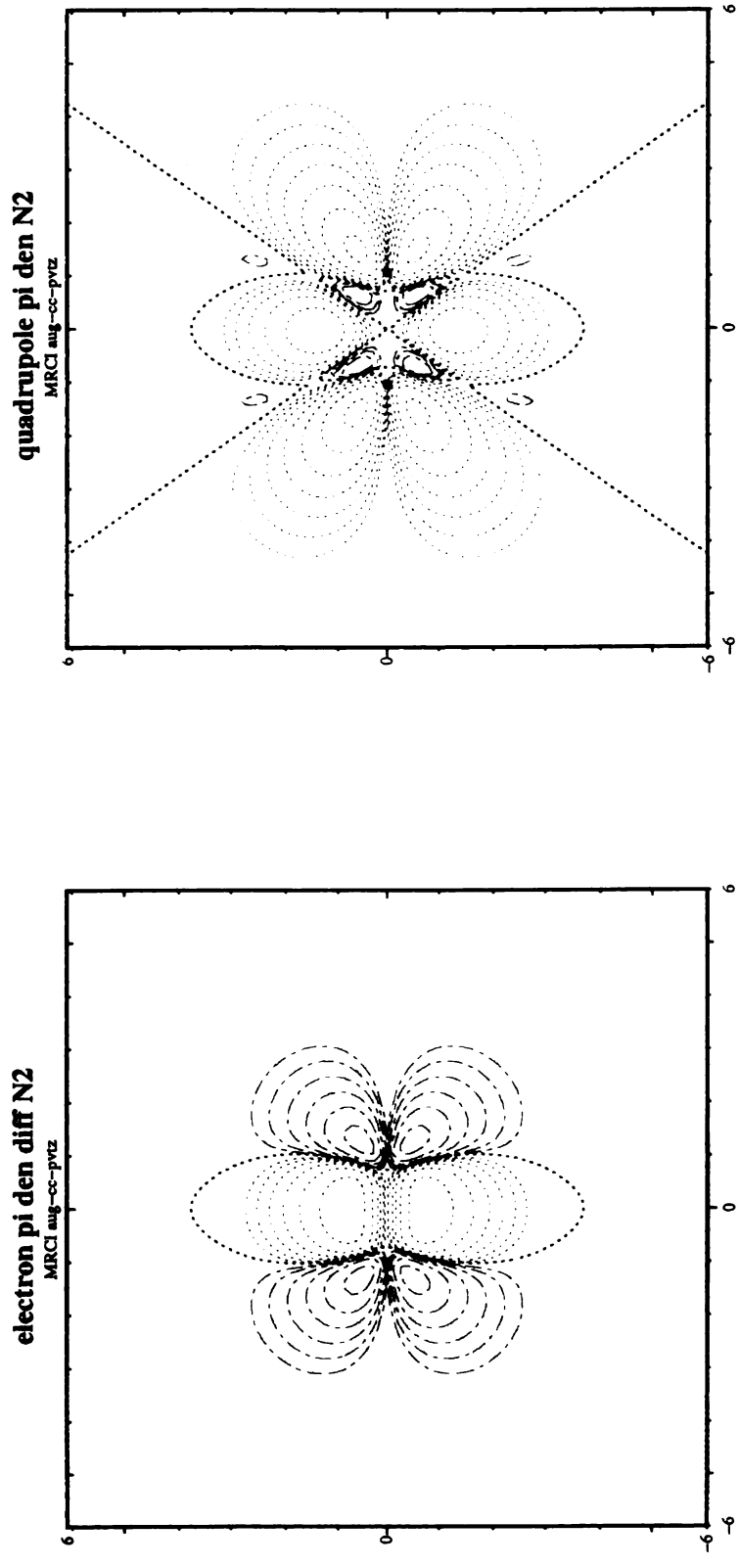

Figure 18. δn_π and $\delta\Theta_\pi$ for N_2 at 2.1 a_0 calculated with MRCI using the aug-cc-pvtz basis. Contours values and colors are same as in Figure 16.

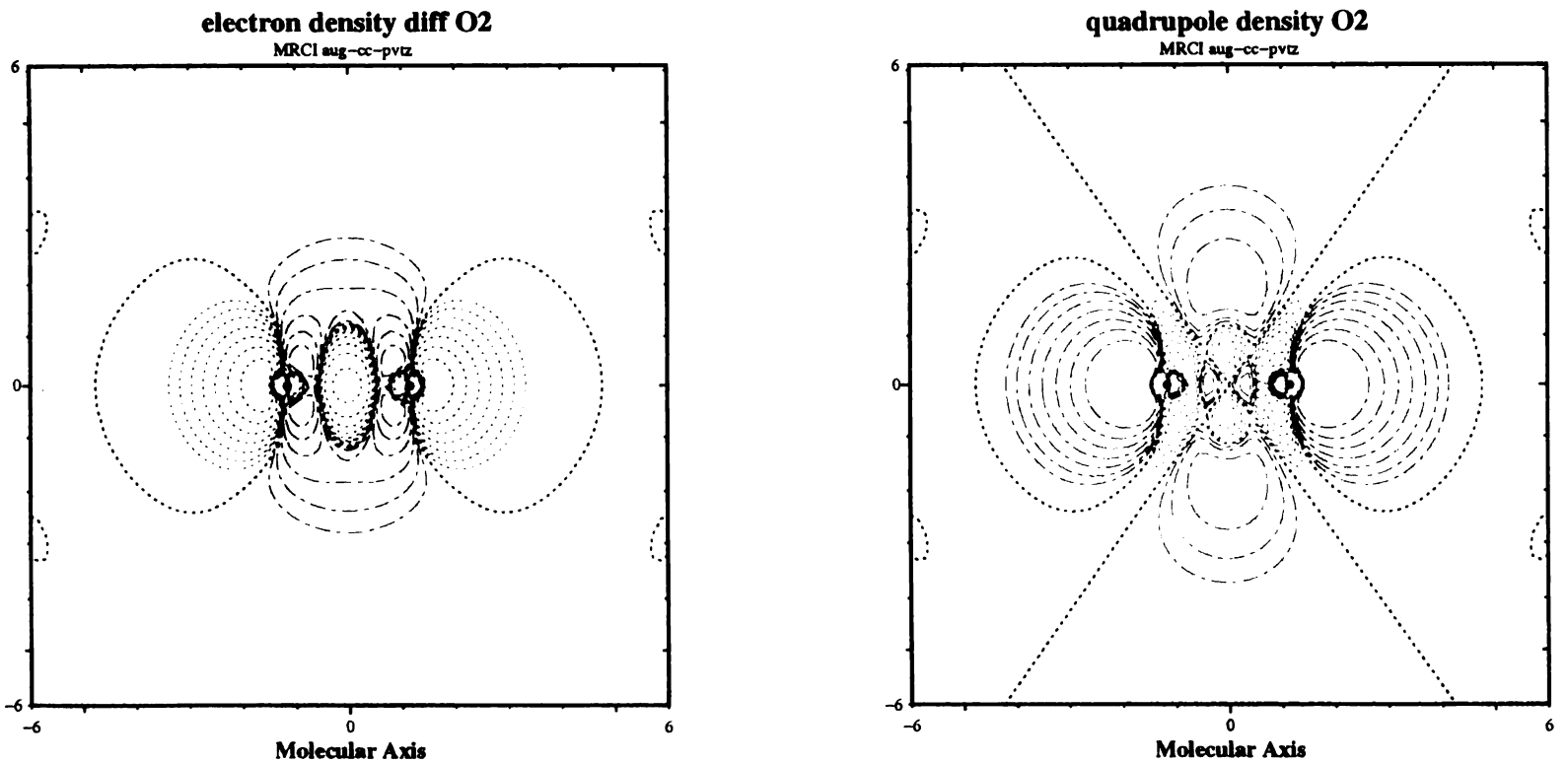

Figure 19. Electron-density difference and the associated quadrupole-density contours for O_2 at 2.3 a_0 calculated with the aug-cc-pvtz basis. Contours values and colors are same as in Figure 16.

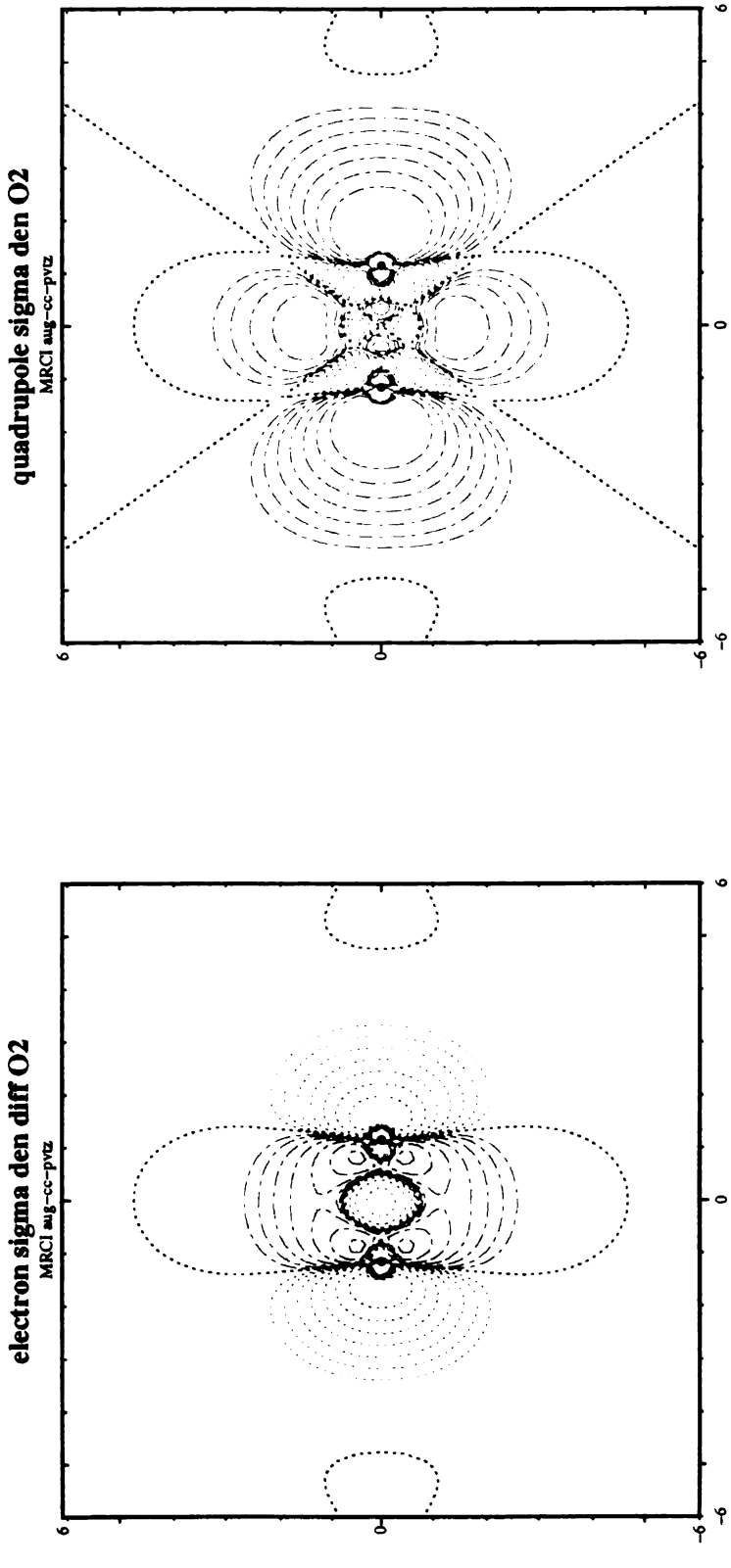

Figure 20. δn_σ and $\delta\Theta_\sigma$ for O_2 at 2.3 a_0 calculated with MRCI using the aug-cc-pvtz basis. Contours values and colors are same as in Figure 16.

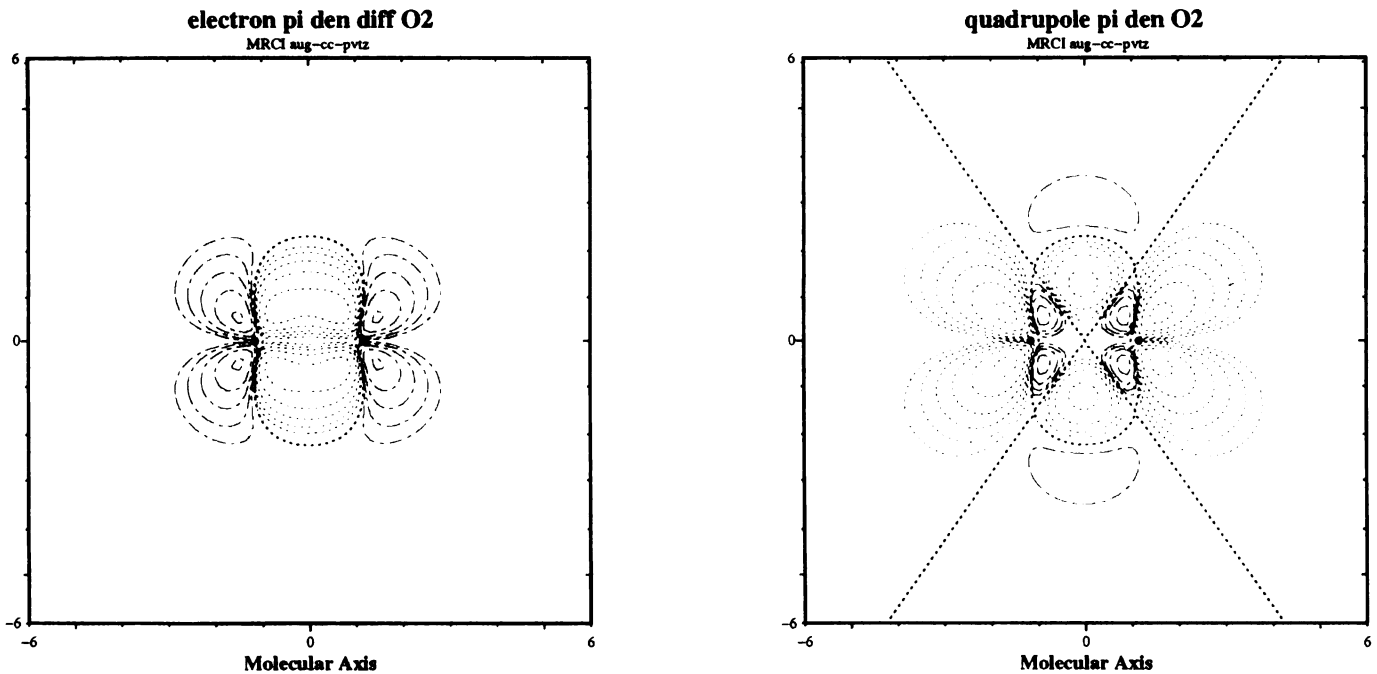

Figure 21. δn_π and $\delta\Theta_\pi$ for O_2 at 2.3 a_0 calculated with MRCI using the aug-cc-pvtz basis. Contours values and colors are same as in Figure 16.

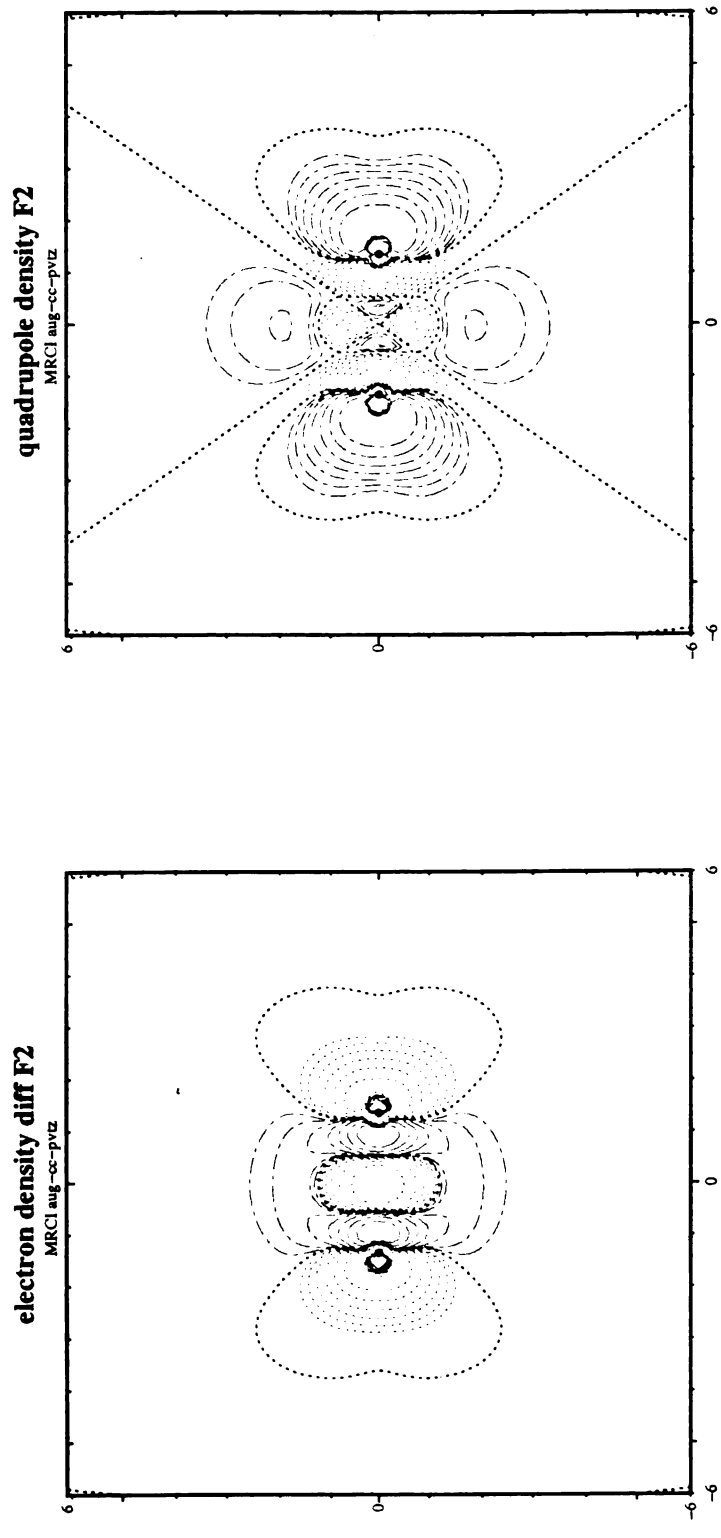

Figure 22. Electron-density difference and the associated quadrupole-density contours for F_2 at 2.7 a_0 calculated with the aug-cc-pvtz basis. Contours values and colors are same as in Figure 16.

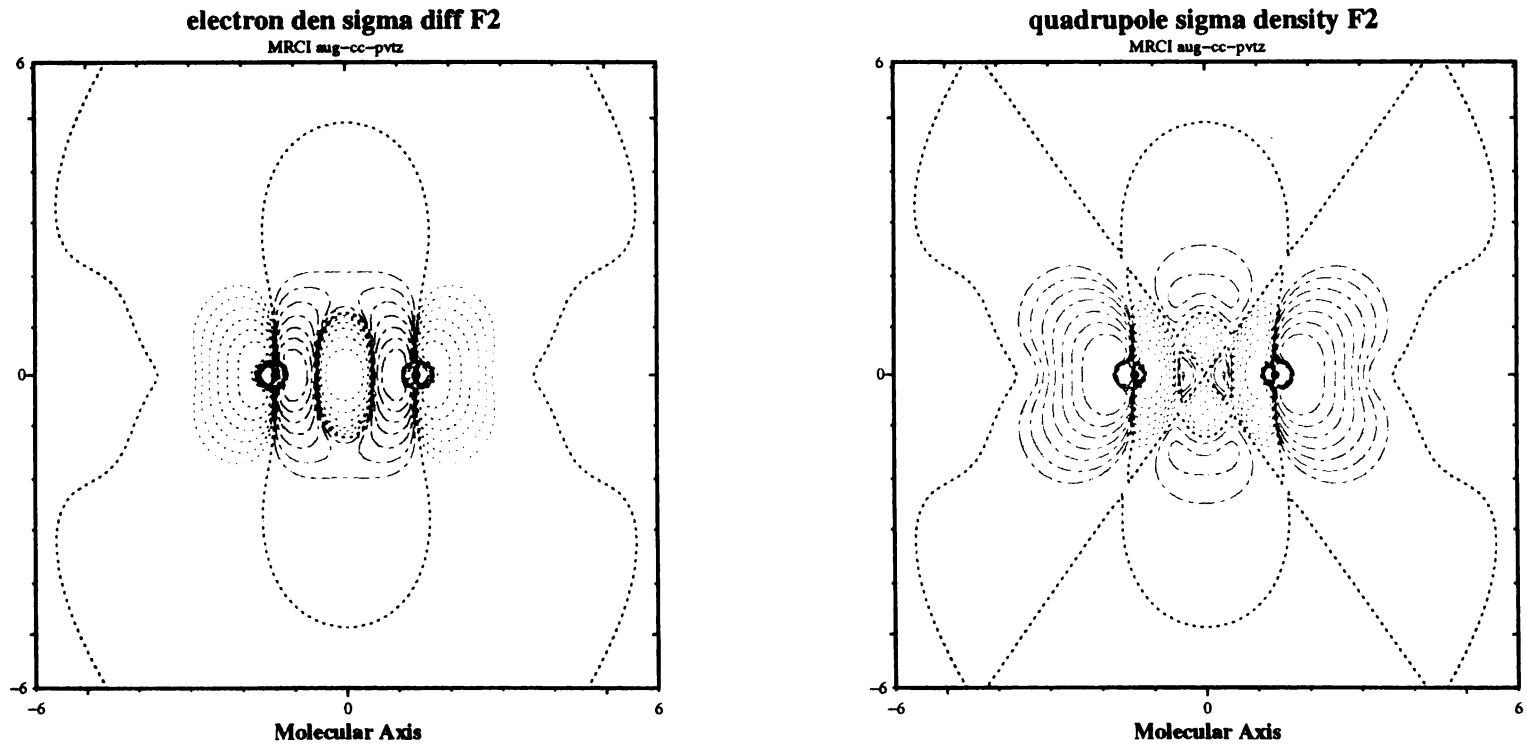

Figure 23. δn_σ and $\delta\Theta_\sigma$ for F_2 at 2.7 a_0 calculated with MRCI using the aug-cc-pvtz basis. Contours values and colors are same as in Figure 16.

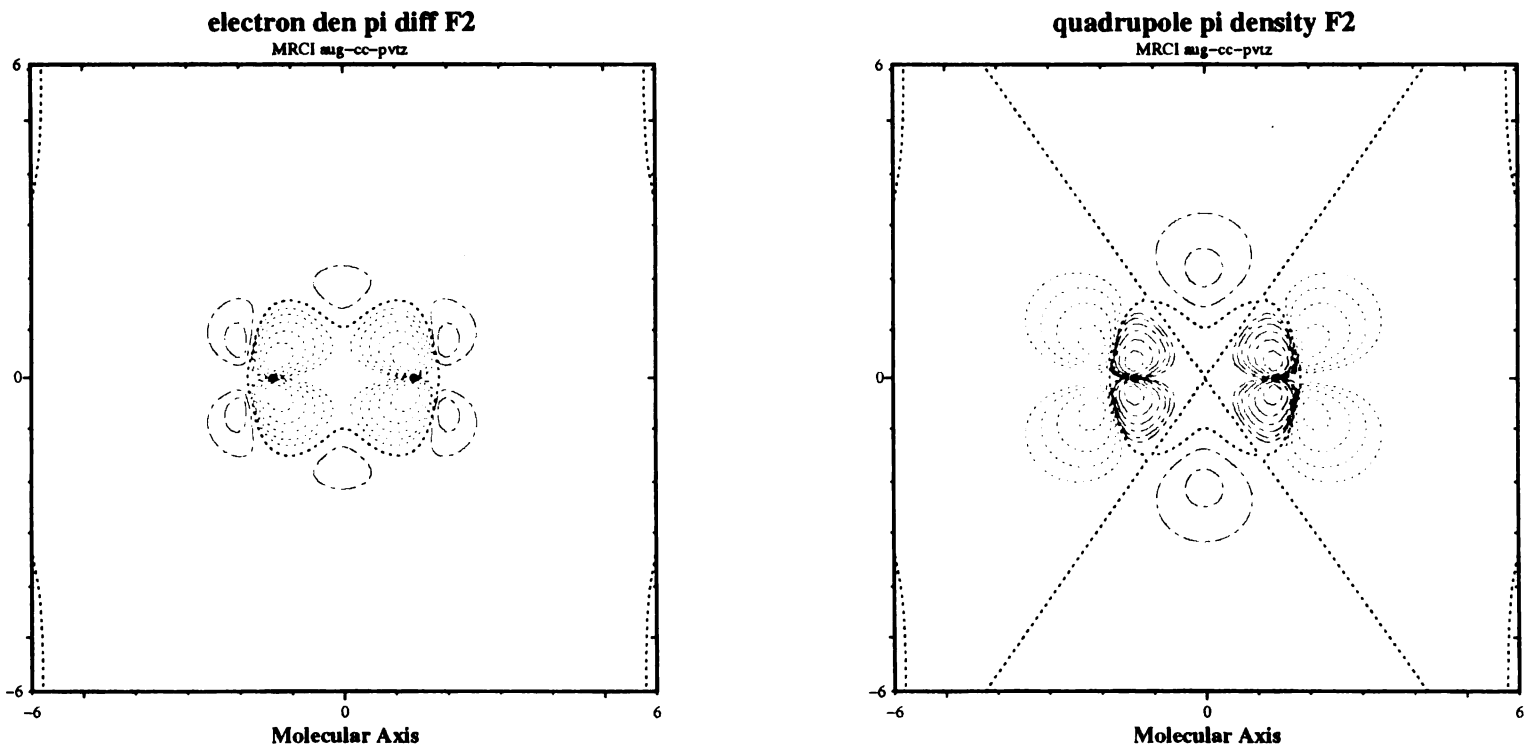

Figure 24. δn_π and $\delta\Theta_\pi$ for F_2 at 2.7 a_0 calculated with MRCI using the aug-cc-pvtz basis. Contours values and colors are same as in Figure 16.

13), which we understand as follows. As the nuclei come together, π electron density accumulates between them (in the P region of Figure 15) and, as R becomes comparable to R_{opt}, some of this density begins to spill over into the N region and thus Θ^{π}_{mol} begins to decrease. The same situation obtains in O_2 and F_2. In O_2, one has less accumulation, a smaller increase in Θ^{π}_{mol}, but the same spilling of δn_{π} into the N region. δn_{π} for F_2 is rather flat, although one still has a slight maximum in Θ^{π}_{mol}. The equilibrium bond length in these molecules is smaller than the internuclear distance where Θ^{π}_{mol} is a maximum, so, the slopes of both the π and σ component of Θ are both positive around R_{opt}.

F. H_2

A similar analysis for H_2 shows that, as the two H atoms approach to form a bond, the density difference δn_{σ} is positive between the nuclei with a large negative region to the rear of each nucleus. Because of the $3\cos^2\theta - 1$ factor in the quadrupole density integrand, the positive region between the nuclei integrate to a small contribution to Θ^{σ}_{mol}, while the decreased density in the N region of Figure 13 contributes to a large positive Θ^{σ}_{mol}. This characteristic of δn_{σ} is common to s-s bonds such as H_2, Li_2, Na_2, etc. and opposite to the sp-sp bonds characteristic of N_2, O_2, and F_2. The maximum in Θ^{σ}_{mol} obtains when large positive components of δn_{σ} in the N region spill over into the P region and this happens a little before the equilibrium separation. Clearly, Θ will go to

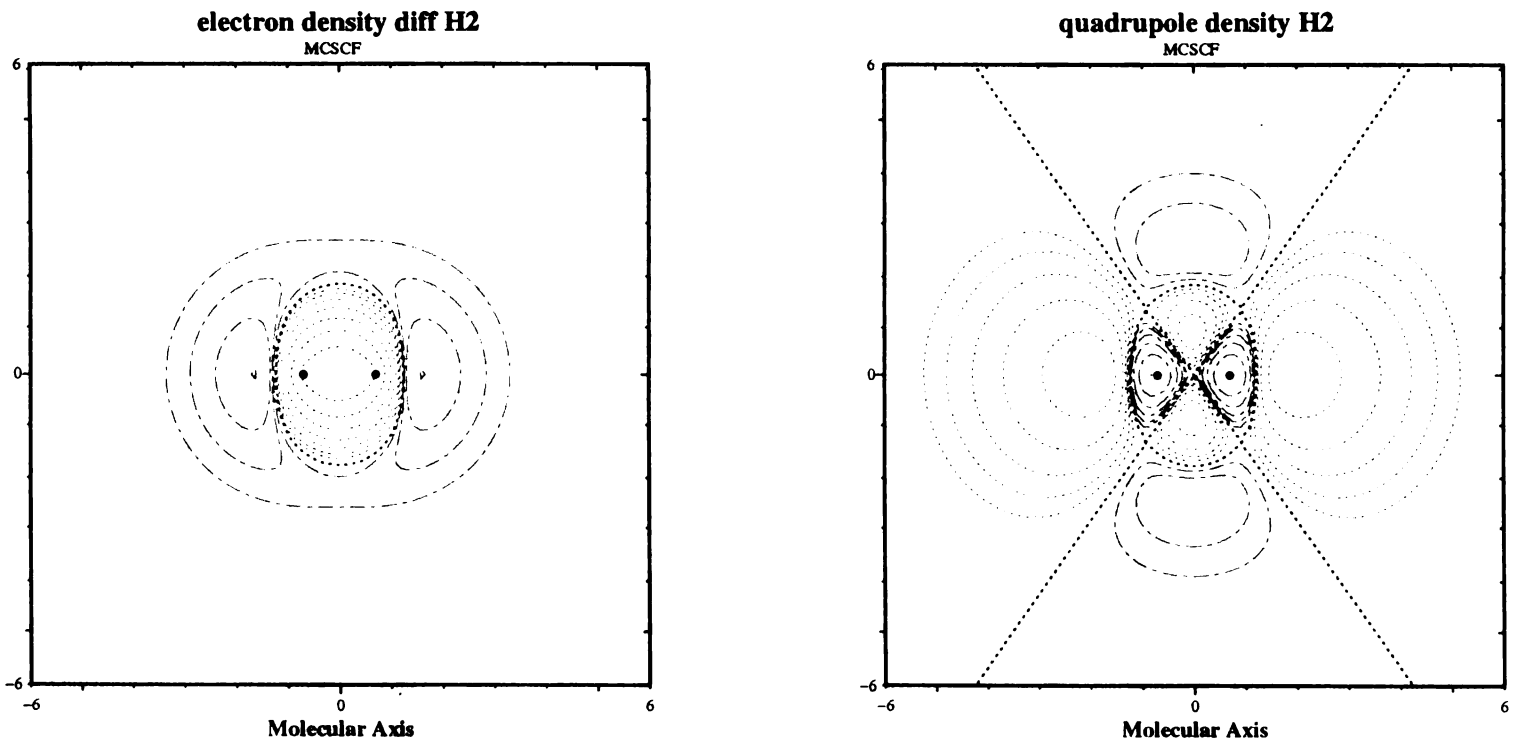

Figure 25. Electron-density difference, δn, and the associated quadrupoledensity, $\delta\Theta$, contours for H_2 at 1.4 a_0 calculated with a 10 CSF MCSCF wavefunction and the aug-cc-pv5z basis. Contour values and conventions are as in Figure 16.

zero as R $\rightarrow$ 0 and $n(\vec{r};R)$ approaches the united atom limit. These observations are illustrated in Figure 25.

G. On the Sign of the Quadrupole Moment

From the preceding discussion, we see that the sign of Θ for N_2, O_2, and F_2 depends on the relative values of Θ_σ (negative) and Θ_π (positive). In F_2, for example, one has a large positive π contribution at ∞, due to the separated atoms, which changes little as the molecule forms because δn_π is small and essentially independent of R. The asymptotically negative σ contribution is reduced further by σ bond formation but not enough to change the sign of Θ, which remains positive. The F_2 σ contribution is anemically negative because of the very slight sp hybridization in F_2. In O_2, the asymptotic value of Θ is less positive than in F_2, and the increased sp hybridization is able to overcome a very positive π contribution and results in a negative quadrupole moment. In N_2, the large sp hybridization causes the Θ_σ to be dominant and Θ is decidedly negative. The situation in H_2 is fundamentally different. The sign is always positive because at large R the s-s bond results in δn_σ being negative in the N region, and this situation obtains until the maximum in Θ (H_2;R), after which Θ decreases toward zero, as described above.

H. Correlation Effects on Θ^{σ}_{mol} and Θ^{π}_{mol}

Further insight into the relationship between electron correlation and the quadrupole moment obtains from an analysis of Θ_σ and Θ_π. In Figure 27, we plot these

quantities for the SCF, MCSCF, and MRCI wavefunction of N_2 (aug-cc-pvqz basis). The distance dependence of Θ_σ (around R_{opt}) for all three wavefunctions is similar, with the SCF and MCSCF contributions being remarkably so. The MRCI value of Θ_σ is the largest of the three and reflects the effect of dynamic correlation in increasing δn_σ in the region between the nuclei. The correlated distance dependence of Θ_π differs markedly from the SCF value and is significantly smaller. These results suggest that the reasonable values of Θ calculated from SCF functions (Table 2-3) obtain because of a cancellation of errors, Θ_σ (SCF) being too negative and Θ_π (SCF) too positive. Our calculated Θ (SCF) is $-0.9306\ ea_0^2$, while Θ (CASSCF+1+2) is $-1.1334\ ea_0^2$, both at R = 2.07432 a_0. These differ by 18 percent, and most of the error is in the π contribution.

The corresponding data for O_2 and F_2 are given in Figures 28 and 29. Note that the scales in these plots are identical and the magnitude of the effect of electron correlation on Θ_σ and Θ_π is similar. In O_2, like N_2, Θ_σ (SCF) is too negative, while Θ_π (SCF) is too positive, resulting in a similar cancellation of errors. At 2.28 a_0, we calculate Θ (O_2; ROHF) = $-0.2634\ ea_0^2$ and Θ (O_2; CASSCF+1+2) = $-0.2530\ ea_0^2$, a difference of only 4 percent, as noted earlier. In F_2, both Θ_σ (SCF) and Θ_π (SCF) are too small, but rather than cancel they add and result in a Θ (SCF) ($0.501\ ea_0^2$ at R = 2.68

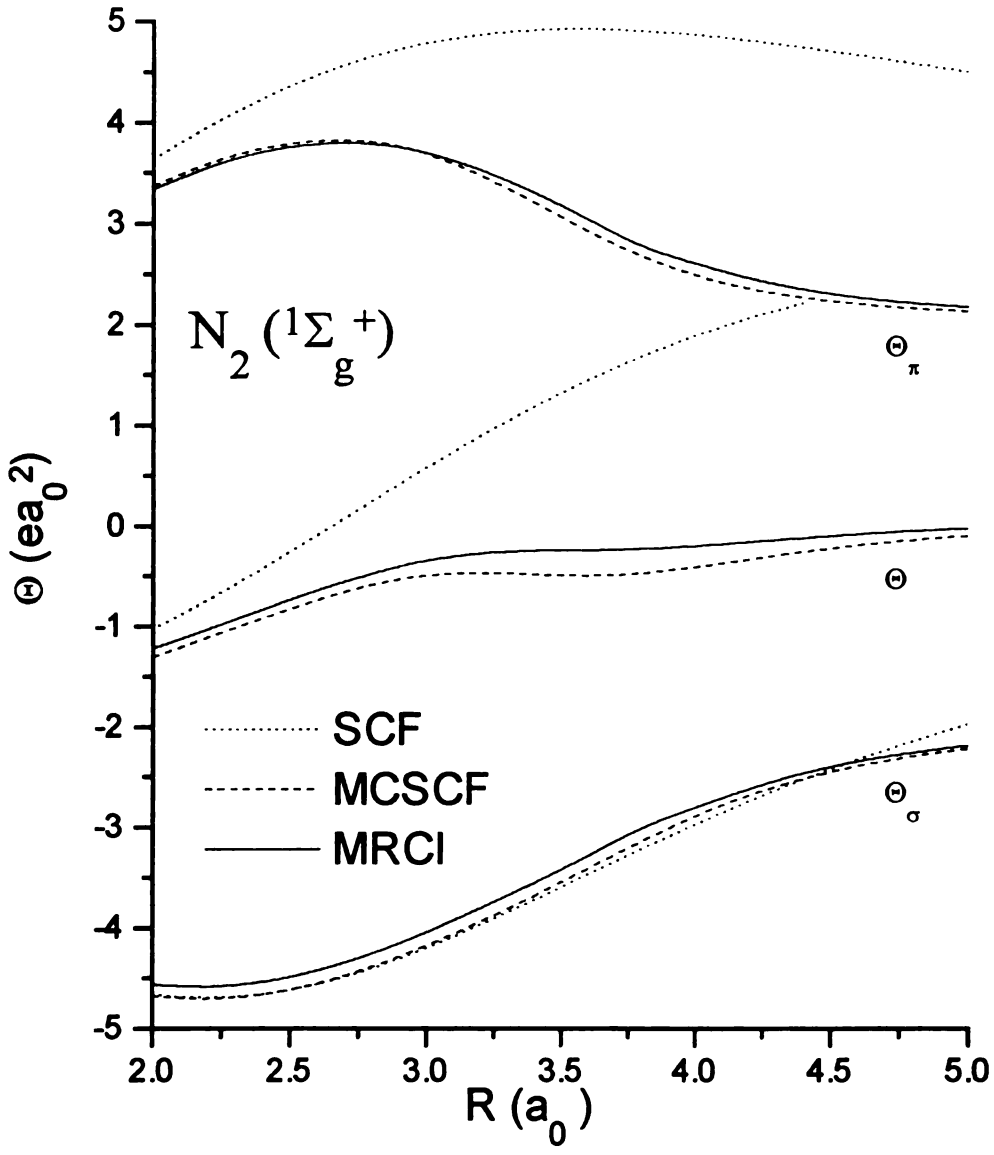

Figure 26. Effect of electron correlation on the magnitude and distance dependence of Θ, Θ_σ, and Θ_π for N_2.

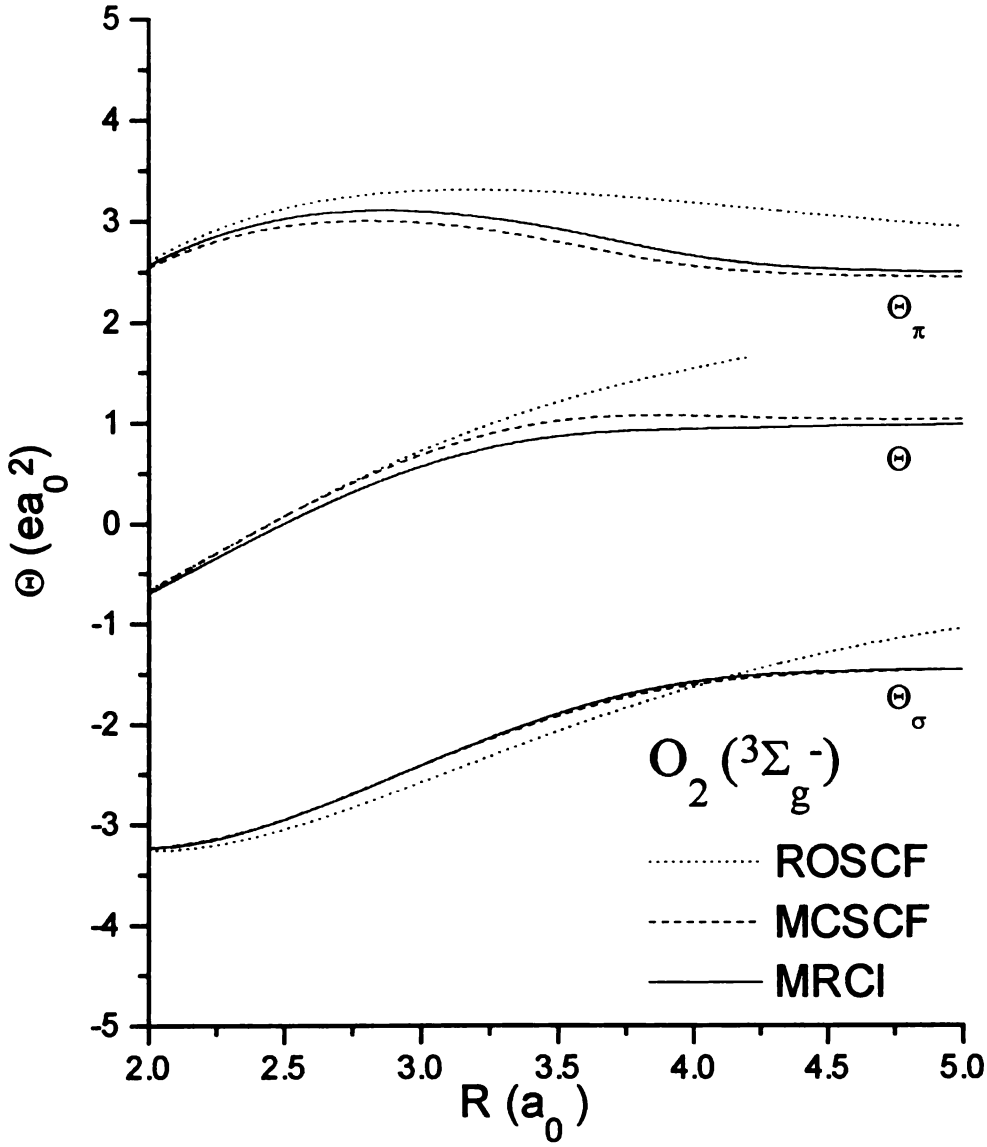

Figure 27. Effect of electron correlation on the magnitude and distance dependence of Θ, Θ_σ, and Θ_π for O_2.

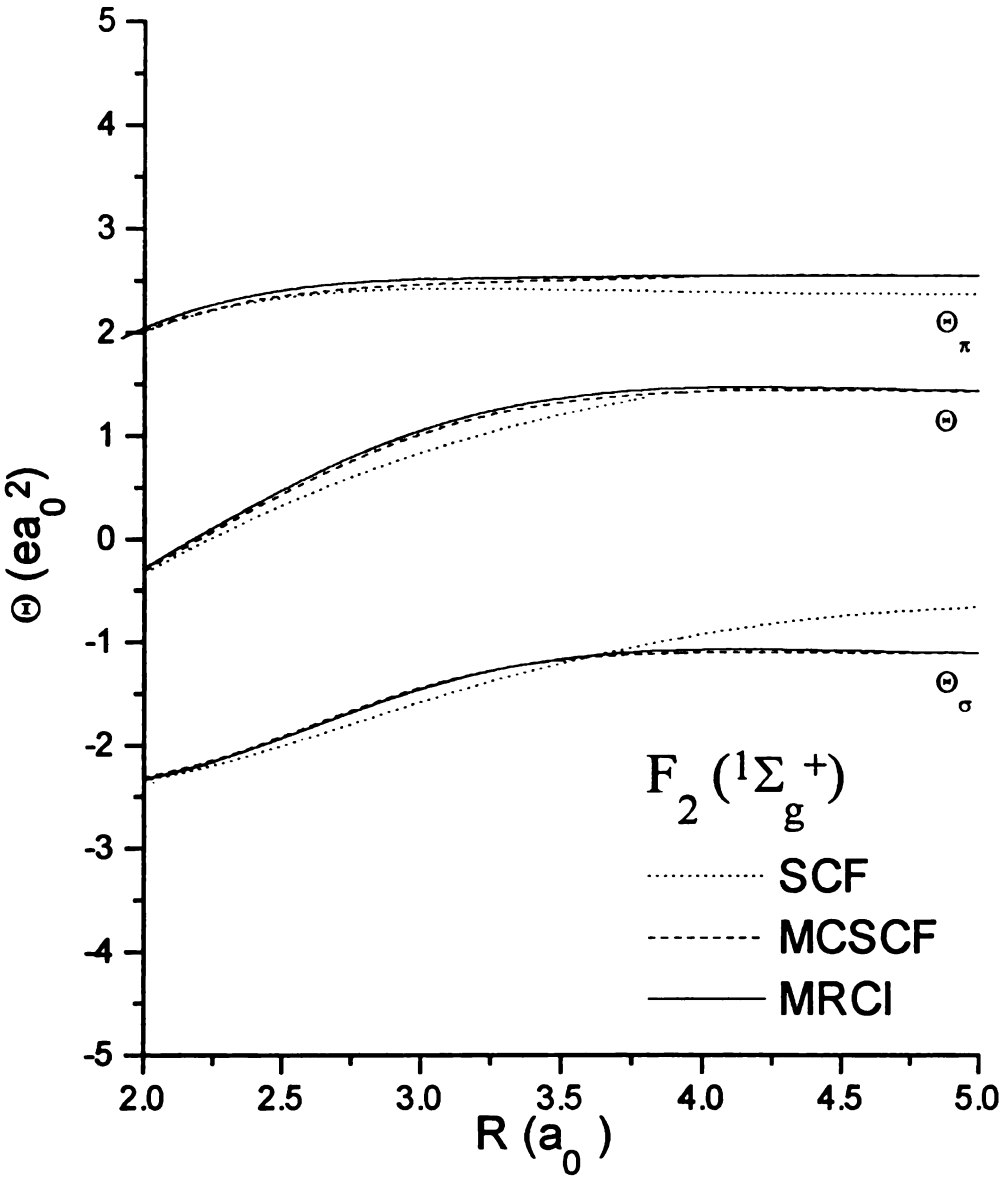

Figure 28. Effect of electron correlation on the magnitude and distance dependence of Θ, Θ_σ, and Θ_π for F_2.

a_0) compared to the Θ (CASSCF+1+2) value of 0.707 ea_0^2 (a difference of 29 percent) at the same bond length.

I. Conclusions

We have studied the quadrupole moments of H_2, N_2, O_2, and F_2 and have estimated the CASSCF+1+2 basis-set limit for the latter three and the CISD limit for H_2. These are in excellent agreement with comparable calculations by others and in good agreement with the existing experimental data. The rather large values of the quadrupole moment derivatives, shown in Table 2-1, result in the quadrupole moment being a very sensitive function of R around R_{opt}. We have written the global quadrupole-moment function as the sum of an atomic contribution and a molecular contribution Θ_{mol}. The atomic contribution is simply the sum of the quadrupole moments of the constituent (oriented) free atoms, while the molecular contribution is an integral over a quadrupole-density function of the form

$$\delta\Theta = -\frac{1}{2}\left(3\cos^2\theta - 1\right)r^2\delta n$$

in which the nuclear contributions are implicit in δn. While not unique, this partitioning of Θ allows us to separate molecular effects from additive atomic effects and provides a deeper understanding of the variation of Θ with R. In particular, the nodal structure of $3\cos^2\theta - 1$ allows us to partition the space in a diatomic molecule into N regions, to the rear of the nuclei and complimentary P regions. Because δΘ is linear in δn, one may define quadrupole densities associated with δn_σ and δn_π and examine the contribution of the σ and π deformation densities to the molecular quadrupole moment. Increases in δn_σ

in the N region contribute to make Θ_{mol}^{σ} negative, while increases in δn_{π} in the P region make Θ_{mol}^{π} positive, and, thus, the molecular contribution to the quadrupole moment is the sum of two opposite-signed terms. The total molecular quadrupole moment is the sum of this molecular contribution and the moment due to the sum of the separated atoms. This perspective is useful in understanding the difference in the quadrupole moments of related systems, such as N_2 and P_2, O_2 and S_2, C_6H_6 and C_6F_6, etc.[44] Additionally, the effect of electron correlation on Θ may be partitioned into σ and π contributions via δn_{σ} and δn_{π}.

We note that the parabolas that delineate the Berlin bonding and antibonding regions are asymptotically tangent to the nodal surfaces separating the N and P regions (Figure 15). Indeed, the largest contribution to Θ_{mol}^{σ} and Θ_{mol}^{π} come from a density difference that is largely localized in the Berlin[45] antibonding and bonding regions, respectively.

Additional contour plots and three-dimensional images of δn and $\delta\Theta$, as well as detailed numerical values of Θ as a function of R, are available via our web page, www.cem.msu.edu/~harrison.

J. References

1. Huber, K. P. and Herzberg, G., "Molecular spectra and molecular structure," Vol. 4, *Constants of Diatomic Molecules* (Van Nostrand-Reinhold, New York, **1979**).

2. McLean, A. D. and Yoshimini, M., *J. Chem. Phys.* **1966**, *45*, 3676.

3. Stogryn, D. E. and Stogryn, A. P., *Mol. Phys.* **1966**, *11*, 371.

4. Ramsy, N. F., *Molecular Beams* (Oxford University Press, London, **1956**).

5. Buckingham, A. D. and Cordle, J. E., *Mol. Phys.* **1974**, *4*, 1037.

6. Amos, R. D., *Mol. Phys.* **1980**, *39*, 1.

7. Laaksonen, L., Pyykkö, P., and Sundholm, D., *Comput. Phys. Rep.* **1986**, *4*, 313.

8. Wolniewicz, L., *J. Chem. Phys.* **1966**, *45*, 515.

9. Kolos, W. and Wolniewicz, L., *J. Chem. Phys.* **1965**, *43*, 2429.

10. Wolinski, K., Sadlej, A. J., Karlström, G., *Mol. Phys.* **1991**, *72*, 425.

11. Kolos, W. and Roothaan, C. C. J., *Rev. Mod. Phys.* **1960**, *32*, 219.

12. Dickson, R. M. and Becke, A. D., *J. Phys. Chem.* **1996**, *100*, 16105.

13. Diercksen, G., Sadlej, A. J., *Theoret. Chim. Acta* **1983**, *63*, xxxx.

14. Kolos, W. and Wolniewicz, L., *J. Chem. Phys.* **1964**, *41*, 3674.

15. Sundholm, D., Pyykkö, P., and Laaksonen, L., *Mol. Phys.* **1985**, *56*, 1411.

16. Maroulis, G. and Thakkar, A. J., *J. Phys. B* **1987**, *20*, L551.

17. McCullough, E. A., Jr., *Mol. Phys.* **1981**, *42*, 943.

18. Maroulis, G. and Thakkar, A. J., *J. Chem. Phys.* **1988**, *88*, 7623.

19. Feller, D., Boyle, C. M., and Davidson, E. R., *J. Chem. Phys.* **1987**, *86*, 3424.

20. Bündgen, P., Green, F., and Thakker, A. J., *J. Molecular Structure* **1995**, *334*, 7.

21. Laaksonen, L., Sundholm, D., and Pyykkö, P., *Int. J. of Quant. Chem.* **1985**, *xxvii*, 601.

22. Duffy, P. and Chong, D. P., *J. Chem. Phys.* **1995**, *102*, 3312.

23. Becke, A. D., *J. Chem. Phys.* **1982**, *76*, 6037.

24. Piecuch, P., Kondo, A. E., Spirko, V., and Paldus, J., *J. Chem. Phys.* **1996**, *104*, 4699.

25. Spirko, V., Piecuch, P., Kondo, A., and Paldus, J., *J. Chem. Phys.* **1996**, *104*, 4716.

26. Buckingham, A. D., Graham, C., and Williams, J. H., *Mol. Phys.* **1983**, *49*, 703.

27. Graham, C., Pierrus, J., and Raab, R. E., *Mol. Phys.* **1989**, *67*, 939.

28. Truhlar, D. G., *Int. J. Quantum Chem.* **1972**, *VI*, 975.

29. Maroulis, G. and Bishop, D. M., *Mol. Phys.* **1986**, *58*, 273.

30. Cartwright, D. C. and Dunning, T. H., *J. Phys. B* **1974**, *7*, 1776.

31. Buckingham, A. D., Disch, R. L., and Dummur, D. A., *J. Am. Chem. Soc.* **1968**, *90*, 3104.

32. Cohen, R. E. and Birnbaum, G., *J. Chem. Phys.* **1977**, *66*, 2443.

33. Camy Plyret, C., Flaud, J. M., Delbouille, L., Roland, G., Brault, J. W., and Testerman, L., *J. Physique Lettres* **1981**, *42*, L279.

34. Reddy, S. P. and Cho, C. W., *Canadian J. Phys.* **1965**, *43*, 2331.

35. Shapiro, M. M. and Gush, H. P., *Canadian J. Phys.* **1966**, *44*, 949.

36. Reuter, D. and Jennings, D. E., *J. Mol. Spec.* **1986**, *115*, 294.

37. Birnbaum, G. J. and Cohen, E. R., *Mol. Phys.* **1976**, *32*, 161.

38. Rijks, W., van Heeringen, M., and Wormer, P. E. S., *J. Chem. Phys.* **1989**, *90*, 6501.

39. Wahl. A. C., *J. Chem. Phys.* **1964**, *41*, 2600.

40. Hellmann,H., *Einfuhrung in die Quantenchemie* (Deuticke, Leipzig, **1937**)

41. Feynman,R.P., Phys.Rev. **1939**, 41,721

42. Raghavachari,K., and Pople, J.A., Int. J. Quant. Chem., **1981**, 20, 1067

43. Amos, R.D., Adv. Chem. Phys., **1987**

44. Lawson, D. and Harrison, J. F., to be published.

45. Berlin, T., *J. Chem. Phys.* **1951**, *19*, 208.

CHAPTER 3

The Quadrupole Moments of P_2, S_2, and Cl_2

A. Introduction

In Chapter 2, the quadrupole moments of H_2, N_2, O_2, and F_2 were discussed in detail. This chapter provides an extension of that discussion to the second row homonuclear diatomics. With the exception of Cl_2, very little theoretical or experimental data could be found for molecules containing heavy atoms. In this Chapter we present calculated quadrupole moment data for the second row homonuclear diatomics and compare them with the first row. Using methods developed in Chapter 2, we also will look at the sign and magnitude of the quadrupole moment as a function of the electronic structure.

B. Computational Technique

The MCSCF and MRCI calculations were done using the COLUMBUS[1] system of codes, while the full CASSCF and CASSCF+1+2 were done using MOLPRO[2]. The UHF, ROHF, and Möller-Plesset calculations were done using g94[3]. Tables 11-13 of Appendix C contain the quadrupole moments of the titled molecules for various wavefunctions and basis sets. The MP2 wavefunctions include excitations from the $4\sigma_g$, $4\sigma_u$, $5\sigma_g$, $5\sigma_u$, $2\pi_{ux}$, $2\pi_{uy}$, $2\pi_{gx}$, and $2\pi_{gy}$ orbitals of P_2, S_2, and Cl_2. The MCSCF wavefunctions are CASSCF functions over the MO's derived from the valence p orbitals (the $5\sigma_g$, $2\pi_{ux}$, $2\pi_{uy}$, $2\pi_{gx}$, $2\pi_{gy}$). The MRCI incorporates all single and double excitations from these six orbitals, as well as all double excitations from the $4\sigma_g$ and $4\sigma_u$ orbitals. The CASSCF wavefunctions include all valence electrons and the 8 orbitals described above, and the CASSCF+1+2 wavefunction consists of all single and double excitations from the

CASSCF reference space. Quadrupole moments were computed in atomic units using the Buckingham convention described in Appendix A. The Dunning basis sets used in this study are described in Appendix B.

C. Discussion

The results of P_2 are summarized in Table C-11 and Figure 1. Unlike H_2, N_2, O_2, and F_2 in Chapter 2, the quadrupole moment does not decrease systematically with increasing basis set. This is an indication that the basis, although fully optimized for the energy, may not be fully optimized for this particular property. Our best SCF value, given as the value associated with the aug-cc-pv5z basis, is 0.7920 ea_0^2 at 3.4950 a_0. This does not compare well with Glaser, Horan, and Haney[4] SCF value of 0.5212 ea_0^2 at 3.5773 a_0, however, this value was calculated with a relatively small basis set. At the experimental separation of 3.5780 a_0 our SCF quadrupole was 1.0629 ea_0^2. This value should be very close to the numerical HF result. Following the SCF calculation, the post-SCF techniques also do not yield CBS-limit quadrupole moments. Our aug-cc-pv5z CASSCF and CASSCF+1+2 values are 0.3162 ea_0^2 at 3.6288 a_0 and 0.5241 ea_0^2 at 3.6055 a_0, respectively. Using the aug-cc-pv5z basis at the experimental geometry, the CASSCF gives 0.2039 ea_0^2 and the CASSCF+1+2 gives 0.4608 ea_0^2.

At the SCF level, the aug-cc-pvdz quadrupole moment is 8.7 % smaller than the aug-cc-pv5z while the aug-cc-pvtz quadrupole moment is 0.6% smaller. For the RHF, MP2, and CASSCF+1+2, the aug-cc-pv5z CASSCF+1+2 value is less than 5.0% higher

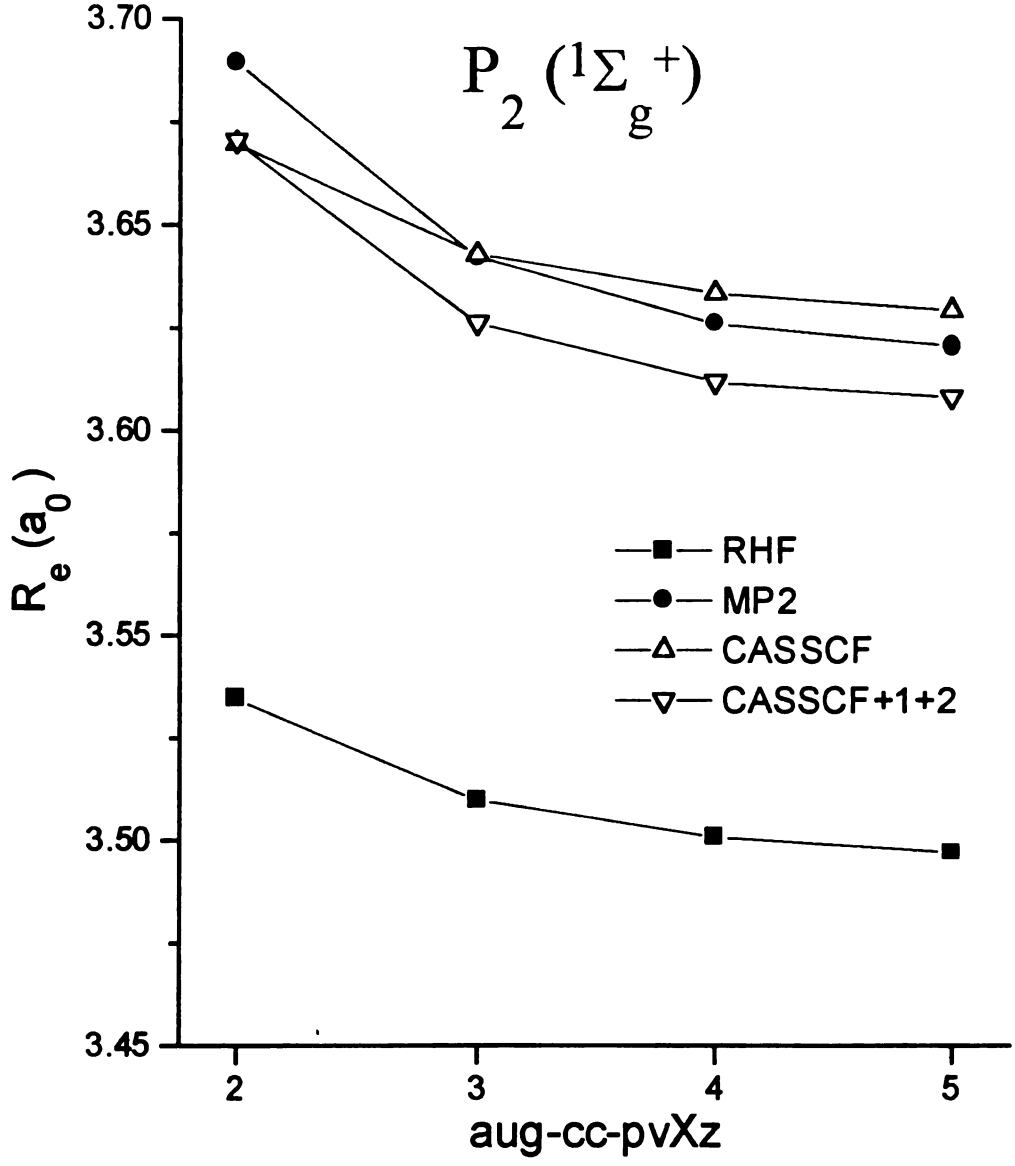

Figure 1. Model dependence of Θ for P_2 as a function of basis set.

than the aug-cc-pvqz quadrupole moment and 3.8% lower than the aug-cc-pvtz quadrupole moment. Adding correlation to the RHF wave function by MP2 and CASSCF+1+2 lowers the value of the quadrupole moment by similar amounts. As in the last chapter MP2 predicts the quadrupole moment comparatively well at little overall computational cost. The CASSCF wavefunction has the greatest differences in the quadrupole moments for each basis set. The CASSCF, also, overestimates the correction to the quadrupole moment, lowering it more than either the MP2 or the CASSCF+1+2.

The distance dependence of Θ around R_{opt} is shown in Figure 2 and 3 for the SCF, CASSCF, and CASSCF+1+2 models, using the aug-cc-pvqz basis. The slopes of the CASSCF and CASSCF+1+2 are parallel to each other, and this is to be found true for S_2 and Cl_2 as can be seen in Table 3-1.

Table 3-1. Equilibrium value of the first and second derivatives of the molecular quadrupole moment function for P_2, S_2, and Cl_2, calculated with various wavefunctions.

Molecule	Wavefunction	$R_{opt}(a_0)$	$\left(\frac{d\Theta}{dR}\right)_{R_{opt}}(ea_0)$	$\left(\frac{d^2\Theta}{dR^2}\right)_{R_{opt}}(e)$
P_2	SCF	3.5007	3.3894	-0.8168
P_2	CASSCF	3.6330	2.1529	-1.6946
P_2	CASSCF+1+2	3.6114	2.0972	-1.6068
S_2	ROSCF	3.5216	1.3023	-1.0148
S_2	CASSCF	3.6457	1.2266	-1.4504
S_2	CASSCF+1+2	3.6101	1.2559	-1.4362
Cl_2	SCF	3.7309	2.2393	-1.0038
Cl_2	CASSCF	3.8574	2.4962	-1.1354
Cl_2	CASSCF+1+2	3.8050	2.3801	-1.1788

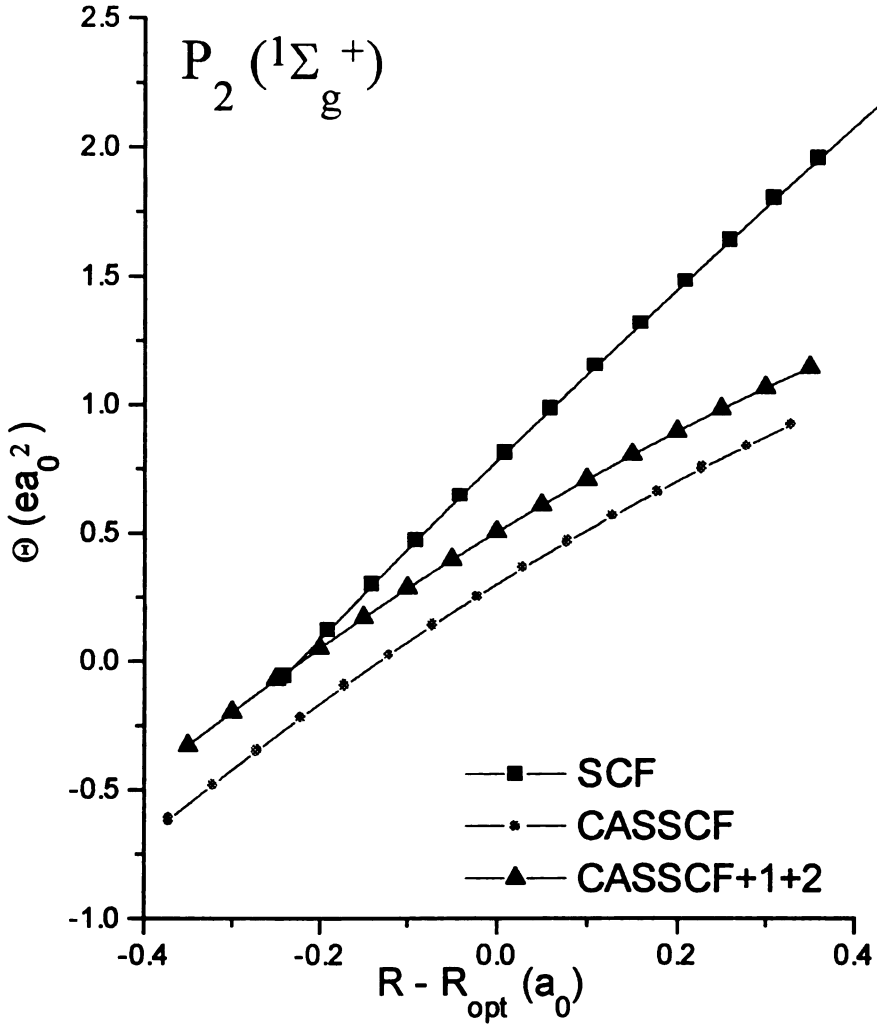

Figure 2. Distance dependence of Θ for P_2 calculated with various models using the aug-cc-pvqz basis.

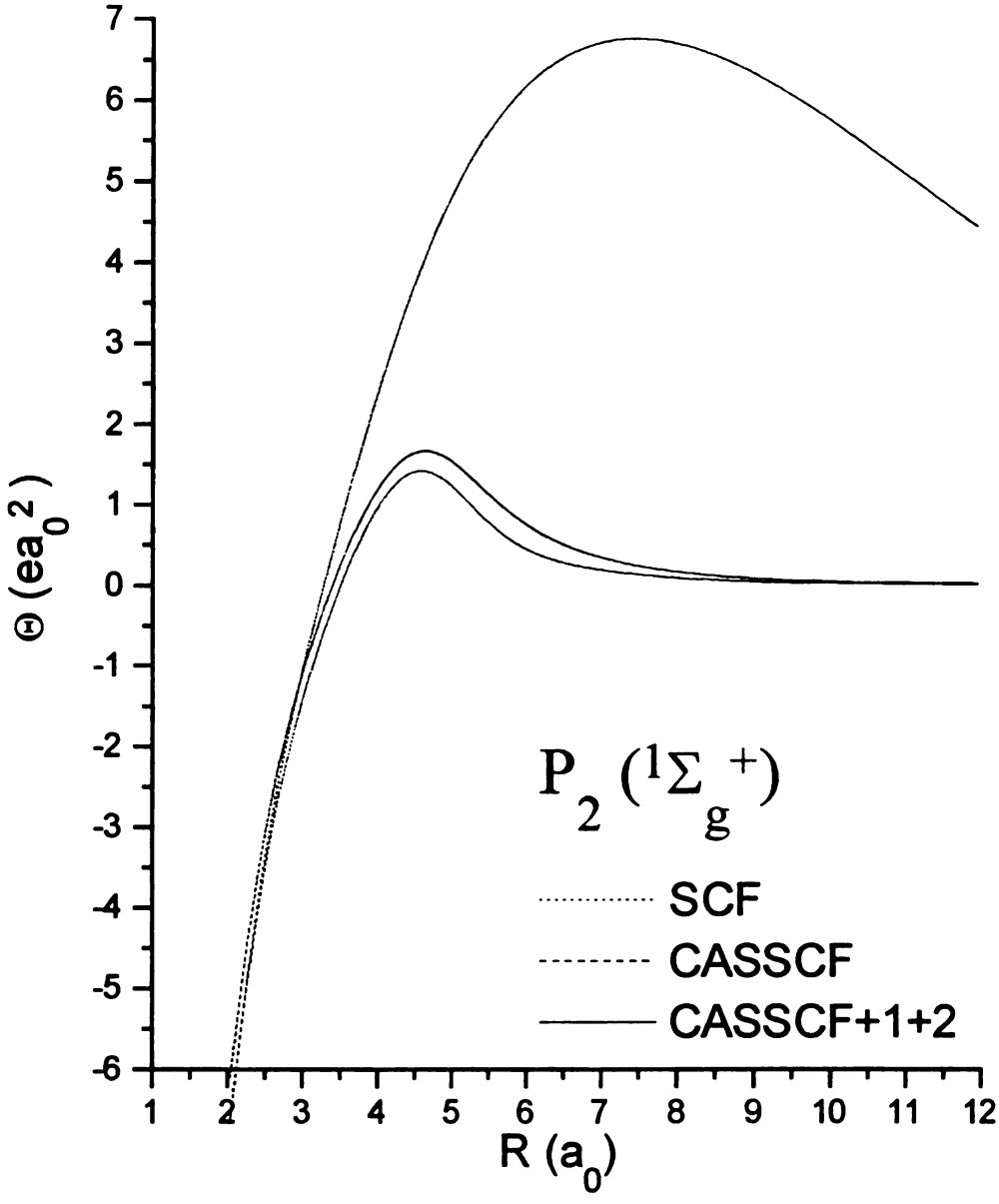

Figure 3. The quadrupole moment of P_2 as a function of internuclear separation with various models using the aug-cc-pvqz basis.

The SCF curve has significantly larger first derivative, while the SCF second derivative is of a smaller magnitude. In comparing P_2 with N_2, the N_2 second derivatives for all methods were positive, while the P_2 second derivatives are negative. This can be better understood by looking at the quadrupole moment as a function of R, $\Theta(R)$. The N_2 $\Theta(R)$ curve is zero at $R=\infty$ and everywhere else negative, while the P_2 $\Theta(R)$ curve is zero at $R=\infty$, positive at large R, and becomes negative as R becomes smaller than R_{opt}. The reasons for the difference between N_2 and P_2 will be described later. Using the CASSCF+1+2 derivatives in Table 3-1, we estimate the vibrational dependence of the aug-cc-pv5z CASSCF+1+2 quadrupole moment as

$$\Theta(P_2;v) = 0.5241 + 0.0197\left(v + \tfrac{1}{2}\right)$$

and so our recommended vibrationally corrected quadrupole moment is $\Theta(P_2;v = 0)$= $+0.5340\ ea_0^2$. There is no experimental value with which to compare our results.

The CBS-ROHF quadrupole moment of S_2 is 1.3966 ea_0^2 at 3.5143 a_0 and our CBS-UHF quadrupole moment is 1.3909 ea_0^2 at 3.5171 a_0. The data at R_{exp} did not extrapolate well for the quadrupole moments at the experimental separation of 3.5701 a_0. The ROHF quadrupole moment with the aug-cc-pv5z basis is 1.5404 ea_0^2 and the aug-cc-pv5z UHF quadrupole moment is 1.5315 ea_0^2. The CBS-CASSCF and CBS-CASSCF+1+2 results were 1.4612 ea_0^2 at 3.6354 a_0 and 1.4585 ea_0^2 at 3.5978 a_0, respectively. The aug-cc-pv5z CASSCF and CASSCF+1+2 where 1.3143 ea_0^2 and 1.3918 ea_0^2, respectively, at the experimental separation. The CBS-Unrestricted-MP2 gave a quadrupole moment of 1.3909 ea_0^2 at 3.5171 a_0. The results for each method and

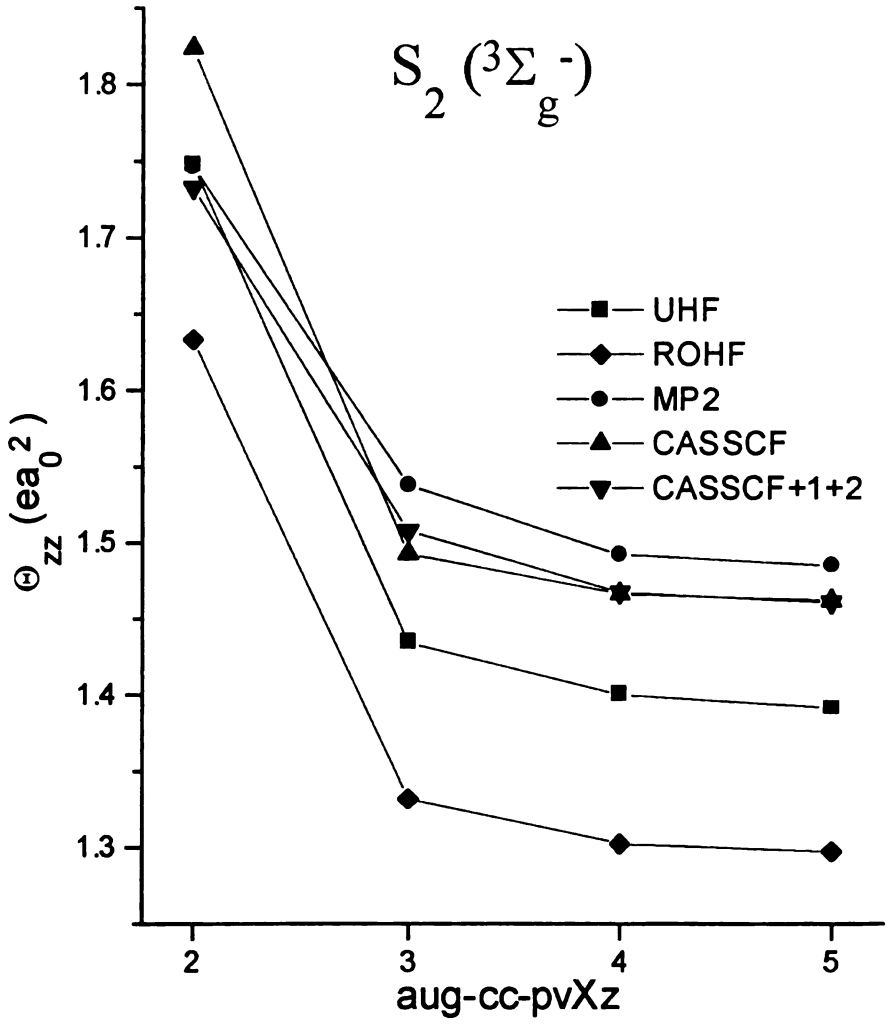

Figure 4. Model dependence of Θ for S_2 as a function of basis set.

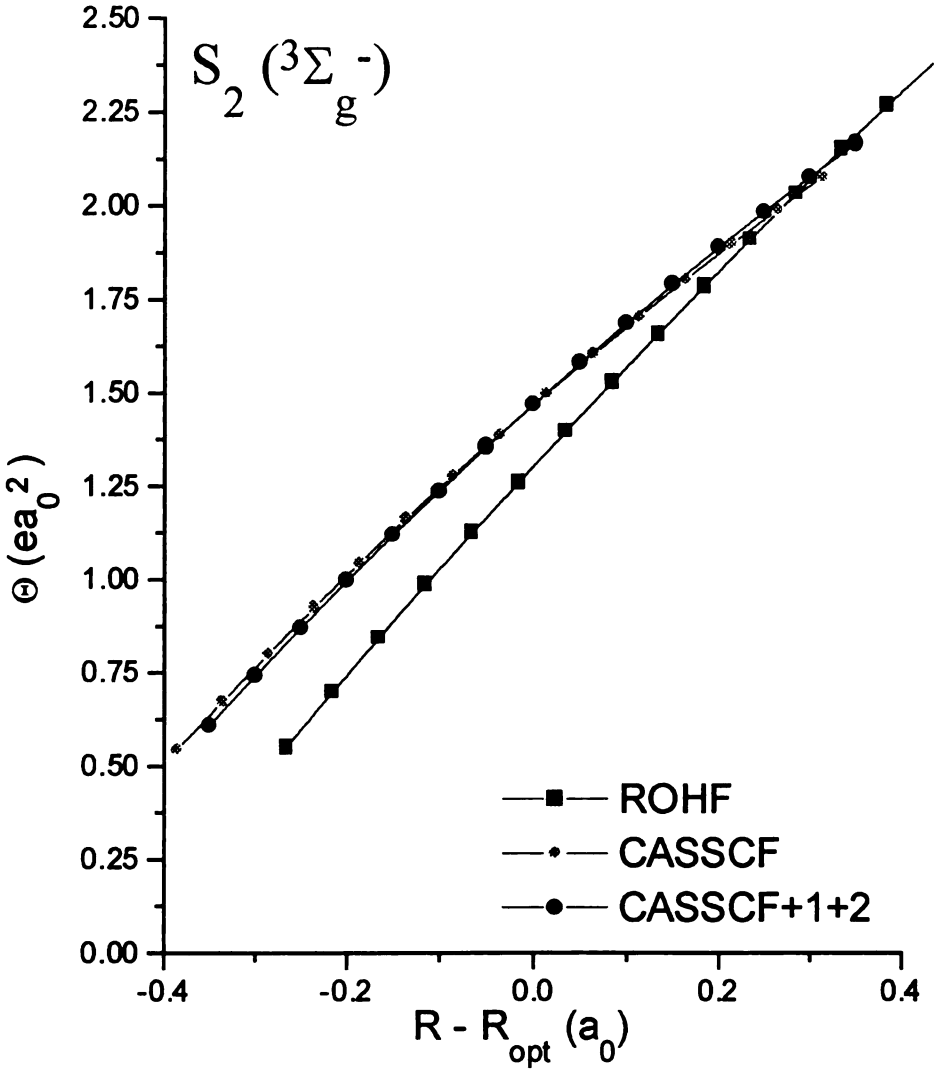

Figure 5. Distance dependence of Θ for S_2 calculated with various models.

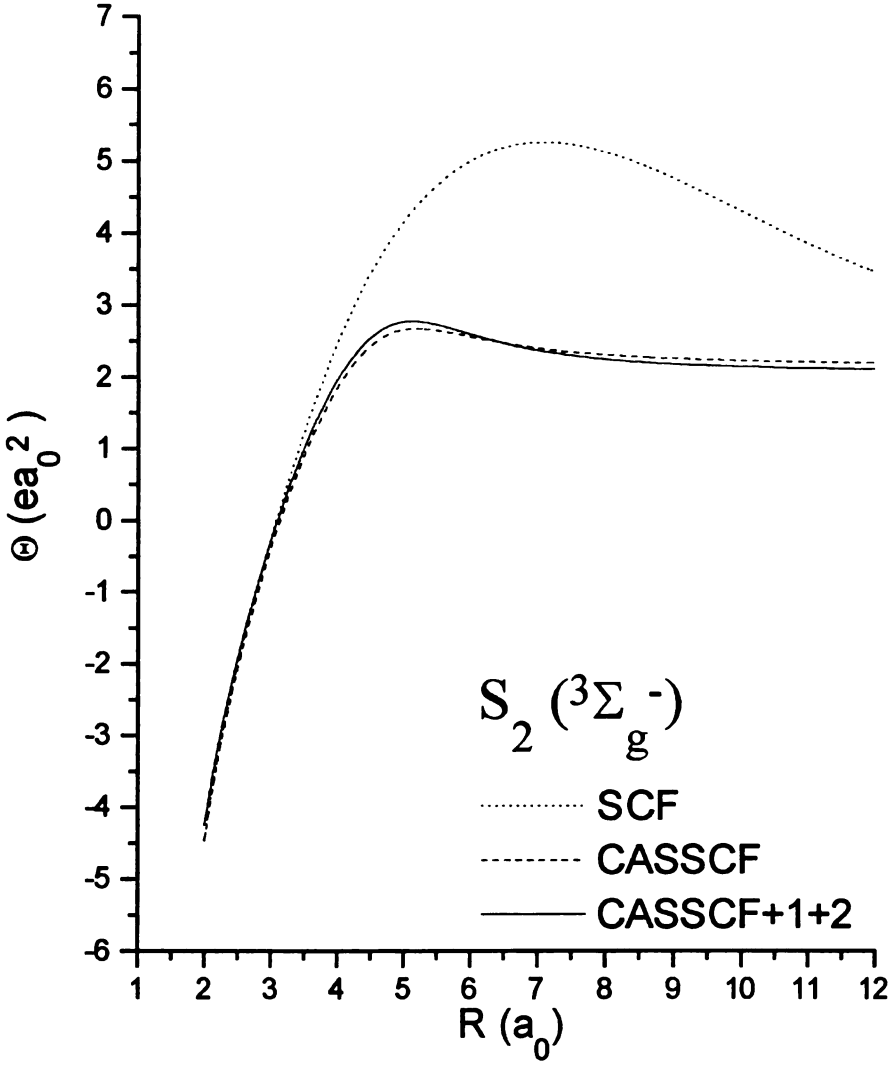

Figure 6. The quadrupole moment of S_2 as a function of internuclear separation with various models using the aug-cc-pvqz basis.

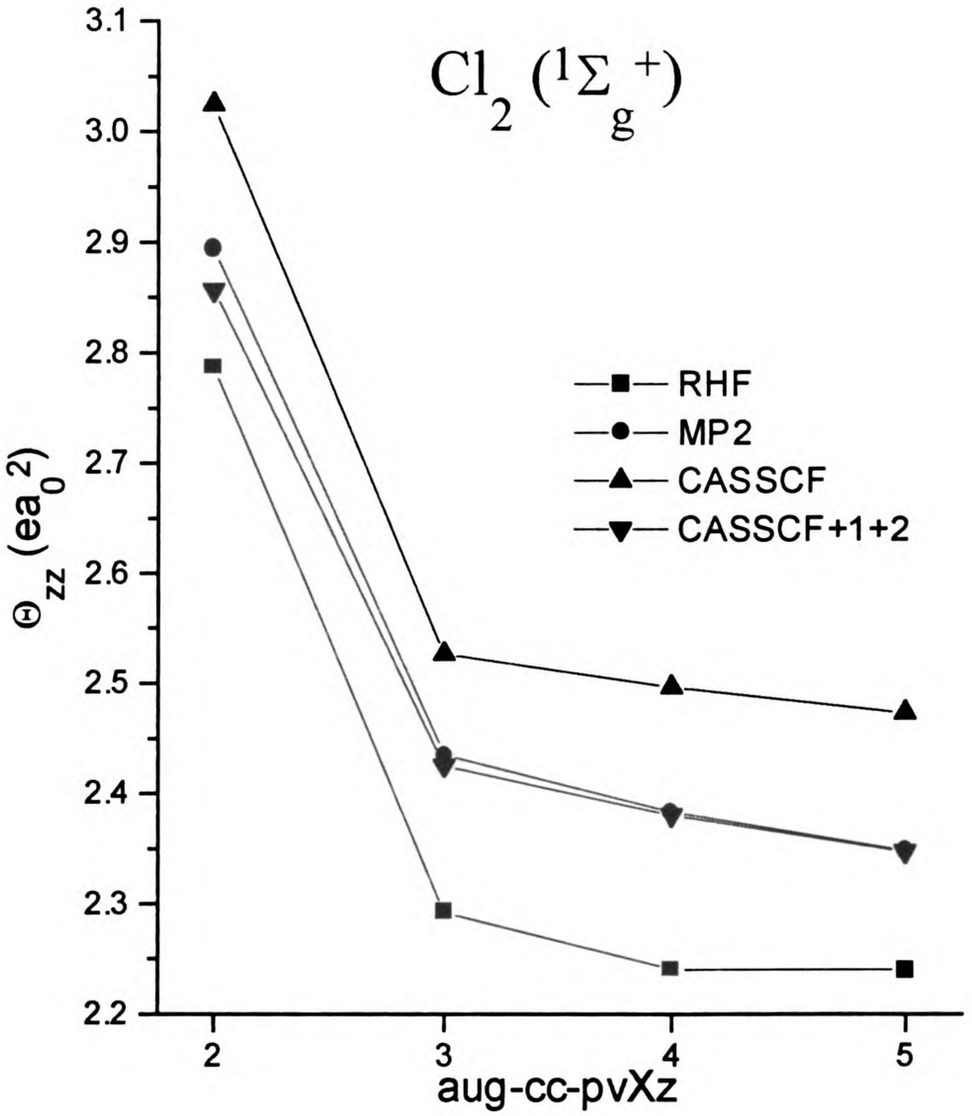

Figure 7. Model dependence of Θ for Cl_2 as a function of basis set.

basis set are collected in Table C-12 and Figure 4. No other theoretical or experimental data exists to compare with our S_2 quadrupole moment.

A plot of the $\Theta(R)$ in the region of R_{opt} is given with the aug-cc-pvqz for various wavefunctions in Figure 5. From the plot we can see the CASSCF and CASSCF+1+2 quadrupole functions are on top of one another while the ROHF quadrupole function has a steeper slope. From Table 3-1, we see that the slope $\Theta(R)$ SCF slope is larger than both the CASSCF and CASSCF+1+2, while the SCF second derivative is a smaller negative number. The CASSCF+1+2 first derivative is +1.2559 and the CASSCF+1+2 second derivative is -1.4362. Using the CASSCF+1+2 derivatives, our vibrationally corrected S_2 quadrupole moment is

$$\Theta(S_2;v) = 1.4585 + 0.0102\left(v+\tfrac{1}{2}\right)$$

and so our recommended vibrationally corrected quadrupole moment is $\Theta(S_2;v = 0)$= +1.4636 ea_0^2. The overall $\Theta(R)$ curve is given in Figure 6 and is very similar to the O_2 curve in Chapter 2. From Chapter 2, the ROHF quadrupole moment of O_2 was 18 % larger than from the UHF quadrupole moment. For S_2, however, the ROHF and UHF quadrupole moments are much closer. This is related to the strong dependence of the quadrupole moment on the internuclear separation. The S_2 ROHF internuclear separation is only 0.003 a_0 larger than the UHF bond length, while the O_2 ROHF internuclear separation is 0.015 a_0 smaller than the UHF separation.

Our Cl_2 results are collected in Table C-13 and Figure 7. As in the previous systems the quadrupole moment decreases within a model with increasing quality of basis. Correlation increases the quadrupole moment from the SCF value and the CASSCF+1+2

decreases the quadrupole moment from its CASSCF value. Our CBS-RHF limit is 2.2373 ea_0^2 at 3.7267 a_0. The aug-cc-pv5z RHF quadrupole moment at the experimental geometry of 3.7567 a_0 is 2.2884 ea_0^2. There are no numerical-HF data for Cl_2, however, our values compare well with other large basis SCF data.[5-7] With the aug-cc-pv5z at the experimental geometry, our CASSCF and CASSCF+1+2 quadrupole moments are 2.3165 ea_0^2 and 2.2896 ea_0^2, respectively.

The distance dependence of $\Theta(Cl_2)$ near the optimized geometry is shown in Figure 8 and 9. Correlation correction effects are relatively small on the first and second derivatives. The SCF, CASSCF, and CASSCF+1+2 first derivatives are positive and SCF, CASSCF, and CASSCF+1+2 second derivatives are negative. The SCF first and second derivatives are 2.2393 and -1.0038, respectively, while the CASSCF+1+2 first derivative is 2.3801 and the second derivative is -1.1788. Using the CASSCF+1+2 first and second derivatives and equation 4 from Chapter 2, we write the vibrational averaged Θ as

$$\Theta(Cl_2;v) = 2.3559 + 0.0301\left(v+\tfrac{1}{2}\right)$$

and, so or vibrationally corrected CASSCF+1+2 quadrupole moment for Cl_2 is 2.371 ea_0^2. This compares well with Buckingham, Graham, and Williams[8] experimental value of 2.405±0.120 ea_0^2. We collect the experimental and select calculated values of Θ in Table 3-2. We have collected the CASSCF+1+2 values of Θ along with estimated CBS limit vibrational corrections in Table 3-3.

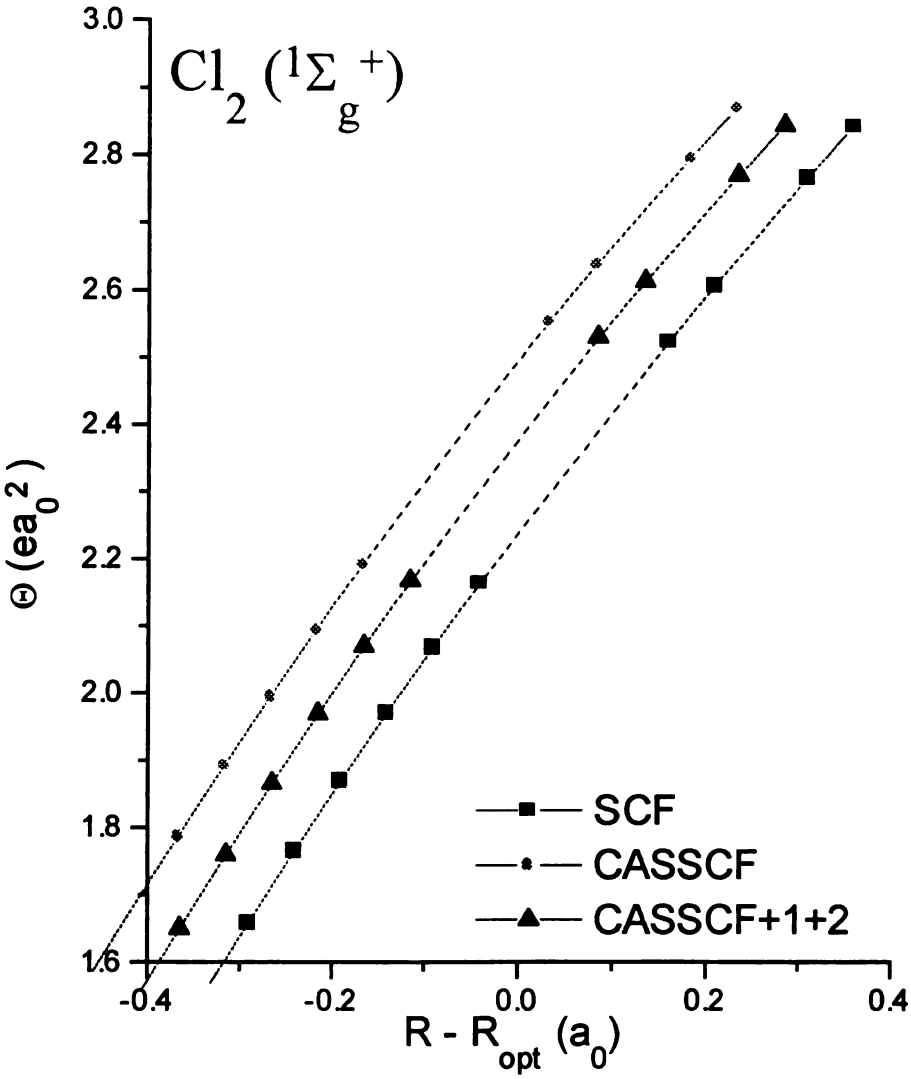

Figure 8. Distance dependence of Θ for Cl_2 calculated with various models using the aug-cc-pvqz basis.

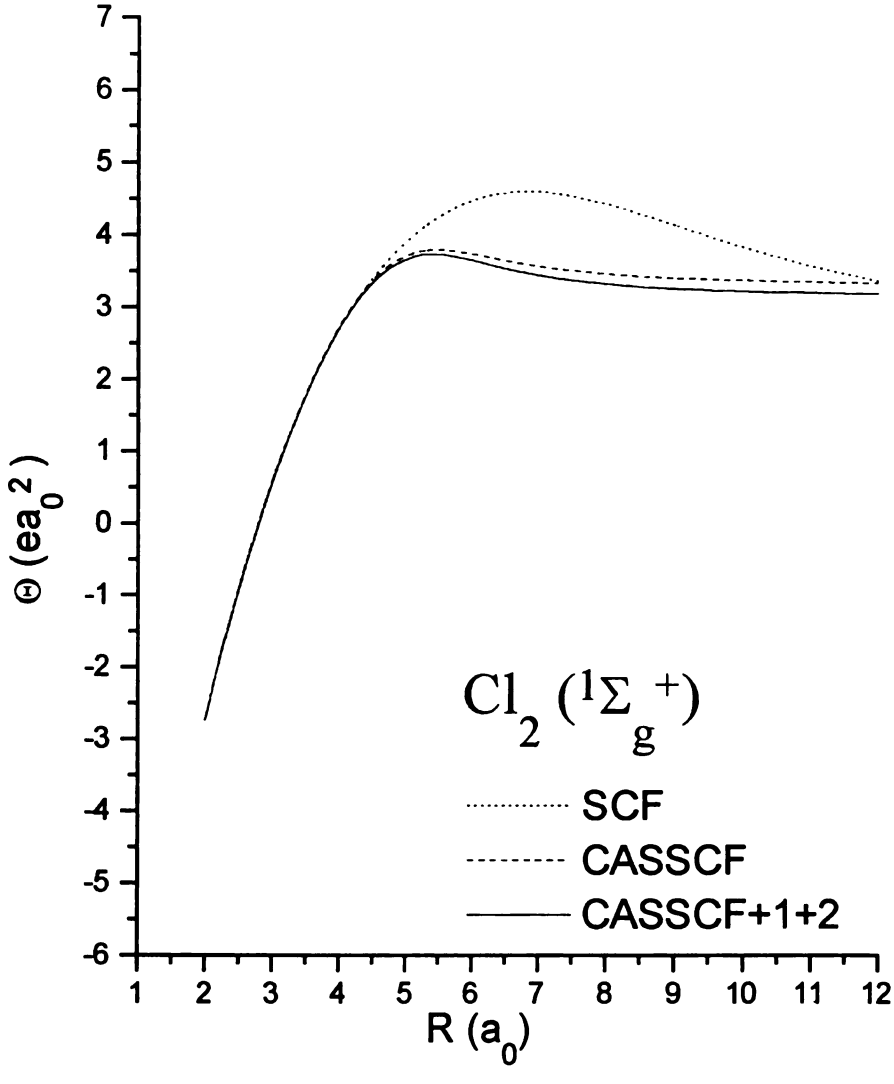

Figure 9. The quadrupole moment of Cl_2 as a function of internuclear separation with various models using the aug-cc-pvqz basis.

Table 3-2. Selection of Cl_2 quadrupole moments.

$R(a_0)$	$\Theta(ea_0^2)$	Reference	Comment
3.7568	2.2696	4	SCF
3.757	2.686	5	SCF
3.7568	2.270	6	SCF
3.7568	2.2884	This Work	aug-cc-pv5z HF;R_{exp}
3.7267	2.2373	This Work	CBS-HF;R_{opt}
3.757	2.652	5	SCF+1+2
3.7568	2.244	6	SDQ-MP4;vibrational average
3.7568	2.274	10	SDQ-MP4;vibrational average
3.7875	2.3559	This Work	CBS-CASSCF+1+2; R_{opt}
3.7568	2.2896	This Work	aug-cc-pv5z CASSCF+1+2; R_{exp}
experimental	3.68±0.38	9	optical birefringence
experimental	2.405±0.120	8	optical birefringence
vibrational average	2.3860	This Work	CBS-CASSCF+1+2

Table 3-3. CASSCF + 1 + 2 results for R_{opt} and Θ.

Molecule	aug-cc-pvqz		estimated complete basis set limit		
	$R_{opt}(a_0)$	$\Theta_{opt}(ea_0^2)$	$R_{opt}(a_0)$	$\Theta_{opt}(ea_0^2)$	vibration correction
P_2	3.6114	+0.5035	3.6055	0.5241	$+0.0197(v+½)$
S_2	3.6101	+1.4670	3.5978	1.4585	$+0.0102(v+½)$
Cl_2	3.8050	+2.3801	3.7875	2.3559	$+0.0301(v+½)$

D. On the Distance Dependence of S_2 and Cl_2

We study the distance dependence of Θ, using the aug-cc-pvqz basis and the SCF, CASSCF, and CASSCF+1+2 wavefunctions. The calculated potential energy curves for N_2, P_2, O_2, S_2, F_2, and Cl_2 are shown in Figure 10, and the calculated properties (R_e, D_e, and ω_e) are very close the CBS CASSCF+1+2 limits. The calculated spectroscopic properties, also compare well with the experimental values taken from Herzberg.[11] The wavefunctions provide a reasonably accurate description of the molecule's electronic structure over a large range of internuclear distances, and we expect the calculated quadrupole-moment function to be realistic.

The quadrupole moment functions for the molecules of interest are shown in Figure 11. The behavior of Θ of the second row molecules at large R is the same as discussed for N_2, O_2, and F_2 in Chapter 2. As with H_2 and N_2, Θ for P_2 is zero at large R because the molecule separates to atoms in S states. Θ for S_2 and Cl_2 separates to the sum of the atomic quadrupole moments of the atoms. For S_2, the oriented S atoms are in $^3P_{|M|=1}$ state. For Cl_2, the oriented Cl atoms are in the $^2P_{|M|=0}$ state. As shown in Figure 10, the minimum in the potential energy of the second row homonuclear molecules is at larger R then the first row molecules. In Figure 11, Θ begins descending at larger R relative to the first row molecules. The core electrons of the second row molecules shield the bonding electrons making the electronic distribution of the second row molecules more diffuse. The more diffuse the electronic distribution the greater the magnitudes of the various

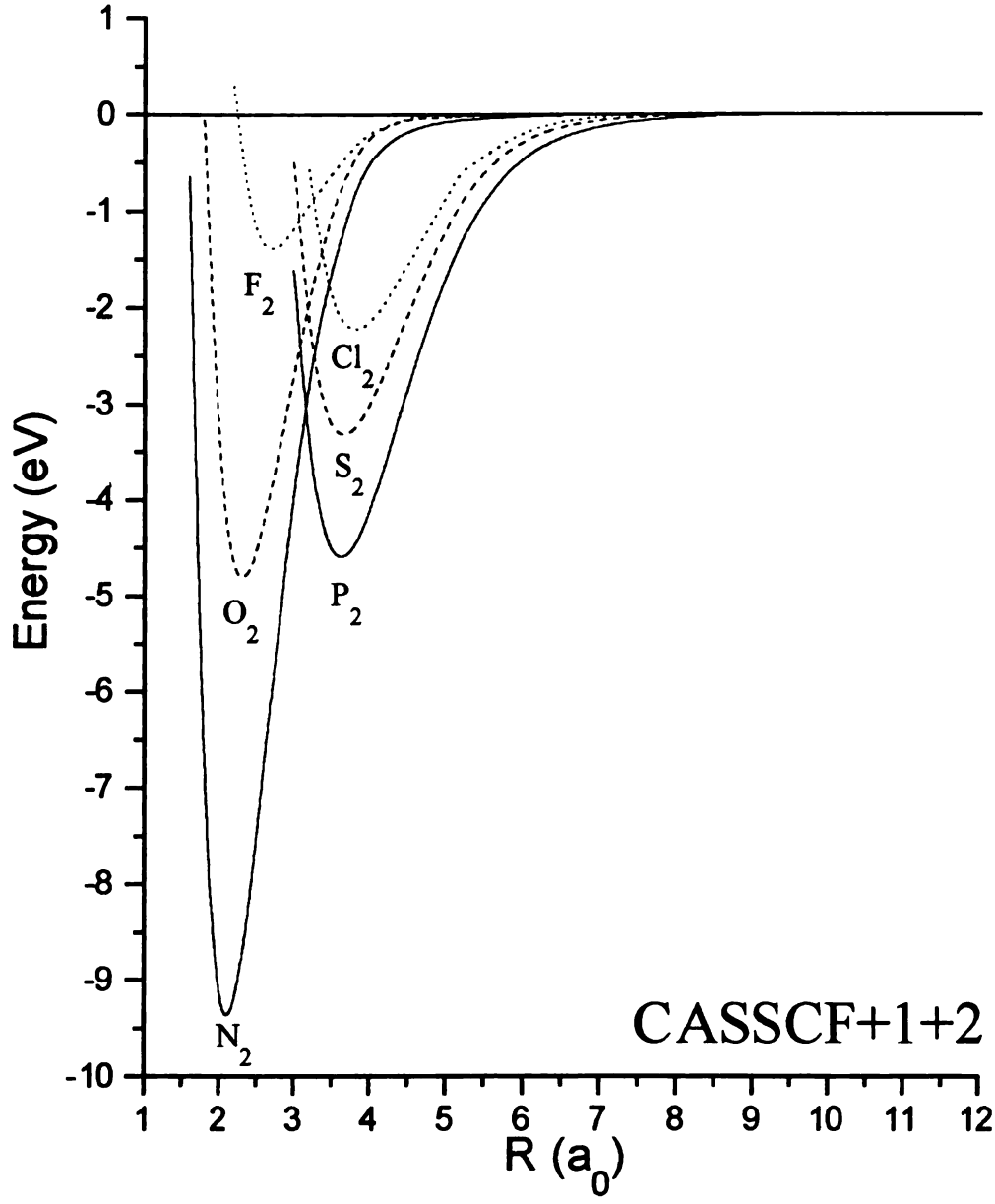

Figure 10. CASSCF+1+2 potential energy curves for N_2, O_2, F_2, P_2, S_2, and Cl_2 using the aug-cc-pvqz basis.

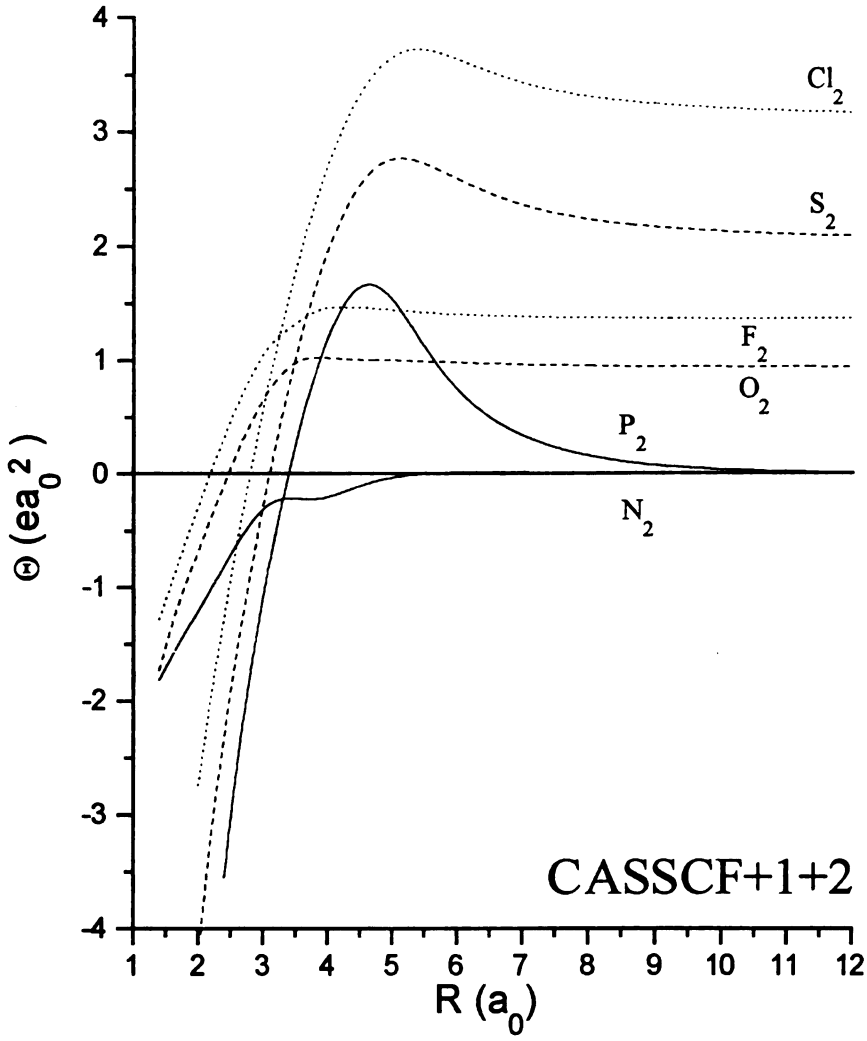

Figure 11. Molecular quadrupole moments of N_2, O_2, F_2, P_2, S_2, and Cl_2 using the CASSCF+1+2 and the aug-cc-pvqz basis.

quadrupole components. This effect is also enhanced by the r^2 term in Equation 13 of chapter 2.

In describing the distance dependence of Θ, we first consider S_2 and Cl_2, returning to P_2 latter. As in Chapter 2, we first partition Θ into its σ and π components. For technical reasons, this is done using the natural orbitals from the MRCI wavefunctions. By setting the occupations of the π or σ electrons to zero, we can select which symmetry components of the electronic distribution we are interested in. These are not precisely in the symmetry determined ratio because our wavefunction has D_{2h} symmetry and our correlated wavefunction results in asymptotic *p* functions that are not equivalent.

The σ components of the quadrupole-moment curves for N_2, P_2, O_2, S_2, F_2, and Cl_2 are given in Figure 12 for a MRCI wavefunction in an aug-cc-pvqz basis. The π components of the quadrupole-moment curves for the same molecules are given in Figure 13. Note that for all molecules Θ_σ is always negative and Θ_π is always positive. The sign of Θ depends on the relative magnitudes of these contributions and Θ usually decreases from its asymptotic value with decreasing R. The relative asymptotic values of S_2 and Cl_2 depend on the signally occupied atomic orbitals and is structurally identical to those of O_2 and F_2, respectively. For S_2 we have, in an orbital model

$$\Theta_\sigma(S) = \Theta(3p_z)$$

$$\Theta_\pi(S) = -3/2\ \Theta_\sigma(S)$$

and for Cl_2

$$\Theta_\sigma(Cl) = \Theta(3pz)$$

$$\Theta_\pi(Cl) = -2\ \Theta_\sigma(Cl)$$

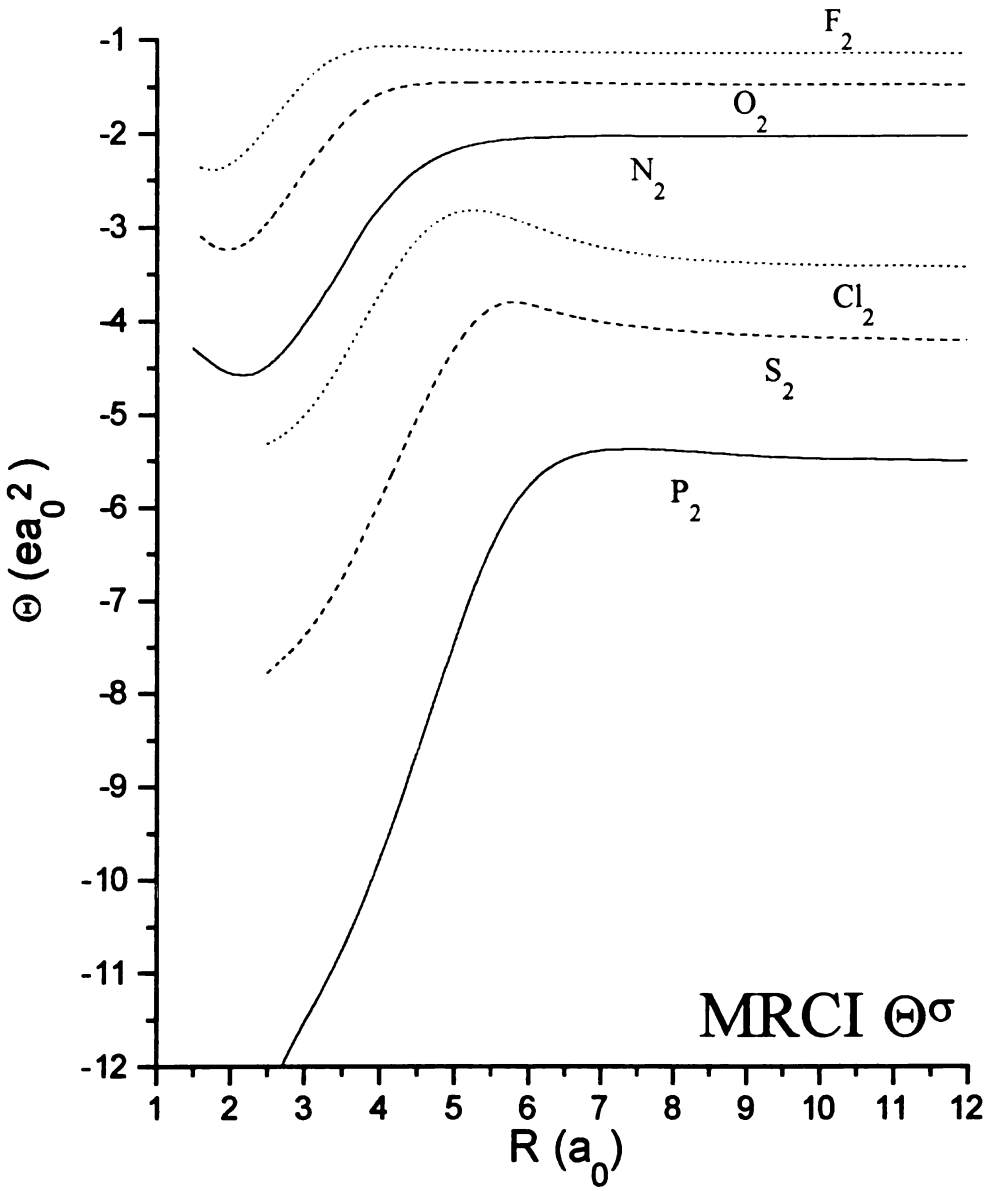

Figure 12. Distance dependence of the sigma component of the quadrupole moment of N_2, O_2, F_2, P_2, S_2, and Cl_2.

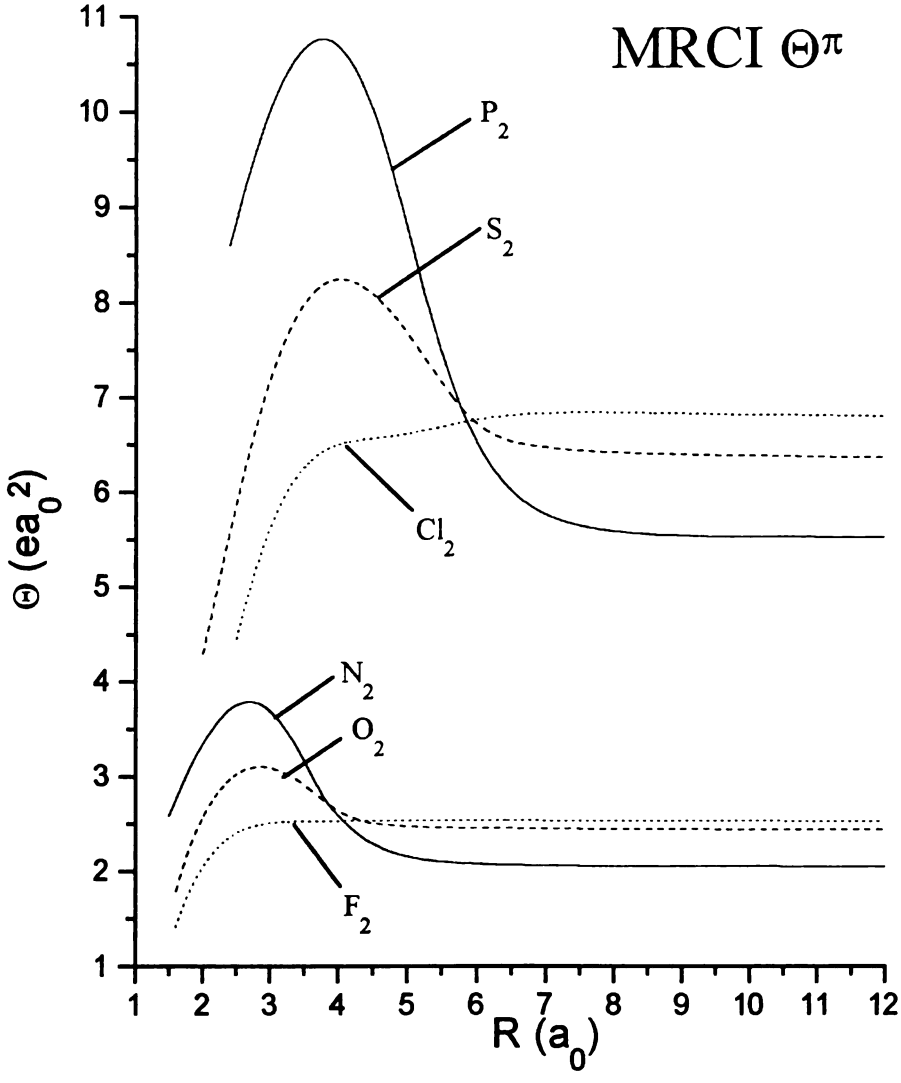

Figure 13. Distance dependence of the pi component of the quadrupole moment of N_2, O_2, F_2, P_2, S_2, and Cl_2.

Our numeric asymptotic values for O_2 and S_2 are

$$\Theta_\pi(O) = +2.435\ ea_0^2 \qquad \Theta_\pi(S) = +6.326\ ea_0^2$$

$$\Theta_\sigma(O) = -1.499\ ea_0^2 \qquad \Theta_\sigma(S) = -4.261\ ea_0^2$$

and the relative asymptotic values for F_2 and Cl_2 are

$$\Theta_\pi(F) = +2.517\ ea_0^2 \qquad \Theta_\pi(Cl) = +6.575\ ea_0^2$$

$$\Theta_\sigma(F) = -1.170\ ea_0^2 \qquad \Theta_\sigma(Cl) = -3.473\ ea_0^2$$

Again, note relative magnitudes of Θ_σ and Θ_π of the second row molecules are much larger their first row counterparts due the larger spatial distribution of the electronic charge.

Referencing each molecular quadrupole-moment function to is asymptotic atomic contribution, we obtain Figures 14-16, which are simply $\Theta_{mol}(R)$ and its component Θ^σ_{mol} and Θ^π_{mol}. In the region near R_{opt}, for S_2 there is an increase in Θ^π_{mol}, which is a result of spilling of δn_π (see Chapter 2) into the P region. For Θ^π_{mol} in Cl_2 there is a small decrease due to δn_π spilling into the N region. These characteristics are illustrated by the contour plots in Figures 17 - 22. The equilibrium bond length in these molecules is smaller than the internuclear distance where Θ^π_{mol} is maximum, so, the slopes of both the π and σ component of Θ are both positive around R_e. The functions for S_2 and Cl_2 are very similar to those of O_2 and F_2 . The sign of the quadrupole moment is determined by the relative internuclear separation while the magnitude of the quadrupole moment is dominated by the Θ_π contribution.

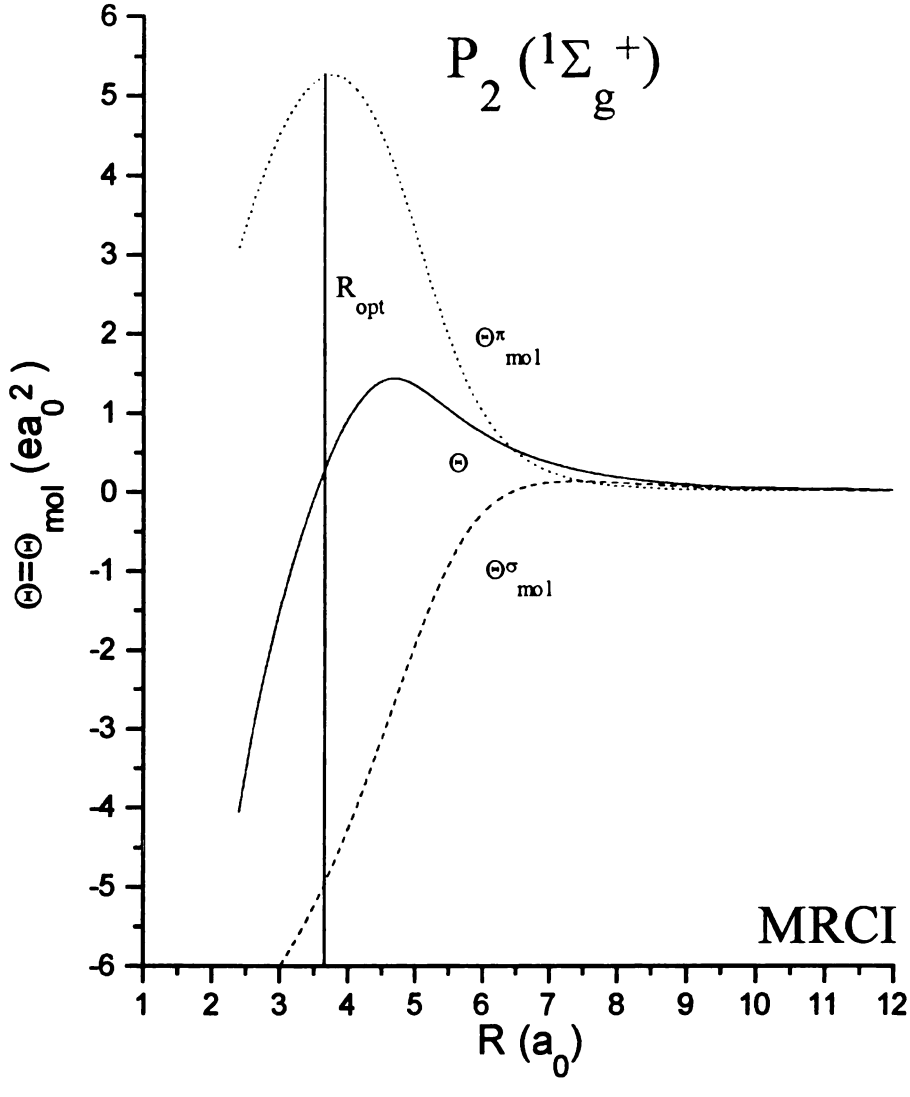

Figure 14. Distance dependence of the quadrupole moment of P_2 partitioned into its Θ^{σ}_{mol} and Θ^{π}_{mol} components.

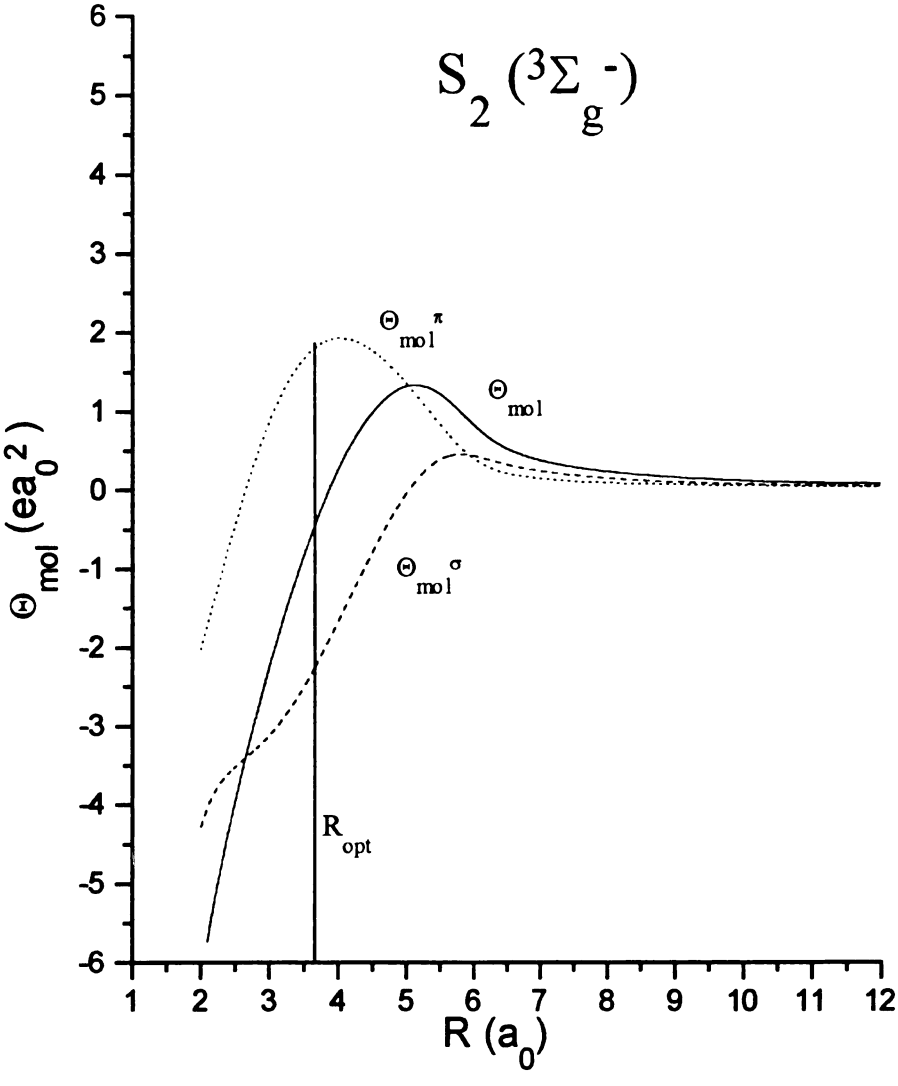

Figure 15. Distance dependence of the quadrupole moment of S_2 partitioned into its Θ^{σ}_{mol} and Θ^{π}_{mol} components.

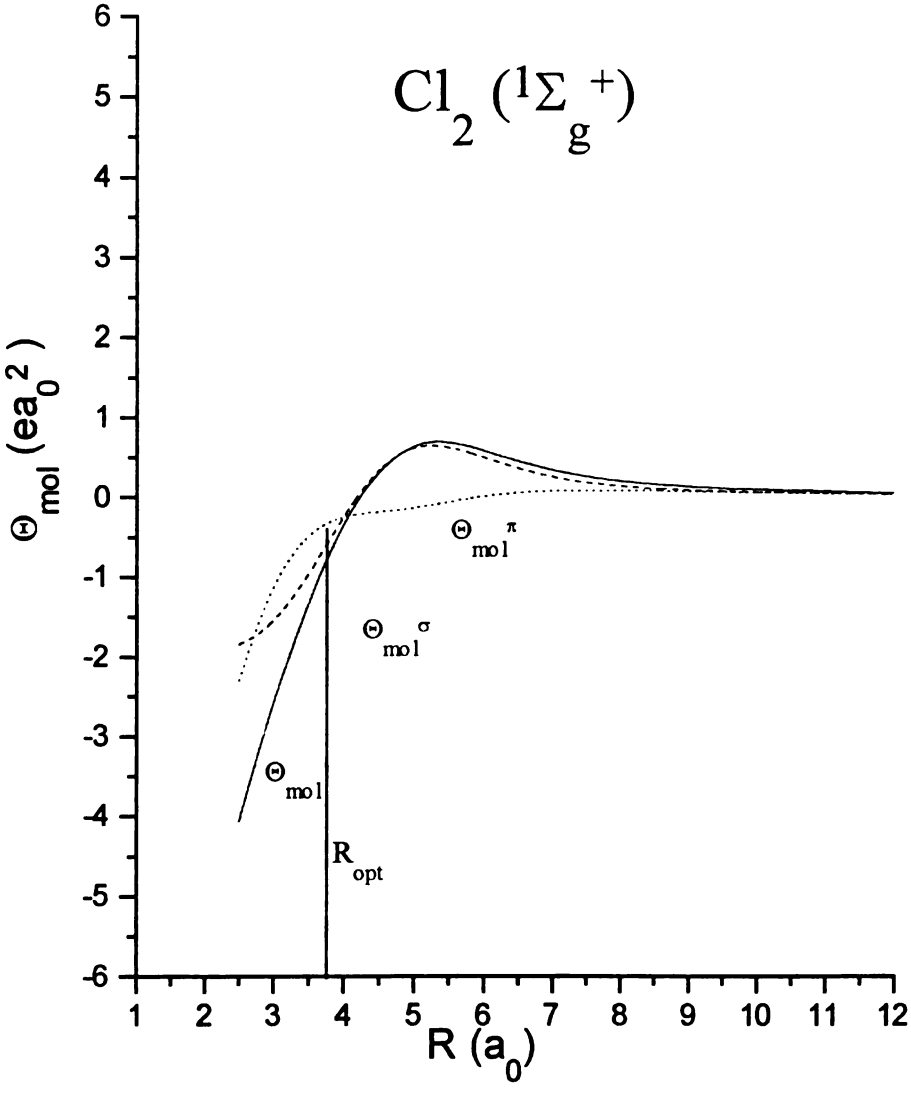

Figure 16. Distance dependence of the quadrupole moment of Cl_2 partitioned into its Θ^{σ}_{mol} and Θ^{π}_{mol} components.

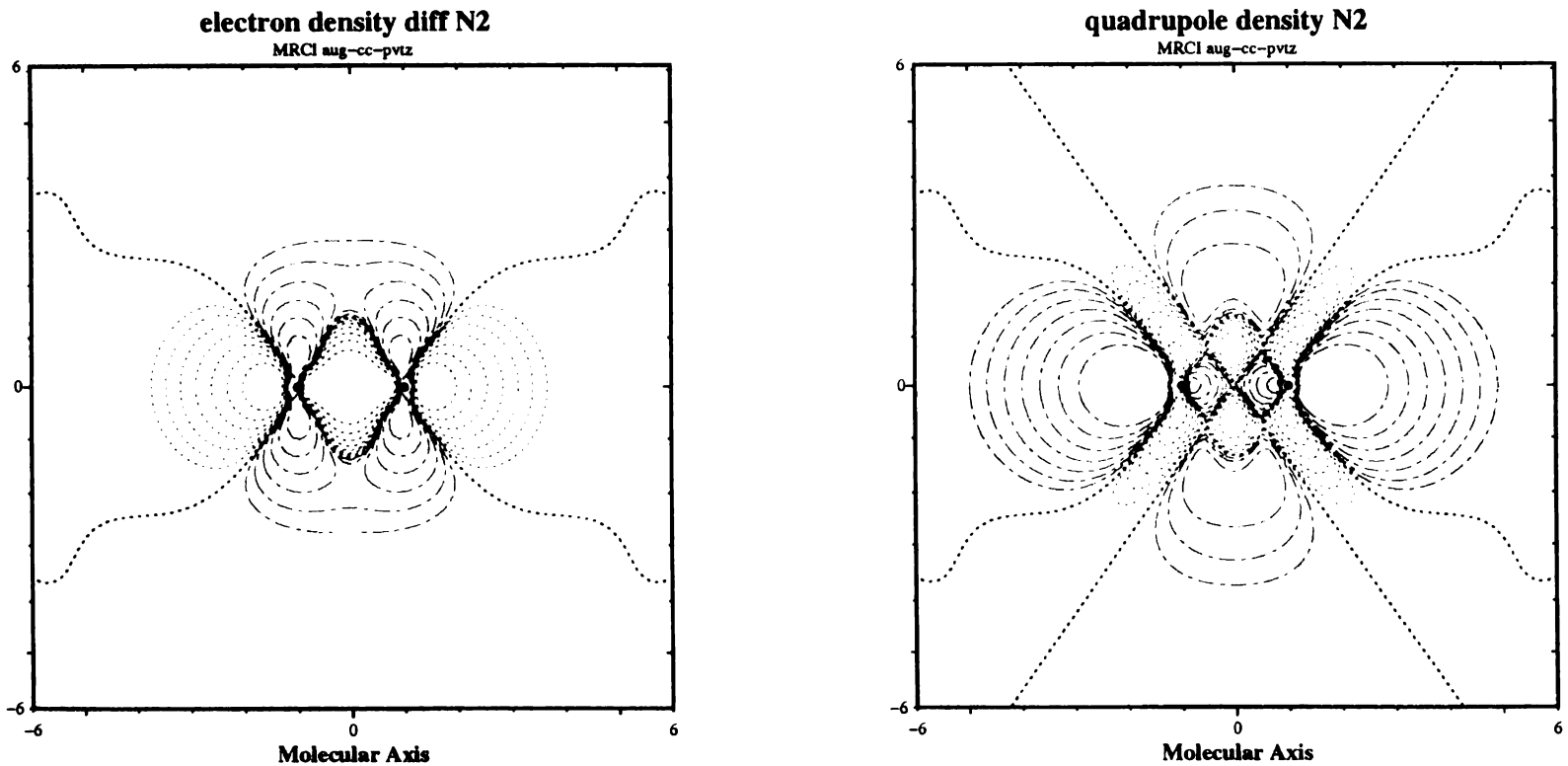

Figure 17. Electron-density difference and the associated quadrupole-density contours for N_2, at 2.1 a_0 calculated with MRCI wavefunction and the aug-cc-pvqz. Contour values are 0.0, ±0.001, ±0.002, ±0.004, ±0.008, ±0.016, ±0.032, and ±0.064. Blue represent positive contours and red represents negative.

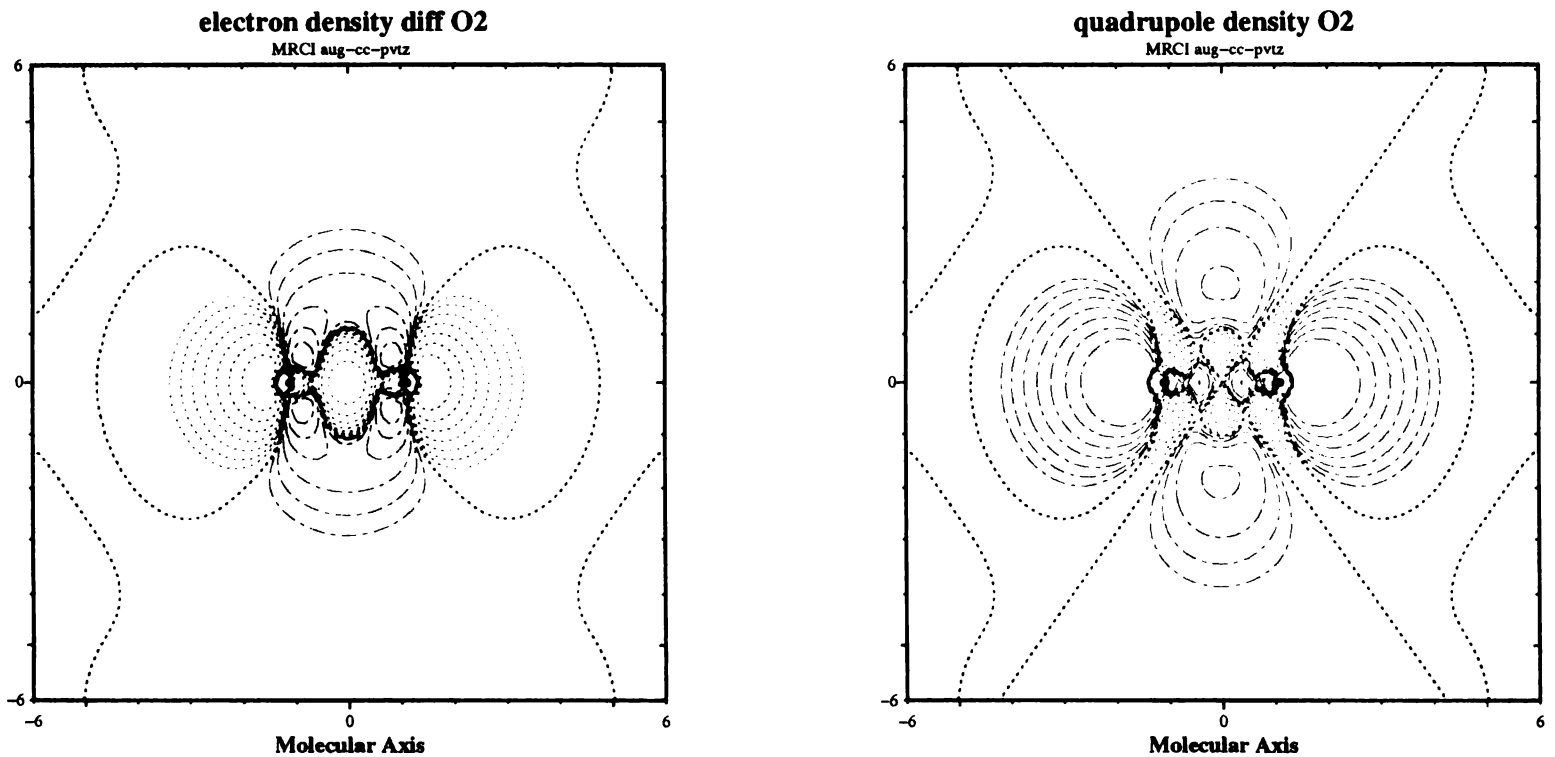

Figure 18. Electron-density difference and the associated quadrupole-density contours for O_2, at 2.3 a_0 calculated with MRCI wavefunction and the aug-cc-pvqz. Contour values are 0.0, ±0.001, ±0.002, ±0.004, ±0.008, ±0.016, ±0.032, and ±0.064. Blue represent positive contours and red represents negative.

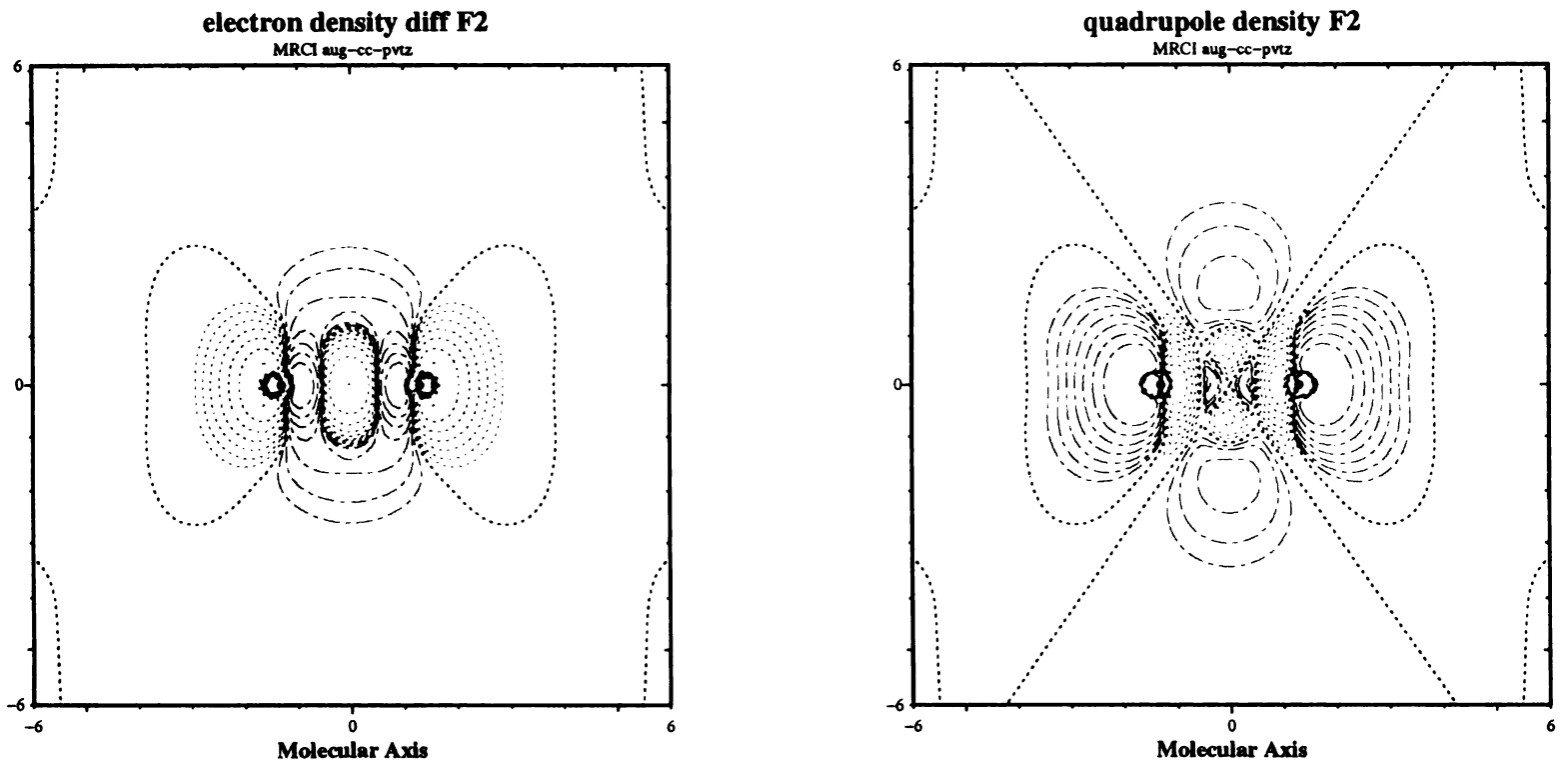

Figure 19. Electron-density difference and the associated quadrupole-density contours for F_2, at 2.6 a_0 calculated with MRCI wavefunction and the aug-cc-pvqz. Contour values are 0.0, ±0.001, ±0.002, ±0.004, ±0.008, ±0.016, ±0.032, and ±0.064. Blue represent positive contours and red represents negative.

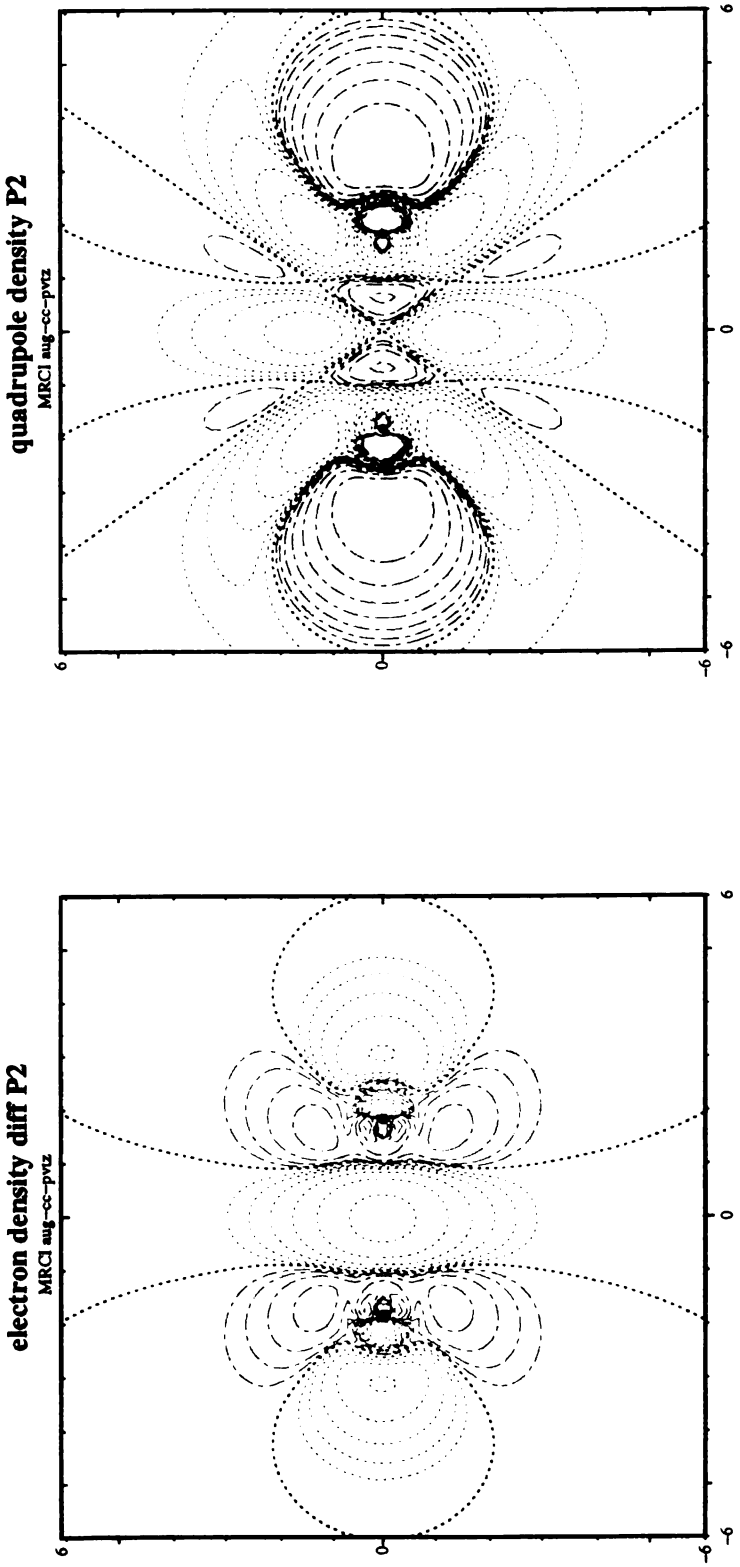

Figure 20. Electron-density difference and the associated quadrupole-density contours for P_2, at 3.6 a_0 calculated with MRCI wavefunction and the aug-cc-pvqz. Contour values are 0.0, ±0.001, ±0.002, ±0.004, ±0.008, ±0.016, ±0.032, and ±0.064. Blue represent positive contours and red represents negative.

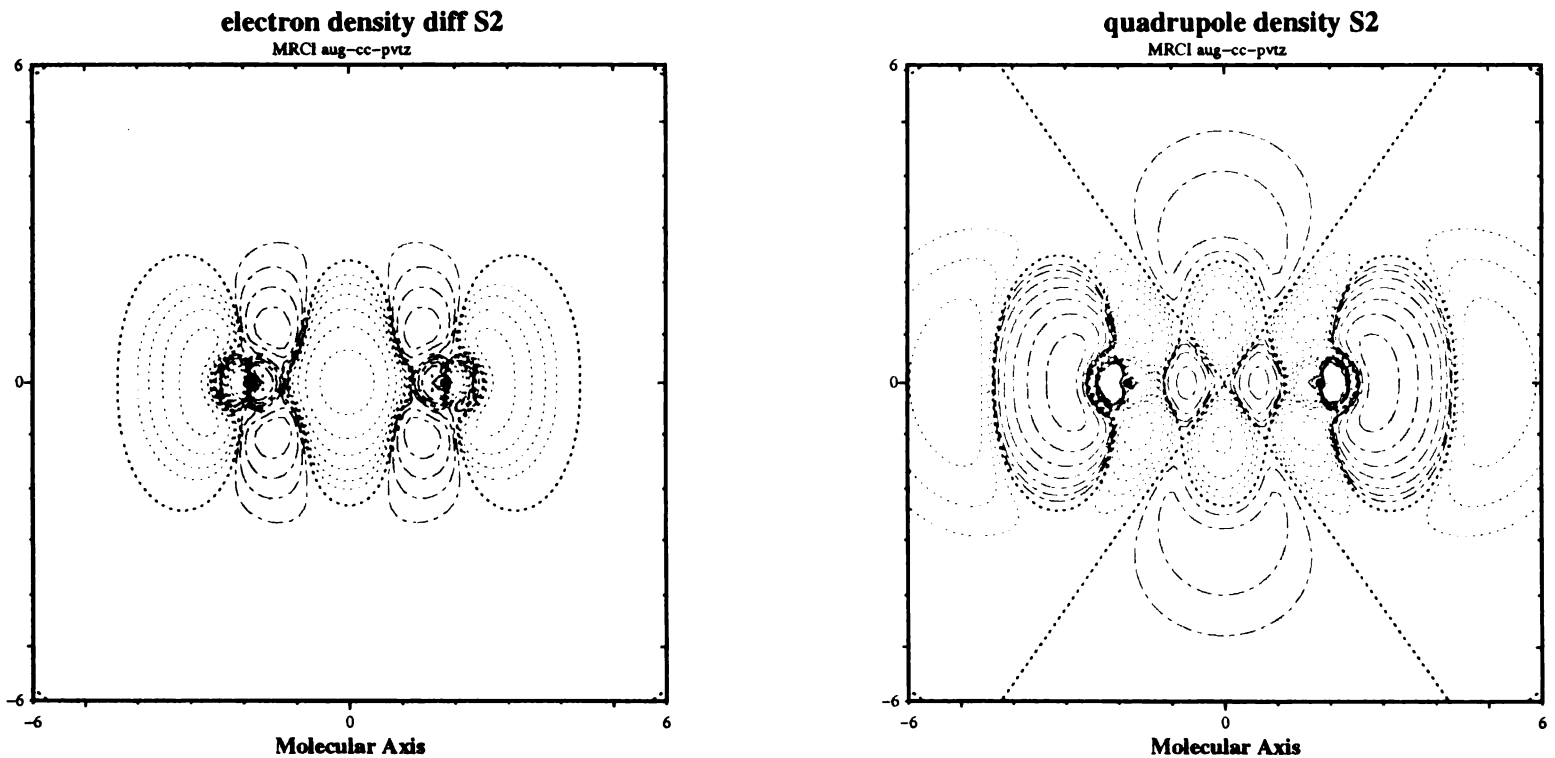

Figure 21. Electron-density difference and the associated quadrupole-density contours for S_2, at 3.6 a_0 calculated with MRCI wavefunction and the aug-cc-pvqz. Contour values are 0.0, ±0.001, ±0.002, ±0.004, ±0.008, ±0.016, ±0.032, and ±0.064. Blue represent positive contours and red represents negative.

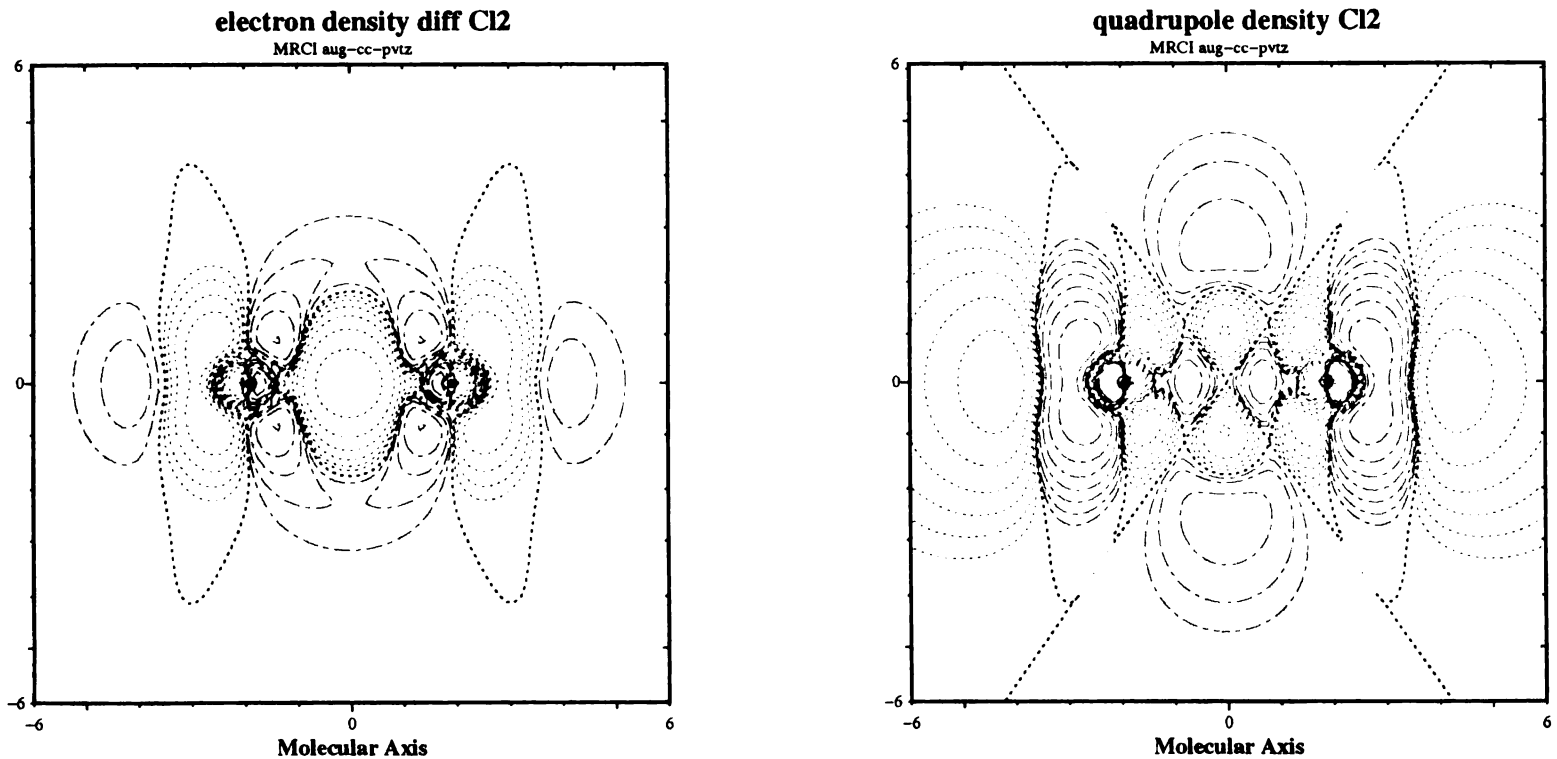

Figure 22. Electron-density difference and the associated quadrupole-density contours for Cl_2, at 3.7 a_0 calculated with MRCI wavefunction and the aug-cc-pvqz. Contour values are 0.0, ±0.001, ±0.002, ±0.004, ±0.008, ±0.016, ±0.032, and ±0.064. Blue represent positive contours and red represents negative.

E. The Quadrupole Moments of N_2 and P_2

The isovalent molecules of N_2 and P_2 have significantly different quadrupole moments. In Chapter 2, we developed methods of analyzing the quadrupole moment in terms of the bonding density. It is our intention to use these techniques to evaluate the significant differences between the quadrupole moment functions of N_2 and P_2.

First lets consider the quadrupole moments of the separate atoms. Both the N atom and the P atom are in the ^4S state and therefore the quadrupole moment is zero. The N_2 and P_2 potential energy surface and the quadrupole moments as a function of internuclear separation is given in Figures 23 and 24. As two nitrogen atoms come together to form N_2, the quadrupole moment immediately becomes negative. With two approaching P atoms, however, the quadrupole moment first shifts positive. Then as the two P atoms approach the energy optimized separation ($R_{P_2} < 5.0\ a_0$) the magnitude of the quadrupole moment begins to decrease. The reason for this can be seen by breaking the quadrupole moment in σ and π symmetry contributions. At infinity the Θ_π and Θ_σ must sum to zero for both N_2 and P_2, as shown in Figure 25. Our numeric asymptotic values of Θ_σ and Θ_π for N_2 and P_2 are

$$\Theta_\pi(N) = +2.041\ ea_0^2 \qquad \Theta_\pi(P) = +5.592\ ea_0^2$$

$$\Theta_\sigma(N) = -2.041\ ea_0^2 \qquad \Theta_\sigma(P) = -5.592\ ea_0^2$$

Referencing each molecular quadrupole-moment function to is asymptotic atomic contribution as in Figure 21, as R approaches R_{exp}, Θ_π increases more in P_2 then in N_2. In the region near R_{opt}, for P_2 there is a greater increase in Θ^π_{mol}, which is a result of spilling of δn_π into the P region. The effect in P_2 is magnified by the greater spatial distribution

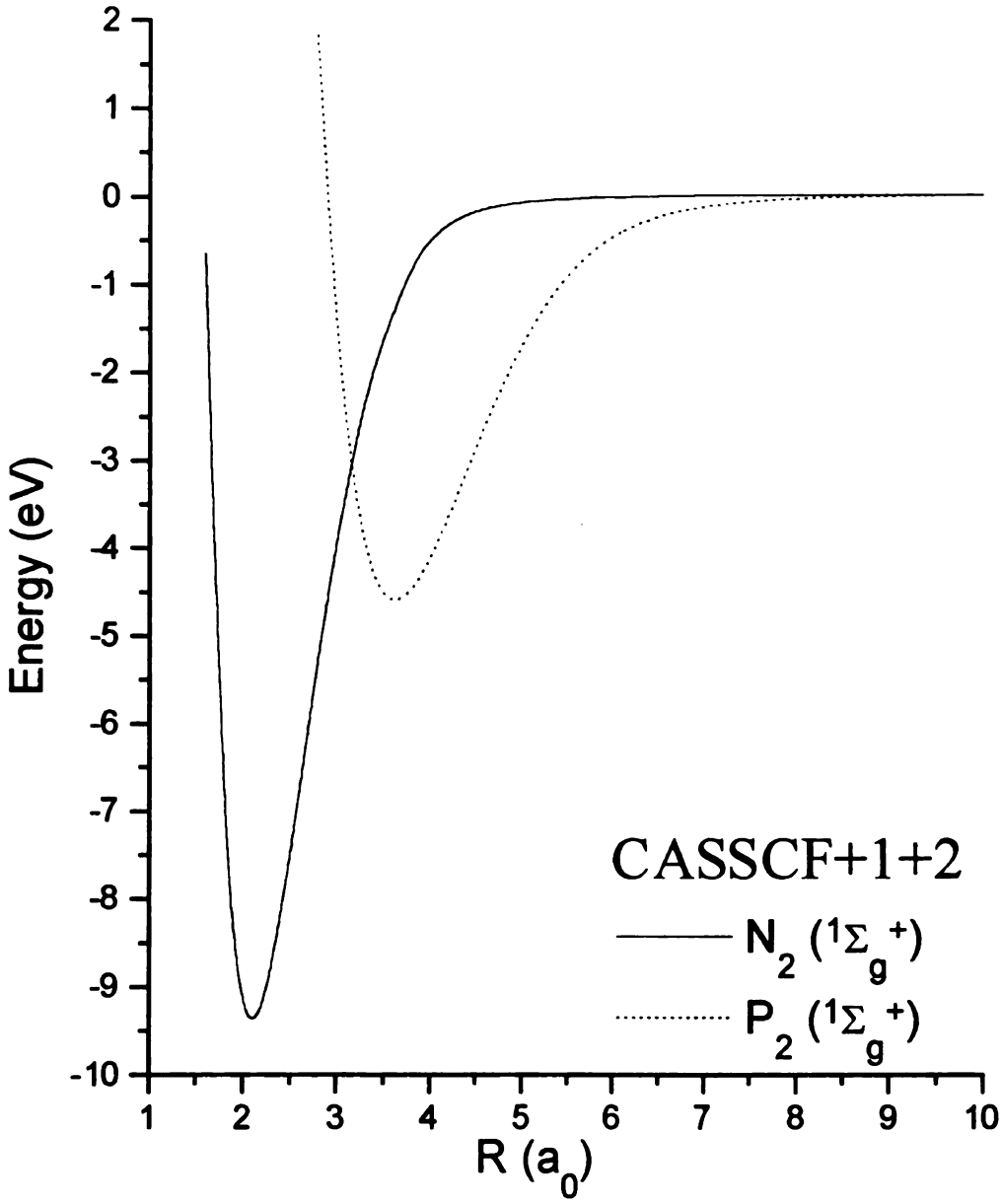

Figure 23. CASSCF+1+2 potential energy curves for N_2 and P_2 using the aug-cc-pvqz basis.

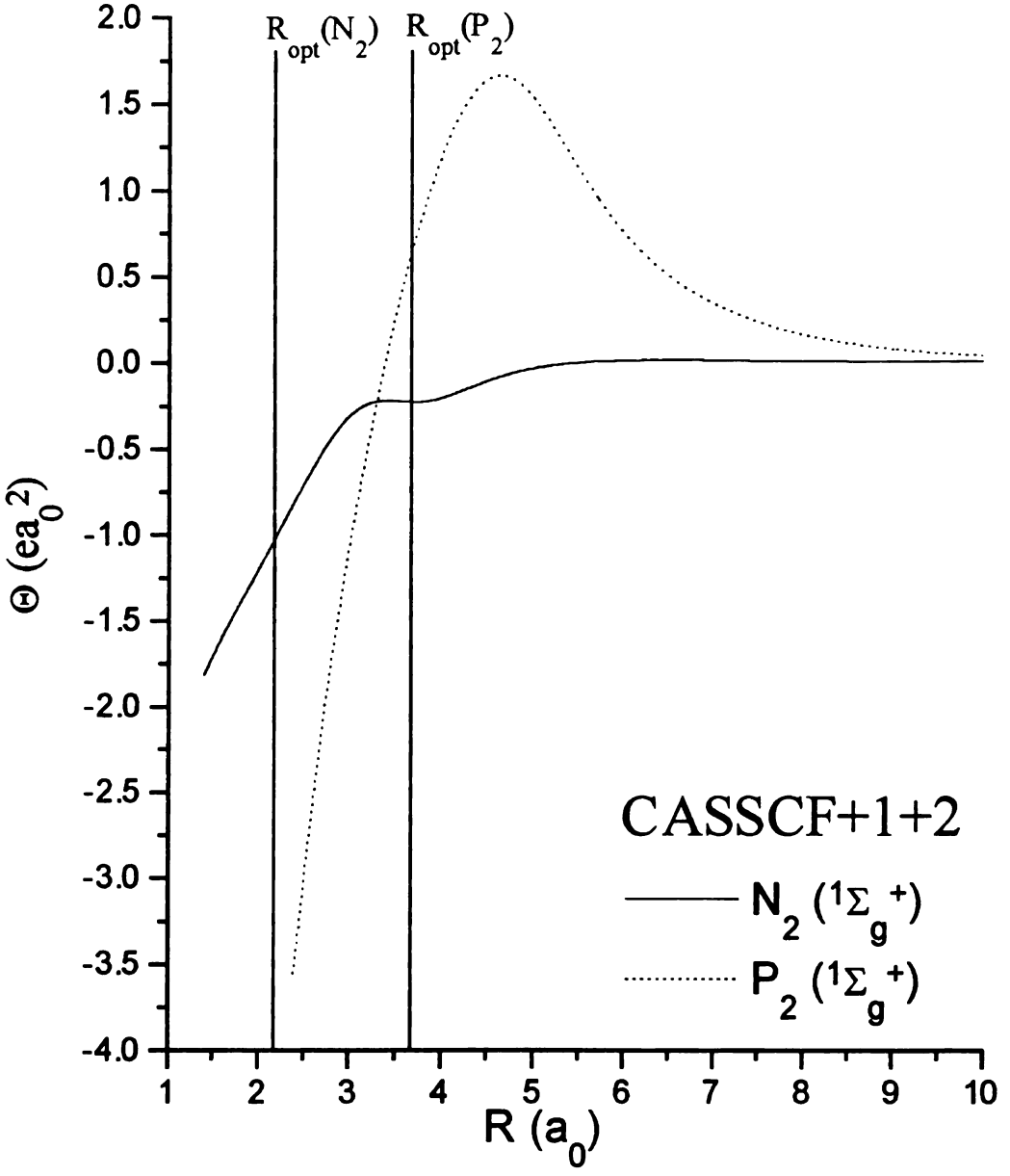

Figure 24. Distance dependence of the molecular quadrupole moments of N_2 and P_2 using the CASSCF+1+2 and the aug-cc-pvqz basis.

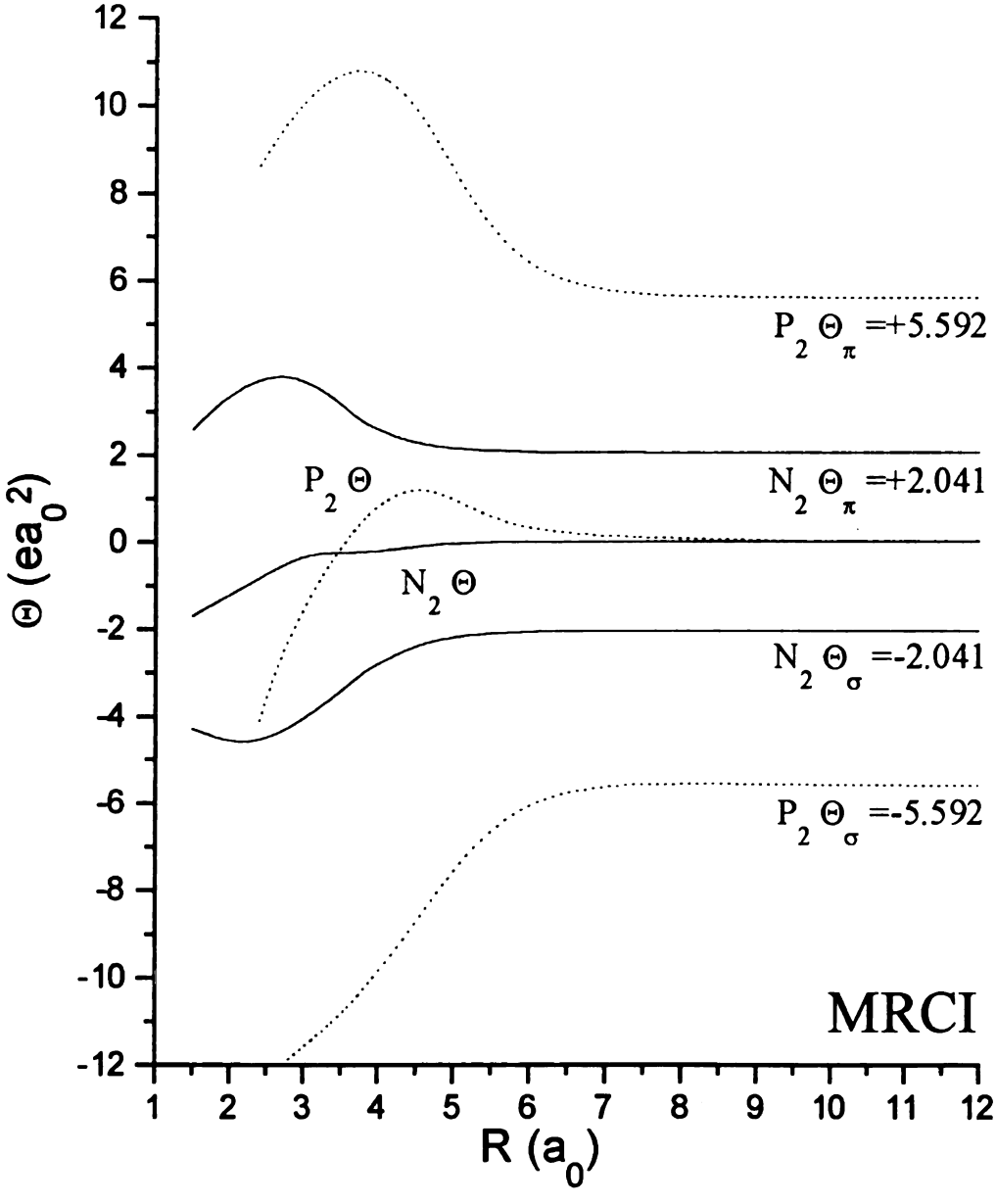

Figure 25. Distance dependence of the molecular quadrupole moments of N_2 and P_2 partitioned into Θ_σ and Θ_π components.

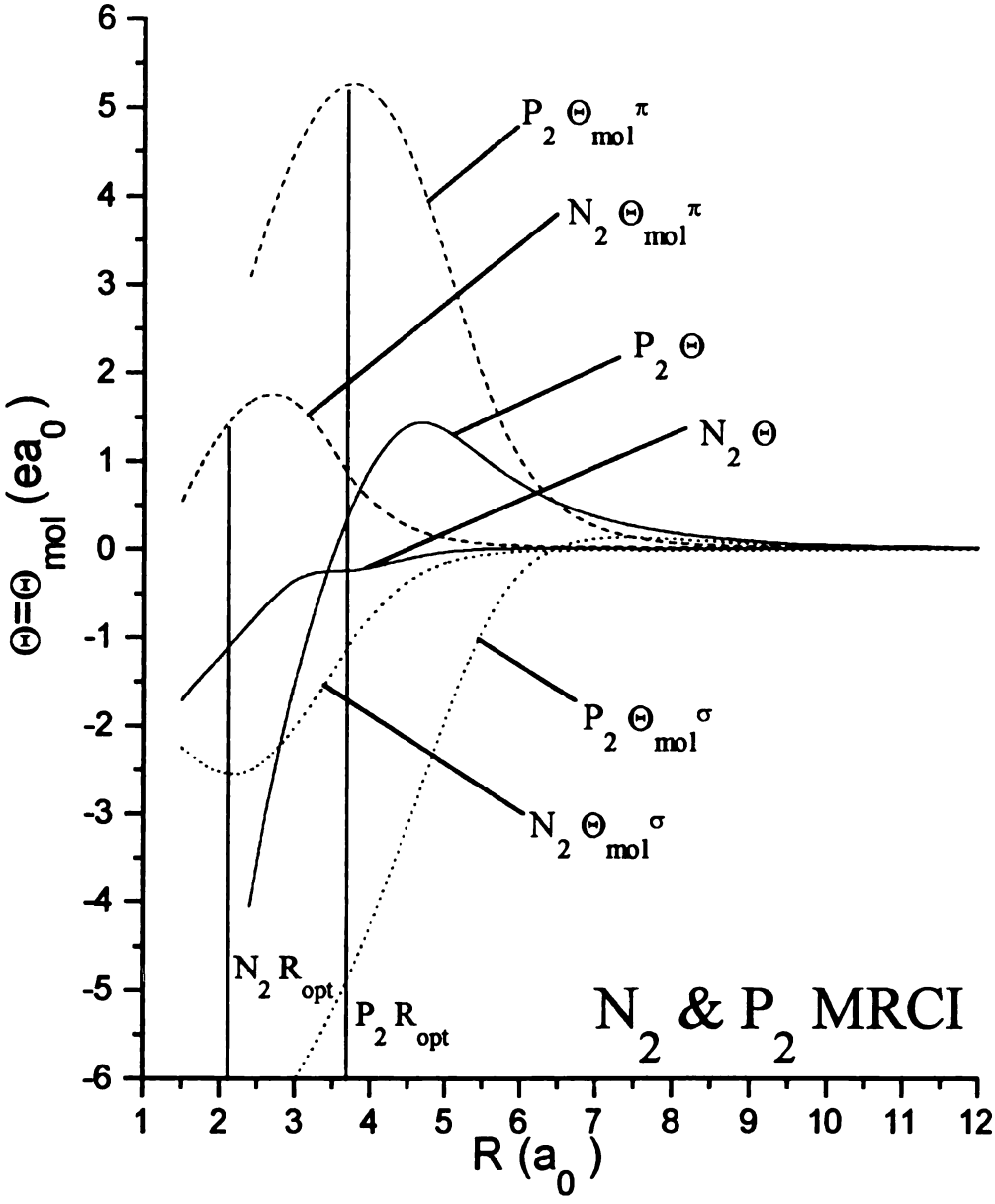

Figure 26. Distance dependence of the quadrupole moment of N_2 and P_2 partitioned into their Θ_{mol}^{σ} and Θ_{mol}^{π} components.

and the r^2 term of the operator, thus giving P_2 its positive quadrupole moment. Since this spatial distribution increases moving down the periodic table, the magnitude of the quadrupole moment should also increase.

F. Conclusion

We have studied the quadrupole moments of P_2, S_2, and Cl_2 and have estimated the CASSCF+1+2 basis-set limit for the latter two. The Cl_2 quadrupole moments are in excellent agreement with calculated values by others and in good agreement with the existing experimental data. The rather large values of the quadrupole moment derivatives, shown in Table 3-1, result in the quadrupole moment being a very sensitive function of R around R_e. We have provided the global quadrupole-moment function as the sum of an atomic contribution and a molecular contribution Θ_{mol}. We have also provided reasons for the differences in the quadrupole moment between the first and second row molecules.

Additional contour plots and three-dimensional images of δn and $\delta\Theta$, as well as detailed numerical values of Θ as a function of R, are available via our web page, www.cem.msu.edu/~harrison.

Table 3-4. Comparison of MP2 and CASSCF + 1 + 2 results.

Molecule	MP2 (estimated CBS)		CASSCF + 1 + 2 (estimated CBS)	
	$R_{opt}(a_0)$	$\Theta_{opt}\left(ea_0^2\right)$	$R_{opt}(a_0)$	$\Theta_{opt}\left(ea_0^2\right)$
P_2	3.6171	+0.5317	3.6055	+0.5241
S_2	3.5801	+1.4812	3.5978	+1.4585
Cl_2	3.7440	+2.3566	3.7875	+2.3559

G. References

1. Shepard, R., Shavitt, I., Pitzer, R. M., Comeau, D. C., Pepper, M., Lischka, H., Szalay, P. G., Ahlrichs, R., Brown, F. B., and Zhao, J. G., *Int. J. Quantum Chem. Symp,* **1988**, *22*, 149.

2. MOLPRO is a package of *ab initio* programs written by H.J.Werner and P.J.Knowles, with contributions from J.Almof, R.D.Amos, M.J.O.Deegan, S.T.Elbert, C.Hampel, W.Meyer, K.Peterson, R.Pitzer, A.J.Stone, P.R.Taylor, R.Lindh, M.E.Mura, and T.Thorsteinsson

3. *Gaussian 92*, Revision A, Frisch, M. J., Trucks, G. W., Head-Gordon, M., Gill, P. M. W., Wong, M. W., Foresman, J. B., Johnson, B. G., Schlegel, H. B., Robb, M. A., Replogle, E. S., Gomperts, R., Andres, J. L., Raghavachari, K., Binkley, J. S., Gonzalez, C., Martin, R. L., Fox, D. J., Defrees, D. J., Baker, J., Stewart, J. J. P., and Pople, J. A., Gaussian, Inc., Pittsburgh PA, 1992.

4. Glasier R., Horan C.J., and Haney P.E., J.Phys.Chem. **1993**, 97, 1835

5. G. Maroulis, J.Mol.Struct.(THEOCHEM), **279** (1993) 79

6. J.F.Williams and R.D.Amos, Chem.Phys.Lett. **70** (1980) 162

7. G.Maroulis, Chem.Phys.Lett. **199** (1992) 244

8. A.D. Buckingham, C.Graham and J.H. Williams, Mol. Phys., **1983**, 49, 703.

9. R.J.Emrich and W. Steele, Mol.Phys. **40** (1980) 469.

10. E.F.Archibong and A.J.Thakkar, Chem.Phys.Lett. **201** (1993) 485

11. Huber, K. P. and Herzberg, G., "Molecular spectra and molecular structure," Vol. 4, *Constants of Diatomic Molecules* (Van Nostrand-Reinhold, New York, **1979**).

CHAPTER 4

The Quadrupole Moment of H_2, Li_2, and Na_2

A. Introduction

From the preceding discussions of Chapters II and III, we see that the sign of Θ for N_2, O_2, F_2, P_2, S_2, and Cl_2 depends on the relative values of Θ_σ (negative) and Θ_π (positive). The relative magnitudes of Θ_σ and Θ_π depends on the extent of hydridization. The magnitude of Θ_π depends on the distance between the nuclei and the number of π orbitals involved in the bonding. The F_2 σ contribution, for instance, is less negative then N_2 because of only slight sp hybridization in F_2. In N_2, the large sp hybridization causes the Θ_σ to be dominant and Θ is decidedly negative. For systems such as H_2, Li_2, and Na_2, however, the situation is fundamentally different. As previously discussed in Chapter II, the sign in H_2 is always positive because at large R the s-s bond results in δn_σ being negative in the region where the quadrupole operator ($\cos^2\theta$-1) inverts the sign to positive. As the nuclear separation decreases $\Theta(H_2;R)$ increases and reaches a maximum before R reaches R_{opt}, after which Θ decreases toward zero. This Chapter presents our results for Li_2 and Na_2 and compares these results with H_2 of Chapter 2.

B. Methods

The Dunning cc-pvXz basis sets are unavailable for Li and Na, so a (14s7p4d3f) Li basis contracted to [6s5p4d3f] was derived from vanDuijenveldt[1] plus J. Williams[2] p functions and augmented with an evenly spaced set of d and f functions. This basis will be refered to as the V5Z basis. A (19s12p3d2f) contracted to [6s5p3d2f] VQZ basis from the MolPro96 library[3] was employed for Na. An ANO basis from Widmark, Malmquist, and Roos[4] (WMR) was used for both Li and Na as comparison basis sets. These basis

sets consisted of (14s9p4d3f) contracted to [6s5p4d3f] for Li and a (17s12p5d4f) contracted to [7s6p4d3f] for Na. Both, the V5Z basis for Li_2 and the VQZ basis for Na_2 gave a lower total energy then did the WMR basis, therefore, we use these results and our 'best' results.

The CASSCF for Li_2 consisted of 8 orbitals including $2\sigma_g$, $2\sigma_u$, $3\sigma_g$, $3\sigma_u$, $2\pi_{xu}$, $2\pi_{yu}$, $2\pi_{xg}$, and the $2\pi_{yg}$. The CASSCF+1+2 wavefunction include all single and double excitations out of the CASSCF reference space. The Na_2 CASSCF wavefunction consisted of similar 8 orbital space including the $4\sigma_g$, $4\sigma_u$, $5\sigma_g$, $5\sigma_u$, $3\pi_{xu}$, $3\pi_{yu}$, $3\pi_{xg}$, and the $3\pi_{yg}$ orbitals. Again, the CASSCF+1+2 wavefunction was derived from the CASSCF reference space and included all single and double excitations. This wavefunction is deemed the best due to its flexibility. All RHF, CASSCF and CASSCF+1+2 calculations were done using the MolPro96 package[3].

C. Results

The values for calculated properties of Li_2 are collected in Table C-2 of Appendix C. Our SCF quadrupole moment for Li_2 was 11.1478 ea_0^2 at the equilibrium geometry of 5.2610 a_0 using our largest basis, the V5Z. This compared well with SCF quadrupole of 11.1486 ea_0^2 calculated with the WMR basis at R_{opt} of 5.2609 a_0. The SCF quadrupole moment for both the V5Z basis and the WMR basis calculated at the experimental geometry of 5.0510 a_0 was 10.6432 ea_0^2 and 10.6411 ea_0^2, respectively.

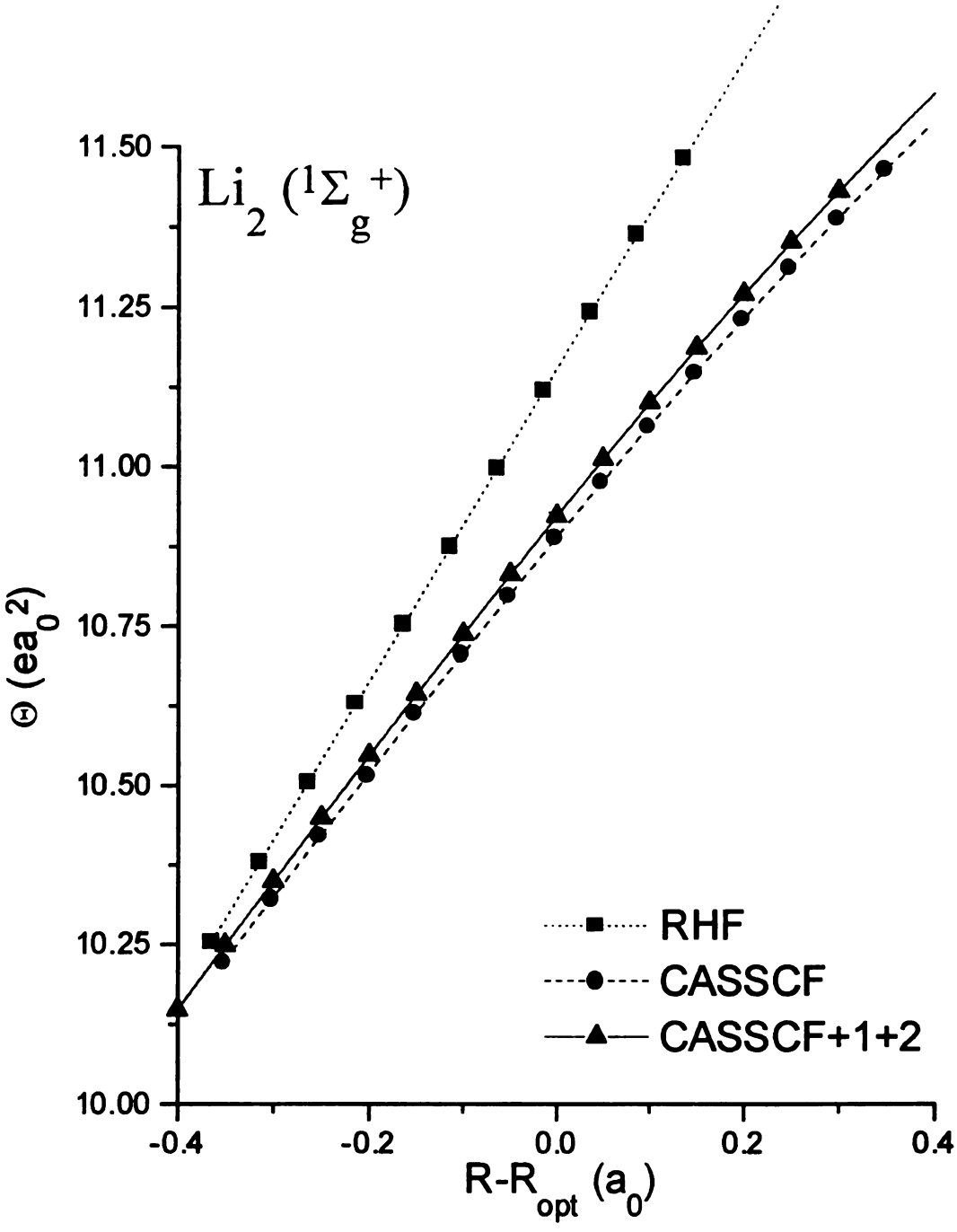

Figure 1. Distance dependence of Θ for Li_2 near R_{opt} calculated with various models using the V5Z basis.

By comparing the optimized SCF geometry, total energy, and dissociation energy to other large basis calculations[5,6], we conclude that our values are very close to the SCF limit. Our CASSCF quadrupole moment was 10.8891 ea_0^2 at the optimized geometry of 5.0986 a_0 using the V5Z basis, while the values determined with the WMR basis was 10.8846 ea_0^2 at an R_{opt} of 5.0972 a_0. The CASSCF quadrupole moment at the experimental separation using the V5Z basis and the WMR basis was 10.8016 ea_0^2 and 10.8034 ea_0^2, respectively. Correlation from configuration interaction of the CASSCF+1+2 changes the quadrupole by a small amount. The CASSCF+1+2 quadrupole moment using the V5Z basis was 10.9213 ea_0^2 at the optimized separation of 5.0971 a_0. Using the WMR basis the optimal separation was the same and the quadrupole moment was 10.9210 ea_0^2. The CASSCF+1+2 quadrupole moment at the experimental geometry was 10.8367 ea_0^2 using the V5Z basis and 10.8372 ea_0^2 using the WMR basis.

A plot of the $\Theta(R)$ in the region of R_{opt} is given with the V5Z for the 3 wavefunctions employed is shown in Figure 1. From the plot we can see the CASSCF and CASSCF+1+2 quadrupole functions are virtually on top of one another while the RHF has a much larger slope then either the CASSCF or the CASSCF+1+2. The first and second derivatives of $\Theta(R)$ near R_{opt} are given in Table 4-1. The first derivative of the SCF $\Theta(R)$ was 2.4293 ea_0 and the second derivative was -0.1976 e. The first derivatives of the CASSCF and CASSCF+1+2 was 1.7718 ea_0 and 1.7974 ea_0,

respectively, while the second derivatives for the CASSCF and CASSCF+1+2 were -0.7220 *e* and -0.7154 *e*. Using the CASSCF+1+2 derivatives, we estimate the vibrational dependence of the CASSCF+1+2 quadrupole moment as

$$\Theta(Li_2; v) = +10.9213 + 0.0650\left(v + \tfrac{1}{2}\right)$$

and so our vibrationally corrected quadrupole moment is $\Theta(Li_2;v = 0) = +10.9538\ ea_0^2$ There is no reported experimental quadrupole moment for Li_2. Plots of $\Theta(R)$ over larger distances is given in Figure 2. The RHF does well near the optimized geometry but fails at larger separations. The CASSCF corrects the SCF curve and follows the CASSCF+1+2 closely.

Table 4-1. First and second derivatives of $\Theta(R)$ near R_{opt} using various models and the V5Z basis for Li_2 and the VQZ basis for Na_2.

Molecule	Wavefunction	$R_{opt}(a_0)$	$\left(\frac{d\Theta}{dR}\right)_{R_{opt}}(ea_0)$	$\left(\frac{d^2\Theta}{dR^2}\right)_{R_{opt}}(e)$
Li_2	SCF	5.2609	2.4293	-0.1976
Li_2	CASSCF	5.0986	1.7718	-0.7220
Li_2	CASSCF+1+2	5.0971	1.7974	-0.7154
Na_2	SCF	6.0365	2.7023	-0.1583
Na_2	CASSCF	6.0118	1.6013	-1.0010
Na_2	CASSCF+1+2	6.0030	1.6377	-0.9963

Our results for Na_2 are collect in Table C-3. Our calculated RHF quadrupole moment for Na_2 was 12.1456 ea_0^2 at 6.0365 a_0 using the VQZ basis. The RHF results with the WMR basis was 12.1456 ea_0^2 at a separation of 6.0414 a_0. The RHF results at the experimental geometry of 5.8182 a_0 was 11.5392 ea_0^2 with WMR basis

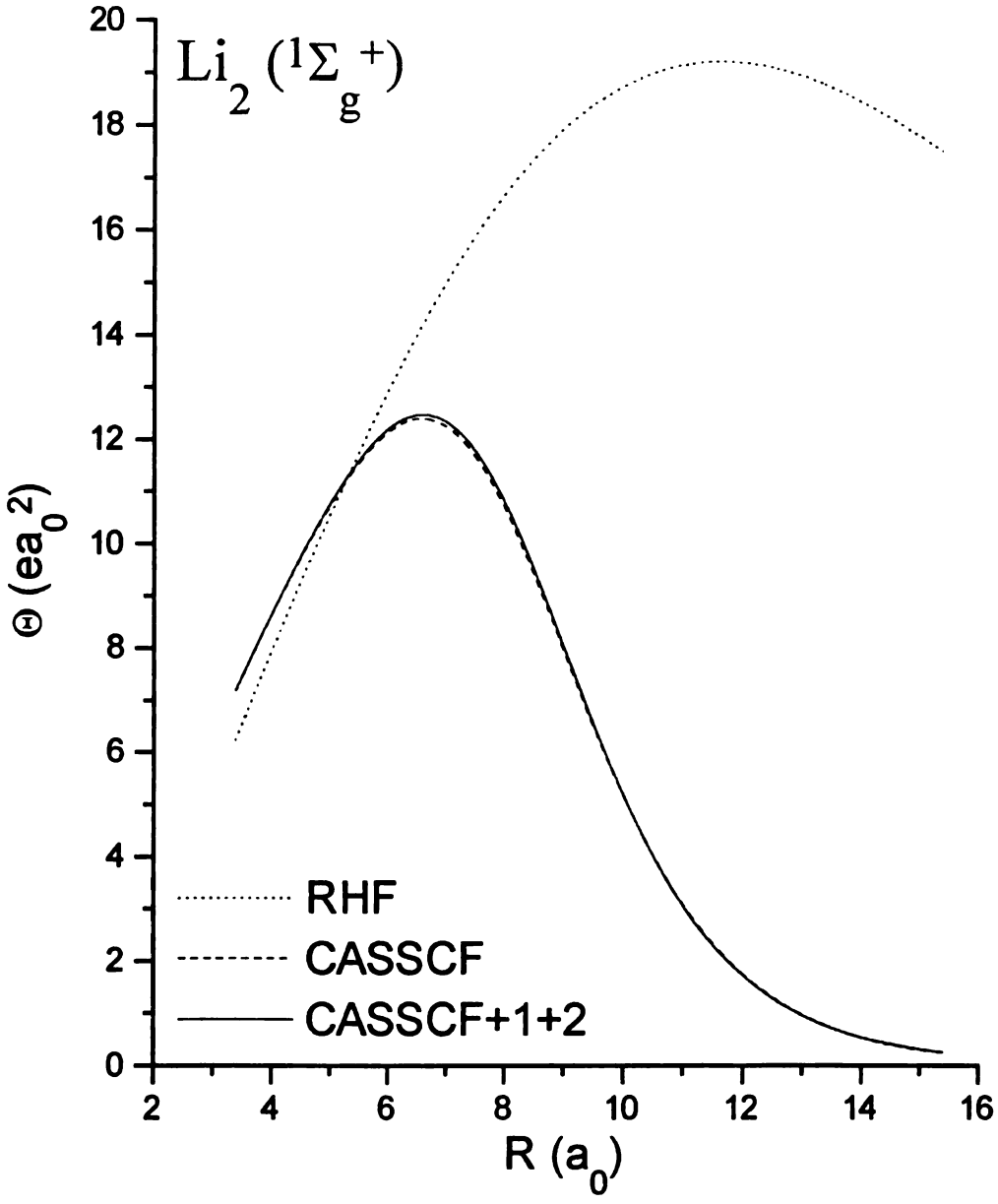

Figure 2. Distance dependence of Θ at large R for Li_2 calculated with various models using the V5Z basis.

and 11.5359 ea_0^2 with the VQZ basis. Our WMR basis, CASSCF quadrupole moment was 11.6614 ea_0^2 at a nuclear separation of 6.0141 a_0 and our VQZ, CASSCF quadrupole moment was 11.5966 ea_0^2 at a separation of 6.0118 a_0. At the experimental geometry, both the WMR, CASSCF and the VQZ, CASSCF gave quadrupole moments of 11.3183 ea_0^2 and 11.2665 ea_0^2. The CASSCF+1+2 quadrupole moments for the WMR and VQZ basis was 11.6905 ea_0^2 at 6.0055 a_0 and 11.6264 ea_0^2 at 6.0030 a_0, respectively. The CASSCF+1+2 results at the experimental geometry were 11.3565 ea_0^2 for the WMR and 11.3054 ea_0^2 for the VQZ.

A plot of the Θ(R) in the region of R_{opt} is given with the VQZ basis for the various wavefunctions in Figure 3. The plot shows the CASSCF and CASSCF+1+2 Θ(R) are very similar while the RHF curve is above and has a larger slope. The RHF first derivative is 2.7023 ea_0 and the second derivative is -0.1583 e. The CASSCF first derivative is 1.6013 ea_0, and as with Li_2, the Na_2 CASSCF+1+2 first derivative has a similar value of 1.6377 ea_0. The second derivatives for the CASSCF and CASSCF+1+2 Θ(R) are -1.0010 e and -0.9963 e, respectively. Using the CASSCF+1+2 first and second derivatives our vibrationally corrected quadrupole moment for Na_2 is

$$\Theta(Na_2;v) = +11.6264 + 0.0215\left(v + \tfrac{1}{2}\right)$$

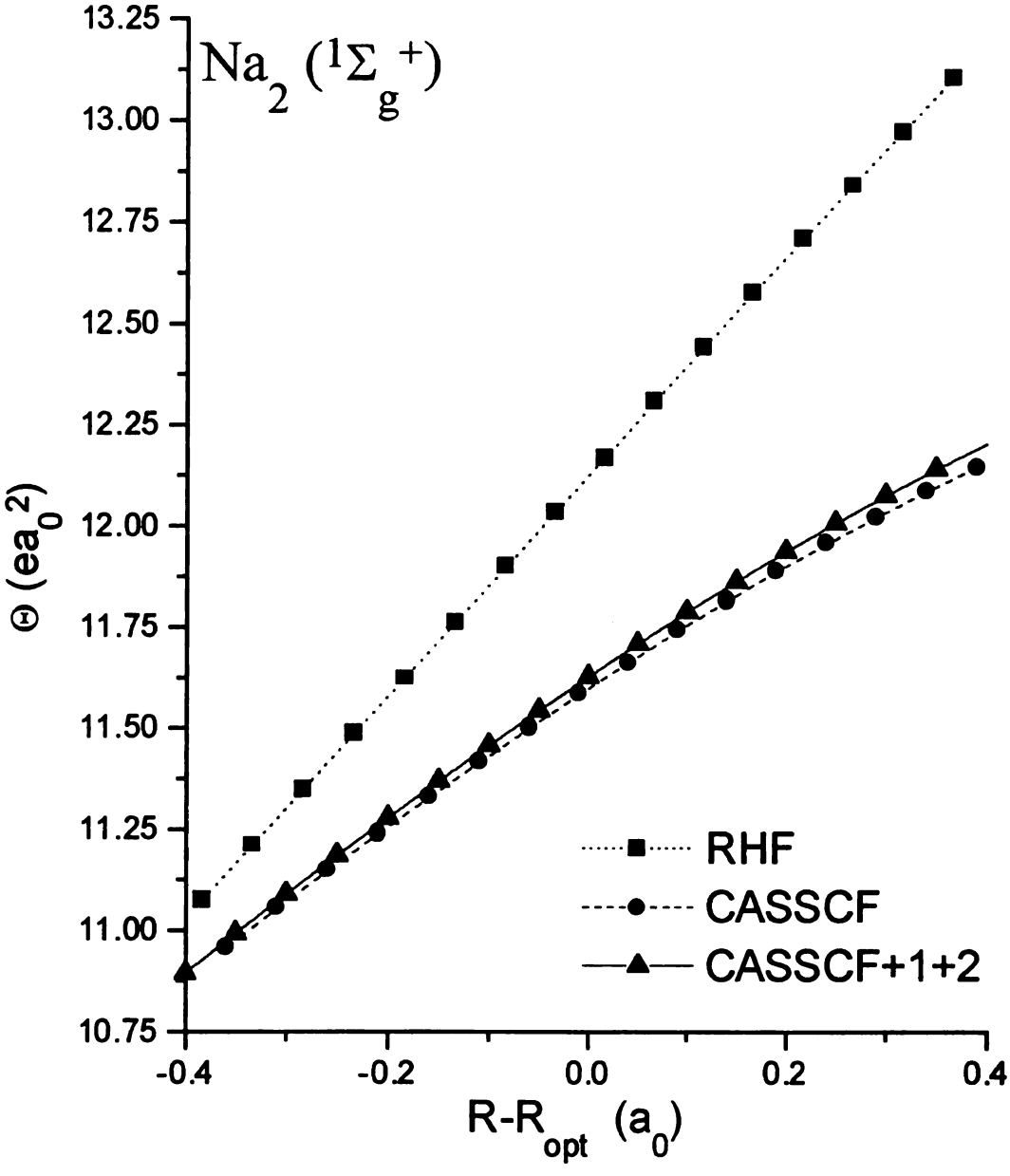

Figure 3. Distance dependence of Θ for Na_2 near R_{opt} calculated with various models using the V5Z basis.

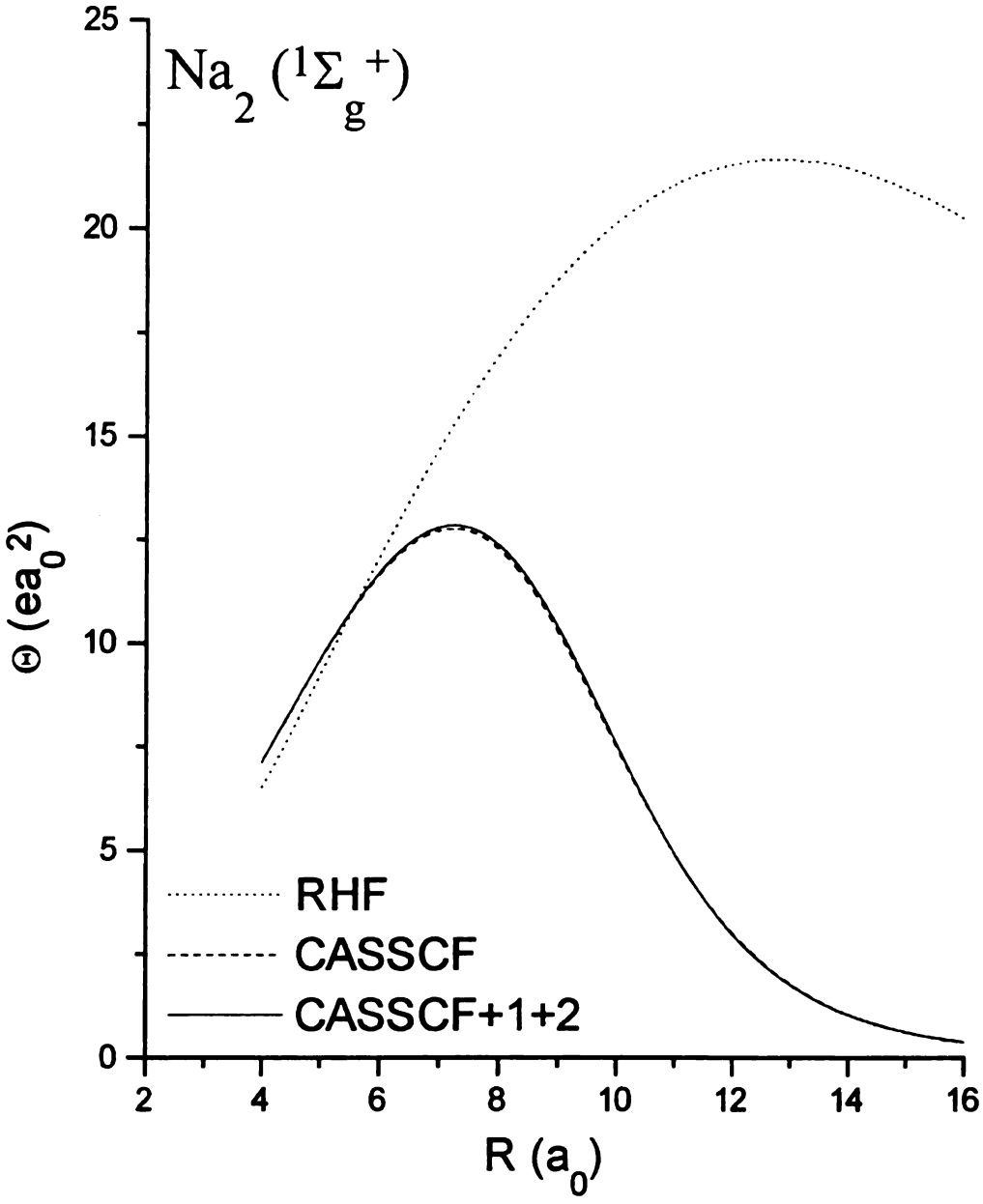

Figure 4. Distance dependence of Θ for Na_2 at large R calculated with various models using the VQZ basis.

and so our vibrationally corrected quadrupole moment is $\Theta(Na_2;v = 0)= +11.6372\ ea_0^2$. The large magnitude of the quadrupole moment makes the vibrational corrections relatively small for both Li_2 and Na_2. There is no reported experimental quadrupole moment for Na_2 dimer. Plots of $\Theta(R)$ over larger distances is given in Figure 4. The figure shows how closely the CASSCF and CASSCF+1+2 follow one another, while the RHF does rather well near the R_{opt} but fails at larger separations.

D. H_2, Li_2, and Na_2

Figure 5 contains the relative potential energy functions and Figure 6 contains $\Theta(R)$ for H_2, Li_2, and Na_2. The dissociation energy of H_2 is much larger than Li_2 or Na_2, while the quadrupole moment is much smaller. A maximum in $\Theta(R)$ occurs on each curve before the nuclear separation reaches the optimized geometry. This maximum in $\Theta(R)$ is attributed to a maximum in the decrease of electron density on either side of the nuclei along the bond axis. As the bond length moves towards zero, the electron density moves towards spherical symmetry and the associated quadrupole density approaches zero. All three molecules have similar shaped $\Theta(R)$ and differ only by magnitude. Li_2 and Na_2 have a significantly larger quadrupole moment due to their diffuse charge distribution and is discussed in the next section.

E. The Quadrupole Density of Li_2 and Na_2

The left-hand diagrams of Figures 7, 8, and 9 are contour plots of the density difference $\delta n(r)$ of H_2, Li_2, and Na_2. Looking first at H_2, we see a density increase,

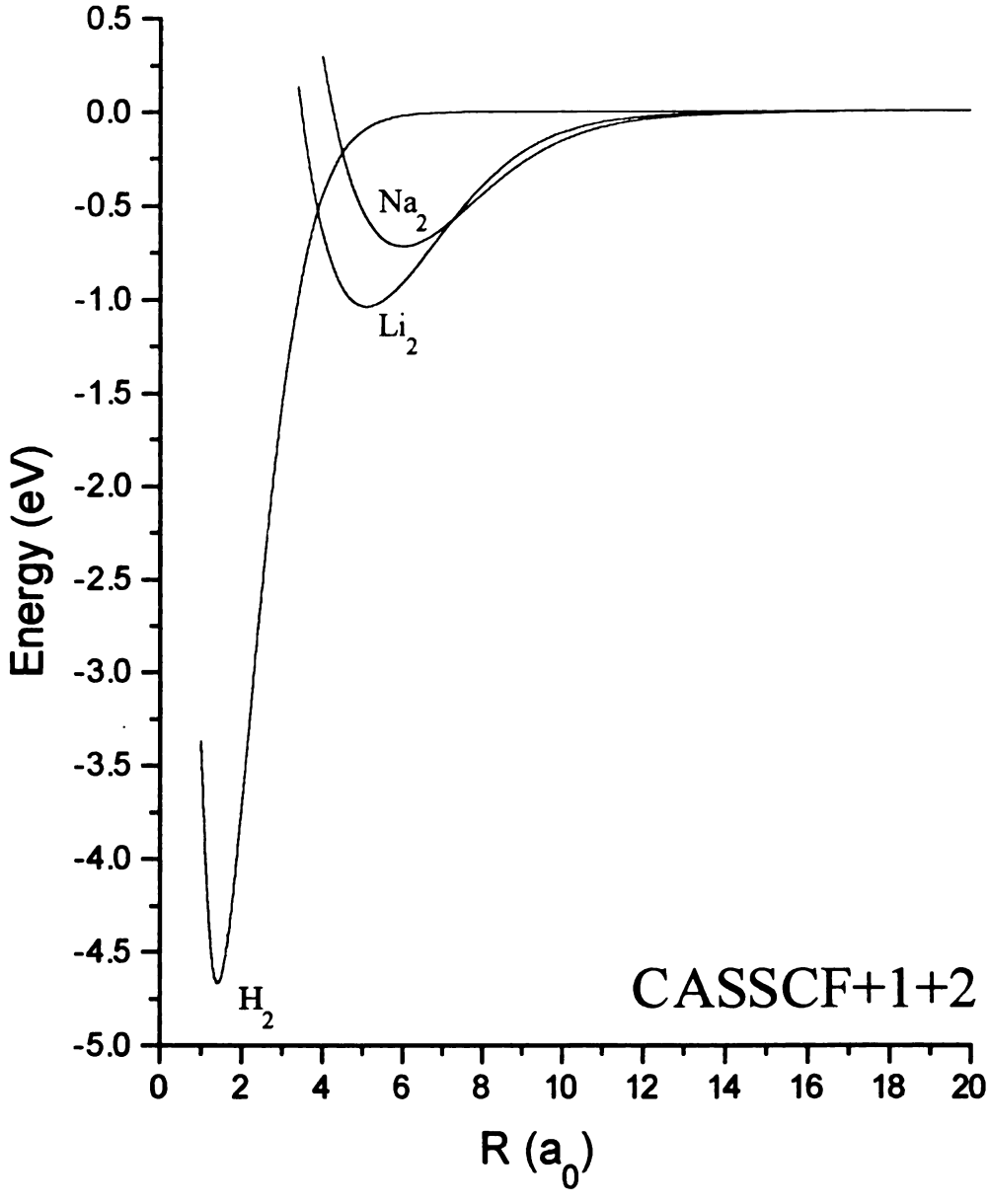

Figure 5. CASSCF+1+2 potential energy curves for H_2, Li_2, and Na_2 using the aug-cc-pv5z, A5Z, and VQZ, respectively.

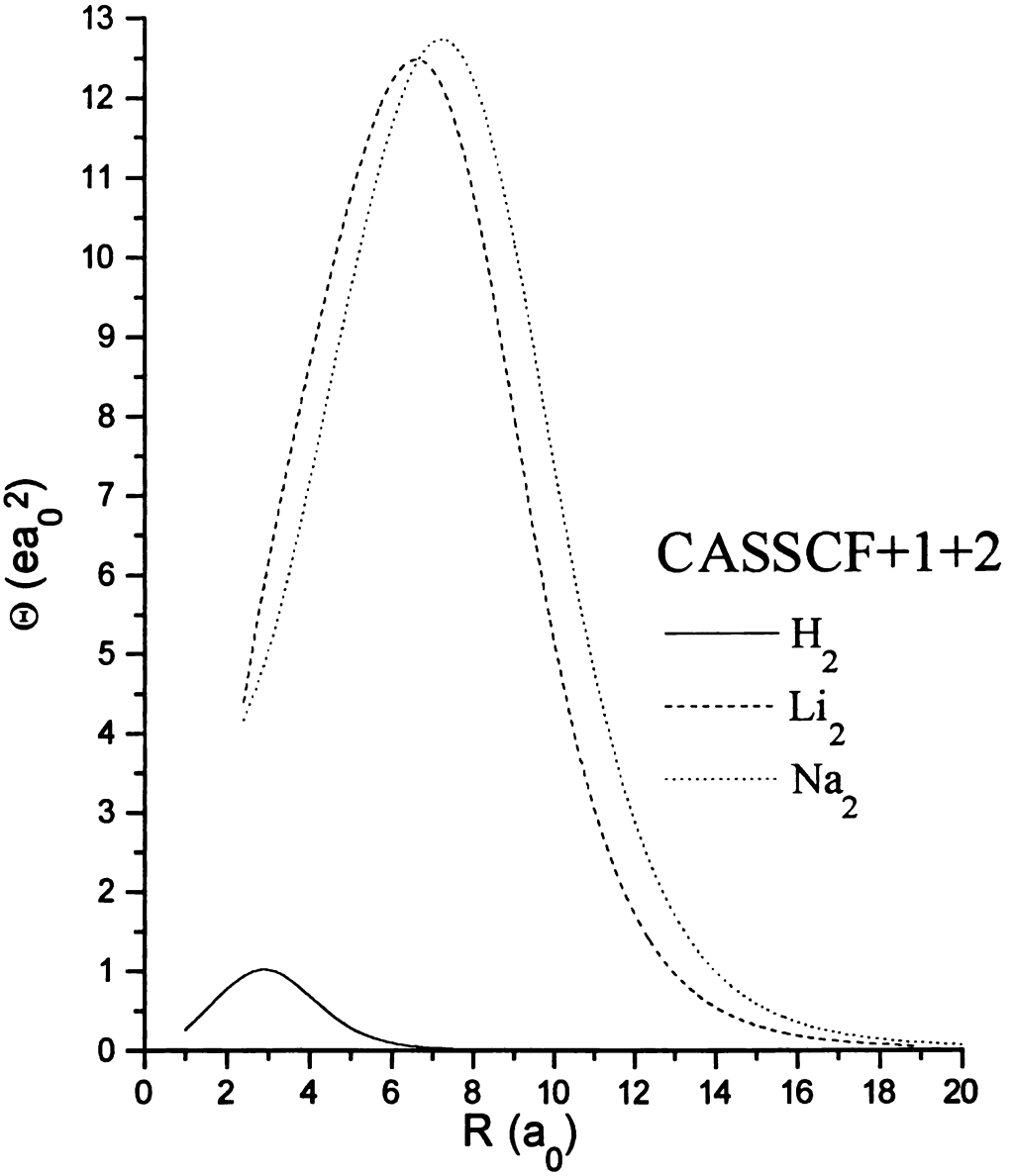

Figure 6. Distance dependence of Θ for H_2, Li_2, and Na_2 using the CASSCF+1+2 wavefuncvtion and aug-cc-pv5z, V5Z, and VQZ basis, respectively.

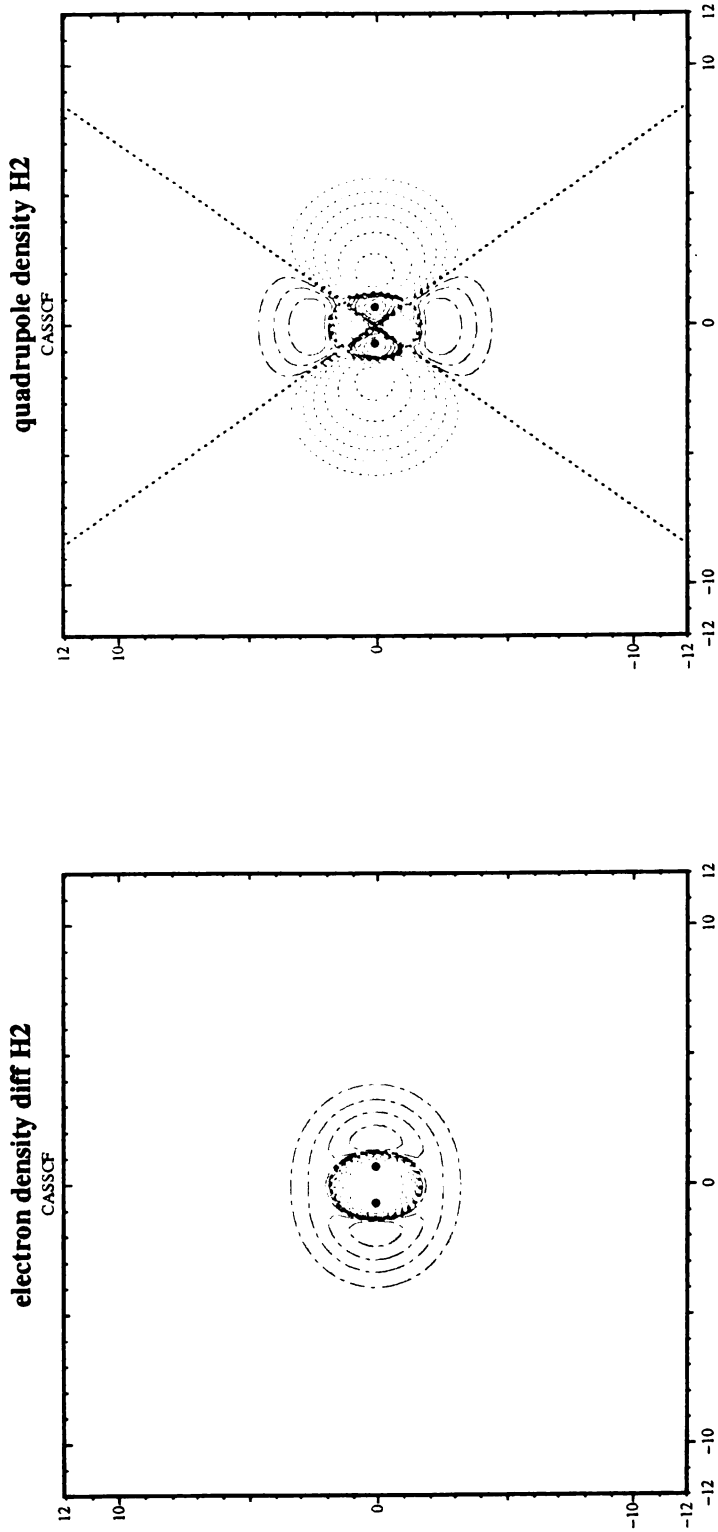

Figure 7. Electron-density difference and the associated quadrupole-density contours for H_2, at 1.4 a_0 calculated with CASSCF wavefunction and the aug-cc-pv5z. Contour values are ±0.0004, ±0.001, ±0.002, ±0.004, ±0.008, ±0.016. Blue represent positive contours and red represents negative.

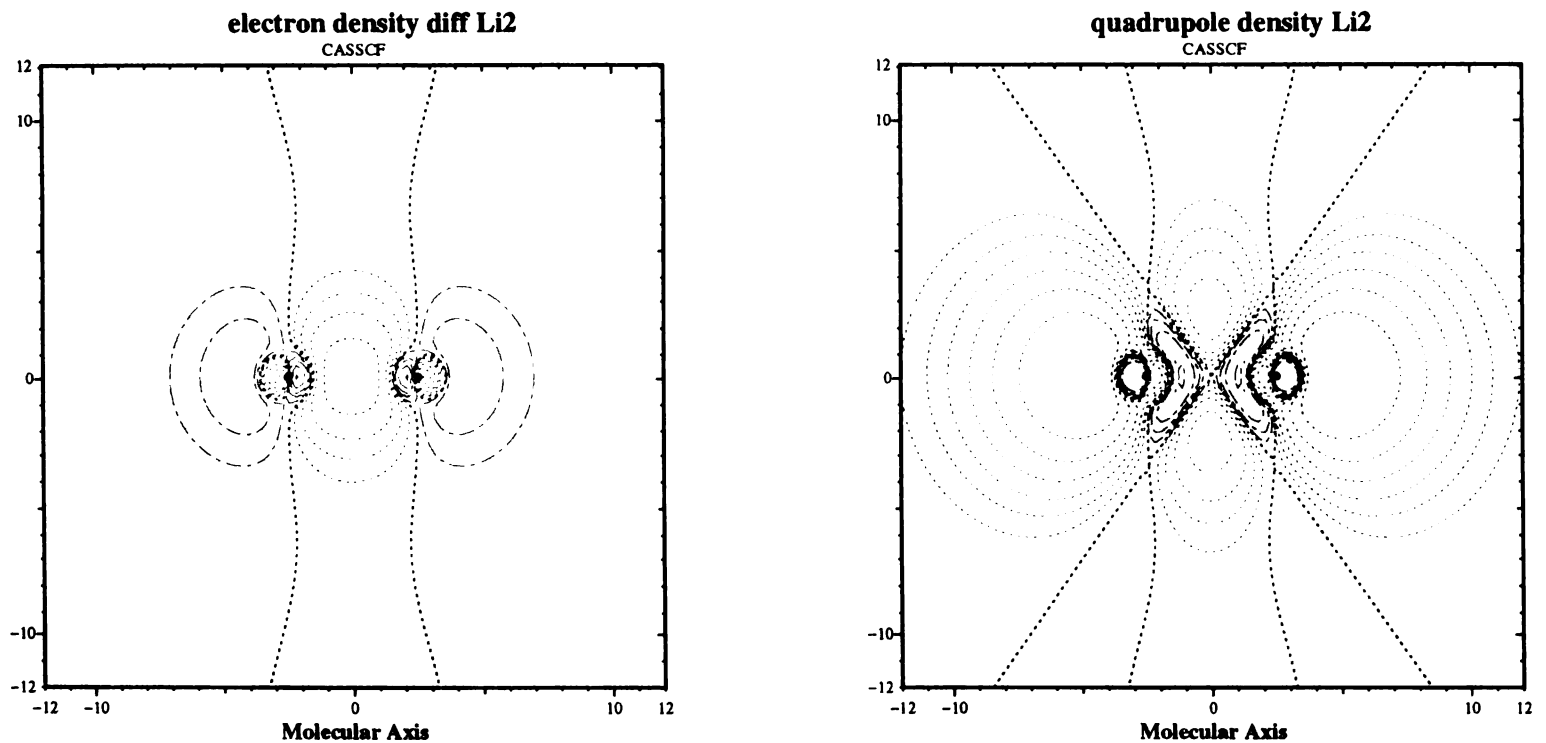

Figure 8. Electron-density difference and the associated quadrupole-density contours for Li_2, at 5.0 a_0 calculated with CASSCF wavefunction and the V5Z. Contour values are ±0.0004, ±0.001, ±0.002, ±0.004, ±0.008, ±0.016. Blue contours represent positive density and red contours represent negative density.

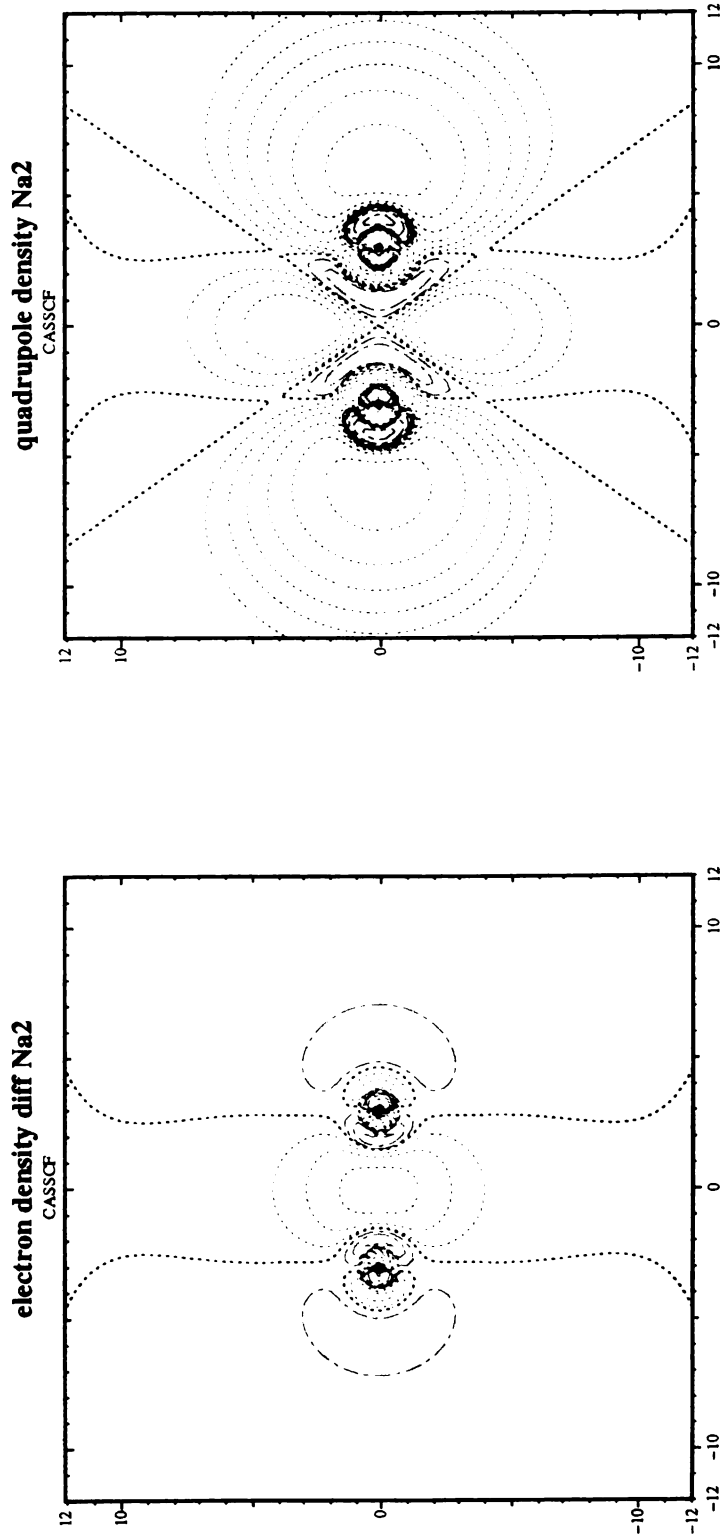

Figure 9. Electron-density difference and the associated quadrupole-density contours for Na_2, at 6.0 a_0 calculated with CASSCF wavefunction and the VQZ. Contour values are ±0.0004, ±0.001, ±0.002, ±0.004, ±0.008, ±0.016. Blue contours represent positive density and red contours represent negative density.

denoted by blue contours, mostly between the nuclei. Outside of this region is the depletion of density, denoted by the red contours. This depletion region is much more diffuse for Li_2 and Na_2 then for H_2. The minimum in this depletion is also closer to the nuclei in H_2, then in either Li_2 or Na_2. When we apply the quadrupole operator on $\delta n(r)$, the r^2 term has a greater effect on Li_2 and Na_2 due to their greater diffusive charge then on H_2. The contour diagrams for the quadrupole moment density for H_2, Li_2, and Na_2 are presented in the diagrams on the right of Figures 7, 8, and 9. The large magnitude of the quadrupole moment of Li_2 and Na_2 are well represented by the blue contours within these figure.

The density difference plots also reveal a complex nodal structure for Li_2 and Na_2 near the core electrons that is not present in the density difference of H_2. When 2 H atoms approach, electron density shifts between the nuclei. This is caused by electron-nuclear attraction pulling the density towards each nucleus. The nuclei are in-tern shielded from one another by the density increase. In Li_2, a similar situation occurs with the valence electrons, however, Li_2 also has 4 core electrons. The increase in density near the center of the molecule creates a repulsive force on the core electrons. The core electrons respond by shifting away from the center to either side of the nuclei as seen in Figure 8. Again Na_2 has a similar increase in electron density near the center of the molecule. Looking at the Figure 9, first at the center of the bond and moving along the z axis towards one of the nuclei, we see $\delta n(r)$ begins positive then becomes negative then again positive up to the nucleus. In bond formation, density from the core is first repelled by the density increase of the bonding region. This depletion in density de-shields the nuclei and attracts electron density closer to the nuclei. Due to the nodal structure of the quadrupole

density, these complex features of the bonding have little effect on the quadrupole. The quadrupole moment is primarily determined by the electron density away from the nuclei.

F. Conclusion

We have studied the quadrupole moments of Li_2 and Na_2 and related them to the quadrupole moment of H_2. There are no experimental values for the quadrupole moments of Li2 or Na2, however, we believe our values to be close to the 'true' quadrupole moments. The CASSCF+1+2 quadrupole moment of Li_2 was +10.9863 ea_0^2 while the CASSCF+1+2 quadrupole moment of Na_2 was +11.6479 ea_0^2. Using techniques developed in Chapter II, we have described why Li_2 and Na_2 have both the sign and magnitude of the quadrupole moment. The lack of sp hybridization keeps $\Theta(R)$ positive over all internuclear separations.

G. References

1. Williams, Jr., J. E.; Streitwieser, Jr., A. Chem. Phys. Lett. **1974**, *25*, 507.

2. van Duijneveldt, F. B. IBM Research Report No. RJ945, **1971**.

3. P.-O.Widmark, P.-A.Malmquist and B.O. Widmark, Malmquist, and Roos, Theor. Chim. Acta 77, 291 **1990**

4. MOLPRO is a package of *ab initio* programs written by H.J.Werner and P.J.Knowles, with contributions from J.Almof, R.D.Amos, M.J.O.Deegan, S.T.Elbert, C.Hampel, W.Meyer, K.Peterson, R.Pitzer, A.J.Stone, P.R.Taylor, R.Lindh, M.E.Mura, and T.Thorsteinsson

5. D.W.Davies and G.J.R.Jones, Chem. Phys. Lett. 81, 179 **1981**

6. R.P.Subramanian, M.A.Lee, K.E.Schmidt, J.W.Moskowitz, J.Chem.Phys. 97, 2600 **1992**

APPENDIX A

Calculation of the Quadrupole Moment

A. Multipole Moments

The potential at an arbitrary point P created by a static molecular charge distribution can be written as

$$V(\vec{R}) = -\int \frac{\eta(\vec{r})}{\left|\vec{R}-\vec{r}\right|} d^3\vec{r} + \sum_k^{nuclei} \frac{Z_k}{\left|\vec{R}-\vec{r}_k\right|} \qquad (1)$$

where the first term is the potential due to the electronic charge distribution $\eta(\vec{r})$ and the latter term represents the contribution due to the nuclei Z_k. This form of the electrostatic potential is written in terms of an arbitrary origin **O** where the distance $\left|\vec{R}-\vec{r}\right|$ is the distance between $\vec{R}$ and the corresponding $\vec{r}$, as shown in the Figure.

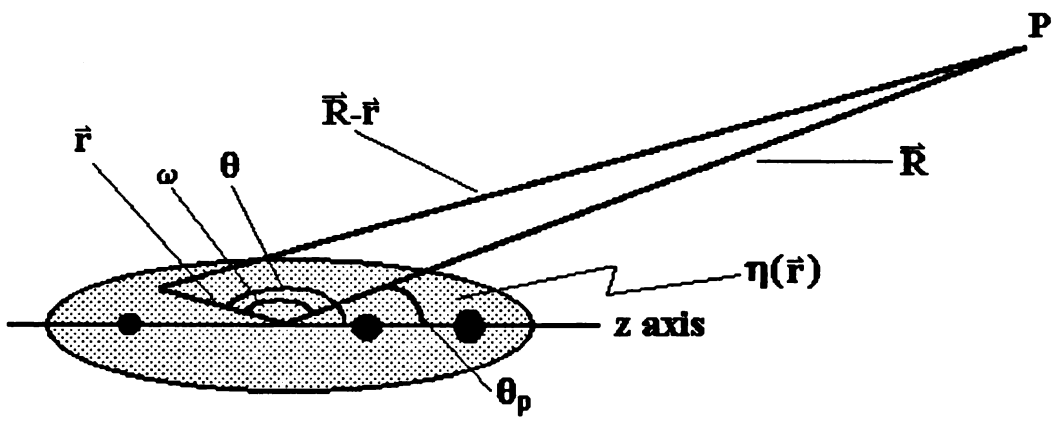

Figure A-1. The potential at an arbitrary point P created by a static molecular charge distribution.

The point P is taken as infinitely away from the charge distribution and the nuclei are considered as fixed point charges. The nuclear contributions can thus be computed analytically as classical charges and the electrostatic potential can be evaluated independently of the origin.[1,2]

If we consider the nuclear component first, θ_p can be taken as the angle between $\vec{R}$ and $\vec{r}_k$, where $\vec{r}_k$ is the correspond nuclear coordinate, by law of cosines $\left|\vec{R}-\vec{r}\right|$ becomes

$$\begin{aligned}\left|\vec{R}-\vec{r}_k\right|^2 &= r_k^2 + R^2 - 2r_k R\cos\theta_p \\ &= R^2\left[1-\left(2\cos\theta_p\right)\left(\frac{r_k}{R}\right)+\left(\frac{r_k}{R}\right)^2\right]\end{aligned} \tag{2}$$

Taking the square root and reciprocal gives

$$\frac{1}{\left|\vec{R}-\vec{r}_k\right|} = \frac{1}{\vec{R}}\left[1-\left(2\cos\theta_p\right)\left(\frac{r_k}{R}\right)+\left(\frac{r_k}{R}\right)^2\right]^{-1/2} \tag{3}$$

Using the series expansion

$$(1+a)^n = 1+na+\frac{n(n-1)}{2!}a^2+\cdots \tag{4}$$

gives

$$\frac{1}{\left|\vec{R}-\vec{r}_k\right|} = \frac{1}{R}\left[1+\cos\theta_p\left(\frac{r_k}{R}\right)+\tfrac{1}{2}\left(3\cos^2\theta_p-1\right)\left(\frac{r_k}{R}\right)^2+\cdots\right] \tag{5}$$

with this expansion the potential at the point P becomes

$$V(\vec{R}) = \frac{1}{R}\sum_{k=1}^{N}\left[1+\cos\theta_p\left(\frac{r_k}{R}\right)+\tfrac{1}{2}\left(3\cos^2\theta_p-1\right)\left(\frac{r_k}{R}\right)^2+\cdots\right]Z_k \tag{6}$$

which can be written as

$$V(\vec{R}) = \frac{1}{R}\sum_{k=1}^{N}Z_k + \frac{1}{R^2}\sum_{k=1}^{N}Z_k r_k\cos\theta_p + \frac{1}{R^3}\sum_{k=1}^{N}Z_k r_k^2\frac{3\cos^2\theta_p-1}{2}+\cdots \tag{7}$$

For a continuous cylindrically symmetric charge distribution as in the electrons about the nuclei, the corresponding expansion of the potential can be written as

$$V(\vec{R}) = -\left[\int \frac{\eta(r)}{R} d^3r + \int \frac{r\eta(r)}{R^2} \cos\omega \; d^3r + \int \frac{r^2\eta(r)}{R^3}\left(\frac{3\cos^2\omega - 1}{2}\right) d^3r + \cdots\right] \quad (8)$$

where $\cos\omega = \cos(\theta - \theta_p)$ The negative sign reflects the negative charge of the electronic distribution. The first terms, $1/R$, is the monopole term, the second term , $1/R^2$, is the dipole, the third term, $1/R^3$, is the quadrupole; the next is the octopole, etc...

Writing sum of both the nuclear and electronic components for a molecule in Cartesian form gives

$$Q = -\int \eta(\vec{r}) d\tau + \sum_{k=1}^{nuc} Z_k \quad (9)$$

$$\mu_\alpha = -\tfrac{1}{2}\int \eta(\vec{r}) r_\alpha d\tau + \sum_{k=1}^{nuc} Z_k r_\alpha \quad (10)$$

$$\begin{aligned} \Theta_{\alpha\beta} &= -\tfrac{1}{2}\int \eta(\vec{r})\left[3r_\alpha r_\beta - r^2\delta_{\alpha\beta}\right] d\tau + \sum_{k=1}^{nuc} Z_k\left[3r_\alpha r_\beta - r^2\delta_{\alpha\beta}\right] \\ &= -\tfrac{1}{2}\int \eta(\vec{r}) r^2\left(3\cos^2\theta - 1\right) d\tau + \sum_{k=1}^{nuc} Z_k r^2\left(3\cos^2\theta - 1\right)/2 \end{aligned} \quad (11)$$

or in general :

$$\begin{aligned} M_{\alpha\beta\cdots\omega} &= \frac{(-1)^m}{m!}\int \eta(\vec{r}) r^{2m+1} \frac{\partial^m}{\partial r_\alpha \partial r_\beta \ldots \partial r_\omega}\left(\frac{1}{r}\right) d\tau \\ &\quad + \sum_{k=1}^{nuc} \frac{(-1)^m}{m!} Z_k r^{2m+1} \frac{\partial^m}{\partial r_\alpha \partial r_\beta \ldots \partial r_\omega}\left(\frac{1}{r}\right) \end{aligned} \quad (12)$$

where Q, μ_α, $\Theta_{\alpha\beta}$, and $M_{\alpha\beta\ldots\omega}$ are components of the charge, dipole, quadrupole, and in general m^{th} rank tensors, respectively.

B. Experimental Evaluation

Most experimentally determined values of molecular quadrupole moments were obtained by indirect methods involving the interaction between two or more molecules. Thus pressure broadening of the pure rotational and inversion spectra of gases can lead to information about molecular quadrupole moments.[4,5] Other indirect methods involve the use of the second virial coefficients[6], heats of sublimation of single crystals at 0 °K [7], and dielectric constants.[8,9] Quadrupole moments determined by any of these methods depend on assumptions made about the sign of the quadrupole and the interaction potential.[10]

In 1958, A.D. Buckingham presented a direct experimental technique to determine the molecular quadrupole moment of gaseous non-dipolar molecules.[11] The apparatus consisted of a glass tube enclosing four parallel wires acting as condensers. The gaseous molecules between the wires experience a torque in the field gradient created by the wires with charge. The quadrupole moment of the molecules can then be evaluated from the index of refraction by the relationship

$$n_z - n_y = 2\pi N F'_{xx}\left[B' + \frac{2\Theta(\alpha_{//} - \alpha_{\perp})}{15kT}\right] \qquad (13)$$

where $(\alpha_{//} - \alpha_{\perp})$ is the anisotropy in the molecular polarizability; B describes the change in the effective polarizability induced by the field gradient, F_{xx}' is the externally generated fieled gradient, and T is temperature. This technique has given N_2 ($^1\Sigma_g^+$) a quadrupole moment of -1.05 ea_0^2.[12] This direct experimental technique, however,

has proven to be extremely difficult, especially for diatomic gases that are highly reactive.[12-15]

C. Theoretical Evaluation

1. Ab-Initio Methods

Throughout this work, we use the Augmented Dunning Correlation Consistent basis sets[16a,16b] and refer to them as aug-cc-pvXz, where X is a cardinal number (2-5) characterizing the basis. Because of technical limitations in the COLUMBUS properties program, we deleted angular functions of g or greater. The SCF, Möller-Plesset and CISD calculations were done using g92/DFT[17], MCSCF and MRCI calculations used the COLUMBUS[18] suite of codes and the full CASSCF and CASSCF+1+2 were done using MOLPRO[19]. We use the traceless form of the quadrupole-moment operator[4], which, for a homonuclear diatomic, reads

$$\hat{\Theta}_{zz} \equiv \hat{\Theta} = -\frac{1}{2}\sum_{i=1}^{N_e}\left(3z_i^2 - r_i^2\right) + \frac{1}{2}ZR^2 \qquad (14)$$

where Z is the atomic number of the nuclei in the diatomic and R is the internuclear separation. We use atomic units throughout, except where explicitly noted. In these units, one atomic unit of quadrupole moment $\left(ea_0^2\right)$ contains 1.344911 Buckinghams, 4.4866×10^{-40} CM^2, and 1.344911×10^{-26} esu cm^2.

We estimate the complete basis set(CBS) limit[16a] of a property by fitting the property values to a function of the form

$$P(X) = P(\infty) + Be^{-CX} \qquad (15)$$

where X is the cardinal number of the basis set and $P(X)$ is the property calculated with that basis.

Appendix C contains the collected tables of the quadrupole moments and other properties of $H_2(^1\Sigma_g^+)$, $Li_2(^1\Sigma_g^+)$, $B_2(^3\Sigma_g^-)$, $C_2(^1\Sigma_g^+)$, $N_2(^1\Sigma_g^+)$, $O_2(^3\Sigma_g^-)$, $F_2(^1\Sigma_g^+)$, Na_2 $(^1\Sigma_g^+)$, $Al_2(^3\Sigma_g^-)$, $Si_2(^3\Sigma_g^-)$, $P_2(^1\Sigma_g^+)$, $S_2(^3\Sigma_g^-)$, and $Cl_2(^1\Sigma_g^+)$ for various wavefunctions as a function of basis set. The MP2 wavefunctions include excitations from the $1\sigma_g$ and $1\sigma_u$ orbitals of H_2 through F_2. For molecules N_2 through F_2, the MCSCF wavefunctions are CASSCF functions over 6 MO's derived from the valence p orbitals (the $3\sigma_g$, $3\sigma_u$, $1\pi_{ux}$, $1\pi_{uy}$, $1\pi_{gx}$, $1\pi_{gy}$). The MRCI incorporates all single and double excitations from these six orbitals, as well as all double excitations from the $2\sigma_g$ and $2\sigma_u$ orbitals. The CASSCF wavefunctions include the $2\sigma_g$ and $2\sigma_u$ orbitals along with the 6 orbitals described above, and the CASSCF+1+2 wavefunction consists of all single and double excitations from the CASSCF reference space. For O_2, both ROHF and UHF results are reported.

For the second row homonuclear diatomics (Na_2 through Cl_2), The MP2 wavefunctions include excitations from the $4\sigma_g$ and $4\sigma_u$ orbitals. The CASSCF wavefunctions include all valence electrons and the 8 orbitals (the $4\sigma_g$, $4\sigma_u$, $5\sigma_g$, $5\sigma_u$, $2\pi_{ux}$, $2\pi_{uy}$, $2\pi_{gx}$, $2\pi_{gy}$), and the CASSCF + 1 + 2 wavefunction consists of all single and double excitations from the CASSCF reference space. As with O_2, both ROHF and UHF results are reported for S_2. Of the wavefunctions used, the best is expected to be the CASSCF+1+2. This wavefunction utilizes the optimized orbitals from the CASSCF to provide much of the correlation energy and a large active space able to accurately describe the valance region of the molecule.

2. Expectation Values

The general procedure for calculating physical properties requires each of the dynamical variables of the system to be represented in the formalism by a linear operator. The process of evaluating a physical quantity then corresponds to operating on the wave function by the corresponding operator. Consider an arbitrary dynamical variable which is represented by the operator $\hat{O}$. Then the 'expectation value' of $\hat{O}$, when the system is in the state ψ, is given by

$$\langle O \rangle = \int \Psi^* \hat{O} \Psi d\tau \tag{16}$$

This is the mean value of $\hat{O}$ which will be obtained by making repeated measurements when the system is known to be in the state ψ prior to each measurement[20,21].

Permanent multipole moments of molecules are first order properties that can be given as expectation values of the corresponding one-electron operator.

$$\Theta = \tfrac{1}{2} \sum_i \left(3 r_{i\alpha} r_{i\beta} - \delta_{\alpha\beta} r_i^2\right) q_i \tag{17}$$

resulting in

$$\Theta_{\alpha\beta} = -\tfrac{1}{2} \int \eta(\vec{r}) \left[3 r_\alpha r_\beta - \vec{r}^{\,2} \delta_{\alpha\beta}\right] d\tau \tag{18}$$

where r_α and r_β are a Cartesian coordinates and $r^2 = \left(x^2 + y^2 + z^2\right)$. For a cylindrically symmetric system

$$-\tfrac{1}{2}\Theta_{zz} = \Theta_{xx} = \Theta_{yy} = -\tfrac{1}{2}\Theta \tag{19}$$

The corresponding quantum mechanical expectation value is

$$\Theta_{\alpha\beta} = \left\langle \Psi \left| \sum_{i=1}^{N} -\tfrac{1}{2} \left[3 r_{i\alpha} r_{i\beta} - r_i^2 \delta_{\alpha\beta}\right] \right| \Psi \right\rangle + \Theta_{zz}^{NUC} \tag{20}$$

where

$$\Theta_{zz}^{NUC} = \tfrac{1}{2}\sum_{\lambda} Z_{\lambda}\left(\left[3r_{\alpha\lambda}r_{\beta\lambda} - \bar{r}_{\lambda}^{2}\delta_{\alpha\beta}\right]\right) \qquad (21)$$

where λ is the index of the nucleus. Given a wavefunction determined by *ab initio* techniques, the quadrupole moment can be determined by effectively operating the wavefunction on the appropriate operator and adding in the nuclear contribution.[22]

3. Point Charge Method

An alternate approach to the calculation of moments and polarizabilities uses one or more fixed charges placed in a vicinity of the molecule.[23] One or more charges are placed around the molecule in regions where the molecular wavefunctions are negligible. This technique allows for the incorporation of uniform and nonuniform electric field contributions due to gradients and higher order field derivatives. The static properties are then determined as extrapolations from the diminishing interaction energies. It is important that the basis set used be adequate to describe any polarization of the molecule in the presence of this field.[24]

In this method the field applied should be small enough to let a truncated expansion accurately represent the moment or energy and strong enough to ensure an effect can be calculated with numerical significance. Generally charges are place 30 - 60 a_0 from the center of the molecule depending on the magnitude of the charge, and the resulting uniform field components range from 0.002 to 0.05 ea_0. If the charges are placed in special arrangements around the molecule, the contributions from the field gradients can be eliminated. For instance, with a homonuclear diatomic, two

charges could be placed along the molecular axis at distances equal but opposite in magnitude to the center of the molecule. This would prevent an additional induced dipole and dipole-quadrupole contribution to the potential.

The Hamiltonian of a molecule $\hat{H}^P$ in the presence of a field may be expanded about the field free Hamiltonian $\hat{H}^0$ in terms of the molecular multipole moment tensors as

$$\hat{H}^P = \hat{H}^0 - \hat{\mu}_\alpha F_\alpha - \tfrac{1}{3}\hat{\Theta}_{\alpha\beta}F_{\alpha\beta} - \tfrac{1}{15}\hat{\Omega}_{\alpha\beta\gamma}F_{\alpha\beta\gamma} - \cdots \qquad (22)$$

and the corresponding perturbed energy[25]

$$\begin{aligned} E^P = E^0 &- \mu_\alpha F_\alpha - \tfrac{1}{3}\Theta_{\alpha\beta}F_{\alpha\beta} - \tfrac{1}{15}\Omega_{\alpha\beta\gamma}F_{\alpha\beta\gamma} \\ &- \tfrac{1}{3}A_{\alpha,\beta\gamma}F_\alpha F_{\beta\gamma} - \tfrac{1}{6}C_{\alpha\beta,\gamma\delta}F_{\alpha\beta}F_{\gamma\delta} - \cdots \\ &- \tfrac{1}{6}B_{\alpha,\beta,\gamma\delta}F_\alpha F_\beta F_{\gamma\delta} + \cdots \end{aligned} \qquad (23)$$

where F_α, $F_{\alpha\beta}$, ... are the field, field gradient, etc. at the origin. E^0, μ, Θ, Ω are the energy, dipole, quadrupole, and octopole moment tenors, respectively and A, B, and C are the pure dipole, dipole-quadrupole, and pure quadrupole polarizability tensors of the field free molecule.[26]

From Equation 23 it can be seen that the energy of a charge system in an electrostatic field is the sum of the energies of a point charge in a potential, a dipole in a uniform field, a quadrupole in a field gradient, and an octopole in the gradient of a field gradient. In general, there will be a torque acting on a rigid charged body in an electric field, the torque about any point being proportional to the multipole moments about that point as origin.

As stated earlier, if the charges are placed in special arrangements around the molecule, the contributions from the field gradients can be eliminated and induced

dipoles can be prevented in such a way to conveniently determine the quadrupole moment for a homonuclear diatomic. By placing two point charges at equi-distant yet opposite sides of the origin along the z axis, the quadrupole moment can be determined by the interaction energy as shown in the figure below.

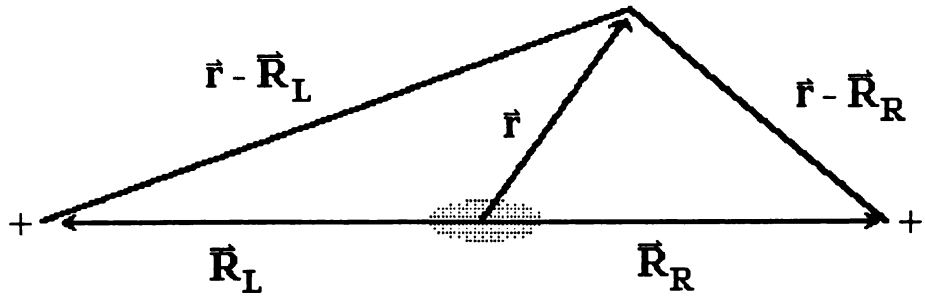

Where $|R_L| = |R_R|$, for a symmetric charge distribution about the Z axis

$$E^p = E^0 - \mu F_z - \tfrac{1}{2}\Theta F_{zz}^{"} - \tfrac{1}{6}\Omega F_{zzz}^{"'} \cdots \tag{24}$$

becomes

$$E^p - E^0 = -\tfrac{1}{2}\Theta F_{zz}^{"} - \tfrac{1}{6}\Omega F_{zzz}^{"'} \cdots \tag{25}$$

where

$$F_{zz}^{"} = 4/R^3; \qquad F_{zzz}^{"'} \propto 1/R^4 \tag{26}$$

where Θ becomes the intercept of the line

$$\tfrac{1}{2}(\Delta E)R^3 = -\Theta - D/R \tag{27}$$

4. Finite Field Method

The *ab initio* calculation of moments and polarizabilites can be accomplished directly from the solution of the Schrodinger equation with an augmented Hamiltonian. The finite-field approach incorporates the electric field terms directly

into the Hamiltonian for a fixed field strength and the wavefunction is solved at that strength.[25] This method has not been employed in this work and is mentioned only briefly. This method is more thoroughly described by Sadjle[26] in and the references therein.

D. References

1. A. Shadowitz, "The Electromagnetic Field", Dover Publications, Inc., New York, **1988**, p.242

2. R. Becker,"Electromagnetic Fielda and Interactions", Dover Publications, Inc., New York, **1982**, p.80

3. A.D. Buckingham, Trans. Faraday Soc. **1956**, 52, 747

4. Gordy, Smith, and Trambarulo, " Microwave Spectroscopy", John Wiley & Sons, Inc., New York, **1953**, Chap. 7

5. W.V. Smith, J.Chem. Phys. **1956**, 25, 510

6. J.A. Pople, Proc. Roy. Soc. (London) **1954**, A221, 508

7. Jansen, Michels, and Lupton, Physica **1954**, 20, 1235

8. A.D. Buckingham and J.A. Pople, Trans. Faraday Soc. **1955**, **51**, 1029

9. R.W. Zwanzig, J. Chem. Phys. **1956**, 25, 211

10. D.E. Stoygryn and A.P. Stogryn, Mol. Phys., **1966**, 11, 371

11. A.D. Buckingham, J.Chem.Phys., **1959**, 30, 1580.

12. A.D. Buckingham, C. Graham, and J.H. Williams, Mol. Phys., **1983**, 49, 703

13. A.D. Buckingham, R.L. Disch, and D.A.Dunmur, J. Amer. Chem., **1968**, 90, 3104

14. C. Graham, J. Pierrus, and R.E. Raab, Mol. Phys., **1989**, 67, 939

15. R.A. Bonham and M. Fink, Phys. Rev. A **1986**, 33, 1569

16a. Dunning, T. H., Jr., *J. Chem. Phys.* **1989**, ***90***, 1007; Kendall, R. A., Dunning, T. H., Jr., and Harrison, R. J., *J. Chem. Phys.* **1992**, *96*, 6796; Peterson, K. A., Kendall, R. A., and Dunning, T. H., Jr., *J. Chem. Phys.* **1993**, *99*, 9790.

16b. Basis sets were obtained from the Extensible Computational Chemistry Environment Basis Set Database, Version 1.0, as developed and distributed by the Molecular Science Computing Facility, Environmental and Molecular Sciences Laboratory, which is part of the Pacific Northwest Laboratory, P. O. Box 999, Richland, Washington 99352, USA, and funded by the U. S.

Department of Energy. The Pacific Northwest Laboratory is a multi-program laboratory operated by Battelle Memorial Institute for the U. S. Department of Energy under contract DE-AC06-76RLO 1830. Contact David Feller, Karen Schuchardt, or Don Jones for further information.

17. *Gaussian 92*, Revision A, Frisch, M. J., Trucks, G. W., Head-Gordon, M., Gill, P. M. W., Wong, M. W., Foresman, J. B., Johnson, B. G., Schlegel, H. B., Robb, M. A., Replogle, E. S., Gomperts, R., Andres, J. L., Raghavachari, K., Binkley, J. S., Gonzalez, C., Martin, R. L., Fox, D. J., Defrees, D. J., Baker, J., Stewart, J. J. P., and Pople, J. A., Gaussian, Inc., Pittsburgh PA, 1992.

18. Shepard, R., Shavitt, I., Pitzer, R. M., Comeau, D. C., Pepper, M., Lischka, H., Szalay, P. G., Ahlrichs, R., Brown, F. B., and Zhao, J. G., *Int. J. Quantum Chem. Symp.* **1988**, *22*, 149.

19. MOLPRO is a package of *ab initio* programs written by H.J.Werner and P.J.Knowles, with contributions from J.Almof, R.D.Amos, M.J.O.Deegan, S.T.Elbert, C.Hampel, W.Meyer, K.Peterson, R.Pitzer, A.J.Stone, P.R.Taylor, R.Lindh, M.E.Mura, and T.Thorsteinsson

20. P.A.M.Dirac,The Priciples of Quantum Mechanics, Oxford Science Publications, 4th Ed., **1991**

21. E.Merzbacher, Quantum Mechanics, John Wiley & Sons, 2nd Ed., **1970**

22. A. Szabo and N.S.Ostlund, Modern Quantum Chemistry, McGraw-Hill Publishing, 1st. Ed. rev., **1982**

23. A.D. Buckingham, in *Intermolecular Interactions: From Diatomics to Biopolymers*, edited by B. Pullman (Wiley, New York, 1978), p. 1.

24. G.C. Maitland, M. Rigby, E.B.Smith, and W.A. Wakeham, Intermolecular Forces: Thier Origin and Determination (Clarendon, Oxford, 1981).

25. A.D. Buckingham, Adv. Chem. Phys., **1967**, 12, 107

26. (a) A.J. Thakkar, J.Chem. Phys.,**1981**, 75, 4496; A.Koide, W.J. Meath, and A.R.Allnatt, J.Phys.Chem., **1982**, 86, 1222; (b) D.M. Bishop and B.Lam, Phys. Rev.A, **1988**, 37, 464

APPENDIX B

Basis Sets

A. Description

The *Dunning correlation consistent basis sets* have been defined as to contain all of the correlating functions which lower the correlation energy by similar amounts as well as all correlating functions which lower the energy by larger amounts.[1] For example, the Nitrogen (9s4p1d) primitive set contracted to [3s2p1d] is the simplest correlation consistent basis set, since the 3*s* and 2*p* spatial functions lower the correlation energy by approximately the same amount as the 1d set; all other functions lower the correlation energy by substantially smaller amounts. This is referred to as the correlation consistent polarized valence double-zeta (cc-pvdz) set. Other correlation consistent basis sets for Boron through Fluorine include a (10s5p2d1f) set contacted to [4s3p2d1f] referred to as the correlation consistent polarized valence triple-zeta (cc-pvtz), a (12s6p3d2f1g) contracted to [5s4p3d2f1g] referred to as the correlation consistent polarized valence quadrupole-zeta (cc-pvqz) set, and a (14s8p4d3f2g1h) contracted to [6s5p4d3f2g] as the correlation consistent polarized valence 5-zeta (cc-pv5z). Due to technical limitations, calculations in this work have only included s, p, d, and, f basis functions unless otherwise stated.

Augmenting these basis sets with spatially diffuse basis functions dramatically improves the description of certain properties, especially those strongly influenced by the outer electron charge distribution. Dunning provides a series of augmented basis functions, constructed specifically for the evaluation of electron affinities of atoms.[2,3] For each correlation consistent basis set, an additional s, p, d, f, g, h basis function is available. Since these functions are spatially diffuse, their contribution to the shape of the molecular potential energy surface is negligible. They do, however, have a

significant effect on the charge distribution, and therefore, properties, away from the nuclei. Figure 1 shows a comparison of the molecular potential energy surface of the cc-pvtz basis set and a CASSCF+1+2 wavefunction to RKR data[4]. Figure 2 is a comparison of the total energy of $O_2(^3\Sigma_g^-)$ using the augmented and non-augmented basis sets at the ROHF and MP2 level. As can be seen in the figure, both the augmented and non-augmented converge rather well to the basis set model limit. The quadrupole moment, however, is much more sensitive to the basis sets used, as can be seen in Figure 3. Figure 3 is a plot comparing $O_2(^3\Sigma_g^-)$ ROHF and MP2 quadrupole moments computed with augment to non-augmented basis functions. By looking at Figure 3, its immediately apparent to the importance of augmenting the basis functions when modeling a property such as the quadrupole moment.

This appendix lists the Dunning Correlation Consistent Basis Sets[5] used in the main component of this thesis. Attached at the end of each basis set are the augmented functions optimized for each particular set. The basis sets are listed in a format that is compatible with the input file for the Gaussian94[6] suite of codes.

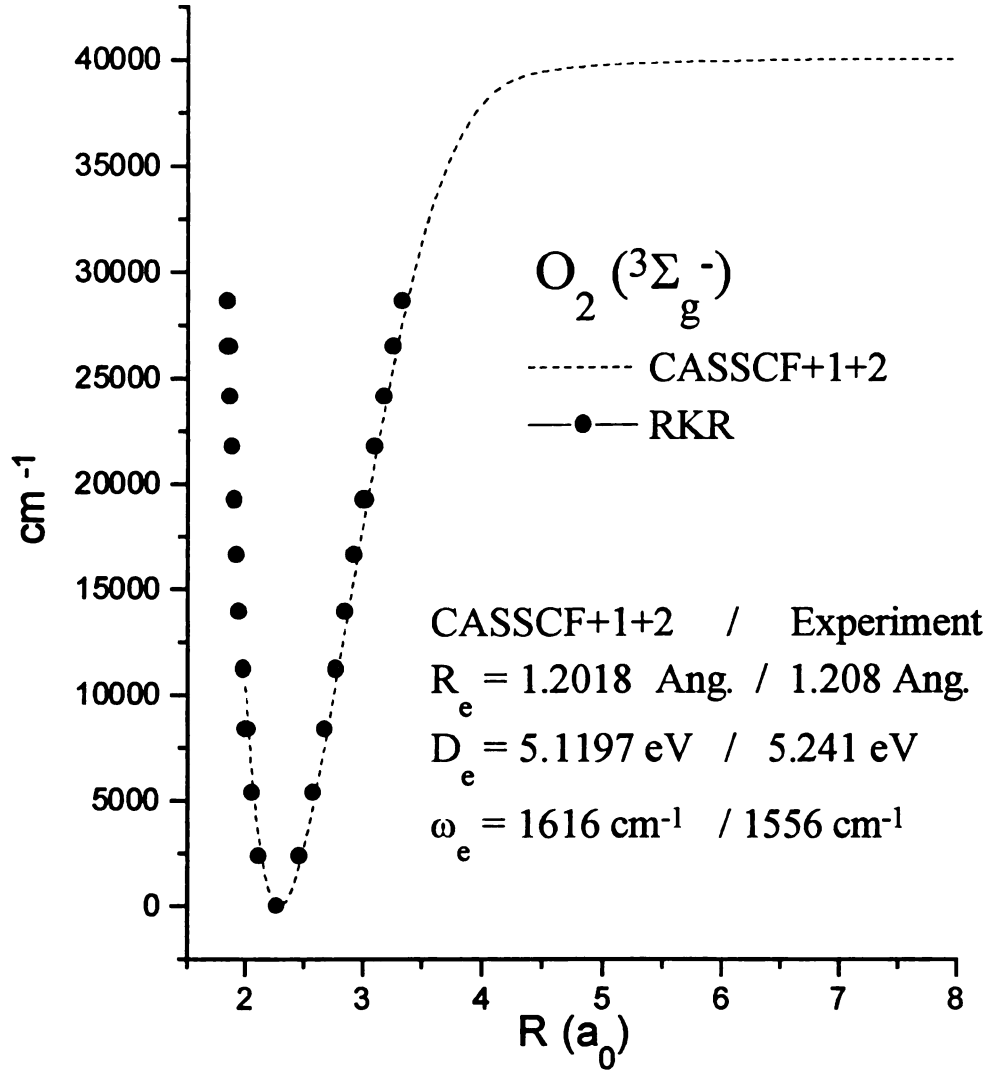

Figure 1. Comparison of O_2 RKR data to CASSCF+1+2 potential energy curve using the cc-pvtz basis.

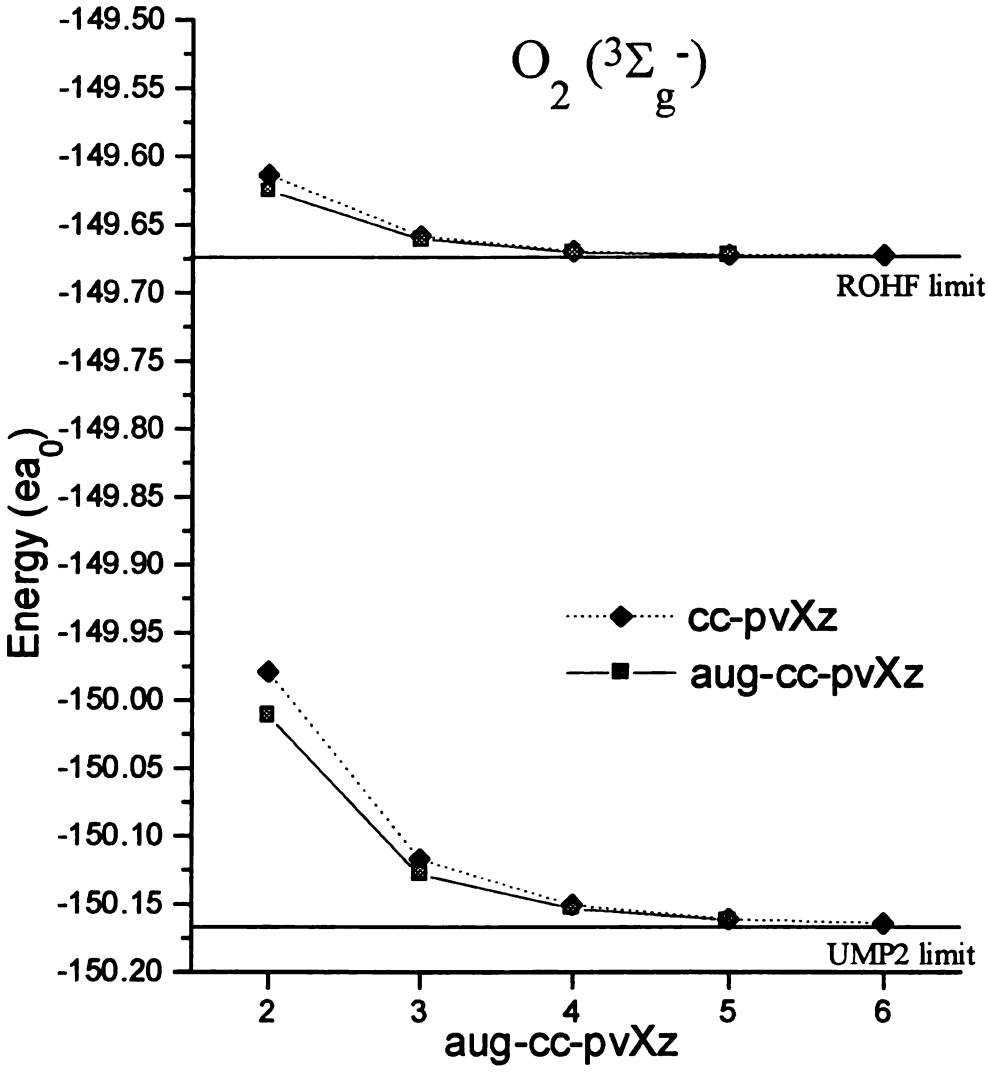

Figure 2. Comparison of ROHF and UMP2 total energy for O_2 using the cc-pvtz and aug-cc-pvtz basis sets.

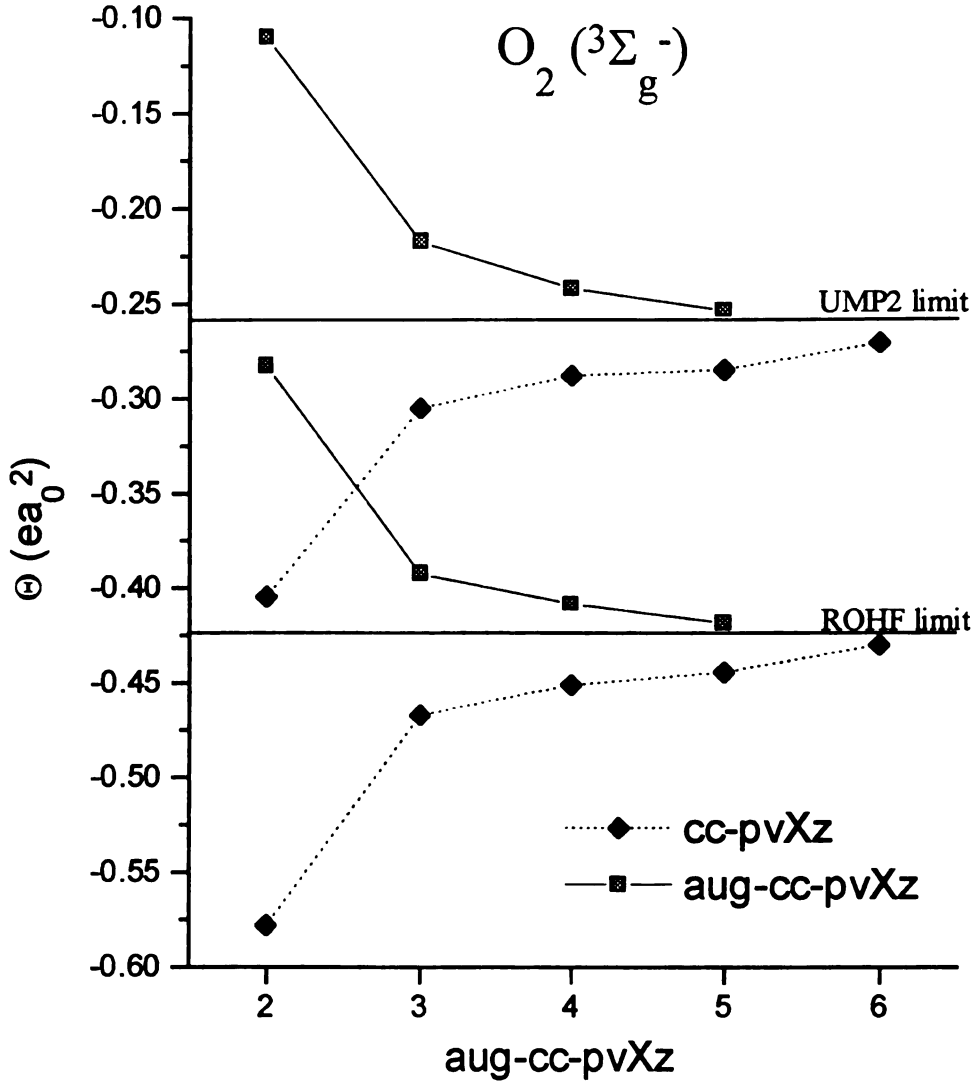

Figure 3. Comparison of the ROHF and UMP2 quadrupole moment of O_2 using the cc-pvtz and aug-cc-pvtz basis sets.

B. References

1. Dunning, T. H., Jr., J. Chem. Phys. **1989**, ***90***, 1007

2. Woon,D.E., and Dunning, T. H., Jr., J. Chem. Phys. **1993**, ***98***, 1358

3. Woon,D.E., and Dunning, T. H., Jr., J. Chem. Phys., **1993**, ***99***, 3730

4. Flugge,S., Walger,P., and Weiguny, A., J. Mol. Phys., **1967**, 23, 243

5. Basis sets were obtained from the Extensible Computational Chemistry Environment Basis Set Database, Version 1.0, as developed and distributed by the Molecular Science Computing Facility, Environmental and Molecular Sciences Laboratory, which is part of the Pacific Northwest Laboratory, P. O. Box 999, Richland, Washington 99352, USA, and funded by the U. S. Department of Energy. The Pacific Northwest Laboratory is a multi-program laboratory operated by Battelle Memorial Institute for the U. S. Department of Energy under contract DE-AC06-76RLO 1830. Contact David Feller, Karen Schuchardt, or Don Jones for further information.

6 Gaussian 94, Revision D.3,M. J. Frisch, G. W. Trucks, H. B. Schlegel, P. M.W. Gill, B. G. Johnson, M. A. Robb, J. R. Cheeseman, T. Keith, G. A. Petersson, J. A. Montgomery, K. Raghavachari, M. A. Al-Laham, V. G. Zakrzewski, J. V. Ortiz, J. B. Foresman, J. Cioslowski, B. B. Stefanov, A. Nanayakkara, M. Challacombe, C. Y. Peng, P. Y. Ayala, W. Chen, M. W. Wong, J. L. Andres, E. S. Replogle, R. Gomperts, R. L. Martin, D. J. Fox, J. S. Binkley, D. J. Defrees, J. Baker, J. P. Stewart, M. Head-Gordon, C. Gonzalez, and J. A. Pople, Gaussian, Inc., Pittsburgh PA, 1995.

Hydrogen

aug-cc-pvdz

```
H          0.000000
S    4 1.00
          13.010000      0.019685
           1.962000      0.137977
           0.444600      0.478148
           0.122000      0.501240
S    1 1.00
           0.122000      1.000000
P    1 1.00
           0.727000      1.000000
S    1 1.00
           0.029740      1.000000
P    1 1.00
           0.141000      1.000000
```

aug-cc-pvtz

```
H          0.000000
S    5 1.00
          33.870000      0.006068
           5.095000      0.045308
           1.159000      0.202822
           0.325800      0.503903
           0.102700      0.383421
S    1 1.00
           0.325800      1.000000
S    1 1.00
           0.102700      1.000000
P    1 1.00
           1.407000      1.000000
P    1 1.00
           0.388000      1.000000
D    1 1.00
           1.057000      1.000000
S    1 1.00
           0.025260      1.000000
P    1 1.00
           0.102000      1.000000
D    1 1.00
           0.247000      1.000000
```

Hydrogen

aug-cc-pvqz

```
H          0.000000
S    6 1.00
           82.640000         0.002006
           12.410000         0.015343
            2.824000         0.075579
            0.797700         0.256875
            0.258100         0.497368
            0.089890         0.296133
S    1 1.00
            0.797700         1.000000
S    1 1.00
            0.258100         1.000000
S    1 1.00
            0.089890         1.000000
P    1 1.00
            2.292000         1.000000
P    1 1.00
            0.838000         1.000000
P    1 1.00
            0.292000         1.000000
D    1 1.00
            2.062000         1.000000
D    1 1.00
            0.662000         1.000000
F    1 1.00
            1.397000         1.000000
S    1 1.00
            0.023630         1.000000
P    1 1.00
            0.084800         1.000000
D    1 1.00
            0.190000         1.000000
F    1 1.00
            0.360000         1.000000
```

aug-cc-pv5z

```
H          0.000000
S    8 1.00
          402.000000         0.000279
           60.240000         0.002165
           13.730000         0.011201
            3.905000         0.044878
            1.283000         0.142299
            0.465500         0.330979
            0.181100         0.436269
            0.072790         0.176440
S    1 1.00
            1.283000         1.000000
S    1 1.00
            0.465500         1.000000
S    1 1.00
            0.181100         1.000000
S    1 1.00
            0.072790         1.000000
P    1 1.00
            4.516000         1.000000
P    1 1.00
            1.712000         1.000000
P    1 1.00
            0.649000         1.000000
P    1 1.00
            0.246000         1.000000
D    1 1.00
            2.950000         1.000000
D    1 1.00
            1.206000         1.000000
D    1 1.00
            0.493000         1.000000
F    1 1.00
            2.506000         1.000000
F    1 1.00
            0.875000         1.000000
G    1 1.00
            2.358000         1.000000
S    1 1.00
            0.020700         1.000000
P    1 1.00
            0.074400         1.000000
D    1 1.00
            0.156000         1.000000
F    1 1.00
            0.274000         1.000000
G    1 1.00
            0.543000         1.000000
```

Boron

aug-cc-pvdz

```
B          0.000000
S   9 1.00
        4,570.000000          0.000696
          685.900000          0.005353
          156.500000          0.027134
           44.470000          0.101380
           14.480000          0.272055
            5.131000          0.448403
            1.898000          0.290123
            0.332900          0.014322
            0.104300         -0.003486
S   9 1.00
        4,570.000000         -0.000139
          685.900000         -0.001097
          156.500000         -0.005444
           44.470000         -0.021916
           14.480000         -0.059751
            5.131000         -0.138732
            1.898000         -0.131482
            0.332900          0.539526
            0.104300          0.580774
S   1 1.00
            0.104300          1.000000
P   4 1.00
            6.001000          0.035481
            1.241000          0.198072
            0.336400          0.505230
            0.095380          0.479499
P   1 1.00
            0.095380          1.000000
D   1 1.00
            0.343000          1.000000
S   1 1.00
            0.031050          1.000000
P   1 1.00
            0.023780          1.000000
D   1 1.00
            0.090400          1.000000
```

aug-cc-pvtz

```
B          0.000000
S   12 1.00
         23,870.000000          0.000088
          3,575.000000          0.000687
            812.800000          0.003600
            229.700000          0.014949
             74.690000          0.051435
             26.810000          0.143302
             10.320000          0.300935
              4.178000          0.403526
              1.727000          0.225340
              0.470400          0.015407
              0.189600         -0.003955
              0.073940          0.001124
S   12 1.00
         23,870.000000         -0.000018
          3,575.000000         -0.000139
            812.800000         -0.000725
            229.700000         -0.003063
             74.690000         -0.010581
             26.810000         -0.031365
             10.320000         -0.071012
              4.178000         -0.132103
              1.727000         -0.123072
              0.470400          0.261819
              0.189600          0.586662
              0.073940          0.290494
S   1 1.00
              0.470400          1.000000
S   1 1.00
              0.189600          1.000000
S   1 1.00
              0.073940          1.000000
P   6 1.00
             22.260000          0.005095
              5.058000          0.033206
              1.487000          0.132314
              0.507100          0.331818
              0.181200          0.472063
              0.064630          0.257979
P   1 1.00
              0.507100          1.000000
P   1 1.00
              0.181200          1.000000
P   1 1.00
              0.064630          1.000000
D   1 1.00
              1.110000          1.000000
```

```
D   1  1.00
                0.402000        1.000000
D   1  1.00
                0.145000        1.000000
F   1  1.00
                0.882000        1.000000
F   1  1.00
                0.311000        1.000000
G   1  1.00
                0.673000        1.000000
S   1  1.00
                0.027210        1.000000
P   1  1.00
                0.018780        1.000000
D   1  1.00
                0.046600        1.000000
F   1  1.00
                0.113000        1.000000
G   1  1.00
                0.273000        1.000000
```

Boron

aug-cc-pvqz

```
B         0.000000
S   10  1.00
        5,473.000000          0.000555
          820.900000          0.004291
          186.800000          0.021949
           52.830000          0.084441
           17.080000          0.238557
            5.999000          0.435072
            2.208000          0.341955
            0.587900          0.036856
            0.241500         -0.009545
            0.086100          0.002368
S   10  1.00
        5,473.000000         -0.000112
          820.900000         -0.000868
          186.800000         -0.004484
           52.830000         -0.017683
           17.080000         -0.053639
            5.999000         -0.119005
            2.208000         -0.165824
            0.587900          0.120107
            0.241500          0.595981
            0.086100          0.411021
S   1  1.00
            0.587900          1.000000
S   1  1.00
            0.086100          1.000000
P   5  1.00
           12.050000          0.013118
            2.613000          0.079896
            0.747500          0.277275
            0.238500          0.504270
            0.076980          0.353680
P   1  1.00
            0.238500          1.000000
P   1  1.00
            0.076980          1.000000
D   1  1.00
            0.661000          1.000000
D   1  1.00
            0.199000          1.000000
F   1  1.00
            0.490000          1.000000
S   1  1.00
            0.029140          1.000000
P   1  1.00
            0.020960          1.000000
D   1  1.00
            0.060400          1.000000
```

aug-cc-pv5z

```
B         0.000000
S   14  1.00
       68,260.000000          0.000024
       10,230.000000          0.000185
        2,328.000000          0.000970
          660.400000          0.004056
          216.200000          0.014399
           78.600000          0.043901
           30.980000          0.113057
           12.960000          0.233825
            5.659000          0.353960
            2.556000          0.301547
            1.175000          0.087521
            0.424900          0.002819
            0.171200          0.000043
            0.069130          0.000078
S   14  1.00
       68,260.000000         -0.000005
       10,230.000000         -0.000037
        2,328.000000         -0.000196
          660.400000         -0.000824
          216.200000         -0.002923
           78.600000         -0.009138
           30.980000         -0.024105
           12.960000         -0.054755
            5.659000         -0.096943
            2.556000         -0.137485
            1.175000         -0.044565
            0.424900          0.324345
            0.171200          0.570414
            0.069130          0.243444
S   1  1.00
            1.175000          1.000000
S   1  1.00
            0.424900          1.000000
S   1  1.00
            0.171200          1.000000
S   1  1.00
            0.069130          1.000000
P   8  1.00
           66.440000          0.000838
           15.710000          0.006409
            4.936000          0.028081
            1.770000          0.092152
            0.700800          0.224164
            0.290100          0.369915
            0.121100          0.374441
            0.049730          0.139086
P   1  1.00
```

```
F    1 1.00
       0.163000       1.000000
       0.700800       1.000000
P    1 1.00
       0.290100       1.000000
P    1 1.00
       0.121100       1.000000
P    1 1.00
       0.049730       1.000000
D    1 1.00
       2.010000       1.000000
D    1 1.00
       0.796000       1.000000
D    1 1.00
       0.316000       1.000000
D    1 1.00
       0.125000       1.000000
F    1 1.00
       1.215000       1.000000
F    1 1.00
       0.525000       1.000000
F    1 1.00
       0.227000       1.000000
G    1 1.00
       1.124000       1.000000
G    1 1.00
       0.461000       1.000000
H    1 1.00
       0.834000       1.000000
S    1 1.00
       0.026100       1.000000
P    1 1.00
       0.015700       1.000000
D    1 1.00
       0.043100       1.000000
F    1 1.00
       0.084300       1.000000
G    1 1.00
       0.202000       1.000000
H    1 1.00
       0.384000       1.000000
```

Carbon

aug-cc-pvdz

```
C          0.000000
S   9 1.00
        6,665.000000      0.000692
        1,000.000000      0.005329
          228.000000      0.027077
           64.710000      0.101718
           21.060000      0.274740
            7.495000      0.448564
            2.797000      0.285074
            0.521500      0.015204
            0.159600     -0.003191
S   9 1.00
        6,665.000000     -0.000146
        1,000.000000     -0.001154
          228.000000     -0.005725
           64.710000     -0.023312
           21.060000     -0.063955
            7.495000     -0.149981
            2.797000     -0.127262
            0.521500      0.544529
            0.159600      0.580496
S   1 1.00
            0.159600      1.000000
P   4 1.00
            9.439000      0.038109
            2.002000      0.209480
            0.545600      0.508557
            0.151700      0.468842
P   1 1.00
            0.151700      1.000000
D   1 1.00
            0.550000      1.000000
S   1 1.00
            0.046900      1.000000
P   1 1.00
            0.040410      1.000000
D   1 1.00
            0.151000      1.000000
```

aug-cc-pvtz

```
C          0.000000
S   10 1.00
        8,236.000000      0.000531
        1,235.000000      0.004108
          280.800000      0.021087
           79.270000      0.081853
           25.590000      0.234817
            8.997000      0.434401
            3.319000      0.346129
            0.905900      0.039378
            0.364300     -0.008983
            0.128500      0.002385
S   10 1.00
        8,236.000000     -0.000113
        1,235.000000     -0.000878
          280.800000     -0.004540
           79.270000     -0.018133
           25.590000     -0.055760
            8.997000     -0.126895
            3.319000     -0.170352
            0.905900      0.140382
            0.364300      0.598684
            0.128500      0.395389
S   1 1.00
            0.905900      1.000000
S   1 1.00
            0.128500      1.000000
P   5 1.00
           18.710000      0.014031
            4.133000      0.086866
            1.200000      0.290216
            0.382700      0.501008
            0.120900      0.343406
P   1 1.00
            0.382700      1.000000
P   1 1.00
            0.120900      1.000000
D   1 1.00
            1.097000      1.000000
D   1 1.00
            0.318000      1.000000
F   1 1.00
            0.761000      1.000000
S   1 1.00
            0.044020      1.000000
P   1 1.00
            0.035690      1.000000
D   1 1.00
            0.100000      1.000000
```

```
F    1  1.00
                0.268000          1.000000
```

Carbon

aug-cc-pvqz

```
C        0.000000
S   12 1.00
     33,980.000000          0.000091
      5,089.000000          0.000704
      1,157.000000          0.003693
        326.600000          0.015360
        106.100000          0.052929
         38.110000          0.147043
         14.750000          0.305631
          6.035000          0.399345
          2.530000          0.217051
          0.735500          0.015894
          0.290500         -0.003084
          0.111100          0.000978
S   12 1.00
     33,980.000000         -0.000019
      5,089.000000         -0.000151
      1,157.000000         -0.000785
        326.600000         -0.003324
        106.100000         -0.011512
         38.110000         -0.034160
         14.750000         -0.077173
          6.035000         -0.141493
          2.530000         -0.118019
          0.735500          0.273806
          0.290500          0.586510
          0.111100          0.285430
S   1 1.00
          0.735500          1.000000
S   1 1.00
          0.290500          1.000000
S   1 1.00
          0.111100          1.000000
P   6 1.00
         34.510000          0.005378
          7.915000          0.036132
          2.368000          0.142493
          0.813200          0.342150
          0.289000          0.463864
          0.100700          0.250028
P   1 1.00
          0.813200          1.000000
P   1 1.00
          0.289000          1.000000
P   1 1.00
          0.100700          1.000000
D   1 1.00
          1.848000          1.000000
D   1 1.00
```

aug-cc-pv5z

```
C        0.000000
S   14 1.00
     96,770.000000          0.000025
     14,500.000000          0.000190
      3,300.000000          0.001000
        935.800000          0.004183
        306.200000          0.014859
        111.300000          0.045301
         43.900000          0.116504
         18.400000          0.240249
          8.054000          0.358799
          3.637000          0.293941
          1.656000          0.077665
          0.633300          0.002333
          0.254500          0.000505
          0.101900          0.000030
S   14 1.00
     96,770.000000         -0.000005
     14,500.000000         -0.000041
      3,300.000000         -0.000213
        935.800000         -0.000897
        306.200000         -0.003187
        111.300000         -0.009961
         43.900000         -0.026375
         18.400000         -0.060001
          8.054000         -0.106825
          3.637000         -0.144166
          1.656000         -0.024644
          0.633300          0.349009
          0.254500          0.558737
          0.101900          0.228102
S   1 1.00
          1.656000          1.000000
S   1 1.00
          0.633300          1.000000
S   1 1.00
          0.254500          1.000000
S   1 1.00
          0.101900          1.000000
P   8 1.00
        101.800000          0.000891
         24.040000          0.006976
          7.571000          0.031669
          2.732000          0.104006
          1.085000          0.241633
          0.449600          0.371946
          0.187600          0.354200
          0.076060          0.131568
P   1 1.00
```

```
                0.649000        1.000000
D   1  1.00
                0.228000        1.000000
F   1  1.00
                1.419000        1.000000
F   1  1.00
                0.485000        1.000000
G   1  1.00
                1.011000        1.000000
S   1  1.00
                0.041450        1.000000
P   1  1.00
                0.032180        1.000000
D   1  1.00
                0.076600        1.000000
F   1  1.00
                0.187000        1.000000
G   1  1.00
                0.424000        1.000000
```

```
                1.085000        1.000000
P   1  1.00
                0.449600        1.000000
P   1  1.00
                0.187600        1.000000
P   1  1.00
                0.076060        1.000000
D   1  1.00
                3.134000        1.000000
D   1  1.00
                1.233000        1.000000
D   1  1.00
                0.485000        1.000000
D   1  1.00
                0.191000        1.000000
F   1  1.00
                2.006000        1.000000
F   1  1.00
                0.838000        1.000000
F   1  1.00
                0.350000        1.000000
G   1  1.00
                1.753000        1.000000
G   1  1.00
                0.678000        1.000000
H   1  1.00
                1.259000        1.000000
S   1  1.00
                0.039400        1.000000
P   1  1.00
                0.027200        1.000000
D   1  1.00
                0.070100        1.000000
F   1  1.00
                0.138000        1.000000
G   1  1.00
                0.319000        1.000000
H   1  1.00
                0.586000        1.000000
```

Nitrogen

aug-cc-pvdz

```
N          0.000000
S   9 1.00
        9,046.000000          0.000700
        1,357.000000          0.005389
          309.300000          0.027406
           87.730000          0.103207
           28.560000          0.278723
           10.210000          0.448540
            3.838000          0.278238
            0.746600          0.015440
            0.224800         -0.002864
S   9 1.00
        9,046.000000         -0.000153
        1,357.000000         -0.001208
          309.300000         -0.005992
           87.730000         -0.024544
           28.560000         -0.067459
           10.210000         -0.158078
            3.838000         -0.121831
            0.746600          0.549003
            0.224800          0.578815
S   1 1.00
            0.224800          1.000000
P   4 1.00
           13.550000          0.039919
            2.917000          0.217169
            0.797300          0.510319
            0.218500          0.462214
P   1 1.00
            0.218500          1.000000
D   1 1.00
            0.817000          1.000000
S   1 1.00
            0.061240          1.000000
P   1 1.00
            0.056110          1.000000
D   1 1.00
            0.230000          1.000000
```

aug-cc-pvtz

```
N          0.000000
S   10 1.00
       11,420.000000          0.000523
        1,712.000000          0.004045
          389.300000          0.020775
          110.000000          0.080727
           35.570000          0.233074
           12.540000          0.433501
            4.644000          0.347472
            1.293000          0.041262
            0.511800         -0.008508
            0.178700          0.002384
S   10 1.00
       11,420.000000         -0.000115
        1,712.000000         -0.000895
          389.300000         -0.004624
          110.000000         -0.018528
           35.570000         -0.057339
           12.540000         -0.132076
            4.644000         -0.172510
            1.293000          0.151814
            0.511800          0.599944
            0.178700          0.387462
S   1 1.00
            1.293000          1.000000
S   1 1.00
            0.178700          1.000000
P   5 1.00
           26.630000          0.014670
            5.948000          0.091764
            1.742000          0.298683
            0.555000          0.498487
            0.172500          0.337023
P   1 1.00
            0.555000          1.000000
P   1 1.00
            0.172500          1.000000
D   1 1.00
            1.654000          1.000000
D   1 1.00
            0.469000          1.000000
F   1 1.00
            1.093000          1.000000
S   1 1.00
            0.057600          1.000000
P   1 1.00
            0.049100          1.000000
D   1 1.00
            0.151000          1.000000
```

F 1 1.00
0.364000 1.000000

Nitrogen

aug-cc-pvqz

```
N          0.000000
S   12 1.00
      45,840.000000          0.000092
       6,868.000000          0.000717
       1,563.000000          0.003749
         442.400000          0.015532
         144.300000          0.053146
          52.180000          0.146787
          20.340000          0.304663
           8.381000          0.397684
           3.529000          0.217641
           1.054000          0.016963
           0.411800         -0.002745
           0.155200          0.000953
S   12 1.00
      45,840.000000         -0.000020
       6,868.000000         -0.000159
       1,563.000000         -0.000824
         442.400000         -0.003478
         144.300000         -0.011966
          52.180000         -0.035388
          20.340000         -0.080077
           8.381000         -0.146722
           3.529000         -0.116360
           1.054000          0.279919
           0.411800          0.585481
           0.155200          0.284028
S   1 1.00
           1.054000          1.000000
S   1 1.00
           0.411800          1.000000
S   1 1.00
           0.155200          1.000000
P   6 1.00
          49.330000          0.005533
          11.370000          0.037962
           3.435000          0.149028
           1.182000          0.348922
           0.417300          0.458972
           0.142800          0.244923
P   1 1.00
           1.182000          1.000000
P   1 1.00
           0.417300          1.000000
P   1 1.00
           0.142800          1.000000
D   1 1.00
           2.837000          1.000000
D   1 1.00
```

aug-cc-pv5z

```
N          0.000000
S   14 1.00
     129,200.000000          0.000025
      19,350.000000          0.000197
       4,404.000000          0.001032
       1,248.000000          0.004325
         408.000000          0.015380
         148.200000          0.046867
          58.500000          0.120116
          24.590000          0.245695
          10.810000          0.361379
           4.882000          0.287283
           2.195000          0.070171
           0.871500          0.001831
           0.350400          0.000835
           0.139700         -0.000006
S   14 1.00
     129,200.000000         -0.000006
      19,350.000000         -0.000043
       4,404.000000         -0.000227
       1,248.000000         -0.000958
         408.000000         -0.003416
         148.200000         -0.010667
          58.500000         -0.028279
          24.590000         -0.064020
          10.810000         -0.113932
           4.882000         -0.146995
           2.195000         -0.007251
           0.871500          0.366183
           0.350400          0.547908
           0.139700          0.216645
S   1 1.00
           2.195000          1.000000
S   1 1.00
           0.871500          1.000000
S   1 1.00
           0.350400          1.000000
S   1 1.00
           0.139700          1.000000
P   8 1.00
         147.000000          0.000892
          34.760000          0.007082
          11.000000          0.032816
           3.995000          0.108209
           1.587000          0.248094
           0.653300          0.374513
           0.268600          0.348414
           0.106700          0.128340
P   1 1.00
```

```
                0.968000        1.000000
D   1  1.00
                0.335000        1.000000
F   1  1.00
                2.027000        1.000000
F   1  1.00
                0.685000        1.000000
G   1  1.00
                1.427000        1.000000
S   1  1.00
                0.054640        1.000000
P   1  1.00
                0.044020        1.000000
D   1  1.00
                0.111000        1.000000
F   1  1.00
                0.245000        1.000000
G   1  1.00
                0.559000        1.000000
                1.587000        1.000000
P   1  1.00
                0.653300        1.000000
P   1  1.00
                0.268600        1.000000
P   1  1.00
                0.106700        1.000000
D   1  1.00
                4.647000        1.000000
D   1  1.00
                1.813000        1.000000
D   1  1.00
                0.707000        1.000000
D   1  1.00
                0.276000        1.000000
F   1  1.00
                2.942000        1.000000
F   1  1.00
                1.204000        1.000000
F   1  1.00
                0.493000        1.000000
G   1  1.00
                2.511000        1.000000
G   1  1.00
                0.942000        1.000000
H   1  1.00
                1.768000        1.000000
S   1  1.00
                0.051800        1.000000
P   1  1.00
                0.036900        1.000000
D   1  1.00
                0.097100        1.000000
F   1  1.00
                0.192000        1.000000
G   1  1.00
                0.436000        1.000000
H   1  1.00
                0.788000        1.000000
```

Oxygen

aug-cc-pvdz

```
O          0.000000
S   9 1.00
       11,720.000000          0.000710
        1,759.000000          0.005470
          400.800000          0.027837
          113.700000          0.104800
           37.030000          0.283062
           13.270000          0.448719
            5.025000          0.270952
            1.013000          0.015458
            0.302300         -0.002585
S   9 1.00
       11,720.000000         -0.000160
        1,759.000000         -0.001263
          400.800000         -0.006267
          113.700000         -0.025716
           37.030000         -0.070924
           13.270000         -0.165411
            5.025000         -0.116955
            1.013000          0.557368
            0.302300          0.572759
S   1 1.00
            0.302300          1.000000
P   4 1.00
           17.700000          0.043018
            3.854000          0.228913
            1.046000          0.508728
            0.275300          0.460531
P   1 1.00
            0.275300          1.000000
D   1 1.00
            1.185000          1.000000
S   1 1.00
            0.078960          1.000000
P   1 1.00
            0.068560          1.000000
D   1 1.00
            0.332000          1.000000
```

aug-cc-pvtz

```
O          0.000000
S   10 1.00
       15,330.000000          0.000508
        2,299.000000          0.003929
          522.400000          0.020243
          147.300000          0.079181
           47.550000          0.230687
           16.760000          0.433118
            6.207000          0.350260
            1.752000          0.042728
            0.688200         -0.008154
            0.238400          0.002381
S   10 1.00
       15,330.000000         -0.000115
        2,299.000000         -0.000895
          522.400000         -0.004636
          147.300000         -0.018724
           47.550000         -0.058463
           16.760000         -0.136463
            6.207000         -0.175740
            1.752000          0.160934
            0.688200          0.603418
            0.238400          0.378765
S   1 1.00
            1.752000          1.000000
S   1 1.00
            0.238400          1.000000
P   5 1.00
           34.460000          0.015928
            7.749000          0.099740
            2.280000          0.310492
            0.715600          0.491026
            0.214000          0.336337
P   1 1.00
            0.715600          1.000000
P   1 1.00
            0.214000          1.000000
D   1 1.00
            2.314000          1.000000
D   1 1.00
            0.645000          1.000000
F   1 1.00
            1.428000          1.000000
S   1 1.00
            0.073760          1.000000
P   1 1.00
            0.059740          1.000000
D   1 1.00
            0.214000          1.000000
```

```
F    1  1.00
                0.500000          1.000000
```

Oxygen

aug-cc-pvqz

```
O          0.000000
S    12 1.00
      61,420.000000        0.000090
       9,199.000000        0.000698
       2,091.000000        0.003664
         590.900000        0.015218
         192.300000        0.052423
          69.320000        0.145921
          26.970000        0.305258
          11.100000        0.398508
           4.682000        0.216980
           1.428000        0.017594
           0.554700       -0.002502
           0.206700        0.000954
S    12 1.00
      61,420.000000       -0.000020
       9,199.000000       -0.000159
       2,091.000000       -0.000829
         590.900000       -0.003508
         192.300000       -0.012156
          69.320000       -0.036261
          26.970000       -0.082992
          11.100000       -0.152090
           4.682000       -0.115331
           1.428000        0.288979
           0.554700        0.586128
           0.206700        0.277624
S    1 1.00
           1.428000        1.000000
S    1 1.00
           0.554700        1.000000
S    1 1.00
           0.206700        1.000000
P    6 1.00
          63.420000        0.006044
          14.660000        0.041799
           4.459000        0.161143
           1.531000        0.356731
           0.530200        0.448309
           0.175000        0.244940
P    1 1.00
           1.531000        1.000000
P    1 1.00
           0.530200        1.000000
P    1 1.00
           0.175000        1.000000
D    1 1.00
           3.775000        1.000000
D    1 1.00
```

aug-cc-pv5z

```
O          0.000000
S    14 1.00
     164,200.000000        0.000026
      24,590.000000        0.000205
       5,592.000000        0.001076
       1,582.000000        0.004522
         516.100000        0.016108
         187.200000        0.049085
          73.930000        0.124857
          31.220000        0.251686
          13.810000        0.362420
           6.256000        0.279051
           2.776000        0.063552
           1.138000        0.001063
           0.460000        0.001144
           0.182900       -0.000040
S    14 1.00
     164,200.000000       -0.000006
      24,590.000000       -0.000046
       5,592.000000       -0.000244
       1,582.000000       -0.001031
         516.100000       -0.003688
         187.200000       -0.011514
          73.930000       -0.030435
          31.220000       -0.068147
          13.810000       -0.120368
           6.256000       -0.148260
           2.776000        0.009905
           1.138000        0.384286
           0.460000        0.536805
           0.182900        0.202687
S    1 1.00
           2.776000        1.000000
S    1 1.00
           1.138000        1.000000
S    1 1.00
           0.460000        1.000000
S    1 1.00
           0.182900        1.000000
P    8 1.00
         195.500000        0.000918
          46.160000        0.007388
          14.580000        0.034958
           5.296000        0.115431
           2.094000        0.256803
           0.847100        0.373938
           0.336800        0.343447
           0.128500        0.129706
P    1 1.00
```

```
                1.300000        1.000000
D       1  1.00
                0.444000        1.000000
F       1  1.00
                2.666000        1.000000
F       1  1.00
                0.859000        1.000000
G       1  1.00
                1.846000        1.000000
S       1  1.00
                0.069590        1.000000
P       1  1.00
                0.053480        1.000000
D       1  1.00
                0.154000        1.000000
F       1  1.00
                0.324000        1.000000
G       1  1.00
                0.714000        1.000000
```

```
                2.094000        1.000000
P       1  1.00
                0.847100        1.000000
P       1  1.00
                0.336800        1.000000
P       1  1.00
                0.128500        1.000000
D       1  1.00
                5.879000        1.000000
D       1  1.00
                2.307000        1.000000
D       1  1.00
                0.905000        1.000000
D       1  1.00
                0.355000        1.000000
F       1  1.00
                4.016000        1.000000
F       1  1.00
                1.554000        1.000000
F       1  1.00
                0.601000        1.000000
G       1  1.00
                3.350000        1.000000
G       1  1.00
                1.189000        1.000000
H       1  1.00
                2.319000        1.000000
S       1  1.00
                0.065500        1.000000
P       1  1.00
                0.044600        1.000000
D       1  1.00
                0.131000        1.000000
F       1  1.00
                0.237000        1.000000
G       1  1.00
                0.517000        1.000000
H       1  1.00
                1.024000        1.000000
```

Fluorine

aug-cc-pvdz

```
F          0.000000
S   9 1.00
      14,710.000000          0.000721
       2,207.000000          0.005553
         502.800000          0.028267
         142.600000          0.106444
          46.470000          0.286814
          16.700000          0.448641
           6.356000          0.264761
           1.316000          0.015333
           0.389700         -0.002332
S   9 1.00
      14,710.000000         -0.000165
       2,207.000000         -0.001308
         502.800000         -0.006495
         142.600000         -0.026691
          46.470000         -0.073690
          16.700000         -0.170776
           6.356000         -0.112327
           1.316000          0.562814
           0.389700          0.568778
S   1 1.00
           0.389700          1.000000
P   4 1.00
          22.670000          0.044878
           4.977000          0.235718
           1.347000          0.508521
           0.347100          0.458120
P   1 1.00
           0.347100          1.000000
D   1 1.00
           1.640000          1.000000
S   1 1.00
           0.098630          1.000000
P   1 1.00
           0.085020          1.000000
D   1 1.00
           0.464000          1.000000
```

aug-cc-pvtz

```
F          0.000000
S   10 1.00
      19,500.000000          0.000507
       2,923.000000          0.003923
         664.500000          0.020200
         187.500000          0.079010
          60.620000          0.230439
          21.420000          0.432872
           7.950000          0.349964
           2.257000          0.043233
           0.881500         -0.007892
           0.304100          0.002384
S   10 1.00
      19,500.000000         -0.000117
       2,923.000000         -0.000912
         664.500000         -0.004717
         187.500000         -0.019086
          60.620000         -0.059655
          21.420000         -0.140010
           7.950000         -0.176782
           2.257000          0.171625
           0.881500          0.605043
           0.304100          0.369512
S   1 1.00
           2.257000          1.000000
S   1 1.00
           0.304100          1.000000
P   5 1.00
          43.880000          0.016665
           9.926000          0.104472
           2.930000          0.317260
           0.913200          0.487343
           0.267200          0.334604
P   1 1.00
           0.913200          1.000000
P   1 1.00
           0.267200          1.000000
D   1 1.00
           3.107000          1.000000
D   1 1.00
           0.855000          1.000000
F   1 1.00
           1.917000          1.000000
S   1 1.00
           0.091580          1.000000
P   1 1.00
           0.073610          1.000000
D   1 1.00
           0.292000          1.000000
```

```
F    1  1.00
                0.724000          1.000000
```

Fluorine

aug-cc-pvqz

```
F          0.000000
S    12 1.00
      74,530.000000        0.000095
      11,170.000000        0.000738
       2,543.000000        0.003858
         721.000000        0.015926
         235.900000        0.054289
          85.600000        0.149513
          33.550000        0.308252
          13.930000        0.394853
           5.915000        0.211031
           1.843000        0.017151
           0.712400       -0.002015
           0.263700        0.000869
S    12 1.00
      74,530.000000       -0.000022
      11,170.000000       -0.000172
       2,543.000000       -0.000891
         721.000000       -0.003748
         235.900000       -0.012862
          85.600000       -0.038061
          33.550000       -0.086239
          13.930000       -0.155865
           5.915000       -0.110914
           1.843000        0.298761
           0.712400        0.585013
           0.263700        0.271159
S    1 1.00
           1.843000        1.000000
S    1 1.00
           0.712400        1.000000
S    1 1.00
           0.263700        1.000000
P    6 1.00
          80.390000        0.006347
          18.630000        0.044204
           5.694000        0.168514
           1.953000        0.361563
           0.670200        0.442178
           0.216600        0.243435
P    1 1.00
           1.953000        1.000000
P    1 1.00
           0.670200        1.000000
P    1 1.00
           0.216600        1.000000
D    1 1.00
           5.014000        1.000000
D    1 1.00
```

aug-cc-pv5z

```
F          0.000000
S    14 1.00
     211,400.000000        0.000026
      31,660.000000        0.000201
       7,202.000000        0.001056
       2,040.000000        0.004432
         666.400000        0.015766
         242.000000        0.048112
          95.530000        0.123232
          40.230000        0.251519
          17.720000        0.364525
           8.005000        0.279766
           3.538000        0.063545
           1.458000        0.001111
           0.588700        0.001258
           0.232400       -0.000035
S    14 1.00
     211,400.000000       -0.000006
      31,660.000000       -0.000047
       7,202.000000       -0.000244
       2,040.000000       -0.001031
         666.400000       -0.003683
         242.000000       -0.011513
          95.530000       -0.030663
          40.230000       -0.069572
          17.720000       -0.123992
           8.005000       -0.150214
           3.538000        0.016460
           1.458000        0.392550
           0.588700        0.532164
           0.232400        0.196524
S    1 1.00
           3.538000        1.000000
S    1 1.00
           1.458000        1.000000
S    1 1.00
           0.588700        1.000000
S    1 1.00
           0.232400        1.000000
P    8 1.00
         241.900000        0.001002
          57.170000        0.008054
          18.130000        0.038048
           6.624000        0.123779
           2.622000        0.266060
           1.057000        0.371796
           0.417600        0.332890
           0.157400        0.128491
P    1 1.00
```

```
                1.725000        1.000000
D       1  1.00
                0.586000        1.000000
F       1  1.00
                3.562000        1.000000
F       1  1.00
                1.148000        1.000000
G       1  1.00
                2.376000        1.000000
S       1  1.00
                0.085940        1.000000
P       1  1.00
                0.065680        1.000000
D       1  1.00
                0.207000        1.000000
F       1  1.00
                0.460000        1.000000
G       1  1.00
                0.924000        1.000000
```

```
                2.622000        1.000000
P       1  1.00
                1.057000        1.000000
P       1  1.00
                0.417600        1.000000
P       1  1.00
                0.157400        1.000000
D       1  1.00
                7.760000        1.000000
D       1  1.00
                3.032000        1.000000
D       1  1.00
                1.185000        1.000000
D       1  1.00
                0.463000        1.000000
F       1  1.00
                5.398000        1.000000
F       1  1.00
                2.078000        1.000000
F       1  1.00
                0.800000        1.000000
G       1  1.00
                4.338000        1.000000
G       1  1.00
                1.513000        1.000000
H       1  1.00
                2.995000        1.000000
S       1  1.00
                0.080600        1.000000
P       1  1.00
                0.055000        1.000000
D       1  1.00
                0.172000        1.000000
F       1  1.00
                0.331000        1.000000
G       1  1.00
                0.663000        1.000000
H       1  1.00
                1.326000        1.000000
```

Aluminum

aug-cc-pvdz

```
Al          0.000000
S    12 1.00
        64,150.000000     0.000290
         9,617.000000     0.002251
         2,189.000000     0.011646
           620.500000     0.046738
           202.700000     0.146299
            73.150000     0.330283
            28.550000     0.415861
            11.770000     0.189253
             3.300000     0.011589
             1.173000    -0.001284
             0.175200     0.000426
             0.064730    -0.000199
S    12 1.00
        64,150.000000    -0.000076
         9,617.000000    -0.000582
         2,189.000000    -0.003081
           620.500000    -0.012311
           202.700000    -0.041978
            73.150000    -0.103371
            28.550000    -0.196308
            11.770000    -0.083000
             3.300000     0.541040
             1.173000     0.578796
             0.175200     0.028815
             0.064730    -0.009538
S    12 1.00
        64,150.000000     0.000018
         9,617.000000     0.000134
         2,189.000000     0.000712
           620.500000     0.002843
           202.700000     0.009768
            73.150000     0.024185
            28.550000     0.047499
            11.770000     0.020362
             3.300000    -0.158788
             1.173000    -0.311694
             0.175200     0.620147
             0.064730     0.520943
S    1 1.00
             0.064730     1.000000
P    8 1.00
           258.800000     0.004068
            60.890000     0.030682
            19.140000     0.129149
             6.881000     0.320831
             2.574000     0.453815
             0.957200     0.275066
```

aug-cc-pvtz

```
Al          0.000000
S    15 1.00
       205,500.000000     0.000068
        30,780.000000     0.000527
         7,006.000000     0.002762
         1,985.000000     0.011473
           649.100000     0.039819
           235.000000     0.115040
            91.620000     0.260887
            37.670000     0.396386
            15.910000     0.284597
             5.850000     0.044458
             2.542000    -0.004898
             1.057000     0.002613
             0.293100    -0.001089
             0.145500     0.000722
             0.056500    -0.000178
S    15 1.00
       205,500.000000    -0.000018
        30,780.000000    -0.000137
         7,006.000000    -0.000719
         1,985.000000    -0.003011
           649.100000    -0.010601
           235.000000    -0.032135
            91.620000    -0.080316
            37.670000    -0.156794
            15.910000    -0.168376
             5.850000     0.126879
             2.542000     0.561494
             1.057000     0.436613
             0.293100     0.035729
             0.145500    -0.011456
             0.056500     0.002202
S    15 1.00
       205,500.000000     0.000004
        30,780.000000     0.000032
         7,006.000000     0.000166
         1,985.000000     0.000695
           649.100000     0.002455
           235.000000     0.007446
            91.620000     0.018825
            37.670000     0.037277
            15.910000     0.041950
             5.850000    -0.035438
             2.542000    -0.175132
             1.057000    -0.276203
             0.293100     0.108729
             0.145500     0.652809
             0.056500     0.394587
```

```
                0.209900        0.019081
                0.059860       -0.003128
P     8 1.00
              258.800000       -0.000748
               60.890000       -0.005458
               19.140000       -0.024537
                6.881000       -0.058214
                2.574000       -0.098376
                0.957200       -0.026006
                0.209900        0.464020
                0.059860        0.648870
P     1 1.00
                0.059860        1.000000
D     1 1.00
                0.189000        1.000000
S     1 1.00
                0.023100        1.000000
P     1 1.00
                0.015300        1.000000
D     1 1.00
                0.053500        1.000000
S     1 1.00
                0.293100        1.000000
S     1 1.00
                0.056500        1.000000
P     9 1.00
              444.400000        0.001628
              105.100000        0.013069
               33.470000        0.061234
               12.330000        0.187870
                4.869000        0.360452
                1.961000        0.408454
                0.783400        0.188640
                0.188800        0.009765
                0.055570       -0.001151
P     9 1.00
              444.400000       -0.000286
              105.100000       -0.002423
               33.470000       -0.010866
               12.330000       -0.036431
                4.869000       -0.064107
                1.961000       -0.097224
                0.783400        0.014744
                0.188800        0.503448
                0.055570        0.597984
P     1 1.00
                0.783400        1.000000
P     1 1.00
                0.055570        1.000000
D     1 1.00
                0.109000        1.000000
D     1 1.00
                0.333000        1.000000
F     1 1.00
                0.244000        1.000000
S     1 1.00
                0.022100        1.000000
P     1 1.00
                0.014600        1.000000
D     1 1.00
                0.035600        1.000000
F     1 1.00
                0.085800        1.000000
```

Aluminum

aug-cc-pvtz

```
Al          0.000000
S   16 1.00
      419,600.000000      0.000028
       62,830.000000      0.000216
       14,290.000000      0.001138
        4,038.000000      0.004796
        1,312.000000      0.017239
          470.500000      0.053807
          181.800000      0.141326
           74.460000      0.289268
           31.900000      0.384825
           13.960000      0.232852
            5.180000      0.029333
            2.265000     -0.003006
            0.966400      0.001667
            0.244700     -0.000606
            0.118400      0.000431
            0.050210     -0.000123
S   16 1.00
      419,600.000000     -0.000007
       62,830.000000     -0.000056
       14,290.000000     -0.000297
        4,038.000000     -0.001249
        1,312.000000     -0.004551
          470.500000     -0.014439
          181.800000     -0.040346
           74.460000     -0.092262
           31.900000     -0.164510
           13.960000     -0.141296
            5.180000      0.195365
            2.265000      0.572475
            0.966400      0.374041
            0.244700      0.023412
            0.118400     -0.009052
            0.050210      0.002112
S   16 1.00
      419,600.000000      0.000002
       62,830.000000      0.000013
       14,290.000000      0.000069
        4,038.000000      0.000288
        1,312.000000      0.001053
          470.500000      0.003339
          181.800000      0.009392
           74.460000      0.021605
           31.900000      0.039587
           13.960000      0.034918
            5.180000     -0.052842
            2.265000     -0.191878
            0.966400     -0.254115
```

aug-cc-pvqz

```
Al          0.000000
S   20 1.00
    3,269,000.000000      0.000002
      489,400.000000      0.000017
      111,400.000000      0.000088
       31,560.000000      0.000369
       10,320.000000      0.001339
        3,731.000000      0.004356
        1,456.000000      0.012896
          604.100000      0.034820
          263.500000      0.084353
          119.800000      0.175907
           56.320000      0.292091
           27.190000      0.328220
           13.260000      0.186927
            6.052000      0.031043
            2.981000     -0.000509
            1.476000      0.001488
            0.733400     -0.000278
            0.244700      0.000119
            0.108800     -0.000066
            0.046720      0.000018
S   20 1.00
    3   269,000.000000     -0.000001
      489,400.000000     -0.000004
      111,400.000000     -0.000023
       31,560.000000     -0.000096
       10,320.000000     -0.000348
        3,731.000000     -0.001138
        1,456.000000     -0.003387
          604.100000     -0.009315
          263.500000     -0.023302
          119.800000     -0.052349
           56.320000     -0.099950
           27.190000     -0.150560
           13.260000     -0.119121
            6.052000      0.108091
            2.981000      0.411129
            1.476000      0.457214
            0.733400      0.175938
            0.244700      0.007706
            0.108800     -0.001662
            0.046720      0.000445
S   20 1.00
    3   269,000.000000      0.000000
      489,400.000000      0.000001
      111,400.000000      0.000005
       31,560.000000      0.000022
       10,320.000000      0.000081
```

```
                0.244700        0.275070
                0.118400        0.604743
                0.050210        0.287629
S    1  1.00
                0.244700        1.000000
S    1  1.00
                0.118400        1.000000
S    1  1.00
                0.050210        1.000000
P    11  1.00
              891.300000        0.000492
              211.300000        0.004158
               68.280000        0.021254
               25.700000        0.076406
               10.630000        0.194277
                4.602000        0.334428
                2.015000        0.375026
                0.870600        0.204041
                0.297200        0.021374
                0.110000       -0.002021
                0.039890        0.000817
P    11  1.00
              891.300000       -0.000089
              211.300000       -0.000746
               68.280000       -0.003870
               25.700000       -0.013935
               10.630000       -0.036686
                4.602000       -0.062780
                2.015000       -0.078960
                0.870600       -0.028859
                0.297200        0.238256
                0.110000        0.551363
                0.039890        0.354385
P    1  1.00
                0.297200        1.000000
P    1  1.00
                0.110000        1.000000
P    1  1.00
                0.039890        1.000000
D    1  1.00
                0.080400        1.000000
D    1  1.00
                0.199000        1.000000
D    1  1.00
                0.494000        1.000000
F    1  1.00
                0.154000        1.000000
F    1  1.00
                0.401000        1.000000
G    1  1.00
                0.357000        1.000000
            3,731.000000        0.000263
            1,456.000000        0.000784
              604.100000        0.002150
              263.500000        0.005420
              119.800000        0.012169
               56.320000        0.023682
               27.190000        0.036094
               13.260000        0.030328
                6.052000       -0.030903
                2.981000       -0.119126
                1.476000       -0.211145
                0.733400       -0.157944
                0.244700        0.339038
                0.108800        0.613097
                0.046720        0.235168
S    1  1.00
                0.733400        1.000000
S    1  1.00
                0.244700        1.000000
S    1  1.00
                0.108800        1.000000
S    1  1.00
                0.046720        1.000000
P    12  1.00
            1,461.000000        0.000209
              346.200000        0.001810
              112.200000        0.009734
               42.510000        0.037827
               17.720000        0.110898
                7.852000        0.234295
                3.571000        0.345245
                1.637000        0.331430
                0.738200        0.147064
                0.257700        0.012141
                0.097730       -0.000872
                0.036900        0.000438
P    12  1.00
            1,461.000000       -0.000037
              346.200000       -0.000329
              112.200000       -0.001743
               42.510000       -0.006948
               17.720000       -0.020281
                7.852000       -0.044866
                3.571000       -0.064328
                1.637000       -0.075267
                0.738200        0.000616
                0.257700        0.287819
                0.097730        0.543030
                0.036900        0.301865
P    1  1.00
                0.738200        1.000000
```

```
S     1  1.00
                0.018300        1.000000
P     1  1.00
                0.012100        1.000000
D     1  1.00
                0.028200        1.000000
F     1  1.00
                0.058200        1.000000
G     1  1.00
                0.153000        1.000000
P     1  1.00
                0.257700        1.000000
P     1  1.00
                0.097730        1.000000
P     1  1.00
                0.036900        1.000000
D     1  1.00
                1.317000        1.000000
D     1  1.00
                0.526000        1.000000
D     1  1.00
                0.210000        1.000000
D     1  1.00
                0.084000        1.000000
F     1  1.00
                0.130000        1.000000
F     1  1.00
                0.258000        1.000000
F     1  1.00
                0.513000        1.000000
G     1  1.00
                0.252000        1.000000
G     1  1.00
                0.543000        1.000000
H     1  1.00
                0.446000        1.000000
S     1  1.00
                0.017700        1.000000
P     1  1.00
                0.011500        1.000000
D     1  1.00
                0.029400        1.000000
F     1  1.00
                0.050900        1.000000
G     1  1.00
                0.106900        1.000000
H     1  1.00
                0.227000        1.000000
```

Silicon

aug-cc-pvdz

```
Si    0
S     12  1.00
          78,860.000000      0.000270
          11,820.000000      0.002097
           2,692.000000      0.010851
             763.400000      0.043675
             249.600000      0.137653
              90.280000      0.316644
              35.290000      0.418581
              14.510000      0.210212
               4.053000      0.014495
               1.482000     -0.002036
               0.251700      0.000624
               0.092430     -0.000283
S     12  1.00
          78,860.000000     -0.000072
          11,820.000000     -0.000555
           2,692.000000     -0.002938
             763.400000     -0.011769
             249.600000     -0.040291
              90.280000     -0.100609
              35.290000     -0.196528
              14.510000     -0.102382
               4.053000      0.527190
               1.482000      0.593251
               0.251700      0.033265
               0.092430     -0.009737
S     12  1.00
          78,860.000000      0.000019
          11,820.000000      0.000142
           2,692.000000      0.000752
             763.400000      0.003023
             249.600000      0.010368
              90.280000      0.026256
              35.290000      0.052399
              14.510000      0.029096
               4.053000     -0.178003
               1.482000     -0.346874
               0.251700      0.623020
               0.092430      0.537712
S     1  1.00
               0.092430      1.000000
P     8  1.00
             315.900000      0.003927
              74.420000      0.029881
              23.480000      0.127212
               8.488000      0.320943
               3.217000      0.455429
               1.229000      0.268563
```

aug-cc-pvtz

```
Si    0
S     15  1.00
          254,900.000000      0.000063
           38,190.000000      0.000486
            8,690.000000      0.002545
            2,462.000000      0.010587
              804.800000      0.036879
              291.300000      0.107479
              113.600000      0.247936
               46.750000      0.390927
               19.820000      0.302026
                7.708000      0.055924
                3.340000     -0.004024
                1.402000      0.002580
                0.438700     -0.001038
                0.207000      0.000608
                0.079440     -0.000154
S     15  1.00
          254,900.000000     -0.000017
           38,190.000000     -0.000129
            8,690.000000     -0.000679
            2,462.000000     -0.002841
              804.800000     -0.010055
              291.300000     -0.030577
              113.600000     -0.077726
               46.750000     -0.154236
               19.820000     -0.180368
                7.708000      0.079822
                3.340000      0.547441
                1.402000      0.480119
                0.438700      0.047485
                0.207000     -0.010700
                0.079440      0.002199
S     15  1.00
          254,900.000000      0.000004
           38,190.000000      0.000033
            8,690.000000      0.000174
            2,462.000000      0.000728
              804.800000      0.002583
              291.300000      0.007864
              113.600000      0.020216
               46.750000      0.040732
               19.820000      0.049936
                7.708000     -0.024940
                3.340000     -0.190350
                1.402000     -0.318350
                0.438700      0.094804
                0.207000      0.681180
                0.079440      0.395672
```

```
                0.296400        0.018834
                0.087680       -0.002624
P     8 1.00
              315.900000       -0.000858
               74.420000       -0.006303
               23.480000       -0.028826
                8.488000       -0.069456
                3.217000       -0.119493
                1.229000       -0.019958
                0.296400        0.510268
                0.087680        0.600382
P     1 1.00
                0.087680        1.000000
D     1 1.00
                0.275000        1.000000
S     1 1.00
                0.033200        1.000000
P     1 1.00
                0.025000        1.000000
D     1 1.00
                0.082300        1.000000
S     1 1.00
                0.438700        1.000000
S     1 1.00
                0.079440        1.000000
P     9 1.00
              481.500000        0.001920
              113.900000        0.015355
               36.230000        0.071399
               13.340000        0.213052
                5.252000        0.390354
                2.120000        0.393721
                0.856100        0.132565
                0.252800        0.003956
                0.078890        0.000332
P     9 1.00
              481.500000       -0.000405
              113.900000       -0.003359
               36.230000       -0.015286
               13.340000       -0.048922
                5.252000       -0.085501
                2.120000       -0.112137
                0.856100        0.061827
                0.252800        0.551919
                0.078890        0.523492
P     1 1.00
                0.856100        1.000000
P     1 1.00
                0.078890        1.000000
D     1 1.00
                0.159000        1.000000
D     1 1.00
                0.481000        1.000000
F     1 1.00
                0.336000        1.000000
S     1 1.00
                0.033000        1.000000
P     1 1.00
                0.023700        1.000000
D     1 1.00
                0.055600        1.000000
F     1 1.00
                0.125000        1.000000
```

Silicon

aug-cc-pvqz

Si	0		
S	16	1.00	
		513,000.000000	0.000026
		76,820.000000	0.000203
		17,470.000000	0.001067
		4,935.000000	0.004506
		1,602.000000	0.016236
		574.100000	0.050891
		221.500000	0.135155
		90.540000	0.281292
		38.740000	0.385336
		16.950000	0.245651
		6.452000	0.034315
		2.874000	-0.003349
		1.250000	0.001876
		0.359900	-0.000693
		0.169900	0.000438
		0.070660	-0.000123
S	16	1.00	
		513,000.000000	-0.000007
		76,820.000000	-0.000054
		17,470.000000	-0.000285
		4,935.000000	-0.001202
		1,602.000000	-0.004384
		574.100000	-0.013978
		221.500000	-0.039352
		90.540000	-0.091428
		38.740000	-0.165609
		16.950000	-0.152505
		6.452000	0.168524
		2.874000	0.569284
		1.250000	0.398056
		0.359900	0.029151
		0.169900	-0.008490
		0.070660	0.001996
S	16	1.00	
		513,000.000000	0.000002
		76,820.000000	0.000014
		17,470.000000	0.000073
		4,935.000000	0.000308
		1,602.000000	0.001126
		574.100000	0.003584
		221.500000	0.010173
		90.540000	0.023752
		38.740000	0.044348
		16.950000	0.041904
		6.452000	-0.050250
		2.874000	-0.216578
		1.250000	-0.286448

aug-cc-pv5z

Si	0		
S	20	1.00	
		3,948,000.000000	0.000002
		591,100.000000	0.000016
		134,500.000000	0.000083
		38,120.000000	0.000351
		12,460.000000	0.001277
		4,504.000000	0.004152
		1,758.000000	0.012303
		729.100000	0.033310
		318.000000	0.080985
		144.600000	0.170290
		67.970000	0.286879
		32.820000	0.330340
		16.030000	0.196602
		7.396000	0.035454
		3.661000	-0.000535
		1.823000	0.001615
		0.914700	-0.000373
		0.339300	0.000146
		0.150000	-0.000079
		0.064380	0.000019
S	20	1.00	
		3948,000.000000	-0.000001
		591,100.000000	-0.000004
		134,500.000000	-0.000022
		38,120.000000	-0.000094
		12,460.000000	-0.000340
		4,504.000000	-0.001111
		1,758.000000	-0.003309
		729.100000	-0.009116
		318.000000	-0.022879
		144.600000	-0.051712
		67.970000	-0.099909
		32.820000	-0.152747
		16.030000	-0.127508
		7.396000	0.094696
		3.661000	0.414036
		1.823000	0.467934
		0.914700	0.173927
		0.339300	0.008439
		0.150000	-0.000998
		0.064380	0.000362
S	20	1.00	
		3948,000.000000	0.000000
		591,100.000000	0.000001
		134,500.000000	0.000006
		38,120.000000	0.000024
		12,460.000000	0.000087

```
                0.359900        0.263256
                0.169900        0.634900
                0.070660        0.290832
S     1  1.00
                0.359900        1.000000
S     1  1.00
                0.169900        1.000000
S     1  1.00
                0.070660        1.000000
P    11  1.00
            1,122.000000        0.000448
              266.000000        0.003816
               85.920000        0.019811
               32.330000        0.072702
               13.370000        0.189839
                5.800000        0.335672
                2.559000        0.379365
                1.124000        0.201193
                0.398800        0.020852
                0.153300       -0.001703
                0.057280        0.000750
P    11  1.00
            1,122.000000       -0.000096
              266.000000       -0.000812
               85.920000       -0.004301
               32.330000       -0.015750
               13.370000       -0.042954
                5.800000       -0.075257
                2.559000       -0.097145
                1.124000       -0.022751
                0.398800        0.291988
                0.153300        0.550670
                0.057280        0.297618
P     1  1.00
                0.398800        1.000000
P     1  1.00
                0.153300        1.000000
P     1  1.00
                0.057280        1.000000
D     1  1.00
                0.120000        1.000000
D     1  1.00
                0.302000        1.000000
D     1  1.00
                0.760000        1.000000
F     1  1.00
                0.212000        1.000000
F     1  1.00
                0.541000        1.000000
G     1  1.00
                0.461000        1.000000
                4,504.000000    0.000284
                1,758.000000    0.000850
                  729.100000    0.002335
                  318.000000    0.005905
                  144.600000    0.013346
                   67.970000    0.026289
                   32.820000    0.040743
                   16.030000    0.036148
                    7.396000   -0.030392
                    3.661000   -0.135961
                    1.823000   -0.250144
                    0.914700   -0.158050
                    0.339300    0.369655
                    0.150000    0.617718
                    0.064380    0.222514
S     1  1.00
                    0.914700    1.000000
S     1  1.00
                    0.339300    1.000000
S     1  1.00
                    0.150000    1.000000
S     1  1.00
                    0.064380    1.000000
P    12  1.00
                1,780.000000    0.000201
                  421.800000    0.001749
                  136.700000    0.009481
                   51.810000    0.037231
                   21.600000    0.110763
                    9.563000    0.237933
                    4.350000    0.353691
                    2.006000    0.328839
                    0.920500    0.132373
                    0.350000    0.010330
                    0.138100   -0.000150
                    0.053380    0.000266
P    12  1.00
                1,780.000000   -0.000043
                  421.800000   -0.000377
                  136.700000   -0.002022
                   51.810000   -0.008128
                   21.600000   -0.024227
                    9.563000   -0.054383
                    4.350000   -0.079905
                    2.006000   -0.088896
                    0.920500    0.018400
                    0.350000    0.335096
                    0.138100    0.532288
                    0.053380    0.254374
P     1  1.00
                    0.920500    1.000000
```

```
S    1  1.00
                0.027500        1.000000
P    1  1.00
                0.020000        1.000000
D    1  1.00
                0.043500        1.000000
F    1  1.00
                0.084600        1.000000
G    1  1.00
                0.212000        1.000000
P    1  1.00
                0.350000        1.000000
P    1  1.00
                0.138100        1.000000
P    1  1.00
                0.053380        1.000000
D    1  1.00
                0.126000        1.000000
D    1  1.00
                0.321000        1.000000
D    1  1.00
                0.817000        1.000000
D    1  1.00
                2.082000        1.000000
F    1  1.00
                0.169000        1.000000
F    1  1.00
                0.341000        1.000000
F    1  1.00
                0.688000        1.000000
G    1  1.00
                0.320000        1.000000
G    1  1.00
                0.705000        1.000000
H    1  1.00
                0.583000        1.000000
S    1  1.00
                0.026000        1.000000
P    1  1.00
                0.019200        1.000000
D    1  1.00
                0.046800        1.000000
F    1  1.00
                0.073500        1.000000
G    1  1.00
                0.151000        1.000000
H    1  1.00
                0.323000        1.000000
```

Phosphorous

aug-cc-pvdz

```
P              0.000000
S    12 1.00
          94,840.000000      0.000256
          14,220.000000      0.001982
           3,236.000000      0.010276
             917.100000      0.041482
             299.500000      0.131984
             108.100000      0.308662
              42.180000      0.420647
              17.280000      0.222878
               4.858000      0.016404
               1.818000     -0.002543
               0.337200      0.000748
               0.123200     -0.000331
S    12 1.00
          94,840.000000     -0.000070
          14,220.000000     -0.000535
           3,236.000000     -0.002837
             917.100000     -0.011398
             299.500000     -0.039293
             108.100000     -0.099636
              42.180000     -0.197983
              17.280000     -0.114860
               4.858000      0.518595
               1.818000      0.601847
               0.337200      0.036861
               0.123200     -0.009708
S    12 1.00
          94,840.000000      0.000019
          14,220.000000      0.000147
           3,236.000000      0.000778
             917.100000      0.003145
             299.500000      0.010820
             108.100000      0.027996
              42.180000      0.056398
              17.280000      0.035819
               4.858000     -0.193387
               1.818000     -0.372097
               0.337200      0.624246
               0.123200      0.551721
S    1 1.00
               0.123200      1.000000
P    8 1.00
             370.500000      0.003950
              87.330000      0.030249
              27.590000      0.129554
              10.000000      0.327594
               3.825000      0.456992
               1.494000      0.253086
```

aug-cc-pvtz

```
P              0.000000
S    15 1.00
         312,400.000000      0.000058
          46,800.000000      0.000448
          10,650.000000      0.002349
           3,018.000000      0.009783
             986.800000      0.034147
             357.400000      0.100204
             139.600000      0.234372
              57.630000      0.382434
              24.600000      0.318088
              10.120000      0.070779
               4.283000     -0.001818
               1.805000      0.002162
               0.615800     -0.000835
               0.278200      0.000432
               0.105500     -0.000114
S    15 1.00
         312,400.000000     -0.000016
          46,800.000000     -0.000122
          10,650.000000     -0.000640
           3,018.000000     -0.002674
             986.800000     -0.009498
             357.400000     -0.028935
             139.600000     -0.074512
              57.630000     -0.149938
              24.600000     -0.189467
              10.120000      0.036327
               4.283000      0.528816
               1.805000      0.519115
               0.615800      0.060555
               0.278200     -0.009257
               0.105500      0.002104
S    15 1.00
         312,400.000000      0.000004
          46,800.000000      0.000033
          10,650.000000      0.000176
           3,018.000000      0.000734
             986.800000      0.002618
             357.400000      0.007979
             139.600000      0.020794
              57.630000      0.042445
              24.600000      0.056344
              10.120000     -0.012736
               4.283000     -0.196495
               1.805000     -0.353555
               0.615800      0.074141
               0.278200      0.700912
               0.105500      0.404739
```

```
                0.392100        0.016880
                0.118600       -0.002071
P       8 1.00
              370.500000       -0.000960
               87.330000       -0.007112
               27.590000       -0.032712
               10.000000       -0.079578
                3.825000       -0.135016
                1.494000       -0.009106
                0.392100        0.537802
                0.118600        0.569066
P       1 1.00
                0.118600        1.000000
D       1 1.00
                0.373000        1.000000
S       1 1.00
                0.041700        1.000000
P       1 1.00
                0.034300        1.000000
D       1 1.00
                0.113000        1.000000
S       1 1.00
                0.615800        1.000000
S       1 1.00
                0.105500        1.000000
P       9 1.00
              504.900000        0.002337
              119.400000        0.018541
               37.960000        0.084969
               13.950000        0.244615
                5.457000        0.422766
                2.177000        0.368439
                0.801000        0.077273
                0.287700       -0.003790
                0.097140        0.001599
P       9 1.00
              504.900000       -0.000555
              119.400000       -0.004459
               37.960000       -0.020635
               13.950000       -0.061769
                5.457000       -0.108924
                2.177000       -0.105599
                0.801000        0.153483
                0.287700        0.576981
                0.097140        0.422439
P       1 1.00
                0.801000        1.000000
P       1 1.00
                0.097140        1.000000
D       1 1.00
                0.216000        1.000000
D       1 1.00
                0.652000        1.000000
F       1 1.00
                0.452000        1.000000
S       1 1.00
                0.040900        1.000000
P       1 1.00
                0.030700        1.000000
D       1 1.00
                0.077500        1.000000
F       1 1.00
                0.165000        1.000000
```

Phosphorous

aug-cc-pvqz

```
P              0.000000
S     16  1.00
        615,200.000000   0.000025
         92,120.000000   0.000192
         20,950.000000   0.001012
          5,920.000000   0.004273
          1,922.000000   0.015416
            688.000000   0.048598
            265.000000   0.130060
            108.200000   0.274514
             46.220000   0.385402
             20.230000   0.255934
              7.859000   0.039124
              3.547000  -0.003680
              1.564000   0.002082
              0.488800  -0.000788
              0.226600   0.000454
              0.093310  -0.000127
S     16  1.00
        615,200.000000  -0.000007
         92,120.000000  -0.000052
         20,950.000000  -0.000275
          5,920.000000  -0.001163
          1,922.000000  -0.004243
            688.000000  -0.013611
            265.000000  -0.038511
            108.200000  -0.090664
             46.220000  -0.166584
             20.230000  -0.161447
              7.859000   0.146781
              3.547000   0.566682
              1.564000   0.416433
              0.488800   0.034384
              0.226600  -0.007806
              0.093310   0.001923
S     16  1.00
        615,200.000000   0.000002
         92,120.000000   0.000014
         20,950.000000   0.000076
          5,920.000000   0.000319
          1,922.000000   0.001169
            688.000000   0.003743
            265.000000   0.010682
            108.200000   0.025266
             46.220000   0.047928
             20.230000   0.047710
              7.859000  -0.046653
              3.547000  -0.234968
              1.564000  -0.311337
```

aug-cc-pv5z

```
P              0.000000
S     20  1.00
      4,666,000.000000   0.000002
        698,600.000000   0.000015
        159,000.000000   0.000080
         45,040.000000   0.000340
         14,720.000000   0.001233
          5,323.000000   0.004013
          2,076.000000   0.011912
            861.100000   0.032251
            375.700000   0.078664
            170.800000   0.166458
             80.290000   0.283039
             38.770000   0.331942
             18.930000   0.203352
              8.796000   0.038318
              4.358000  -0.000385
              2.174000   0.001587
              1.095000  -0.000413
              0.440000   0.000153
              0.194500  -0.000083
              0.083760   0.000018
S     20  1.00
      4,666,000.000000  -0.000001
        698,600.000000  -0.000004
        159,000.000000  -0.000022
         45,040.000000  -0.000092
         14,720.000000  -0.000335
          5,323.000000  -0.001095
          2,076.000000  -0.003268
            861.100000  -0.009000
            375.700000  -0.022653
            170.800000  -0.051465
             80.290000  -0.100186
             38.770000  -0.155075
             18.930000  -0.133818
              8.796000   0.087836
              4.358000   0.422581
              2.174000   0.474899
              1.095000   0.165002
              0.440000   0.008469
              0.194500  -0.000292
              0.083760   0.000285
S     20  1.00
      4,666,000.000000   0.000000
        698,600.000000   0.000001
        159,000.000000   0.000006
         45,040.000000   0.000025
         14,720.000000   0.000092
```

```
                0.488800  0.257109
                0.226600  0.653655
                0.093310  0.294212
S     1  1.00
                0.488800  1.000000
S     1  1.00
                0.226600  1.000000
S     1  1.00
                0.093310  1.000000
P     11  1.00
            1,367.000000  0.000421
              324.000000  0.003610
              104.600000  0.018922
               39.370000  0.070556
               16.260000  0.188157
                7.056000  0.338709
                3.130000  0.381943
                1.394000  0.195261
                0.517900  0.019942
                0.203200 -0.001351
                0.076980  0.000517
P     11  1.00
            1,367.000000 -0.000101
              324.000000 -0.000855
              104.600000 -0.004571
               39.370000 -0.017033
               16.260000 -0.047520
                7.056000 -0.085279
                3.130000 -0.109676
                1.394000 -0.016118
                0.517900  0.322893
                0.203200  0.545738
                0.076980  0.268538
P     1  1.00
                0.517900  1.000000
P     1  1.00
                0.203200  1.000000
P     1  1.00
                0.076980  1.000000
D     1  1.00
                0.165000  1.000000
D     1  1.00
                0.413000  1.000000
D     1  1.00
                1.036000  1.000000
F     1  1.00
                0.280000  1.000000
F     1  1.00
                0.703000  1.000000
G     1  1.00
                0.597000  1.000000
            5,323.000000  0.000301
            2,076.000000  0.000900
              861.100000  0.002474
              375.700000  0.006268
              170.800000  0.014260
               80.290000  0.028277
               38.770000  0.044512
               18.930000  0.040722
                8.796000 -0.030191
                4.358000 -0.152894
                2.174000 -0.282411
                1.095000 -0.148522
                0.440000  0.393563
                0.194500  0.617327
                0.083760  0.214612
S     1  1.00
                1.095000  1.000000
S     1  1.00
                0.440000  1.000000
S     1  1.00
                0.194500  1.000000
S     1  1.00
                0.083760  1.000000
P     12  1.00
            2,010.000000  0.000216
              476.300000  0.001875
              154.400000  0.010174
               58.510000  0.039986
               24.400000  0.118563
               10.800000  0.251816
                4.913000  0.366565
                2.269000  0.316177
                1.043000  0.104700
                0.431300  0.006099
                0.176700  0.000502
                0.070090 -0.000030
P     12  1.00
            2,010.000000 -0.000051
              476.300000 -0.000448
              154.400000 -0.002423
               58.510000 -0.009698
               24.400000 -0.029097
               10.800000 -0.064173
                4.913000 -0.094507
                2.269000 -0.093470
                1.043000  0.052061
                0.431300  0.374624
                0.176700  0.509097
                0.070090  0.215116
P     1  1.00
                1.043000  1.000000
```

```
S     1  1.00
                  0.035400  1.000000
P     1  1.00
                  0.027200  1.000000
D     1  1.00
                  0.059400  1.000000
F     1  1.00
                  0.109000  1.000000
G     1  1.00
                  0.250000  1.000000
P     1  1.00
                  0.431300  1.000000
P     1  1.00
                  0.176700  1.000000
P     1  1.00
                  0.070090  1.000000
D     1  1.00
                  0.166000  1.000000
D     1  1.00
                  0.418000  1.000000
D     1  1.00
                  1.054000  1.000000
D     1  1.00
                  2.656000  1.000000
F     1  1.00
                  0.219000  1.000000
F     1  1.00
                  0.450000  1.000000
F     1  1.00
                  0.923000  1.000000
G     1  1.00
                  0.412000  1.000000
G     1  1.00
                  0.903000  1.000000
H     1  1.00
                  0.745000  1.000000
S     1  1.00
                  0.033500  1.000000
P     1  1.00
                  0.025300  1.000000
D     1  1.00
                  0.062400  1.000000
F     1  1.00
                  0.095000  1.000000
G     1  1.00
                  0.184000  1.000000
H     1  1.00
                  0.372000  1.000000
```

Sulfur

aug-cc-pvdz

```
S              0.000000
S     12 1.00
        110,800.000000  0.000248
         16,610.000000  0.001920
          3,781.000000  0.009962
          1,071.000000  0.040298
            349.800000  0.128604
            126.300000  0.303480
             49.260000  0.421432
             20.160000  0.230781
              5.720000  0.017897
              2.182000 -0.002975
              0.432700  0.000850
              0.157000 -0.000368
S     12 1.00
        110,800.000000 -0.000069
         16,610.000000 -0.000528
          3,781.000000 -0.002797
          1,071.000000 -0.011265
            349.800000 -0.038883
            126.300000 -0.099503
             49.260000 -0.199740
             20.160000 -0.123360
              5.720000  0.513194
              2.182000  0.607120
              0.432700  0.039675
              0.157000 -0.009469
S     12 1.00
        110,800.000000  0.000020
         16,610.000000  0.000153
          3,781.000000  0.000810
          1,071.000000  0.003290
            349.800000  0.011297
            126.300000  0.029639
             49.260000  0.059985
             20.160000  0.041325
              5.720000 -0.207474
              2.182000 -0.392889
              0.432700  0.632840
              0.157000  0.556924
S     1 1.00
              0.157000  1.000000
P     8 1.00
            399.700000  0.004475
             94.190000  0.034171
             29.750000  0.144250
             10.770000  0.353928
              4.119000  0.459085
              1.625000  0.206383
```

aug-cc-pvtz

```
S              0.000000
S     15 1.00
        374,100.000000  0.000054
         56,050.000000  0.000421
         12,760.000000  0.002207
          3,615.000000  0.009193
          1,183.000000  0.032112
            428.800000  0.094668
            167.800000  0.223630
             69.470000  0.374393
             29.840000  0.329108
             12.720000  0.084704
              5.244000  0.000441
              2.219000  0.001648
              0.776700 -0.000622
              0.349000  0.000301
              0.132200 -0.000084
S     15 1.00
        374,100.000000 -0.000015
         56,050.000000 -0.000116
         12,760.000000 -0.000612
          3,615.000000 -0.002554
          1,183.000000 -0.009087
            428.800000 -0.027705
            167.800000 -0.072002
             69.470000 -0.146439
             29.840000 -0.195150
             12.720000  0.008192
              5.244000  0.516601
              2.219000  0.542178
              0.776700  0.068843
              0.349000 -0.009181
              0.132200  0.002268
S     15 1.00
        374,100.000000  0.000004
         56,050.000000  0.000034
         12,760.000000  0.000178
          3,615.000000  0.000741
          1,183.000000  0.002646
            428.800000  0.008075
            167.800000  0.021228
             69.470000  0.043832
             29.840000  0.061272
             12.720000 -0.003615
              5.244000 -0.204510
              2.219000 -0.381871
              0.776700  0.082684
              0.349000  0.714147
              0.132200  0.393791
```

```
                0.472600  0.010214
                0.140700 -0.000060
P     8 1.00
              399.700000 -0.001163
               94.190000 -0.008657
               29.750000 -0.039089
               10.770000 -0.093463
                4.119000 -0.147994
                1.625000  0.030190
                0.472600  0.561573
                0.140700  0.534776
P     1 1.00
                0.140700  1.000000
D     1 1.00
                0.479000  1.000000
S     1 1.00
                0.050700  1.000000
P     1 1.00
                0.039900  1.000000
D     1 1.00
                0.152000  1.000000
S     1 1.00
                0.776700  1.000000
S     1 1.00
                0.132200  1.000000
P     9 1.00
              574.400000  0.002423
              135.800000  0.019280
               43.190000  0.088540
               15.870000  0.254654
                6.208000  0.433984
                2.483000  0.354953
                0.868800  0.061894
                0.322900 -0.005030
                0.109800  0.002098
P     9 1.00
              574.400000 -0.000620
              135.800000 -0.004939
               43.190000 -0.023265
               15.870000 -0.068520
                6.208000 -0.123896
                2.483000 -0.096950
                0.868800  0.228215
                0.322900  0.569394
                0.109800  0.366302
P     1 1.00
                0.868800  1.000000
P     1 1.00
                0.109800  1.000000
D     1 1.00
                0.269000  1.000000
D     1 1.00
                0.819000  1.000000
F     1 1.00
                0.557000  1.000000
S     1 1.00
                0.049700  1.000000
P     1 1.00
                0.035100  1.000000
D     1 1.00
                0.101000  1.000000
F     1 1.00
                0.218000  1.000000
```

Sulfur

aug-cc-pvqz

S	0.000000	
S	16 1.00	
	727,800.000000	0.000024
	109,000.000000	0.000183
	24,800.000000	0.000964
	7,014.000000	0.004065
	2,278.000000	0.014697
	814.700000	0.046508
	313.400000	0.125508
	127.700000	0.268433
	54.480000	0.384809
	23.850000	0.265372
	9.428000	0.043733
	4.290000	-0.003788
	1.909000	0.002181
	0.627000	-0.000837
	0.287300	0.000448
	0.117200	-0.000125
S	16 1.00	
	727,800.000000	-0.000007
	109,000.000000	-0.000051
	24,800.000000	-0.000267
	7,014.000000	-0.001126
	2,278.000000	-0.004112
	814.700000	-0.013245
	313.400000	-0.037700
	127.700000	-0.089855
	54.480000	-0.167098
	23.850000	-0.169354
	9.428000	0.127824
	4.290000	0.564862
	1.909000	0.431767
	0.627000	0.038940
	0.287300	-0.007303
	0.117200	0.001923
S	16 1.00	
	727,800.000000	0.000002
	109,000.000000	0.000015
	24,800.000000	0.000078
	7,014.000000	0.000327
	2,278.000000	0.001197
	814.700000	0.003848
	313.400000	0.011054
	127.700000	0.026465
	54.480000	0.050877
	23.850000	0.053003
	9.428000	-0.042552
	4.290000	-0.250853
	1.909000	-0.333152

aug-cc-pv5z

S	0.000000	
S	20 1.00	
	5,481,000.000000	0.000002
	820,600.000000	0.000015
	186,700.000000	0.000078
	52,880.000000	0.000327
	17,250.000000	0.001194
	6,226.000000	0.003884
	2,429.000000	0.011534
	1,007.000000	0.031275
	439.500000	0.076439
	199.800000	0.162700
	93.920000	0.279328
	45.340000	0.333145
	22.150000	0.209836
	10.340000	0.041597
	5.119000	-0.000451
	2.553000	0.001689
	1.282000	-0.000517
	0.545000	0.000189
	0.241100	-0.000100
	0.103500	0.000021
S	20 1.00	
	5,481,000.000000	-0.000001
	820,600.000000	-0.000004
	186,700.000000	-0.000021
	52,880.000000	-0.000090
	17,250.000000	-0.000330
	6,226.000000	-0.001078
	2,429.000000	-0.003219
	1,007.000000	-0.008872
	439.500000	-0.022377
	199.800000	-0.051058
	93.920000	-0.100225
	45.340000	-0.156795
	22.150000	-0.139748
	10.340000	0.081006
	5.119000	0.430883
	2.553000	0.481688
	1.282000	0.156862
	0.545000	0.007888
	0.241100	0.000394
	0.103500	0.000224
S	20 1.00	
	5,481,000.000000	0.000000
	820,600.000000	0.000001
	186,700.000000	0.000006
	52,880.000000	0.000026
	17,250.000000	0.000096

```
                0.627000        0.263796
                0.287300        0.666849
                0.117200        0.288451
S     1  1.00
                0.627000        1.000000
S     1  1.00
                0.287300        1.000000
S     1  1.00
                0.117200        1.000000
P    11  1.00
            1,546.000000        0.000441
              366.400000        0.003776
              118.400000        0.019836
               44.530000        0.074206
               18.380000        0.197327
                7.965000        0.351851
                3.541000        0.378687
                1.591000        0.170931
                0.620500        0.015159
                0.242000        0.000067
                0.090140        0.000405
P    11  1.00
            1,546.000000       -0.000113
              366.400000       -0.000959
              118.400000       -0.005135
               44.530000       -0.019264
               18.380000       -0.053598
                7.965000       -0.096033
                3.541000       -0.118183
                1.591000        0.009232
                0.620500        0.358841
                0.242000        0.525818
                0.090140        0.248872
P     1  1.00
                0.620500        1.000000
P     1  1.00
                0.242000        1.000000
P     1  1.00
                0.090140        1.000000
D     1  1.00
                0.203000        1.000000
D     1  1.00
                0.504000        1.000000
D     1  1.00
                1.250000        1.000000
F     1  1.00
                0.335000        1.000000
F     1  1.00
                0.869000        1.000000
G     1  1.00
                0.683000        1.000000
            6,226.000000        0.000313
            2,429.000000        0.000936
            1,007.000000        0.002578
              439.500000        0.006541
              199.800000        0.014963
               93.920000        0.029894
               45.340000        0.047695
               22.150000        0.044956
               10.340000       -0.029301
                5.119000       -0.168916
                2.553000       -0.311014
                1.282000       -0.136491
                0.545000        0.423195
                0.241100        0.613888
                0.103500        0.200473
S     1  1.00
                1.282000        1.000000
S     1  1.00
                0.545000        1.000000
S     1  1.00
                0.241100        1.000000
S     1  1.00
                0.103500        1.000000
P    12  1.00
            2,200.000000        0.000239
              521.400000        0.002077
              169.000000        0.011236
               64.050000        0.044069
               26.720000        0.129168
               11.830000        0.269083
                5.378000        0.378611
                2.482000        0.296779
                1.116000        0.077968
                0.484800        0.002052
                0.200600        0.001436
                0.079510       -0.000060
P    12  1.00
            2,200.000000       -0.000061
              521.400000       -0.000530
              169.000000       -0.002879
               64.050000       -0.011440
               26.720000       -0.034276
               11.830000       -0.073581
                5.378000       -0.107782
                2.482000       -0.087977
                1.116000        0.108261
                0.484800        0.407082
                0.200600        0.468994
                0.079510        0.184877
P     1  1.00
                1.116000        1.000000
```

S 1 1.00
0.042800 1.000000
P 1 1.00
0.031700 1.000000
D 1 1.00
0.074800 1.000000
F 1 1.00
0.140000 1.000000
G 1 1.00
0.297000 1.000000

P 1 1.00
0.484800 1.000000
P 1 1.00
0.200600 1.000000
P 1 1.00
0.079510 1.000000
D 1 1.00
0.205000 1.000000
D 1 1.00
0.512000 1.000000
D 1 1.00
1.281000 1.000000
D 1 1.00
3.203000 1.000000
F 1 1.00
0.255000 1.000000
F 1 1.00
0.529000 1.000000
F 1 1.00
1.096000 1.000000
G 1 1.00
0.463000 1.000000
G 1 1.00
1.071000 1.000000
H 1 1.00
0.872000 1.000000
S 1 1.00
0.042000 1.000000
P 1 1.00
0.029400 1.000000
D 1 1.00
0.079400 1.000000
F 1 1.00
0.118800 1.000000
G 1 1.00
0.220000 1.000000
H 1 1.00
0.472000 1.000000

Chlorine

aug-cc-pvdz

```
Cl          0.000000
S    12 1.00
      127,900.000000     0.000241
       19,170.000000     0.001871
        4,363.000000     0.009708
        1,236.000000     0.039315
          403.600000     0.125932
          145.700000     0.299341
           56.810000     0.421886
           23.230000     0.237201
            6.644000     0.019153
            2.575000    -0.003348
            0.537100     0.000930
            0.193800    -0.000396
S    12 1.00
      127,900.000000    -0.000068
       19,170.000000    -0.000522
        4,363.000000    -0.002765
        1,236.000000    -0.011154
          403.600000    -0.038592
          145.700000    -0.099485
           56.810000    -0.201392
           23.230000    -0.130313
            6.644000     0.509443
            2.575000     0.610725
            0.537100     0.042155
            0.193800    -0.009234
S    12 1.00
      127,900.000000     0.000021
       19,170.000000     0.000158
        4,363.000000     0.000834
        1,236.000000     0.003399
          403.600000     0.011674
          145.700000     0.030962
           56.810000     0.062953
           23.230000     0.046026
            6.644000    -0.219312
            2.575000    -0.408773
            0.537100     0.638465
            0.193800     0.562362
S    1 1.00
            0.193800     1.000000
P    8 1.00
          417.600000     0.005260
           98.330000     0.039833
           31.040000     0.164655
           11.190000     0.387322
            4.249000     0.457072
            1.624000     0.151636
```

aug-cc-pvtz

```
Cl          0.000000
S    15 1.00
      456,100.000000     0.000049
       68,330.000000     0.000383
       15,550.000000     0.002009
        4,405.000000     0.008386
        1,439.000000     0.029470
          520.400000     0.087833
          203.100000     0.211473
           83.960000     0.365364
           36.200000     0.340884
           15.830000     0.102133
            6.334000     0.003117
            2.694000     0.001058
            0.976800    -0.000378
            0.431300     0.000156
            0.162500    -0.000051
S    15 1.00
      456,100.000000    -0.000014
       68,330.000000    -0.000107
       15,550.000000    -0.000565
        4,405.000000    -0.002361
        1,439.000000    -0.008459
          520.400000    -0.025964
          203.100000    -0.068636
           83.960000    -0.141874
           36.200000    -0.199319
           15.830000    -0.019566
            6.334000     0.499741
            2.694000     0.563736
            0.976800     0.079033
            0.431300    -0.008351
            0.162500     0.002325
S    15 1.00
      456,100.000000     0.000004
       68,330.000000     0.000032
       15,550.000000     0.000171
        4,405.000000     0.000714
        1,439.000000     0.002567
          520.400000     0.007886
          203.100000     0.021087
           83.960000     0.044226
           36.200000     0.065167
           15.830000     0.006030
            6.334000    -0.206495
            2.694000    -0.405871
            0.976800     0.075956
            0.431300     0.725661
            0.162500     0.394423
```

```
                0.532200        0.001816
                0.162000        0.001883
P       8 1.00
              417.600000       -0.001436
               98.330000       -0.010780
               31.040000       -0.047008
               11.190000       -0.111030
                4.249000       -0.153275
                1.624000        0.089461
                0.532200        0.579444
                0.162000        0.483272
P       1 1.00
                0.162000        1.000000
D       1 1.00
                0.600000        1.000000
S       1 1.00
                0.060800        1.000000
P       1 1.00
                0.046600        1.000000
D       1 1.00
                0.196000        1.000000
S       1 1.00
                0.976800        1.000000
S       1 1.00
                0.162500        1.000000
P       9 1.00
              663.300000        0.002404
              156.800000        0.019215
               49.980000        0.088510
               18.420000        0.256020
                7.240000        0.436927
                2.922000        0.350334
                1.022000        0.058550
                0.381800       -0.004584
                0.130100        0.002270
P       9 1.00
              663.300000       -0.000652
              156.800000       -0.005194
               49.980000       -0.024694
               18.420000       -0.072817
                7.240000       -0.134030
                2.922000       -0.094774
                1.022000        0.262289
                0.381800        0.564667
                0.130100        0.341250
P       1 1.00
                1.022000        1.000000
P       1 1.00
                0.130100        1.000000
D       1 1.00
                1.046000        1.000000
D       1 1.00
                0.344000        1.000000
F       1 1.00
                0.706000        1.000000
S       1 1.00
                0.059100        1.000000
P       1 1.00
                0.041900        1.000000
D       1 1.00
                0.135000        1.000000
F       1 1.00
                0.312000        1.000000
```

Chlorine

aug-cc-pvqz

```
Cl          0.000000
S    16 1.00
      834,900.000000    0.000023
      125,000.000000    0.000180
       28,430.000000    0.000948
        8,033.000000    0.004001
        2,608.000000    0.014463
          933.900000    0.045659
          360.000000    0.123248
          147.000000    0.264369
           62.880000    0.382989
           27.600000    0.270934
           11.080000    0.047140
            5.075000   -0.003718
            2.278000    0.002192
            0.777500   -0.000850
            0.352700    0.000425
            0.143100   -0.000120
S    16 1.00
      834,900.000000   -0.000007
      125,000.000000   -0.000050
       28,430.000000   -0.000266
        8,033.000000   -0.001125
        2,608.000000   -0.004105
          933.900000   -0.013199
          360.000000   -0.037534
          147.000000   -0.089723
           62.880000   -0.167671
           27.600000   -0.174763
           11.080000    0.114909
            5.075000    0.563618
            2.278000    0.441606
            0.777500    0.042670
            0.352700   -0.006672
            0.143100    0.001907
S    16 1.00
      834,900.000000    0.000002
      125,000.000000    0.000015
       28,430.000000    0.000081
        8,033.000000    0.000340
        2,608.000000    0.001246
          933.900000    0.003996
          360.000000    0.011475
          147.000000    0.027550
           62.880000    0.053292
           27.600000    0.057125
           11.080000   -0.039520
            5.075000   -0.264343
            2.278000   -0.349291
```

aug-cc-pv5z

```
Cl          0.000000
S    20 1.00
    6,410,000.000000    0.000002
      959,600.000000    0.000014
      218,300.000000    0.000074
       61,810.000000    0.000314
       20,140.000000    0.001146
        7,264.000000    0.003739
        2,832.000000    0.011095
        1,175.000000    0.030115
          512.600000    0.073915
          233.000000    0.158258
          109.500000    0.274753
           52.860000    0.334066
           25.840000    0.217589
           12.170000    0.045728
            6.030000   -0.000135
            3.012000    0.001639
            1.511000   -0.000522
            0.660400    0.000181
            0.292600   -0.000100
            0.125400    0.000019
S    20 1.00
    6,410,000.000000   -0.000001
      959,600.000000   -0.000004
      218,300.000000   -0.000021
       61,810.000000   -0.000088
       20,140.000000   -0.000322
        7,264.000000   -0.001053
        2,832.000000   -0.003142
        1,175.000000   -0.008664
          512.600000   -0.021935
          233.000000   -0.050258
          109.500000   -0.099541
           52.860000   -0.157647
           25.840000   -0.146024
           12.170000    0.069223
            6.030000    0.430412
            3.012000    0.490802
            1.511000    0.158390
            0.660400    0.008399
            0.292600    0.000768
            0.125400    0.000227
S    20 1.00
    6,410,000.000000    0.000000
      959,600.000000    0.000001
      218,300.000000    0.000006
       61,810.000000    0.000027
       20,140.000000    0.000097
```

```
                0.777500        0.269671
                0.352700        0.676073
                0.143100        0.284679
S    1  1.00
                0.777500        1.000000
S    1  1.00
                0.352700        1.000000
S    1  1.00
                0.143100        1.000000
P    11  1.00
            1,703.000000        0.000474
              403.600000        0.004064
              130.300000        0.021336
               49.050000        0.079461
               20.260000        0.208927
                8.787000        0.364945
                3.919000        0.371725
                1.765000        0.146292
                0.720700        0.010791
                0.283900        0.001170
                0.106000        0.000339
P    11  1.00
            1,703.000000       -0.000128
              403.600000       -0.001094
              130.300000       -0.005834
               49.050000       -0.021926
               20.260000       -0.060139
                8.787000       -0.106929
                3.919000       -0.122454
                1.765000        0.038362
                0.720700        0.385256
                0.283900        0.507265
                0.106000        0.227218
P    1  1.00
                0.720700        1.000000
P    1  1.00
                0.283900        1.000000
P    1  1.00
                0.106000        1.000000
D    1  1.00
                0.254000        1.000000
D    1  1.00
                0.628000        1.000000
D    1  1.00
                1.551000        1.000000
F    1  1.00
                0.423000        1.000000
F    1  1.00
                1.089000        1.000000
G    1  1.00
                0.827000        1.000000
            7,264.000000        0.000318
            2,832.000000        0.000952
            1,175.000000        0.002624
              512.600000        0.006682
              233.000000        0.015360
              109.500000        0.030943
               52.860000        0.050064
               25.840000        0.048978
               12.170000       -0.026081
                6.030000       -0.178426
                3.012000       -0.332324
                1.511000       -0.132008
                0.660400        0.440556
                0.292600        0.611891
                0.125400        0.193172
S    1  1.00
                1.511000        1.000000
S    1  1.00
                0.660400        1.000000
S    1  1.00
                0.292600        1.000000
S    1  1.00
                0.125400        1.000000
P    12  1.00
            2,548.000000        0.000236
              603.700000        0.002052
              195.600000        0.011154
               74.150000        0.043982
               30.940000        0.129994
               13.690000        0.272959
                6.229000        0.383690
                2.878000        0.291870
                1.282000        0.070446
                0.564100        0.001288
                0.234800        0.001826
                0.093120        0.000020
P    12  1.00
            2,548.000000       -0.000064
              603.700000       -0.000553
              195.600000       -0.003028
               74.150000       -0.012065
               30.940000       -0.036635
               13.690000       -0.079076
                6.229000       -0.117422
                2.878000       -0.086094
                1.282000        0.140308
                0.564100        0.422336
                0.234800        0.446363
                0.093120        0.166634
P    1  1.00
                1.282000        1.000000
```

```
S    1  1.00
                0.051900        1.000000
P    1  1.00
                0.037600        1.000000
D    1  1.00
                0.095200        1.000000
F    1  1.00
                0.217000        1.000000
G    1  1.00
                0.378000        1.000000
P    1  1.00
                0.564100        1.000000
P    1  1.00
                0.234800        1.000000
P    1  1.00
                0.093120        1.000000
D    1  1.00
                0.250000        1.000000
D    1  1.00
                0.618000        1.000000
D    1  1.00
                1.529000        1.000000
D    1  1.00
                3.781000        1.000000
F    1  1.00
                0.320000        1.000000
F    1  1.00
                0.656000        1.000000
F    1  1.00
                1.345000        1.000000
G    1  1.00
                0.556000        1.000000
G    1  1.00
                1.302000        1.000000
H    1  1.00
                1.053000        1.000000
S    1  1.00
                0.047900        1.000000
P    1  1.00
                0.034800        1.000000
D    1  1.00
                0.100300        1.000000
F    1  1.00
                0.164000        1.000000
G    1  1.00
                0.277000        1.000000
H    1  1.00
                0.607000        1.000000
```

APPENDIX C

Tabulated Properties

In this appendix tables are given of properties for various types of wavefunctions and basis sets. Selected experimental values are given for comparison. The properties computed are: r_e the internuclear separation in atomic units at the model energy minimum, E the model total energy minimum, D_e the energy difference between model minimum and asymptotic limit, Θ_{zz} the expectation of quadrupole moment $\left\langle \frac{1}{2}\sum_i q_i\left(3z_i^2 - r_i^2\right)\right\rangle$ in atomic units taken at center of mass, and q_{zz} the expectation value of the field gradient $\left\langle \sum_{i\neq A} q_i \frac{3z_{iA}^2 - r_{iA}^2}{r_{iA}^5}\right\rangle$ in atomic units taken at nucleus. In both the quadrupole moment and the field gradient q_i denotes the charge of particle i, and the summation index runs over nuclei and electrons. The last table contains experimental spectroscopic values used in the determination of vibration corrections of calculated properties.

Table C-1. Calculated and experimental constants for the ground state, $X\ ^1\Sigma_g^+$, of H_2

Method/basis	r_e (a_0)	$E_T\left(e/a_0\right)$	D_e (ev)	$\Theta_{zz}\left(ea_0^2\right)$	$q_{zz}\left(e/a_0^3\right)$
RHF					
aug-cc-pvdz	1.4137	-1.128826	3.5066	0.4613	-0.3665
aug-cc-pvtz	1.3880	-1.133056	3.6207	0.4916	-0.3639
aug-cc-pvqz	1.3865	-1.133508	3.6330	0.4867	-0.3608
aug-cc-pv5z	1.3863	-1.133648	3.6368	0.4852	-0.3591
CBS limit	1.3863	-1.1336	3.6355	0.4845	-0.3589
MP2					
aug-cc-pvdz	1.4271	-1.156216	4.2509	0.4401	-0.3513
aug-cc-pvtz	1.3933	-1.165023	4.4906	0.4719	-0.3550
aug-cc-pvqz	1.3912	-1.166740	4.5373	0.4679	-0.3520
aug-cc-pv5z	1.3902	-1.167191	4.5496	0.4662	-0.3507
CBS limit	1.3893		4.5498	0.4649	-0.3504
CASSCF					
aug-cc-pvdz	1.4332	-1.149819	4.0769	0.4589	-0.3350
aug-cc-pvtz	1.4273	-1.151743	4.1292	0.4455	-0.3164
aug-cc-pvqz	1.4262	-1.152121	4.1395	0.4422	-0.3147
aug-cc-pv5z	1.4258	-1.152259	4.1433	0.4408	-0.3144
CBS limit	1.4256		4.1439	0.4404	-0.3142
CISD					
aug-cc-pvdz	1.4392	-1.164900	4.4873	0.4275	-0.3383
aug-cc-pvtz	1.4041	-1.172636	4.6978	0.4616	-0.3447
aug-cc-pvqz	1.4022	-1.173867	4.7313	0.4585	-0.3393
aug-cc-pv5z	1.4014	-1.174175	4.7397	0.4569	-0.3380
CBS limit	1.4010		4.7403	0.4552	-0.3374
CASSCF+1+2					
aug-cc-pvdz	1.4117	-1.168170	4.5762	0.4666	-0.3606
aug-cc-pvtz	1.4043	-1.172910	4.7052	0.4620	-0.3014
aug-cc-pvqz	1.4021	-1.173905	4.7323	0.4587	-0.3392
aug-cc-pv5z	1.4014	-1.174187	4.7400	0.4570	-0.3380
CBS limit	1.4012		4.7405	0.4567	-0.3377
Exptl.	1.4011[12]		4.7487[12]	0.460 ± 0.021[10]	

Table C-2. Calculated and experimental constants for the ground state, $X\ ^1\Sigma_g^+$, of Li_2

Method/basis	r_e (a_0)	$E_T\left(e/a_0\right)$	D_e (ev)	$\Theta_{zz}\left(ea_0^2\right)$	$q_{zz}\left(e/a_0^3\right)$
RHF					
roos	5.2609	-14.8718858	0.1758	11.1486	0.005577
a5z	5.2609	-14.8719081	0.1759	11.14507	0.005468
CASSCF					
roos	5.0972	-14.9032651	1.0272	10.8846	0.004657
a5z	5.0986	-14.9033815	1.0273	10.8891	0.004653
CASSCF+1+2					
roos	5.0971	-14.9037444	1.0396	10.9210	0.004896
a5z	5.0971	-14.9037781	1.0397	10.9213	0.004653
Exptl.	5.0510		1.046		

Table C-3. Calculated and experimental constants for the ground state, $X\ ^1\Sigma_g^+$, of Na_2

Method/basis	r_e (a_0)	$E_T\left(e/a_0\right)$	D_e (ev)	$\Theta_{zz}\left(ea_0^2\right)$	$q_{zz}\left(e/a_0^3\right)$
RHF					
roos	6.0414	-323.715883	-0.01458	12.1456	0.02574
vqz	6.0365	-323.716628	-0.01973	12.1212	0.02541
CASSCF					
roos	6.0141	-323.742751	0.7117	11.6614	0.02054
vqz	6.0118	-323.743497	0.7079	11.5966	0.02041
CASSCF+1+2					
roos	6.0055	-323.743156	0.7227	11.6905	0.02134
vqz	6.0030	-323.743890	0.7175	11.6264	0.02112
Exptl.	5.8182		0.720		

Table C-4 Calculated and experimental constants for the ground state, $X\ ^3\Sigma_g^-$, of B_2

Method/basis	r_e (a_0)	E_T $\left(e/a_0\right)$	D_e (ev)	Θ_{zz} $\left(ea_0^2\right)$	$q_{zz}\left(e/a_0^3\right)$
UHF					
aug-cc-pvdz	3.1188	-49.088087	0.7331	1.5809	-0.1310
aug-cc-pvtz	3.0942	-49.092796	0.7743	1.4246	-0.1132
aug-cc-pvqz	3.0900	-49.094648	0.7805	1.4000	-0.1126
aug-cc-pv5z	3.0897	-49.094949	0.7807	1.3758	-0.1123
CBS limit	3.0867		0.7808	1.2103	-0.1122
MP2					
aug-cc-pvdz	3.0642	-49.229733	2.4950	1.0072	-0.034542
aug-cc-pvtz	3.0205	-49.255513	2.7043	0.8777	-0.007246
aug-cc-pvqz	3.0118	-49.261555	2.7245	0.8528	-0.005252
aug-cc-pv5z	3.0103	-49.263164	2.7309	0.8476	-0.006043
CBS limit	3.0081		2.7338	0.8462	
CASSCF					
aug-cc-pvdz	3.0698	-49.2144360	2.4825	1.0066	0.03152
aug-cc-pvtz	3.0525	-49.2192017	2.2614	0.9064	0.04575
aug-cc-pvqz	3.0507	-49.2210594	2.2781	0.8887	0.04870
aug-cc-pv5z	3.0503	-49.2213994	2.2792	0.8843	0.04804
CBS limit	3.0503			0.8832	0.04800
CASSCF+1+2					
aug-cc-pvdz	3.0753	-49.2815040	2.2868	1.0414	0.01255
aug-cc-pvtz	3.0283	-49.2995716	2.4153	0.9260	0.03609
aug-cc-pvqz	3.0214	-49.3030189	2.4347	0.8931	0.04108
aug-cc-pv5z	3.0198	-49.3039741	2.4358	0.8858	0.05683
CBS limit	3.0152			0.8802	
Exptl.					

Table C-5. Calculated and experimental constants for the ground state, $X\ ^1\Sigma_g^+$, of C_2

Method/basis	r_e (a_0)	E_T (e/a_0)	D_e (ev)	Θ_{zz} (ea_0^2)	q_{zz} (e/a_0^3)
RHF					
aug-cc-pvdz	2.3673	-75.388372	0.6017	2.9023	-0.8553
aug-cc-pvtz	2.3442	-75.401798	0.7653	2.7844	-0.8274
aug-cc-pvqz	2.3408	-75.405643	0.7891	2.7693	-0.8265
aug-cc-pv5z	2.3406	-75.406302	0.7894	2.7657	-0.8239
CBS limit	2.3405		0.7896	2.7645	-0.8231
MP2					
aug-cc-pvdz	2.4153	-75.706322	6.1068	2.2683	-0.6051
aug-cc-pvtz	2.3805	-75.760793	6.5844	2.1823	-0.5828
aug-cc-pvqz	2.3737	-75.772458	6.6526	2.1615	-0.5843
aug-cc-pv5z	2.3726	-75.775764	6.6730	2.1556	-0.5848
CBS limit	2.3721		6.7104	2.1533	-0.5852
CASSCF					
aug-cc-pvdz	2.3877	-75.6266524	4.7080	2.3403	-0.4309
aug-cc-pvtz	2.3704	-75.6396363	5.9879	2.2628	-0.4051
aug-cc-pvqz	2.3688	-75.6432811	6.1743	2.2505	-0.4002
aug-cc-pv5z	2.3685	-75.6440411	6.1765	2.2463	-0.3987
CBS limit	2.3683			2.2425	-0.3980
CASSCF+1+2					
aug-cc-pvdz	2.3963	-75.7429896	4.7480	2.3700	-0.4815
aug-cc-pvtz	2.3631	-75.7839690	6.0386	2.2987	-0.4554
aug-cc-pvqz	2.3575	-75.7914593	6.2266	2.2757	-0.4489
aug-cc-pv5z	2.3562	-75.7936075	6.2287	2.2694	-0.4470
CBS limit	2.3557			2.2684	-0.4464
Exptl.	2.0744[12]		9.9065[12]	-1.09±0.07[31]	

Table C-6. Calculated and experimental constants for the ground state, $X\ ^1\Sigma_g^+$, of N_2

Method/basis	r_e (a_0)	$E_T\left(e/a_0\right)$	D_e (ev)	$\Theta_{zz}\left(ea_0^2\right)$	$q_{zz}\left(e/a_0^3\right)$
RHF					
aug-cc-pvdz	2.0377	-108.961925	4.9576	-0.9490	1.1237
aug-cc-pvtz	2.0163	-108.987796	5.2404	-1.0090	1.3857
aug-cc-pvqz	2.0135	-108.994616	5.2836	-1.0118	1.4060
aug-cc-pv5z	2.0133	-108.995999	5.2870	-1.0149	1.4042
CBS limit	2.0133		5.2891	-1.0158	
MP2					
aug-cc-pvdz	2.1388	-109.280650	9.4100	-1.1262	0.8417
aug-cc-pvtz	2.1053	-109.364800	10.0293	-1.1626	1.0637
aug-cc-pvqz	2.0985	-109.383055	10.1363	-1.1710	1.0858
aug-cc-pv5z	2.0976	-109.388586	10.1731	-1.1747	1.0854
CBS limit	2.0970		10.1724	-1.1751	
MCSCF					
aug-cc-pvdz	2.1076	-109.097018	8.6337	-1.1683	
aug-cc-pvtz	2.0853	-109.120694	8.8568	-1.2260	
aug-cc-pvqz	2.0825	-109.127412	8.8973	-1.2292	
CBS limit	2.0821		8.9063	-1.2294	
CASSCF					
aug-cc-pvdz	2.1063	-109.111025	9.0131	-1.1263	1.0345
aug-cc-pvtz	2.0873	-109.133920	9.2165	-1.1675	1.1462
aug-cc-pvqz	2.0860	-109.139872	9.2364	-1.1753	1.1763
aug-cc-pv5z	2.0856	-109.141326	9.2759	-1.1790	1.1780
CBS limit	2.0857			-1.1795	1.1870
MRCI					
aug-cc-pvdz	2.1144	-109.284004	8.7673	-1.1079	
aug-cc-pvtz	2.0866	-109.367229	9.5037	-1.1390	
aug-cc-pvqz	2.0806	-109.383822	9.5698	-1.1464	
CBS limit	2.0789		9.5721	-1.1487	
CASSCF+1+2					
aug-cc-pvdz	2.1135	-109.305121	8.9126	-1.0878	0.9881
aug-cc-pvtz	2.0855	-109.372107	9.5294	-1.1162	1.1095
aug-cc-pvqz	2.0827	-109.386811	9.6725	-1.1247	1.1432
aug-cc-pv5z	2.0802	-109.388891	9.7291	-1.1322	1.1478
CBS limit	2.0810			-1.1345	1.1518
Exptl.	2.0744[12]		9.9065[12]	-1.09±0.07[31]	

Table C-7. Calculated and experimental constants for the ground state, $X\ ^3\Sigma_g^-$, of O_2

Method/basis	r_e (a_0)	E_T (e/a_0)	D_e (ev)	Θ_{zz} (ea_0^2)	q_{zz} (e/a_0^3)
RoHF					
aug-cc-pvdz	2.1840	-149.625220	1.1784	-0.2833	-2.4415
aug-cc-pvtz	2.1779	-149.660506	1.2923	-0.3928	-2.4657
aug-cc-pvqz	2.1749	-149.670308	1.3110	-0.4085	-2.4927
aug-cc-pv5z	2.1747	-149.672974	1.3186	-0.4183	-2.5006
CBS limit	2.1739		1.3181	-0.4188	-2.5012
UHF					
aug-cc-pvdz	2.1979	-149.646215	1.7497	-0.2341	-1.2547
aug-cc-pvtz	2.1915	-149.682470	1.8899	-0.3134	-1.2472
aug-cc-pvqz	2.1885	-149.692404	1.9124	-0.3273	-1.2591
aug-cc-pv5z	2.1885	-149.695099	1.9207	-0.3356	-1.2578
CBS limit	2.1889		1.9172	-0.3427	-1.2565
UMP2					
aug-cc-pvdz	2.3314	-150.011480	5.2852	-0.1107	-1.3375
aug-cc-pvtz	2.3138	-150.128401	5.6078	-0.2178	-1.3771
aug-cc-pvqz	2.3064	-150.153761	5.6322	-0.2421	-1.3934
aug-cc-pv5z	2.3049	-150.162153	5.6548	-0.2537	-1.3901
CBS limit	2.3032		5.6472	-0.2546	-1.3894
MCSCF					
aug-cc-pvdz	2.3022	-149.718078	3.7982	-0.1457	
aug-cc-pvtz	2.2975	-149.752814	3.9146	-0.2618	
aug-cc-pvqz	2.2939	-149.763505	3.9606	-0.2858	
CBS limit	2.2936		3.9906	-0.2920	
CASSCF					
aug-cc-pvdz	2.3065	-149.725943	3.9798	-0.1669	-1.3470
aug-cc-pvtz	2.3009	-149.759501	4.0959	-0.2650	-1.3442
aug-cc-pvqz	2.2973	-149.768890	4.1072	-0.2822	-1.3465
aug-cc-pv5z	2.2970	-149.771592	4.1161	-0.2930	-1.3532
CBS limit	2.2957		4.1189	-0.2921	-1.3548
MRCI					
aug-cc-pvdz	2.3072	-150.003808	4.4229	-0.1213	
aug-cc-pvtz	2.2921	-150.114527	4.9575	-0.2156	
aug-cc-pvqz	2.2864	-150.138411	5.0034	-0.2474	
CBS limit	2.2830		5.0077	-0.2636	
CASSCF+1+2					
aug-cc-pvdz	2.3069	-150.027600	4.7815	-0.1448	-1.3594
aug-cc-pvtz	2.2944	-150.118085	4.8974	-0.2269	-1.3543
aug-cc-pvqz	2.2907	-150.140112	5.0056	-0.2368	-1.3605
aug-cc-pv5z	2.2868	-150.142995	5.0148	-0.2612	-1.3639
CBS limit	2.2854		5.0152	-0.2588	-1.3643
Exptl.	2.2818[12]		5.2318[12]	-0.3±0.1[36]	

Table C-8. Calculated and experimental constants for the ground state, $X\ ^1\Sigma_g^+$, of F_2

Method/basis	r_e (a_0)	E_T (e/a_0)	D_e (ev)	Θ_{zz} (ea_0^2)	q_{zz} (e/a_0^3)
RHF					
aug-cc-pvdz	2.5288	-198.703251	1.3847	0.5229	-6.4144
aug-cc-pvtz	2.5099	-198.760936	1.1764	0.3558	-6.6284
aug-cc-pvqz	2.5090	-198.774915	1.1770	0.3321	-6.7109
aug-cc-pv5z	2.5071	-198.779081	1.1786	0.3149	-6.7190
CBS limit	2.5079	-198.7801	1.1792	0.3180	-6.7198
MP2					
aug-cc-pvdz	2.6959	-199.126917	1.5039	0.9254	-5.7669
aug-cc-pvtz	2.6490	-199.290907	1.7987	0.7588	-6.1000
aug-cc-pvqz	2.6471	-199.326593	1.7931	0.7374	-6.1953
aug-cc-pv5z	2.6452	-199.338340	1.8004	0.7199	-6.2094
CBS limit	2.6460	-199.3399	1.7970	0.7236	-6.2109
MCSCF					
aug-cc-pvdz	2.8257	-198.777612	0.6388	0.9873	
aug-cc-pvtz	2.7643	-198.832379	0.7677	0.7899	
aug-cc-pvqz	2.7632	-198.846561	0.7658	0.7651	
CBS limit	2.7632	-198.8515	0.7681	0.7616	
CASSCF					
aug-cc-pvdz	2.8021	-198.780304	0.7041	0.9585	-6.0449
aug-cc-pvtz	2.7654	-198.834724	0.7305	0.7778	-6.2151
aug-cc-pvqz	2.7586	-198.848763	0.8257	0.7611	-6.2788
aug-cc-pv5z	2.7560	-198.852728	0.8261	0.7426	-6.2969
CBS limit	2.7560		0.8262	0.7481	-6.3098
MRCI					
aug-cc-pvdz	2.7520	-199.119575	1.2603	0.9370	
aug-cc-pvtz	2.6838	-199.277054	1.4875	0.7356	
aug-cc-pvqz	2.6825	-199.310003	1.4879	0.7111	
CBS limit	2.6827	-199.3187	1.4906	0.7077	
CASSCF+1+2					
aug-cc-pvdz	2.7329	-199.158133	1.2056	0.9032	-5.9777
aug-cc-pvtz	2.6955	-199.285251	1.4407	0.7352	-6.1519
aug-cc-pvqz	2.6853	-199.311735	1.4421	0.7165	-6.2275
aug-cc-pv5z	2.6802	-199.320173	1.4490	0.6927	-6.2496
CBS limit	2.6791		1.4496	0.6985	-6.2699
Exptl.	2.6681[12]		1.6916[12]	None Available	

Table C-9. Calculated and experimental constants for the ground state, $X\ ^3\Sigma_g^-$, of Al_2

Method/basis	r_e (a_0)	$E_T\left(e/a_0\right)$	D_e (ev)	$\Theta_{zz}\left(ea_0^2\right)$	$q_{zz}\left(e/a_0^3\right)$
UHF					
aug-cc-pvdz	4.8475	-483.762718	0.3919	7.9896	-0.3016
aug-cc-pvtz	4.8180	-483.774231	0.4322	7.6578	-0.3168
aug-cc-pvqz	4.8048	-483.776836	0.4351	7.5442	-0.2935
aug-cc-pv5z	4.8027	-483.777656	0.4365	7.5292	-0.3275
CBS limit	4.8023			7.5269	
MP2					
aug-cc-pvdz	4.7366	-483.853878	1.1071	7.2889	-0.2365
aug-cc-pvtz	4.6765	-483.879735	1.2532	7.1173	-0.2381
aug-cc-pvqz	4.6599	-483.884449	1.2616	7.0273	-0.2205
aug-cc-pv5z	4.6553	-483.777050	1.2625	7.0348	-0.2422
CBS limit	4.5542				
CASSCF					
aug-cc-pvdz	4.7984	-483.826309	1.1890	6.6022	-0.2122
aug-cc-pvtz	4.7766	-483.837438	1.2381	6.3208	-0.2006
aug-cc-pvqz	4.7661	-483.840329	1.2431	6.2268	-0.1965
aug-cc-pv5z	4.7634	-483.841074	1.2511	6.2208	
CBS limit	4.7625			6.2204	
CASSCF+1+2					
aug-cc-pvdz	4.7957	-483.888899	1.1989	6.6022	
aug-cc-pvtz	4.7263	-483.910444	1.3468	6.3208	
aug-cc-pvqz	4.7086	-483.914596	1.3906	6.1937	
aug-cc-pv5z	4.7063	-483.915684	1.5268	6.1914	
CBS limit	4.7060			6.1912	
Exptl.	4.660		1.55		

Table C-10. Calculated and experimental constants for the ground state, $X\ ^3\Sigma_g^-$, of Si_2

Method/basis	r_e (a_0)	$E_T\left(e/a_0\right)$	D_e (ev)	$\Theta_{zz}\left(ea_0^2\right)$	$q_{zz}\left(e/a_0^3\right)$
UHF					
aug-cc-pvdz	4.2256	-577.764760	1.7113	-4.6444	1.6932
aug-cc-pvtz	4.2016	-577.779332	1.7981	-4.7239	2.0001
aug-cc-pvqz	4.1927	-577.783621	1.8183	-4.7584	1.8211
aug-cc-pv5z	4.1884	-577.785048	1.8317	-4.7514	2.0860
CBS limit	4.1880				
MP2					
aug-cc-pvdz	4.3122	-577.897246	2.7258	-4.2857	1.4929
aug-cc-pvtz	4.2689	-577.939991	3.0221	-4.1696	1.7909
aug-cc-pvqz	4.2541	-577.947457	3.0519	-4.1973	1.6408
aug-cc-pv5z	4.2517	-577.951384	3.1002	-4.1834	1.8302
CBS limit	4.2511				
CASSCF					
aug-cc-pvdz	4.3555	-577.814916	2.6587	-4.3142	
aug-cc-pvtz	4.3300	-577.828330	2.7862	-4.3936	
aug-cc-pvqz	4.3205	-577.832431	2.8095	-4.4238	
aug-cc-pv5z	4.3162	-577.833570	2.8241	-4.4151	
CBS limit	4.3158				
CASSCF+1+2					
aug-cc-pvdz	4.3429	-577.932991	2.6835	-4.0188	
aug-cc-pvtz	4.2952	-577.970127	3.0642	-4.0175	
aug-cc-pvqz	4.2788	-577.976584	3.1821	-4.0593	
aug-cc-pv5z	4.2750	-577.978619	3.2318	-4.0425	
CBS limit	4.2741				
Exptl.	4.2443		3.21		

Table C-11. Calculated and experimental constants for the ground state, $X\ ^1\Sigma_g^+$, of P_2

Method/basis	r_e (a_0)	$E_T\left(e/a_0\right)$	D_e (ev)	$\Theta_{zz}\left(ea_0^2\right)$	$q_{zz}\left(e/a_0^3\right)$
RHF					
aug-cc-pvdz	3.5345	-681.470428	1.3826	0.7231	1.6350
aug-cc-pvtz	3.5096	-681.491898	1.6232	0.7870	1.8942
aug-cc-pvqz	3.5007	-681.498395	1.6788	0.7785	1.8316
aug-cc-pv5z	3.4969	-681.500786	1.7288	0.7920	2.0363
CBS limit	3.4950				
MP2					
aug-cc-pvdz	3.6895	-681.707199	4.1800	0.4203	1.1365
aug-cc-pvtz	3.6421	-681.775016	4.7259	0.5137	1.3700
aug-cc-pvqz	3.6256	-681.786020	4.8047	0.5080	1.3519
aug-cc-pv5z	3.6201	-681.790680	4.8396	0.5317	1.5039
CBS limit	3.6171				
CASSCF					
aug-cc-pvdz	3.6698	-681.564365	3.9380	0.3758	1.4625
aug-cc-pvtz	3.6425	-681.583508	4.1160	0.3042	1.5462
aug-cc-pvqz	3.6330	-681.589364	4.1543	0.3001	1.5705
aug-cc-pv5z	3.6288	-681.591273	4.1882	0.3162	1.5712
CBS limit	3.6268				
CASSCF+1+2					
aug-cc-pvdz	3.6704	-681.731599	4.0398	0.4989	1.3901
aug-cc-pvtz	3.6259	-681.791347	4.5810	0.5166	1.5007
aug-cc-pvqz	3.6114	-681.800869	4.6585	0.5035	1.5323
aug-cc-pv5z	3.6077	-681.804154	4.7094	0.5241	1.5319
CBS limit	3.6055				
Exptl.	3.5780		5.033		

Table C-12. Calculated and experimental constants for the ground state, $X\ ^3\Sigma_g^-$, of S_2

Method/basis	r_e (a_0)	$E_T\left(e/a_0\right)$	D_e (ev)	$\Theta_{zz}\left(ea_0^2\right)$	$q_{zz}\left(e/a_0^3\right)$
ROHF					
aug-cc-pvdz	3.5654	-795.054156	2.1420	1.4897	-1.7751
aug-cc-pvtz	3.5321	-795.083129	2.4563	1.4286	-1.7635
aug-cc-pvqz	3.5216	-795.090308	2.5118	1.3940	-1.7337
aug-cc-pv5z	3.5146	-795.093390	2.5791	1.3931	-1.7639
CBS limit	3.5123			1.3930	
UHF					
aug-cc-pvdz	3.5712	-795.067319	2.5002	1.7471	-0.8210
aug-cc-pvtz	3.5373	-795.098276	2.8685	1.4342	-0.7869
aug-cc-pvqz	3.5268	-795.105711	2.9309	1.4001	-0.7198
aug-cc-pv5z	3.5194	-795.109046	2.9768	1.3911	-0.7730
CBS limit	3.5171			1.3910	
UMP2					
aug-cc-pvdz	3.6679	-795.323675	3.9239	1.7466	-0.9704
aug-cc-pvtz	3.6109	-795.420906	4.0521	1.5373	-0.9648
aug-cc-pvqz	3.5937	-795.435561	4.4509	1.4916	-0.8856
aug-cc-pv5z	3.5831	-795.441961	4.4968	1.4845	-0.9510
CBS limit	3.5801			1.4831	
CASSCF					
aug-cc-pvdz	3.6975	-795.104169	3.1746	1.8238	-1.1505
aug-cc-pvtz	3.6570	-795.130461	3.4201	1.4922	-1.0727
aug-cc-pvqz	3.6457	-795.137012	3.4541	1.4660	-1.0454
aug-cc-pv5z	3.6372	-795.139513	3.5000	1.4614	-1.0226
CBS limit	3.6354		3.4927	1.4604	-1.0112
CASSCF+1+2					
aug-cc-pvdz	3.6780	-795.337615	3.6018	1.7322	-1.1505
aug-cc-pvtz	3.6258	-795.423487	3.9994	1.5075	-1.0249
aug-cc-pvqz	3.6101	-795.435364	4.0591	1.4670	-0.9931
aug-cc-pv5z	3.6005	-795.440183	4.1289	1.4602	-0.9689
CBS limit	3.5978		4.1191	1.4585	-0.9656
Exptl.	3.5701		4.3693		

Table C-13. Calculated and experimental constants for the ground state, $X\ ^1\Sigma_g^+$, of Cl_2

Method/basis	r_e (a_0)	$E_T\left(e/a_0\right)$	D_e (ev)	$\Theta_{zz}\left(ea_0^2\right)$	$q_{zz}\left(e/a_0^3\right)$
RHF					
aug-cc-pvdz	3.7915	-918.966152	0.7945	2.7868	-5.5182
aug-cc-pvtz	3.7496	-919.000062	1.0793	2.2923	-5.8076
aug-cc-pvqz	3.7309	-919.007029	1.1005	2.2401	-5.7488
aug-cc-pv5z	3.7308	-919.009640	1.1441	2.2400	-6.0858
CBS limit	3.7267			2.2400	-6.0866
MP2					
aug-cc-pvdz	3.8532	-919.259803	2.0128	2.8937	-5.1629
aug-cc-pvtz	3.7770	-919.387079	2.4579	2.4349	-5.4837
aug-cc-pvqz	3.7538	-919.404287	2.4938	2.3833	-5.4457
aug-cc-pv5z	3.7471	-919.410504	2.5252	2.3476	-5.7545
CBS limit	3.7440			2.3412	-5.7520
CASSCF					
aug-cc-pvdz	3.9130	-918.993656	1.7089	3.0242	-6.1467
aug-cc-pvtz	3.8652	-919.024862	1.7526	2.5262	-6.0555
aug-cc-pvqz	3.8554	-919.031537	1.7668	2.4962	-6.0503
aug-cc-pv5z	3.8439	-919.033687	1.7982	2.4725	-6.0136
CBS limit	3.8434		1.7935	2.3833	-6.0168
CASSCF+1+2					
aug-cc-pvdz	3.8846	-919.277887	1.8873	2.8560	-5.9721
aug-cc-pvtz	3.8182	-919.388888	2.2294	2.4251	-5.8841
aug-cc-pvqz	3.8050	-919.402437	2.2633	2.3801	-5.8801
aug-cc-pv5z	3.7881	-919.407181	2.3082	2.3468	-5.8389
CBS limit	3.7875		2.3159	2.3214	-5.8390
Exptl.	3.7566		2.4794	2.405±0.120	

APPENDIX D

Distance Dependence of Select Properties

This Appendix contains lists of the total energy(E), quadrupole moment(Θ) and the field gradient (q_{zz}) in atomic units as functions of internuclear separation for SCF, CASSCF, and CASSCF+1+2. The CASSCF and CASSCF+1+2 wavefunctions as those described in chapter 2,3, and 4. Molecules with multiplicities greater than 1 use the Restricted Open Shell Hartree-Fock wavefunction. All calculations use the Dunning aug-cc-pvqz basis sets which are described in Appendix B. The quadrupole moment and the field gradient were computed using the MOLPRO package.

Table D-1. H_2 ($^1\Sigma_g^+$) aug-cc-pvqz : Internuclear separation v.s. property, R increments of 0.2 a_0
Energy in atomic units plus 1.0000

R	$E^{(SCF)}$	$\Theta^{(SCF)}$	$q_{zz}^{(SCF)}$	$E^{(CASSCF)}$	$\Theta^{(CASSCF)}$	$q_{zz}^{(CASSCF)}$	$E^{(CASSCF+1+2)}$	$\Theta^{(CASSCF+1+2)}$	$q_{zz}^{(CASSCF+1+2)}$
0.80	0.01959	0.17809	-3.16989	0.00816	0.15741	-3.16182	-0.01906	0.17123	-3.16269
1.00	-0.08491	0.27006	-1.40539	-0.09836	0.23925	-1.40022	-0.12376	0.25699	-1.39951
1.20	-0.12484	0.37647	-0.68188	-0.14064	0.33108	-0.67909	-0.16428	0.35364	-0.67756
1.40	-0.13348	0.49507	-0.34453	-0.15200	0.42911	-0.34377	-0.17390	0.45755	-0.34173
1.60	-0.12622	0.62358	-0.17301	-0.14788	0.52915	-0.17406	-0.16807	0.56470	-0.17164
1.80	-0.11085	0.75972	-0.08165	-0.13609	0.62664	-0.08436	-0.15460	0.67063	-0.08168
2.00	-0.09152	0.90138	-0.03181	-0.12087	0.71680	-0.03608	-0.13770	0.77064	-0.03322
2.20	-0.07055	1.04651	-0.00420	-0.10456	0.79476	-0.01000	-0.11973	0.85978	-0.00703
2.40	-0.04924	1.19310	0.01112	-0.08853	0.85575	0.00383	-0.10205	0.93301	0.00685
2.60	-0.02835	1.33916	0.01934	-0.07355	0.89562	0.01062	-0.08544	0.98555	0.01363
2.80	-0.00829	1.48284	0.02331	-0.06005	0.91142	0.01325	-0.07035	1.01350	0.01619
3.00	0.01072	1.62246	0.02472	-0.04822	0.90204	0.01347	-0.05701	1.01453	0.01626
3.20	0.02857	1.75651	0.02463	-0.03813	0.86854	0.01240	-0.04551	0.98846	0.01498
3.40	0.04524	1.88363	0.02375	-0.02972	0.81418	0.01077	-0.03581	0.93756	0.01308
3.60	0.06073	2.00265	0.02246	-0.02285	0.74398	0.00900	-0.02780	0.86642	0.01102
3.80	0.07509	2.11264	0.02098	-0.01736	0.66386	0.00730	-0.02133	0.78120	0.00901
4.00	0.08836	2.21293	0.01942	-0.01305	0.57976	0.00578	-0.01619	0.68867	0.00720
4.20	0.10061	2.30300	0.01785	-0.00971	0.49676	0.00448	-0.01218	0.59504	0.00564
4.40	0.11190	2.38263	0.01631	-0.00716	0.41867	0.00341	-0.00909	0.50528	0.00434
4.60	0.12231	2.45162	0.01484	-0.00524	0.34789	0.00256	-0.00674	0.42277	0.00329
4.80	0.13188	2.50994	0.01347	-0.00381	0.28563	0.00190	-0.00497	0.34938	0.00247
5.00	0.14069	2.55768	0.01220	-0.00275	0.23212	0.00139	-0.00365	0.28578	0.00184
5.20	0.14880	2.59504	0.01104	-0.00196	0.18701	0.00102	-0.00266	0.23178	0.00136
5.40	0.15626	2.62233	0.00998	-0.00139	0.14956	0.00074	-0.00194	0.18668	0.00100
5.60	0.16312	2.63991	0.00903	-0.00098	0.11885	0.00053	-0.00140	0.14949	0.00074
5.80	0.16944	2.64824	0.00817	-0.00067	0.09394	0.00039	-0.00101	0.11915	0.00055
6.00	0.17525	2.64780	0.00739	-0.00045	0.07393	0.00028	-0.00072	0.09370	0.00041
6.20	0.18061	2.63913	0.00668	-0.00030	0.05797	0.00021	-0.00050	0.07416	0.00030

6.40	0.18555	2.62280	0.00605	-0.00018	0.04534	0.00016	-0.00035	0.05861	0.00023
6.60	0.19010	2.59940	0.00547	-0.00010	0.03541	0.00012	-0.00023	0.04629	0.00018
6.80	0.19430	2.56956	0.00495	-0.00004	0.02763	0.00009	-0.00015	0.03658	0.00013
7.00	0.19818	2.53390	0.00448	0.00000	0.02156	0.00006	-0.00009	0.02893	0.00010

Table D-2. H_2 ($^1\Sigma_g^+$) aug-cc-pvqz : Internuclear separation v.s. property, R increments of 0.05 a_0
Energy in atomic units plus 1.0000

R	$E^{(SCF)}$	$\Theta^{(SCF)}$	$q_{zz}^{(SCF)}$	$E^{(CASSCF)}$	$\Theta^{(CASSCF)}$	$q_{zz}^{(CASSCF)}$	$E^{(CASSCF+1+2)}$	$\Theta^{(CASSCF+1+2)}$	$q_{zz}^{(CASSCF+1+2)}$
1.0022	-0.08561	0.27115	-1.39370	-0.09908	0.24021	-1.38856	-0.12447	0.25800	-1.38784
1.0522	-0.09973	0.29653	-1.15597	-0.11375	0.26240	-1.15146	-0.13869	0.28130	-1.15049
1.1022	-0.11067	0.32277	-0.96338	-0.12528	0.28516	-0.95948	-0.14978	0.30523	-0.95829
1.1522	-0.11898	0.34984	-0.80610	-0.13418	0.30842	-0.80278	-0.15824	0.32973	-0.80141
1.2022	-0.12507	0.37771	-0.67669	-0.14090	0.33213	-0.67392	-0.16451	0.35475	-0.67239
1.2522	-0.12929	0.40634	-0.56946	-0.14577	0.35623	-0.56723	-0.16895	0.38021	-0.56555
1.3022	-0.13194	0.43569	-0.48006	-0.14909	0.38065	-0.47835	-0.17183	0.40607	-0.47653
1.3522	-0.13327	0.46574	-0.40511	-0.15110	0.40533	-0.40389	-0.17342	0.43226	-0.40196
1.4022	-0.13346	0.49643	-0.34197	-0.15202	0.43020	-0.34123	-0.17391	0.45872	-0.33918
1.4522	-0.13271	0.52775	-0.28855	-0.15201	0.45520	-0.28828	-0.17347	0.48538	-0.28613
1.5022	-0.13115	0.55964	-0.24321	-0.15122	0.48026	-0.24339	-0.17225	0.51218	-0.24115
1.5522	-0.12891	0.59208	-0.20461	-0.14977	0.50530	-0.20524	-0.17038	0.53903	-0.20290
1.6022	-0.12608	0.62503	-0.17167	-0.14778	0.53024	-0.17273	-0.16796	0.56588	-0.17031
1.6522	-0.12278	0.65846	-0.14350	-0.14532	0.55503	-0.14499	-0.16508	0.59266	-0.14250
1.7022	-0.11906	0.69233	-0.11938	-0.14249	0.57958	-0.12129	-0.16182	0.61928	-0.11873
1.7522	-0.11500	0.72660	-0.09869	-0.13934	0.60382	-0.10101	-0.15825	0.64567	-0.09839
1.8022	-0.11065	0.76125	-0.08093	-0.13594	0.62768	-0.08365	-0.15443	0.67177	-0.08096

Table D-3. N_2 ($^3\Sigma_g^-$) aug-cc-pvqz : Internuclear separation v.s. property, R increments of 0.2 a_0
Energy in atomic units plus 108.0

R	$E^{(SCF)}$	$\Theta^{(SCF)}$	$q_{zz}^{(SCF)}$	$E^{(CASSCF)}$	$\Theta^{(CASSCF)}$	$q_{zz}^{(CASSCF)}$	$E^{(CASSCF+1+2)}$	$\Theta^{(CASSCF+1+2)}$	$q_{zz}^{(CASSCF+1+2)}$
1.4000	-0.15025	-1.81106	1.10671	-0.23072	-1.87049	1.02139	-0.48445	-1.81776	0.99566
1.6000	-0.70754	-1.54891	1.45993	-0.80476	-1.64894	1.34777	-1.05532	-1.59420	1.31979
1.8000	-0.93605	-1.29665	1.50577	-1.05293	-1.45268	1.36513	-1.30072	-1.39855	1.33369
2.0000	-0.99452	-1.03052	1.41708	-1.13395	-1.25954	1.24777	-1.37965	-1.20703	1.21297
2.2000	-0.96704	-0.74068	1.26775	-1.13181	-1.06160	1.07119	-1.37622	-1.01004	1.03401
2.4000	-0.89874	-0.42705	1.09534	-1.09147	-0.86121	0.87431	-1.33545	-0.80858	0.83660
2.6000	-0.81394	-0.09624	0.92078	-1.03702	-0.66928	0.67862	-1.28129	-0.61209	0.64297
2.8000	-0.72548	0.24108	0.75596	-0.98110	-0.50414	0.49540	-1.22617	-0.43725	0.46439
3.0000	-0.63981	0.57289	0.60730	-0.93017	-0.38897	0.32970	-1.17618	-0.30435	0.30560
3.2000	-0.55990	0.88846	0.47731	-0.88751	-0.34330	0.18459	-1.13413	-0.23055	0.16874
3.4000	-0.48686	1.18003	0.36590	-0.85471	-0.36248	0.06696	-1.10110	-0.21583	0.05847
3.6000	-0.42087	1.44313		-0.83193	-0.40071		-1.07696	-0.22985	
3.8000	-0.36165	1.67606	0.19236	-0.81772	-0.40542	-0.04841	-1.06056	-0.23274	-0.05436
4.0000	-0.30871	1.87903	0.12619	-0.80962	-0.36637	-0.05513	-1.05007	-0.21002	-0.06319
4.2000	-0.26150	2.05337	0.07130	-0.80527	-0.30403	-0.04812	-1.04359	-0.17136	-0.05732
4.4000	-0.21945	2.20099	0.02608	-0.80302	-0.23847	-0.03772	-1.03963	-0.12936	-0.04678
4.6000	-0.18199	2.32399	-0.01076	-0.80188	-0.18000	-0.02821	-1.03719	-0.09158	-0.03634
4.8000	-0.14862	2.42446	-0.04034	-0.80129	-0.13196	-0.02070	-1.03563	-0.06056	-0.02759
5.0000	-0.11887	2.50438	-0.06366	-0.80099	-0.09445	-0.01510	-1.03461	-0.03665	-0.02076
5.2000	-0.09229	2.56555	-0.08162	-0.80082	-0.06582	-0.01102	-1.03391	-0.01913	-0.01558
5.4000	-0.06852	2.60962	-0.09500	-0.80072	-0.04461	-0.00805	-1.03340	-0.00662	-0.01170
5.6000	-0.04721	2.63804	-0.10453	-0.80066	-0.02919	-0.00591	-1.03302	0.00149	-0.00880
5.8000	-0.02807	2.65219	-0.11082	-0.80062	-0.01822	-0.00434	-1.03273	0.00702	-0.00665
6.0000	-0.01084	2.65330	-0.11442	-0.80059	-0.01052	-0.00319	-1.03250	0.01030	-0.00503
6.2000	0.00471	2.64257		-0.80056	-0.00540		-1.03232	0.01196	
6.4000	0.01878	2.62114	-0.11540	-0.80054	-0.00196	-0.00171	-1.03216	0.01244	-0.00289
6.6000	0.03154	2.59025	-0.11343	-0.80053	0.00015	-0.00124	-1.03204	0.01220	-0.00219
6.8000	0.04315	2.55079	-0.11047	-0.80051	0.00129	-0.00089	-1.03194	0.01146	-0.00166
7.0000	0.05374	2.50391	-0.10666	-0.80050	0.00182	-0.00063	-1.03186	0.01038	-0.00125
7.2000	0.06341	2.45064	-0.10222	-0.80049	0.00189	-0.00043	-1.03179	0.00914	-0.00093

7.4000	0.07229	2.39202		-0.80049	0.00165		-1.03174	0.00782	
7.6000	0.08044	2.32903	-0.09218	-0.80048	0.00127	-0.00018	-1.03170	0.00653	-0.00052
7.8000	0.08796	2.26256	-0.08686	-0.80047	0.00082	-0.00011	-1.03167	0.00532	-0.00038
8.0000	0.09491	2.19346	-0.08150	-0.80047	0.00039	-0.00006	-1.03165	0.00424	-0.00028
8.2000	0.10134	2.12246	-0.07618	-0.80047	-0.00002	-0.00002	-1.03163	0.00332	-0.00021
8.4000	0.10731	2.05019	-0.07095	-0.80046	-0.00034	0.00000	-1.03161	0.00255	-0.00016
8.6000	0.11288	1.97723	-0.06589	-0.80046	-0.00058	0.00001	-1.03160	0.00193	-0.00012
8.8000	0.11807	1.90405	-0.06101	-0.80046	-0.00074	0.00002	-1.03159	0.00148	-0.00009
9.0000	0.12292	1.83111	-0.05636	-0.80046	-0.00080	0.00002	-1.03158	0.00116	-0.00007
9.2000	0.12747	1.75880	-0.05196	-0.80046	-0.00081	0.00003	-1.03158	0.00095	-0.00005
9.4000	0.13175	1.68749	-0.04781	-0.80046	-0.00077	0.00003	-1.03157	0.00081	-0.00003
9.6000	0.13578	1.61753	-0.04393	-0.80046	-0.00070	0.00003	-1.03157	0.00073	-0.00002
9.8000	0.13958	1.54925	-0.04031	-0.80046	-0.00062	0.00003	-1.03156	0.00068	-0.00001
10.0000	0.14318	1.48296	-0.03695	-0.80046	-0.00052	0.00003	-1.03156	0.00065	0.00000
10.2000	0.14658	1.41892	-0.03384	-0.80046	-0.00043	0.00003	-1.03156	0.00064	0.00000
10.4000	0.14982	1.36017	-0.03109	-0.80045	-0.00034	0.00003	-1.03156	0.00063	0.00001
10.6000	0.15289	1.30159	-0.02847	-0.80045	-0.00026	0.00003	-1.03155	0.00061	0.00001
10.8000	0.15582	1.24550	-0.02606	-0.80045	-0.00019	0.00003	-1.03155	0.00060	0.00001
11.0000	0.15861	1.19226	-0.02384	-0.80045	-0.00014	0.00003	-1.03155	0.00058	0.00001
11.2000	0.16127	1.14198	-0.02181	-0.80045	-0.00009	0.00003	-1.03155	0.00056	0.00001
11.4000	0.16382	1.09465		-0.80045	-0.00006		-1.03155	0.00054	
11.6000	0.16627	1.05025	-0.01827	-0.80045	-0.00003	0.00002	-1.03155	0.00051	0.00001
11.8000	0.16861	1.00870	-0.01673	-0.80045	-0.00001	0.00002	-1.03154	0.00048	0.00001
12.0000	0.17087	0.96991	-0.01533	-0.80045	0.00000	0.00002	-1.03154	0.00044	0.00001
12.2000	0.17303	0.93375	-0.01405	-0.80045	0.00001	0.00002	-1.03154	0.00040	0.00001
12.4000	0.17512	0.90007		-0.80045	0.00002		-1.03154	0.00037	
12.6000	0.17713	0.87090	-0.01190	-0.80045	0.00002	0.00001	-1.03154	0.00033	0.00000
12.8000	0.17906	0.84215	-0.01095	-0.80045	0.00002	0.00001	-1.03154	0.00030	0.00000
13.0000	0.18094	0.81498	-0.01008	-0.80045	0.00002	0.00001	-1.03154	0.00027	0.00000

Table D-4. N_2 ($^1\Sigma_g^+$) aug-cc-pvqz : Internuclear separation v.s. property, R increments of 0.05 a_0
Energy in atomic units plus 108.0

R	$E^{(SCF)}$	$\Theta^{(SCF)}$	$q_{zz}^{(SCF)}$	$E^{(CASSCF)}$	$\Theta^{(CASSCF)}$	$q_{zz}^{(CASSCF)}$	$E^{(CASSCF+1+2)}$	$\Theta^{(CASSCF+1+2)}$	$q_{zz}^{(CASSCF+1+2)}$
1.7135	-0.86510	-1.40613	1.50922	-0.97312	-1.53627	1.38087	-1.22205	-1.48165	1.35094
1.7635	-0.91041	-1.34302	1.51067	-1.02349	-1.48783	1.37521	-1.27174	-1.43347	1.34441
1.8135	-0.94411	-1.27909	1.50296	-1.06242	-1.43969	1.36029	-1.31005	-1.38566	1.32862
1.8635	-0.96797	-1.21448		-1.09171	-1.39163		-1.33875	-1.33798	
1.9135	-0.98353	-1.14834	1.46597	-1.11286	-1.34346	1.30902	-1.35936	-1.29024	1.27561
1.9635	-0.99207	-1.08083	1.43926	-1.12717	-1.29507	1.27515	-1.37319	-1.24226	1.24093
2.0135	-0.99471	-1.01184	1.40833	-1.13577	-1.24636	1.23714	-1.38135	-1.19395	1.20215
2.0635	-0.99240	-0.94132	1.37397	-1.13958	-1.19729	1.19579	-1.38477	-1.14522	1.16009
2.1135	-0.98596	-0.86920	1.33685	-1.13943	-1.14786	1.15181	-1.38429	-1.09607	1.11548
2.1635	-0.97607	-0.79551	1.29754	-1.13602	-1.09810	1.10578	-1.38060	-1.04648	1.06892
2.2135	-0.96336	-0.72025	1.25655	-1.12993	-1.04807	1.05822	-1.37429	-0.99651	1.02095
2.2635	-0.94831	-0.64349	1.21429	-1.12168	-0.99788	1.00960	-1.36587	-0.94624	0.97203
2.3135	-0.93139	-0.56532	1.17116	-1.11172	-0.94766	0.96028	-1.35579	-0.89578	0.92256
2.3635	-0.91296	-0.48583	1.12746	-1.10040	-0.89757	0.91062	-1.34440	-0.84537	0.87282
2.4135	-0.89335	-0.40514	1.08349	-1.08805	-0.84782	0.86089	-1.33203	-0.79502	0.82324
2.4635	-0.87283	-0.32340	1.03948	-1.07494	-0.79862	0.81135	-1.31894	-0.74499	0.77401
2.5135	-0.85163	-0.24077	0.99566	-1.06130	-0.75023	0.76221	-1.30537	-0.69554	0.72534

Table D-5. O_2 ($^3\Sigma_g^-$) aug-cc-pvqz : Internuclear separation v.s. property, R increments of 0.2 a_0
Energy in Atomic units plus 149.0

R	$E^{(SCF)}$	$\Theta^{(SCF)}$	$q_{zz}^{(SCF)}$	$E^{(CASSCF)}$	$\Theta^{(CASSCF)}$	$q_{zz}^{(CASSCF)}$	$E^{(CASSCF+1+2)}$	$\Theta^{(CASSCF+1+2)}$	$q_{zz}^{(CASSCF+1+2)}$
1.40	0.41607	-1.72063	0.02118	0.39029	-1.68885	-0.01595	0.01569	-1.73171	-0.07708
1.60	1.16968	-2.49514	-0.56613	-0.27245	-1.27817	-0.26497	-0.64569	-1.29634	-0.31046
1.80	0.56403	-2.23030	-1.04438	-0.58611	-0.97858	-0.58768	-0.95779	-0.97609	-0.62663
2.00	0.21038	-1.97744	-1.44461	-0.72077	-0.69813	-0.91665	-1.09089	-0.67706	-0.94989
2.20	0.00300	-1.71352	-1.76770	-0.76513	-0.41791	-1.21686	-1.13377	-0.37925	-1.24298
2.40	-0.11719	-1.43709	-2.02347	-0.76565	-0.14066	-1.47010	-1.13292	-0.08572	-1.48756
2.60	-0.18415	-1.15533	-2.22384	-0.74638	0.12306	-1.67037	-1.11231	0.19240	-1.67877
2.80	-0.21793	-0.87650	-2.38021	-0.71970	0.36149	-1.81923	-1.08410	0.44304	-1.81991
3.00	-0.23085	-0.60680	-2.50212	-0.69211	0.56484	-1.92104	-1.05454	0.65631	-1.91701
3.20	-0.23072	-0.35000	-2.59687	-0.66715	0.72582	-1.97901	-1.02698	0.82489	-1.97419
3.40	-0.22259	-0.10821	-2.66979	-0.64689	0.83922	-1.99415	-1.00338	0.94274	-1.99252
3.60	-0.20980	0.11730	-2.72484	-0.63238	0.90391	-1.96831	-0.98491	1.00668	-1.97239
3.80	-0.19450	0.32560	-2.76490	-0.62364	0.92950	-1.91386	-0.97207	1.02412	-1.92282
4.00	-0.17811	0.51631	-2.79245	-0.61941	0.93679	-1.85656	-0.96440	1.01770	-1.86699
4.20	-0.16152	0.68900	-2.80934	-0.61782	0.94137	-1.81478	-0.96041	1.00857	-1.82413
4.40	-0.14529	0.84354	-2.81730	-0.61740	0.94677	-1.78945	-0.95847	1.00314	-1.79704
4.60	-0.12975	0.97999	-2.81792	-0.61741	0.95188	-1.77502	-0.95751	1.00031	-1.78103
4.80	-0.11508	1.09860	-2.81266	-0.61754	0.95565	-1.76679	-0.95699	0.99825	-1.77160
5.00	-0.10136	1.19985	-2.80281	-0.61767	0.95775	-1.76193	-0.95668	0.99594	-1.76587
5.20	-0.08862	1.28443	-2.78950	-0.61777	0.95829	-1.75891	-0.95647	0.99305	-1.76223
5.40	-0.07684	1.35316	-2.77368	-0.61784	0.95756	-1.75690	-0.95631	0.98959	-1.75978
5.60	-0.06597	1.40703	-2.75614	-0.61789	0.95590	-1.75548	-0.95618	0.98569	-1.75805
5.80	-0.05597	1.44712	-2.73755	-0.61792	0.95359	-1.75441	-0.95607	0.98155	-1.75678
6.00	-0.04678	1.47449	-2.71823	-0.61794	0.95089	-1.75357	-0.95598	0.97731	-1.75579
6.20	-0.03832	1.49085	-2.69910	-0.61795	0.94803	-1.75290	-0.95590	0.97313	-1.75502
6.40	-0.03054	1.49730	-2.68026	-0.61796	0.94506	-1.75234	-0.95583	0.96909	-1.75440
6.60	-0.02338	1.49517	-2.66198	-0.61796	0.94210	-1.75189	-0.95578	0.96527	-1.75391
6.80	-0.01678	1.48578	-2.64443	-0.61796	0.93930	-1.75151	-0.95573	0.96173	-1.75350
7.00	-0.01068	1.47032	-2.62776	-0.61796	0.93669	-1.75121	-0.95569	0.95848	-1.75318
7.20	-0.00505	1.44987	-2.61204	-0.61796	0.93428	-1.75097	-0.95566	0.95555	-1.75292

7.40	0.00016	1.42532	-2.59732	-0.61796	0.93210	-1.75077	-0.95564	0.95293	-1.75271
7.60	0.00500	1.39743	-2.58363	-0.61796	0.93015	-1.75060	-0.95562	0.95060	-1.75254
7.80	0.00949	1.36684	-2.57096	-0.61796	0.92841	-1.75046	-0.95561	0.94855	-1.75239
8.00	0.01368	1.33411	-2.55929	-0.61796	0.92686	-1.75034	-0.95560	0.94674	-1.75227
8.20	0.01758	1.29975	-2.54861	-0.61796	0.92547	-1.75024	-0.95559	0.94512	-1.75216
8.40	0.02124	1.26425	-2.53886	-0.61796	0.92423	-1.75015	-0.95559	0.94367	-1.75206
8.60	0.02466	1.22810	-2.53002	-0.61796	0.92310	-1.75007	-0.95558	0.94236	-1.75198
8.80	0.02787	1.19175	-2.52201	-0.61796	0.92206	-1.74999	-0.95558	0.94116	-1.75191
9.00	0.03090	1.15563	-2.51479	-0.61796	0.92111	-1.74993	-0.95557	0.94006	-1.75184
9.20	0.03375	1.12155	-2.50844	-0.61796	0.92022	-1.74987	-0.95557	0.93905	-1.75179
9.40	0.03644	1.08717	-2.50263	-0.61796	0.91940	-1.74983	-0.95557	0.93810	-1.75174
9.60	0.03899	1.05391	-2.49741	-0.61796	0.91863	-1.74978	-0.95556	0.93722	-1.75170
9.80	0.04140	1.02212	-2.49274	-0.61796	0.91790	-1.74975	-0.95556	0.93640	-1.75166
10.00	0.04370	0.99196	-2.48856	-0.61796	0.91723	-1.74971	-0.95556	0.93564	-1.75163
10.20	0.04588	0.96355	-2.48484	-0.61796	0.91660	-1.74969	-0.95556	0.93493	-1.75160
10.40	0.04796	0.93692	-2.48151	-0.61796	0.91601	-1.74966	-0.95556	0.93426	-1.75158
10.60	0.04994	0.91209	-2.47855	-0.61796	0.91546	-1.74964	-0.95556	0.93364	-1.75156
10.80	0.05183	0.88901	-2.47590	-0.61796	0.91494	-1.74963	-0.95555	0.93306	-1.75155
11.00	0.05364	0.86761	-2.47354	-0.61796	0.91446	-1.74961	-0.95555	0.93252	-1.75153
11.20	0.05538	0.84912	-2.47152	-0.61796	0.91400	-1.74960	-0.95555	0.93202	-1.75152
11.40	0.05705	0.83099	-2.46965	-0.61796	0.91358	-1.74958	-0.95555	0.93163	-1.75142
11.60	0.05865	0.81400	-2.46797	-0.61796	0.91318	-1.74957	-0.95555	0.93119	-1.75141
11.80	0.06019	0.79823	-2.46647	-0.61796	0.91281	-1.74956	-0.95555	0.93078	-1.75140
12.00	0.06167	0.78359	-2.46513	-0.61796	0.91246	-1.74955	-0.95555	0.93040	-1.75139
12.20	0.06310	0.76999	-2.46393	-0.61796	0.91213	-1.74954	-0.95555	0.93004	-1.75138
12.40	0.06448	0.75733	-2.46286	-0.61796	0.91182	-1.74954	-0.95555	0.92970	-1.75138
12.60	0.06581	0.74552	-2.46191	-0.61796	0.91153	-1.74953	-0.95555	0.92939	-1.75137
12.80	0.06710	0.73447	-2.46106	-0.61796	0.91126	-1.74952	-0.95555	0.92909	-1.75136
13.00	0.06834	0.72412	-2.46031	-0.61796	0.91101	-1.74952	-0.95555	0.92882	-1.75136

Table D-6. O_2 ($^3\Sigma_g^-$) aug-cc-pvqz : Internuclear separation v.s. property, R increments of 0.05 a_0
Energy in atomic units plus 149.0

R	$E^{(SCF)}$	$\Theta^{(SCF)}$	$q_{zz}^{(SCF)}$	$E^{(CASSCF)}$	$\Theta^{(CASSCF)}$	$q_{zz}^{(CASSCF)}$	$E^{(CASSCF+1+2)}$	$\Theta^{(CASSCF+1+2)}$	$q_{zz}^{(CASSCF+1+2)}$
1.8877	-0.59811	-0.83540	-0.70858	-0.66065	-0.85513	-0.73368	-1.03165	-0.84435	-0.77023
1.9377	0.30110	-2.05683	-1.32852	-0.69158	-0.78521	-0.81600	-1.06218	-0.76981	-0.85112
1.9877	0.22712	-1.99321	-1.42213	-0.71573	-0.71533	-0.89698	-1.08595	-0.69537	-0.93061
2.0377	0.16236	-1.92877	-1.51105	-0.73420	-0.64538	-0.97619	-1.10404	-0.62092	-1.00822
2.0877	0.10569	-1.86346	-1.59522	-0.74790	-0.57535	-1.05323	-1.11736	-0.54644	-1.08358
2.1377	0.05612	-1.79724	-1.67477	-0.75761	-0.50524	-1.12780	-1.12670	-0.47195	-1.15634
2.1877	0.01279	-1.73013	-1.74987	-0.76400	-0.43514	-1.19963	-1.13273	-0.39753	-1.22624
2.2377	-0.02504	-1.66219	-1.82070	-0.76763	-0.36516	-1.26851	-1.13600	-0.32331	-1.29309
2.2877	-0.05801	-1.59349	-1.88745	-0.76897	-0.29544	-1.33427	-1.13700	-0.24944	-1.35674
2.3377	-0.08670	-1.52416	-1.95030	-0.76843	-0.22614	-1.39681	-1.13612	-0.17609	-1.41708
2.3877	-0.11160	-1.45432	-2.00946	-0.76636	-0.15745	-1.45604	-1.13371	-0.10346	-1.47406
2.4377	-0.13314	-1.38411	-2.06511	-0.76304	-0.08955	-1.51193	-1.13006	-0.03174	-1.52766
2.4877	-0.15169	-1.31367	-2.11744	-0.75872	-0.02264	-1.56447	-1.12541	0.03888	-1.57790
2.5377	-0.16759	-1.24314	-2.16664	-0.75360	0.04309	-1.61367	-1.11996	0.10818	-1.62483
2.5877	-0.18114	-1.17265	-2.21289	-0.74787	0.10745	-1.65957	-1.11388	0.17598	-1.66851
2.6377	-0.19260	-1.10232	-2.25635	-0.74167	0.17027	-1.70224	-1.10733	0.24209	-1.70903
2.6877	-0.20219	-1.03227	-2.29720	-0.73512	0.23136	-1.74173	-1.10042	0.30633	-1.74647

7.4	-0.44670	1.42648	-7.12959	-0.81831	1.36271	-5.55761	-1.25864	1.37466	-5.57489
7.6	-0.44387	1.39151		-0.81833	1.36087		-1.25868	1.37261	
7.8	-0.44128	1.35699		-0.81834	1.35919		-1.25870	1.37075	
8	-0.43891	1.32334	-7.09111	-0.81835	1.35766	-5.55680	-1.25872	1.36905	-5.57376
8.2	-0.43673	1.29093	-7.08096	-0.81836	1.35625	-5.55661	-1.25873	1.36749	-5.57351
8.4	-0.43472	1.26005	-7.07197	-0.81836	1.35495	-5.55644	-1.25874	1.36606	-5.57331
8.6	-0.43286	1.23175	-7.06419	-0.81837	1.35375	-5.55630	-1.25875	1.36475	-5.57315
8.8	-0.43113	1.20459	-7.05718	-0.81837	1.35265	-5.55618	-1.25876	1.36353	-5.57301
9	-0.42952	1.17935	-7.05099	-0.81838	1.35163	-5.55607	-1.25876	1.36241	-5.57290
9.2	-0.42801	1.15609	-7.04555	-0.81838	1.35068	-5.55599	-1.25877	1.36138	-5.57281
9.4	-0.42660	1.13479	-7.04075	-0.81839	1.34981	-5.55591	-1.25877	1.36042	-5.57273
9.6	-0.42527	1.11535	-7.03654	-0.81839	1.34900	-5.55584	-1.25877	1.35954	-5.57266
9.8	-0.42402	1.09765	-7.03282	-0.81839	1.34825	-5.55578	-1.25877	1.35872	-5.57260
10	-0.42283	1.08157	-7.02956	-0.81839	1.34755	-5.55573	-1.25878	1.35797	-5.57255
10.2	-0.42171	1.06768	-7.02679	-0.81840	1.34691	-5.55569	-1.25878	1.35727	-5.57251
10.4	-0.42064	1.05447	-7.02427	-0.81840	1.34631	-5.55564	-1.25878	1.35662	-5.57248
10.6	-0.41963	1.04235	-7.02203	-0.81840	1.34575	-5.55561	-1.25876	1.35600	-5.57273
10.8	-0.41866	1.03128	-7.02005	-0.81840	1.34523	-5.55558	-1.25873	1.35541	-5.57307
11	-0.41773	1.02114	-7.01831	-0.81840	1.34475	-5.55555	-1.25873	1.35490	-5.57304
11.2	-0.41685	1.01184	-7.01678	-0.81840	1.34430	-5.55553	-1.25873	1.35441	-5.57302
11.4	-0.41600	1.00328	-7.01544	-0.81841	1.34388	-5.55550	-1.25873	1.35396	-5.57300
11.6	-0.41518	0.99538	-7.01425	-0.81841	1.34349	-5.55548	-1.25873	1.35354	-5.57299
11.8	-0.41440	0.98807	-7.01321	-0.81841	1.34312	-5.55546	-1.25873	1.35315	-5.57297
12	-0.41365	0.98129	-7.01229	-0.81841	1.34278	-5.55545	-1.25874	1.35279	-5.57296
12.2	-0.41292	0.97498	-7.01149	-0.81841	1.34246	-5.55543	-1.25874	1.35245	-5.57295
12.4	-0.41222	0.96912	-7.01078	-0.81841	1.34216	-5.55542	-1.25874	1.35213	-5.57293
12.6	-0.41155	0.96365	-7.01016	-0.81841	1.34187	-5.55540	-1.25874	1.35183	-5.57293
12.8	-0.41090	0.95855	-7.00961	-0.81841	1.34161	-5.55539	-1.25874	1.35155	-5.57292
13	-0.41027	0.95378	-7.00913	-0.81841	1.34136	-5.55538	-1.25874	1.35129	-5.57291
13.2	-0.40966	0.94934	-7.00870	-0.81841	1.34112	-5.55537	-1.25874	1.35104	-5.57290

Table D-7. F_2 ($^1\Sigma_g^+$) aug-cc-pvqz : Internuclear separation v.s. property, R increments of 0.2 a_0
Energy in atomic units plus 198.0

R	$E^{(SCF)}$	$\Theta^{(SCF)}$	$q_{zz}^{(SCF)}$	$E^{(CASSCF)}$	$\Theta^{(CASSCF)}$	$q_{zz}^{(CASSCF)}$	$E^{(CASSCF+1+2)}$	$\Theta^{(CASSCF+1+2)}$	$q_{zz}^{(CASSCF+1+2)}$
1.4	0.82411	-1.28204	-4.39874	0.81214	-1.27915	-4.35275	0.42802	-1.28413	-4.41902
1.6	-0.00678	-0.93288	-4.91738	-0.02336	-0.92595	-4.85116	-0.48375	-0.93632	-4.83130
1.8	-0.42993	-0.62742	-5.42934	-0.45288	-0.61249	-5.32615	-0.92146	-0.60879	-5.28605
2	-0.63984	-0.33600	-5.88030	-0.67129	-0.30532	-5.71962	-1.14091	-0.28626	-5.66279
2.2	-0.73617	-0.05777	-6.25510	-0.77870	-0.00125	-6.00842	-1.24785	0.03048	-5.93995
2.4	-0.77112	0.20093	-6.55676	-0.82749	0.29226	-6.18940	-1.29507	0.33166	-6.11899
2.6	-0.77278	0.43545	-6.79605	-0.84567	0.56499	-6.27205	-1.31062	0.60704	-6.21110
2.8	-0.75686	0.64456	-6.98457	-0.84863	0.80670	-6.27359	-1.31012	0.84834	-6.23081
3	-0.73238	0.82924	-7.13180	-0.84488	1.00876	-6.21586	-1.30254	1.04925	-6.19435
3.2	-0.70455	0.99135	-7.24494	-0.83900	1.16631	-6.12254	-1.29288	1.20613	-6.11986
3.4	-0.67631	1.13279		-0.83324	1.27973		-1.28374	1.31929	
3.6	-0.64928	1.25527		-0.82850	1.35448		-1.27621	1.39348	
3.8	-0.62425	1.36014	-7.42869	-0.82495	1.39892	-5.82059	-1.27049	1.43659	-5.84104
4	-0.60155	1.44871	-7.45083	-0.82246	1.42190	-5.74695	-1.26637	1.45745	-5.76751
4.2	-0.58121	1.52186	-7.45904	-0.82079	1.43098	-5.69083	-1.26349	1.46391	-5.71031
4.4	-0.56312	1.58044	-7.45628	-0.81970	1.43180	-5.65013	-1.26152	1.46191	-5.66825
4.6	-0.54712	1.62530	-7.44510	-0.81903	1.42808	-5.62174	-1.26015	1.45545	-5.63857
4.8	-0.53301	1.65735	-7.42767	-0.81862	1.42212	-5.60236	-1.25915	1.44697	-5.61811
5	-0.52058	1.67759	-7.40581	-0.81838	1.41524	-5.58918	-1.25833	1.43788	-5.60402
5.2	-0.50963	1.68714	-7.38103	-0.81825	1.40820	-5.58013	-1.25743	1.42899	-5.59413
5.4	-0.49998	1.68724	-7.35459	-0.81819	1.40143	-5.57380	-1.25594	1.42078	-5.58698
5.6	-0.49146	1.67917	-7.32722	-0.81817	1.39515	-5.56931	-1.25170	1.41368	-5.58183
5.8	-0.48392	1.66444	-7.30027	-0.81817	1.38946	-5.56607	-1.25879	1.40550	-5.58294
6	-0.47725	1.64427	-7.27400	-0.81819	1.38439	-5.56371	-1.25874	1.39950	-5.58048
6.2	-0.47131	1.61981	-7.24881	-0.81820	1.37992	-5.56199	-1.25872	1.39428	-5.57870
6.4	-0.46603	1.59205	-7.22497	-0.81822	1.37602	-5.56071	-1.25713	1.38966	-5.58152
6.6	-0.46130	1.56175	-7.20264	-0.81824	1.37263	-5.55975	-1.25795	1.38578	-5.57898
6.8	-0.45707	1.52955		-0.81826	1.36966		-1.25831	1.38242	
7	-0.45326	1.49596		-0.81828	1.36706		-1.25849	1.37951	
7.2	-0.44982	1.46145	-7.14541	-0.81830	1.36476	-5.55799	-1.25858	1.37694	-5.57548

Table D-8. F_2 ($^1\Sigma_g^+$) aug-cc-pvqz : Internuclear separation v.s. property, R increments of 0.05 a_0
Energy in atomic units plus 198.0

R	$E^{(SCF)}$	$\Theta^{(SCF)}$	$q_{zz}^{(SCF)}$	$E^{(CASSCF)}$	$\Theta^{(CASSCF)}$	$q_{zz}^{(CASSCF)}$	$E^{(CASSCF+1+2)}$	$\Theta^{(CASSCF+1+2)}$	$q_{zz}^{(CASSCF+1+2)}$
2.28436	-0.75639	0.05403	-6.39079	-0.80442	0.12441	-6.09759	-1.27305	0.16004	-6.02692
2.33436	-0.76436	0.11853	-6.46521	-0.81589	0.19771	-6.14151	-1.28410	0.23519	-6.07047
2.38436	-0.76985	0.18153	-6.53556	-0.82504	0.26992	-6.17898	-1.29279	0.30892	-6.10830
2.43436	-0.77322	0.24301	-6.60196	-0.83225	0.34089	-6.21019	-1.29945	0.38106	-6.14062
2.48436	-0.77477	0.30294	-6.66459	-0.83780	0.41044	-6.23539	-1.30439	0.45149	-6.16764
2.53436	-0.77477	0.36128	-6.72364	-0.84196	0.47842	-6.25482	-1.30788	0.52005	-6.18959
2.58436	-0.77344	0.41803	-6.77930	-0.84495	0.54466	-6.26876	-1.31013	0.58664	-6.20671
2.63436	-0.77098	0.47317	-6.83174	-0.84696	0.60900	-6.27752	-1.31136	0.65112	-6.21921
2.68436	-0.76758	0.52673	-6.88114	-0.84817	0.67128	-6.28140	-1.31174	0.71339	-6.22735
2.73436	-0.76337	0.57870	-6.92765	-0.84871	0.73137	-6.28075	-1.31141	0.77333	-6.23137
2.78436	-0.75850	0.62911	-6.97141	-0.84872	0.78913	-6.27591	-1.31050	0.83086	-6.23152
2.83436	-0.75308	0.67798	-7.01256	-0.84829	0.84443	-6.26724	-1.30915	0.88587	-6.22807
2.88436	-0.74721	0.72534	-7.05123	-0.84753	0.89715	-6.25511	-1.30743	0.93829	-6.22128
2.93436	-0.74098	0.77122	-7.08753	-0.84651	0.94722	-6.23989	-1.30544	0.98806	-6.21143
2.98436	-0.73447	0.81564	-7.12158	-0.84529	0.99453	-6.22197	-1.30325	1.03510	-6.19882
3.03436	-0.72773	0.85865	-7.15348	-0.84393	1.03906	-6.20171	-1.30093	1.07938	-6.18374
3.08436	-0.72084	0.90027	-7.18332	-0.84249	1.08075	-6.17949	-1.29852	1.12088	-6.16648

Table D-9. P_2 ($^1\Sigma_g^+$) aug-cc-pvqz : Internuclear separation v.s. property, R increments of 0.2 a_0
Energy in atomic units plus 681.0

R	$E^{(SCF)}$	$\Theta^{(SCF)}$	$q_{zz}^{(SCF)}$	$E^{(CASSCF)}$	$\Theta^{(CASSCF)}$	$q_{zz}^{(CASSCF)}$	$E^{(CASSCF+1+2)}$	$\Theta^{(CASSCF+1+2)}$	$q_{zz}^{(CASSCF+1+2)}$
3.4000	-0.49577	0.43307	2.15473	-0.57828	-0.24864	1.90974	-0.79162	0.02367	1.83901
3.6000	-0.49621	1.10966	1.88078	-0.58918	0.22771	1.61675	-0.80085	0.47935	1.54825
3.8000	-0.48096	1.75557	1.62855	-0.58534	0.63774	1.34593	-0.79566	0.87190	1.28091
4.0000	-0.45619	2.36714	1.39908	-0.57291	0.97401	1.09858	-0.78217	1.19585	1.03812
4.2000	-0.42601	2.94089	1.19215	-0.55601	1.22594	0.87392	-0.76443	1.44376	0.81901
4.4000	-0.39315	3.47346	1.00681	-0.53741	1.38175	0.67044	-0.74513	1.60560	0.62192
4.6000	-0.35942	3.96224	0.84170	-0.51898	1.43229	0.48711	-0.72603	1.67465	0.44559
4.8000	-0.32597	4.40580	0.69531	-0.50195	1.37840	0.32468	-0.70827	1.65040	0.29016
5.0000	-0.29354	4.80388	0.56606	-0.48711	1.23928	0.18650	-0.69253	1.54607	0.15814
5.2000	-0.26257	5.15687	0.45247	-0.47480	1.05247	0.07735	-0.67913	1.38911	0.05341
5.4000	-0.23330	5.46742	0.35288	-0.46504	0.85946	0.00005	-0.66812	1.21205	-0.02138
5.6000	-0.20587	5.73715	0.26597	-0.45756	0.68856	-0.04719	-0.65933	1.04006	-0.06752
5.8000	-0.18029	5.96863	0.19048	-0.45198	0.55028	-0.07039	-0.65245	0.88537	-0.09012
6.0000	-0.15654	6.16457	0.12523	-0.44789	0.44334	-0.07716	-0.64716	0.75205	-0.09611
6.2000	-0.13455	6.32768	0.06917	-0.44492	0.36196	-0.07430	-0.64313	0.63910	-0.09203
6.4000	-0.11425	6.46056	0.02135	-0.44277	0.29988	-0.06673	-0.64008	0.54400	-0.08284
6.6000	-0.09552	6.56567	-0.01910	-0.44120	0.25242	-0.05751	-0.63776	0.46446	-0.07179
6.8000	-0.07826	6.64523	-0.05299	-0.44007	0.21433	-0.04830	-0.63601	0.39747	-0.06072
7.0000	-0.06236	6.70132	-0.08104	-0.43923	0.18342	-0.03989	-0.63467	0.34085	-0.05053
7.2000	-0.04772	6.73579	-0.10392	-0.43861	0.15744	-0.03256	-0.63364	0.29280	-0.04160
7.4000	-0.03424	6.75036	-0.12223	-0.43815	0.13553	-0.02636	-0.63285	0.25170	-0.03400
7.6000	-0.02181	6.74662	-0.13653	-0.43780	0.11652	-0.02120	-0.63223	0.21637	-0.02764
7.8000	-0.01036	6.72603	-0.14734	-0.43754	0.09998	-0.01697	-0.63175	0.18607	-0.02238
8.0000	0.00021	6.69102	-0.15468	-0.43735	0.08559	-0.01352	-0.63137	0.15990	-0.01807
8.2000	0.00997	6.64096	-0.15986	-0.43720	0.07306	-0.01073	-0.63108	0.13739	-0.01456
8.4000	0.01899	6.57796	-0.16281	-0.43708	0.06217	-0.00848	-0.63084	0.11800	-0.01172
8.6000	0.02734	6.50320	-0.16386	-0.43700	0.05273	-0.00668	-0.63065	0.10131	-0.00942
8.8000	0.03508	6.41781	-0.16330	-0.43693	0.04454	-0.00524	-0.63049	0.08691	-0.00756
9.0000	0.04226	6.32286	-0.16141	-0.43688	0.03755	-0.00410	-0.63037	0.07446	-0.00607
9.2000	0.04892	6.21942	-0.15842	-0.43684	0.03156	-0.00319	-0.63027	0.06385	-0.00487

9.4000	0.05513	6.10849	-0.15453	-0.43681	0.02658	-0.00247	-0.63018	0.05481	-0.00391
9.6000	0.06090	5.99107	-0.14994	-0.43679	0.02216	-0.00191	-0.63011	0.04699	-0.00314
9.8000	0.06630	5.86810	-0.14480	-0.43677	0.01837	-0.00147	-0.63006	0.04027	-0.00253
10.0000	0.07133	5.74050	-0.13926	-0.43676	0.01512	-0.00112	-0.63001	0.03449	-0.00203
10.2000	0.07605	5.60916	-0.13342	-0.43675	0.01234	-0.00085	-0.62997	0.02951	-0.00164
10.4000	0.08046	5.47491	-0.12740	-0.43674	0.00997	-0.00064	-0.62994	0.02521	-0.00133
10.6000	0.08461	5.33854	-0.12128	-0.43673	0.00794	-0.00048	-0.62992	0.02149	-0.00108
10.8000	0.08851	5.20081	-0.11514	-0.43672	0.00619	-0.00036	-0.62989	0.01827	-0.00088
11.0000	0.09218	5.06821	-0.10903	-0.43672	0.00470	-0.00026	-0.62987	0.01549	-0.00072
11.2000	0.09564	4.93107	-0.10305	-0.43672	0.00343	-0.00019	-0.62986	0.01306	-0.00059
11.4000	0.09891	4.79363	-0.09720	-0.43671	0.00236	-0.00014	-0.62985	0.01100	-0.00049
11.6000	0.10200	4.65709	-0.09150	-0.43671	0.00145	-0.00010	-0.62983	0.00923	-0.00041
11.8000	0.10493	4.52205	-0.08600	-0.43671	0.00071	-0.00007	-0.62982	0.00771	-0.00034
12.0000	0.10771	4.38892	-0.08070	-0.43671	0.00012	-0.00005	-0.62982	0.00642	-0.00029
12.2000	0.11036	4.25807	-0.07561	-0.43671	-0.00035	-0.00003	-0.62981	0.00535	-0.00025
12.4000	0.11287	4.12980	-0.07076	-0.43671	-0.00069	-0.00002	-0.62980	0.00447	-0.00021
12.6000	0.11526	4.00437	-0.06615	-0.43671	-0.00093	-0.00001	-0.62980	0.00377	-0.00018
12.8000	0.11755	3.88199	-0.06177	-0.43671	-0.00108	-0.00001	-0.62979	0.00321	-0.00016
13.0000	0.11973	3.76286	-0.05764	-0.43670	-0.00115	0.00000	-0.62979	0.00278	-0.00014
13.2000	0.12182	3.64714	-0.05374	-0.43670	-0.00116	0.00000	-0.62978	0.00244	-0.00012
13.4000	0.12383	3.53496	-0.05008	-0.43670	-0.00113	0.00001	-0.62978	0.00217	-0.00011
13.6000	0.12575	3.42643	-0.04664	-0.43670	-0.00106	0.00001	-0.62978	0.00197	-0.00010
13.8000	0.12759	3.33211	-0.04363	-0.43670	-0.00097	0.00001	-0.62977	0.00182	-0.00008
14.0000	0.12936	3.22180	-0.04044	-0.43670	-0.00087	0.00001	-0.62977	0.00167	-0.00008
14.2000	0.13107	3.13442	-0.03782	-0.43670	-0.00076	0.00001	-0.62977	0.00158	-0.00007
14.4000	0.13271	3.04420	-0.03527	-0.43670	-0.00065	0.00001	-0.62977	0.00152	-0.00006
14.6000	0.13429	2.95577		-0.43670	-0.00055		-0.62977	0.00146	
14.8000	0.13582	2.87051	-0.03061	-0.43670	-0.00045	0.00002	-0.62976	0.00141	-0.00005
15.0000	0.13730	2.78884	-0.02851	-0.43670	-0.00036	0.00002	-0.62976	0.00136	-0.00004
15.2000	0.13873	2.71086	-0.02657	-0.43670	-0.00028	0.00002	-0.62976	0.00132	-0.00004

Table D-10. P_2 ($^1\Sigma_g^+$) aug-cc-pvqz : Internuclear separation v.s. property, R increments of 0.05 a_0
Energy in atomic units plus 681.0

R	$E^{(SCF)}$	$\Theta^{(SCF)}$	$q_{zz}^{(SCF)}$	$E^{(CASSCF)}$	$\Theta^{(CASSCF)}$	$q_{zz}^{(CASSCF)}$	$E^{(CASSCF+1+2)}$	$\Theta^{(CASSCF+1+2)}$	$q_{zz}^{(CASSCF+1+2)}$
3.2114	-0.47281	-0.23611	2.42691	-0.54636	-0.75637	2.20115	-0.76160	-0.46253	2.12983
3.2614	-0.48160	-0.05718	2.35338	-0.55744	-0.61612	2.12301	-0.77215	-0.32818	2.05167
3.3114	-0.48832	0.12121	2.28091	-0.56651	-0.47999	2.04537	-0.78070	-0.19782	1.97414
3.3614	-0.49317	0.29741	2.20914	-0.57378	-0.34790	1.96847	-0.78748	-0.07133	1.89748
3.4114	-0.49636	0.47150	2.13824	-0.57944	-0.21978	1.89251	-0.79268	0.05129	1.82187
3.4614	-0.49805	0.64355	2.06838	-0.58367	-0.09562	1.81765	-0.79646	0.17009	1.74746
3.5114	-0.49841	0.81360	1.99966	-0.58663	0.02458	1.74401	-0.79900	0.28507	1.67435
3.5614	-0.49758	0.98167	1.93218	-0.58846	0.14078	1.67166	-0.80042	0.39621	1.60263
3.6114	-0.49569	1.14776	1.86600	-0.58929	0.25292	1.60069	-0.80087	0.50346	1.53236
3.6614	-0.49286	1.31185	1.80116	-0.58923	0.36091	1.53113	-0.80046	0.60675	1.46358
3.7114	-0.48920	1.47391	1.73771	-0.58841	0.46467	1.46302	-0.79929	0.70606	1.39632
3.7614	-0.48480	1.63391	1.67567	-0.58691	0.56407	1.39637	-0.79747	0.80127	1.33059
3.8114	-0.47976	1.79181	1.61505	-0.58482	0.65898	1.33120	-0.79507	0.89228	1.26641
3.8614	-0.47414	1.94755	1.55586	-0.58222	0.74927	1.26751	-0.79218	0.97898	1.20378
3.9114	-0.46803	2.10108	1.49810	-0.57918	0.83477	1.20528	-0.78887	1.06127	1.14267
3.9614	-0.46149	2.25235	1.44177	-0.57577	0.91532	1.14451	-0.78521	1.13902	1.08309
4.0114	-0.45458	2.40130	1.38686	-0.57204	0.99074	1.08518	-0.78124	1.21209	1.02500

Table D-11. S_2 ($^3\Sigma_g^-$) aug-cc-pvqz : Internuclear separation v.s. property, R increments of 0.2 a_0
Energy in atomic units plus 795.0

R	$E^{(SCF)}$	$Q^{(SCF)}$	$q_{zz}^{(SCF)}$	$E^{(CASSCF)}$	$Q^{(CASSCF)}$	$q_{zz}^{(CASSCF)}$	$E^{(CASSCF+1+2)}$	$Q^{(CASSCF+1+2)}$	$q_{zz}^{(CASSCF+1+2)}$
2.00	2.11383	-4.46449	1.98744	2.09523	-4.46043	1.91285	1.77265	-4.24837	1.84782
2.20	1.25288	-3.31650	2.79669	1.23234	-3.32877	2.72118	0.91449	-3.15631	2.60686
2.40	0.70027	-2.39830	2.50715	0.67669	-2.42855	2.42692	0.36329	-2.28676	2.30970
2.60	0.35801	-1.61386	1.87810	0.33039	-1.66937	1.79200	0.02076	-1.54720	1.68934
2.80	0.15334	-0.90553	1.20166	0.12063	-0.99536	1.10899	-0.18576	-0.88452	1.02571
3.00	0.03700	-0.24625	0.57349	-0.00187	-0.38238	0.47477	-0.30538	-0.27724	0.41148
3.20	-0.02312	0.37313	0.01957	-0.06922	0.17694	-0.08384	-0.37016	0.27983	-0.12776
3.40	-0.04774	0.95608	-0.45884	-0.10214	0.68259	-0.56415	-0.40079	0.78500	-0.59007
3.60	-0.05018	1.50027	-0.86757	-0.11391	1.13218	-0.97137	-0.41061	1.23481	-0.98171
3.80	-0.03905	2.00368	-1.21488	-0.11303	1.52356	-1.31292	-0.40815	1.62680	-1.31030
4.00	-0.01989	2.46474	-1.50905	-0.10499	1.85568	-1.59599	-0.39881	1.96036	-1.58263
4.20	0.00371	2.88284	-1.75756	-0.09328	2.12909	-1.82661	-0.38595	2.23624	-1.80454
4.40	0.02943	3.25843	-1.96701	-0.08019	2.34422	-2.00914	-0.37165	2.45413	-1.98076
4.60	0.05577	3.59296	-2.14307	-0.06716	2.50194	-2.14671	-0.35726	2.61347	-2.11477
4.80	0.08178	3.88835	-2.29036	-0.05516	2.60382	-2.24164	-0.34369	2.71468	-2.20896
5.00	0.10686	4.14758	-2.41330	-0.04472	2.65603	-2.29648	-0.33161	2.76331	-2.26537
5.20	0.13066	4.37302	-2.51508	-0.03614	2.66852	-2.31568	-0.32137	2.76871	-2.28759
5.40	0.15299	4.56722	-2.59857	-0.02939	2.65377	-2.30686	-0.31306	2.74268	-2.28212
5.60	0.17376	4.73259	-2.66623	-0.02430	2.62417	-2.27984	-0.30655	2.69814	-2.25782
5.80	0.19297	4.87132	-2.72018	-0.02056	2.58833	-2.24428	-0.30159	2.64504	-2.22388
6.00	0.21065	4.98538	-2.76228	-0.01786	2.55095	-2.20737	-0.29788	2.58988	-2.18752
6.20	0.22688	5.07658	-2.79417	-0.01593	2.51431	-2.17330	-0.29513	2.53614	-2.15322
6.40	0.24174	5.14653	-2.81729	-0.01456	2.47954	-2.14393	-0.29309	2.48572	-2.12317
6.60	0.25532	5.19676	-2.83295	-0.01358	2.44720	-2.11969	-0.29159	2.43949	-2.09809
6.80	0.26773	5.22869	-2.84230	-0.01289	2.41760	-2.10028	-0.29048	2.39780	-2.07786
7.00	0.27905	5.24388	-2.84591	-0.01240	2.39082	-2.08511	-0.28966	2.36065	-2.06195
7.20	0.28939	5.24340	-2.84567	-0.01206	2.36682	-2.07348	-0.28905	2.32776	-2.04969
7.40	0.29883	5.22869	-2.84189	-0.01182	2.34541	-2.06466	-0.28859	2.29883	-2.04036
7.60	0.30745	5.20102	-2.83525	-0.01165	2.32637	-2.05804	-0.28825	2.27340	-2.03333
7.80	0.31534	5.16166	-2.82638	-0.01153	2.30945	-2.05308	-0.28799	2.25105	-2.02805

8.00	0.32255	5.11184	-2.81579	-0.01145	2.29438	-2.04935	-0.28779	2.23137	-2.02407
8.20	0.32916	5.05278	-2.80395	-0.01140	2.28093	-2.04653	-0.28763	2.21401	-2.02105
8.40	0.33523	4.98566	-2.79124	-0.01137	2.26891	-2.04438	-0.28751	2.19867	-2.01874
8.60	0.34080	4.91164	-2.77797	-0.01135	2.25815	-2.04273	-0.28742	2.18507	-2.01696
8.80	0.34593	4.83182	-2.76444	-0.01134	2.24844	-2.04144	-0.28735	2.17296	-2.01557
9.00	0.35066	4.74726	-2.75084	-0.01133	2.23967	-2.04042	-0.28730	2.16216	-2.01447
9.20	0.35502	4.65898	-2.73738	-0.01133	2.23173	-2.03961	-0.28725	2.15248	-2.01359
9.40	0.35906	4.56791	-2.72419	-0.01134	2.22451	-2.03896	-0.28722	2.14378	-2.01287
9.60	0.36281	4.47494	-2.71140	-0.01134	2.21793	-2.03842	-0.28720	2.13592	-2.01229
9.80	0.36628	4.38090	-2.69908	-0.01134	2.21189	-2.03799	-0.28718	2.12879	-2.01181
10.00	0.36952	4.28971	-2.68737	-0.01135	2.20634	-2.03762	-0.28717	2.12231	-2.01141
10.20	0.37254	4.19622	-2.67621	-0.01136	2.20122	-2.03732	-0.28716	2.11640	-2.01108
10.40	0.37536	4.10323	-2.66565	-0.01136	2.19650	-2.03706	-0.28715	2.11099	-2.01080
10.60	0.37800	4.01157	-2.65570	-0.01137	2.19213	-2.03683	-0.28714	2.10604	-2.01055
10.80	0.38048	3.92171	-2.64636	-0.01137	2.18809	-2.03664	-0.28714	2.10150	-2.01035
11.00	0.38281	3.83398	-2.63764	-0.01138	2.18436	-2.03648	-0.28713	2.09734	-2.01017
11.20	0.38501	3.74866	-2.62952	-0.01138	2.18090	-2.03633	-0.28713	2.09352	-2.01001
11.40	0.38708	3.66595	-2.62198	-0.01138	2.17771	-2.03620	-0.28713	2.09001	-2.00987
11.60	0.38904	3.58600	-2.61500	-0.01139	2.17474	-2.03608	-0.28713	2.08677	-2.00974
11.80	0.39090	3.50891	-2.60855	-0.01139	2.17199	-2.03598	-0.28713	2.08378	-2.00963
12.00	0.39266	3.43477	-2.60261	-0.01139	2.16942	-2.03588	-0.28712	2.08102	-2.00953
12.20	0.39434	3.36364	-2.59716	-0.01140	2.16703	-2.03580	-0.28712	2.07845	-2.00944
12.40	0.39594	3.29553	-2.59215	-0.01140	2.16479	-2.03572	-0.28712	2.07606	-2.00936
12.60	0.39746	3.23619	-2.58785	-0.01140	2.16268	-2.03564	-0.28712	2.07382	-2.00928
12.80	0.39892	3.16886	-2.58340	-0.01140	2.16070	-2.03557	-0.28712	2.07172	-2.00921
13.00	0.40031	3.11520	-2.57983	-0.01141	2.15882	-2.03551	-0.28712	2.06975	-2.00914
13.20	0.40165	3.06050	-2.57640	-0.01141	2.15705	-2.03545	-0.28712	2.06789	-2.00908
13.40	0.40293	3.00767	-2.57323	-0.01141	2.15536	-2.03540	-0.28712	2.06613	-2.00903
13.60	0.40417	2.95741	-2.57034	-0.01141	2.15376	-2.03535	-0.28712	2.06446	-2.00898
13.80	0.40535	2.90985	-2.56771	-0.01141	2.15224	-2.03531	-0.28712	2.06288	-2.00893

Table D-12. S_2 ($^3\Sigma_g^-$) aug-cc-pvqz : Internuclear separation v.s. property, R increments of 0.05 a_0
Energy in atomic units plus 795.0

R	$E^{(SCF)}$	$\Theta^{(SCF)}$	$q_{zz}^{(SCF)}$	$E^{(CASSCF)}$	$\Theta^{(CASSCF)}$	$q_{zz}^{(CASSCF)}$	$E^{(CASSCF+1+2)}$	$\Theta^{(CASSCF+1+2)}$	$q_{zz}^{(CASSCF+1+2)}$
3.2101	-0.02508	0.40454	-0.00677	-0.09725	0.40851	-0.13148	-0.40040	0.47369	-0.16149
3.2601	0.66511	1.39063	-7.72271	-0.10735	0.54213	-0.25456	-0.40988	0.60864	-0.28169
3.3101	1.46665	-6.93323	-7.33220	-0.11561	0.67264	-0.37269	-0.41753	0.74064	-0.39706
3.3601	1.43977	-6.73010	-7.40025	-0.12224	0.80001	-0.48596	-0.42356	0.86961	-0.50767
3.4101	1.41478	-6.53425	-7.46323	-0.12742	0.92421	-0.59447	-0.42816	0.99550	-0.61363
3.4601	1.39152	-6.34642	-7.52110	-0.13133	1.04521	-0.69835	-0.43150	1.11823	-0.71503
3.5101	1.36984	-6.16675	-7.57401	-0.13412	1.16298	-0.79770	-0.43372	1.23774	-0.81201
3.5601	1.34959	-5.99521	-7.62213	-0.13591	1.27750	-0.89266	-0.43497	1.35398	-0.90467
3.6101	1.33065	-5.83173	-7.66565	-0.13683	1.38873	-0.98336	-0.43536	1.46690	-0.99315
3.6601	1.31291	-5.67616	-7.70478	-0.13698	1.49665	-1.06993	-0.43501	1.57644	-1.07757
3.7101	1.29627	-5.52836	-7.73976	-0.13647	1.60124	-1.15250	-0.43399	1.68260	-1.15805
3.7601	1.28064	-5.38812	-7.77080	-0.13537	1.70248	-1.23121	-0.43241	1.78532	-1.23474
3.8101	1.26595	-5.25523	-7.79815	-0.13376	1.80035	-1.30620	-0.43034	1.88458	-1.30775
3.8601	1.25210	-5.12944	-7.82206	-0.13171	1.89485	-1.37757	-0.42784	1.98037	-1.37722
3.9101	1.23905	-5.01049	-7.84276	-0.12929	1.98594	-1.44547	-0.42498	2.07267	-1.44325
3.9601	1.22674	-4.89809	-7.86050	-0.12654	2.07363	-1.51002	-0.42182	2.16145	-1.50599
4.0101	1.21510	-4.79195	-7.87551	-0.12352	2.15789	-1.57132	-0.41839	2.24649	-1.56553

Table D-13. Cl_2 ($^1\Sigma_g^+$) aug-cc-pvqz : Internuclear separation v.s. property, R increments of 0.2 a_0
Energy in atomic units plus 919.0

R	$E^{(SCF)}$	$\Theta^{(SCF)}$	$q_{zz}^{(SCF)}$	$E^{(CASSCF)}$	$\Theta^{(CASSCF)}$	$q_{zz}^{(CASSCF)}$	$E^{(CASSCF+1+2)}$	$\Theta^{(CASSCF+1+2)}$	$q_{zz}^{(CASSCF+1+2)}$
2.00	2.32745	-2.72282	1.03504	2.32259	-2.73096	1.02069	1.91847	-2.74408	0.89073
2.20	1.39596	-1.90848	0.06940	1.39074	-1.91788	0.06348	0.99465	-1.94734	-0.02787
2.40	0.82003	-1.20110	-1.20482	0.81415	-1.21030	-1.20448	0.42360	-1.24681	-1.25150
2.60	0.46677	-0.55512	-2.39066	0.45988	-0.56181	-2.38209	0.07314	-0.60046	-2.38791
2.80	0.25206	0.04321	-3.39676	0.24367	0.04238	-3.37164	-0.14016	0.00339	-3.34488
3.00	0.12402	0.59742	-4.22220	0.11354	0.60210	-4.17291	-0.26726	0.56594	-4.12172
3.20	0.05068	1.10648	-4.88960	0.03758	1.11727	-4.81270	-0.34034	1.08536	-4.73970
3.40	0.01210	1.57007	-5.42619	-0.00418	1.58808	-5.31360	-0.37958	1.56012	-5.22331
3.60	-0.00432	1.98890	-5.85692	-0.02440	2.01417	-5.69785	-0.39759	1.98896	-5.59525
3.80	-0.00670	2.36483	-6.20254	-0.03124	2.39528	-5.98410	-0.40244	2.37114	-5.87414
4.00	-0.00030	2.70071	-6.47963	-0.03003	2.73103	-6.18737	-0.39937	2.70617	-6.07476
4.20	0.01139	2.99986	-6.70123	-0.02427	3.02067	-6.31991	-0.39186	2.99340	-6.20890
4.40	0.02608	3.26571	-6.87729	-0.01630	3.26303	-6.39230	-0.38221	3.23196	-6.28648
4.60	0.04222	3.50111	-7.01612	-0.00767	3.45712	-6.41455	-0.37199	3.42103	-6.31691
4.80	0.05879	3.70871	-7.12377	0.00065	3.60294	-6.39692	-0.36216	3.56044	-6.31100
5.00	0.07514	3.89055	-7.20529	0.00809	3.70247	-6.35014	-0.35177	3.64966	-6.29321
5.20	0.09084	4.04827	-7.26487	0.01439	3.76029	-6.28508	-0.34099	3.71486	-6.16761
5.40	0.10565	4.18324	-7.30606	0.01949	3.78330	-6.21165	-0.33785	3.72440	-6.11922
5.60	0.11945	4.29664	-7.33190	0.02346	3.77982	-6.13792	-0.33329	3.71100	-6.05268
5.80	0.13217	4.38960	-7.34502	0.02647	3.75824	-6.06964	-0.32958	3.67983	-5.98778
6.00	0.14384	4.46324	-7.34775	0.02869	3.72601	-6.01017	-0.32674	3.63834	-5.92996
6.20	0.15446	4.51863	-7.34164	0.03029	3.68893	-5.96088	-0.32461	3.59261	-5.88142
6.40	0.16411	4.55724	-7.32945	0.03142	3.65103	-5.92169	-0.32305	3.54689	-5.84250
6.60	0.17285	4.58023	-7.31220	0.03221	3.61477	-5.89157	-0.32191	3.50374	-5.81243
6.80	0.18075	4.58894	-7.29118	0.03275	3.58140	-5.86898	-0.32107	3.46443	-5.78982
7.00	0.18788	4.58473	-7.26751	0.03311	3.55134	-5.85229	-0.32046	3.42942	-5.77313
7.20	0.19432	4.56900	-7.24211	0.03334	3.52460	-5.84005	-0.31996	3.39870	-5.76096
7.40	0.20012	4.54310	-7.21575	0.03349	3.50094	-5.83105	-0.31945	3.37225	-5.75240
7.60	0.20535	4.50841		0.03358	3.48004		-0.31827	3.35138	
7.80	0.21008	4.46622		0.03363	3.46159		-0.31941	3.32458	

8.00	0.21435	4.41779	-7.13656	0.03365	3.44522	-5.81568	-0.31931	3.30602	-5.73712
8.20	0.21822	4.36432	-7.11144	0.03366	3.43069	-5.81281	-0.31925	3.28972	-5.73425
8.40	0.22172	4.30692	-7.08739	0.03365	3.41772	-5.81060	-0.31834	3.27531	-5.73449
8.60	0.22490	4.24663	-7.06458	0.03364	3.40610	-5.80886	-0.31876	3.26223	-5.73161
8.80	0.22780	4.18442	-7.04310	0.03363	3.39563	-5.80749	-0.31892	3.25072	-5.72971
9.00	0.23044	4.12277	-7.02314	0.03361	3.38615	-5.80638	-0.31900	3.24043	-5.72833
9.20	0.23285	4.05939	-7.00450	0.03359	3.37754	-5.80549	-0.31905	3.23116	-5.72727
9.40	0.23506	3.99616	-6.98724	0.03358	3.36969	-5.80475	-0.31907	3.22277	-5.72643
9.60	0.23709	3.93374	-6.97132	0.03356	3.36250	-5.80413	-0.31910	3.21514	-5.72574
9.80	0.23896	3.87260	-6.95672	0.03355	3.35591	-5.80361	-0.31911	3.20818	-5.72517
10.00	0.24068	3.81308	-6.94337	0.03353	3.34984	-5.80317	-0.31912	3.20182	-5.72469
10.20	0.24228	3.75542	-6.93120	0.03352	3.34424	-5.80278	-0.31913	3.19598	-5.72429
10.40	0.24376	3.69983	-6.92015	0.03351	3.33906	-5.80245	-0.31914	3.19060	-5.72394
10.60	0.24514	3.64644	-6.91012	0.03350	3.33425	-5.80215	-0.31915	3.18563	-5.72363
10.80	0.24643	3.59535	-6.90106	0.03349	3.32978	-5.80189	-0.31915	3.18102	-5.72336
11.00	0.24764	3.54661	-6.89289	0.03348	3.32560	-5.80166	-0.31916	3.17674	-5.72312
11.20	0.24877	3.50026	-6.88554	0.03347	3.32170	-5.80144	-0.31916	3.17274	-5.72291
11.40	0.24984	3.45631	-6.87893	0.03347	3.31803	-5.80125	-0.31917	3.16901	-5.72272
11.60	0.25084	3.41787	-6.87333	0.03346	3.31459	-5.80108	-0.31917	3.16551	-5.72255
11.80	0.25179	3.37571	-6.86770	0.03345	3.31135	-5.80092	-0.31917	3.16222	-5.72239
12.00	0.25269	3.34172	-6.86323	0.03345	3.30830	-5.80078	-0.31918	3.15913	-5.72225
12.20	0.25355	3.30766	-6.85902	0.03344	3.30542	-5.80065	-0.31918	3.15622	-5.72212
12.40	0.25436	3.27529	-6.85522	0.03344	3.30269	-5.80053	-0.31918	3.15347	-5.72201
12.60	0.25514	3.24493	-6.85181	0.03344	3.30012	-5.80042	-0.31918	3.15088	-5.72190
12.80	0.25588	3.21659	-6.84877	0.03343	3.29768	-5.80033	-0.31919	3.14843	-5.72181
13.00	0.25659	3.19019	-6.84605	0.03343	3.29538	-5.80024	-0.31919	3.14611	-5.72172
13.20	0.25726	3.16565	-6.84362	0.03343	3.29319	-5.80015	-0.31919	3.14392	-5.72164
13.40	0.25792	3.14287	-6.84145	0.03342	3.29112	-5.80008	-0.31919	3.14185	-5.72157
13.60	0.25854	3.12175	-6.83952	0.03342	3.28915	-5.80001	-0.31919	3.13989	-5.72150
13.80	0.25914	3.10217	-6.83779	0.03342	3.28729	-5.79995	-0.31919	3.13803	-5.72144

Table D-14. Cl_2 ($^1\Sigma_g^+$) aug-cc-pvqz : Internuclear separation v.s. property, R increments of 0.05 a_0
Energy in atomic units plus 919.0

R	$E^{(SCF)}$	$\Theta^{(SCF)}$	$q_{zz}^{(SCF)}$	$E^{(CASSCF)}$	$\Theta^{(CASSCF)}$	$q_{zz}^{(CASSCF)}$	$E^{(CASSCF+1+2)}$	$\Theta^{(CASSCF+1+2)}$	$q_{zz}^{(CASSCF+1+2)}$
3.3902	0.01340	1.54835	-5.40263	-0.00271	1.56605	-5.29194	-0.37824	1.53792	-5.20239
3.4402	0.00734	1.65778	-5.52047	-0.00966	1.67733	-5.39954	-0.38460	1.65003	-5.30638
3.4902	0.00252	1.76439	-5.63215	-0.01539	1.78580	-5.50013	-0.38977	1.75926	-5.40367
3.5402	-0.00118	1.86824	-5.73785	-0.02006	1.89147	-5.59400	-0.39388	1.86560	-5.49455
3.5902	-0.00389	1.96936	-5.83789	-0.02377	1.99434	-5.68144	-0.39707	1.96903	-5.57932
3.6402	-0.00572	2.06780	-5.93258	-0.02665	2.09440	-5.76272	-0.39942	2.06954	-5.65825
3.6902	-0.00676	2.16358	-6.02219	-0.02877	2.19164	-5.83810	-0.40104	2.16713	-5.73158
3.7402	-0.00710	2.25674		-0.03024	2.28606		-0.40201	2.26179	
3.7902	-0.00682	2.34735		-0.03113	2.37766		-0.40242	2.35351	
3.8402	-0.00598	2.43544		-0.03151	2.46643		-0.40232	2.44229	
3.8902	-0.00466	2.52106	-6.33509	-0.03145	2.55236	-6.08526	-0.40179	2.52811	-5.97355
3.9402	-0.00290	2.60428	-6.40308	-0.03100	2.63543	-6.13452	-0.40088	2.61097	-6.02223
3.9902	-0.00076	2.68513		-0.03022	2.71565		-0.39965	2.69086	
4.0402	0.00171	2.76367	-6.52822	-0.02915	2.79298	-6.21933	-0.39813	2.76777	-6.10673
4.0902	0.00447	2.83997	-6.58573	-0.02783	2.86743	-6.25524	-0.39637	2.84168	-6.14287
4.1402	0.00749	2.91406	-6.64009	-0.02631	2.93896	-6.28704	-0.39441	2.91258	-6.17515
4.1902	0.01073	2.98601	-6.69145	-0.02462	3.00756	-6.31490	-0.39229	2.98045	-6.20372

Table D-15. Li_2 ($^1\Sigma_g^+$) aug-cc-pvqz : Internuclear separation v.s. property, R increments of 0.05 a_0
Energy in atomic units plus 14.0

3.40	-0.820932	6.231350	-0.029848	-0.860422	7.185859	-0.032562	-0.860662	7.188502	-0.032408
3.60	-0.834022	6.801962	-0.020161	-0.872177	7.675110	-0.022083	-0.872456	7.680155	-0.021885
3.80	-0.844621	7.369031	-0.012781	-0.881582	8.149161	-0.014138	-0.881898	8.157318	-0.013917
4.00	-0.853009	7.921888	-0.007306	-0.888896	8.611072	-0.008300	-0.889242	8.622730	-0.008071
4.20	-0.859474	8.460243	-0.003158	-0.894394	9.061542	-0.003849	-0.894764	9.076970	-0.003623
4.40	-0.864298	8.987029	-0.000165	-0.898347	9.499472	-0.000680	-0.898733	9.518875	-0.000462
4.60	-0.867738	9.504783		-0.901005	9.922464		-0.901401	9.946048	
4.80	-0.870020	10.014471	0.003537	-0.902591	10.327240	0.003182	-0.902991	10.355220	0.003374
5.00	-0.871345	10.516241	0.004604	-0.903302	10.709873	0.004266	-0.903700	10.742489	0.004443
5.20	-0.871879	11.009796	0.005315	-0.903303	11.065967	0.004968	-0.903697	11.103478	0.005131
5.40	-0.871769	11.494564	0.005760	-0.902739	11.390767	0.005383	-0.903124	11.433441	0.005534
5.60	-0.871133	11.969804	0.006008	-0.901730	11.679267	0.005585	-0.902104	11.727397	0.005724
5.80	-0.870073	12.434680	0.006110	-0.900378	11.926307	0.005630	-0.900739	11.980148	0.005758
6.00	-0.868675	12.888308	0.006106	-0.898769	12.126685	0.005560	-0.899116	12.186462	0.005678
6.20	-0.867008	13.329804	0.006026	-0.896976	12.275287	0.005407	-0.897306	12.341135	0.005515
6.40	-0.865131	13.758311	0.005891	-0.895058	12.367255	0.005193	-0.895370	12.439201	0.005292
6.60	-0.863094	14.173026	0.005718	-0.893067	12.398177	0.004936	-0.893361	12.476099	0.005028
6.80	-0.860937	14.573214	0.005518	-0.891046	12.364319	0.004650	-0.891320	12.447914	0.004735
7.00	-0.858693	14.958214	0.005303	-0.889030	12.262887	0.004347	-0.889285	12.351644	0.004424
7.20	-0.856391	15.327445	0.005078	-0.887049	12.092296	0.004034	-0.887283	12.185483	0.004105
7.40	-0.854054	15.680408	0.004849	-0.885127	11.852450	0.003719	-0.885341	11.949101	0.003784
7.60	-0.851701	16.016681	0.004621	-0.883283	11.544976	0.003406	-0.883477	11.643898	0.003466
7.80	-0.849348	16.335923	0.004395	-0.881533	11.173394	0.003101	-0.881707	11.273179	0.003155
8.00	-0.847008	16.637869	0.004175	-0.879886	10.743169	0.002807	-0.880042	10.843125	0.002856
8.20	-0.844690	16.922330	0.003961	-0.878352	10.261650	0.002526	-0.878489	10.358845	0.002571
8.40	-0.842404	17.189191	0.003755	-0.876933	9.737747	0.002262	-0.877054	9.830112	0.002302
8.60	-0.840157	17.438407	0.003558	-0.875632	9.181527	0.002015	-0.875738	9.266927	0.002051
8.80	-0.837953	17.670002	0.003369	-0.874447	8.603635	0.001788	-0.874540	8.680026	0.001820
9.00	-0.835798	17.897527	0.003193	-0.873375	8.014685	0.001580	-0.873457	8.080322	0.001608
9.20	-0.833694	18.095398	0.003021	-0.872412	7.424699	0.001391	-0.872485	7.478343	0.001416

9.40	-0.831644	18.274696	0.002859	-0.871551	6.842676	0.001222	-0.871616	6.883726	0.001244
9.60	-0.829649	18.436770	0.002705	-0.870784	6.276308	0.001070	-0.870845	6.304828	0.001090
9.80	-0.827711	18.582051	0.002559	-0.870106	5.731834	0.000936	-0.870163	5.748488	0.000953
10.00	-0.825830	18.710853	0.002421	-0.869508	5.214018	0.000816	-0.869562	5.219939	0.000833
10.20	-0.824006	18.823481	0.002290	-0.868982	4.726222	0.000711	-0.869035	4.722858	0.000727
10.40	-0.822239	18.920260	0.002167	-0.868521	4.270543	0.000619	-0.868574	4.259517	0.000634
10.60	-0.820530	19.001527	0.002050	-0.868118	3.847988	0.000538	-0.868172	3.830986	0.000553
10.80	-0.818876	19.067637	0.001940	-0.867766	3.458666	0.000468	-0.867822	3.435622	0.000482
11.00	-0.817277	19.118959	0.001836	-0.867460	3.101980	0.000406	-0.867517	3.076078	0.000421
11.20	-0.815733	19.155879	0.001737	-0.867194	2.776796	0.000353	-0.867253	2.749418	0.000368
11.40	-0.814242	19.178798	0.001645	-0.866963	2.481604	0.000306	-0.867024	2.453926	0.000321
11.60	-0.812803	19.188135	0.001557	-0.866763	2.214643	0.000265	-0.866825	2.187633	0.000281
11.80	-0.811414	19.184327	0.001474	-0.866590	1.974005	0.000230	-0.866652	1.948429	0.000246
12.00	-0.810075	19.167829	0.001396	-0.866439	1.757717	0.000199	-0.866503	1.734138	0.000215
12.20	-0.808783	19.139113	0.001323	-0.866309	1.563801	0.000172	-0.866373	1.542582	0.000189
12.40	-0.807538	19.098667	0.001253	-0.866196	1.390324	0.000149	-0.866261	1.371879	0.000165
12.60	-0.806337	19.046990	0.001187	-0.866099	1.235430	0.000129	-0.866164	1.220242	0.000145
12.80	-0.805180	18.984589	0.001126	-0.866014	1.097352	0.000111	-0.866079	1.085562	0.000128
13.00	-0.804065	18.911973	0.001067	-0.865941	0.974444	0.000096	-0.866005	0.965806	0.000112
13.20	-0.802991	18.829647	0.001012	-0.865878	0.865180	0.000083	-0.865941	0.859593	0.000099
13.40	-0.801955	18.738102	0.000960	-0.865823	0.768099	0.000071	-0.865885	0.765400	0.000087
13.60	-0.800958	18.637810	0.000911	-0.865776	0.681954	0.000061	-0.865837	0.682051	0.000077
13.80	-0.799997	18.529221	0.000864	-0.865735	0.605554	0.000053	-0.865794	0.608260	0.000068
14.00	-0.799071	18.412755	0.000821	-0.865699	0.537843	0.000045	-0.865757	0.542944	0.000060
14.20	-0.798178	18.288803		-0.865668	0.477841		-0.865724	0.485152	
14.40	-0.797318	18.157725	0.000740	-0.865641	0.424697	0.000033	-0.865696	0.433980	0.000047
14.60	-0.796489	18.050443		-0.865617	0.377632		-0.865671	0.388682	
14.80	-0.795691	17.877709	0.000667	-0.865597	0.335978	0.000024	-0.865648	0.348561	0.000038
15.00	-0.794921	17.757348		-0.865579	0.299102		-0.865629	0.312971	
15.20	-0.794178	17.608687	0.000604	-0.865564	0.266473	0.000018	-0.865611	0.281439	0.000030
15.40	-0.793463	17.448951		-0.865550	0.237587		-0.865596	0.253473	

Table D-16. Li_2 ($^1\Sigma_g^+$) aug-cc-pvqz : Internuclear separation v.s. property, R increments of 0.05 a_0
Energy in atomic units plus 14.0

R	$E^{(SCF)}$	$\Theta^{(SCF)}$	$q_{zz}^{(SCF)}$	$E^{(CASSCF)}$	$\Theta^{(CASSCF)}$	$q_{zz}^{(CASSCF)}$	$E^{(CASSCF+1+2)}$	$\Theta^{(CASSCF+1+2)}$	$q_{zz}^{(CASSCF+1+2)}$
4.697088	-0.86898	9.75251	0.002810	-0.90190	10.12146	0.002436	-0.90229	10.14715	0.002634
4.747088	-0.86952	9.87728	0.003187	-0.90226	10.22213	0.002816	-0.90266	10.24893	0.003012
4.797088	-0.86999	10.00329		-0.90258	10.32149		-0.90297	10.34941	
4.847088	-0.87041	10.12917	0.003831	-0.90283	10.41947	0.003478	-0.90323	10.44852	0.003666
4.897088	-0.87077	10.25464	0.004110	-0.90303	10.51600	0.003763	-0.90343	10.54621	0.003948
4.947088	-0.87108	10.37963	0.004365	-0.90319	10.61103	0.004021	-0.90359	10.64240	0.004202
4.997088	-0.87133	10.50412		-0.90330	10.70447		-0.90370	10.73703	
5.047088	-0.87154	10.62810	0.004803	-0.90336	10.79626	0.004462	-0.90376	10.83002	0.004636
5.097088	-0.87169	10.75157	0.004991	-0.90338	10.88632	0.004648	-0.90378	10.92130	0.004819
5.147088	-0.87181	10.87452	0.005159	-0.90336	10.97459	0.004813	-0.90376	11.01079	0.004981
5.197088	-0.87188	10.99694	0.005310	-0.90331	11.06098	0.004960	-0.90370	11.09843	0.005124
5.247088	-0.87191	11.11881	0.005444	-0.90322	11.14542	0.005088	-0.90361	11.18414	0.005249
5.297088	-0.87190	11.24013	0.005562	-0.90309	11.22784	0.005200	-0.90348	11.26783	0.005357
5.347088	-0.87185	11.36090	0.005667	-0.90294	11.30815	0.005297	-0.90332	11.34944	0.005451
5.397088	-0.87177	11.48108		-0.90275	11.38627		-0.90314	11.42888	
5.447088	-0.87166	11.60068	0.005836	-0.90254	11.46213	0.005447	-0.90292	11.50608	0.005595
5.497088	-0.87152	11.71967	0.005903	-0.90230	11.53565	0.005504	-0.90268	11.58096	0.005649

Table D-17. Na_2 ($^1\Sigma_g^+$) aug-cc-pvqz : Internuclear separation v.s. property, R increments of 0.05 a_0
Energy in atomic units plus 323.0

R	$E^{(SCF)}$	$\Theta^{(SCF)}$	$q_{zz}^{(SCF)}$	$E^{(CASSCF)}$	$\Theta^{(CASSCF)}$	$q_{zz}^{(CASSCF)}$	$E^{(CASSCF+1+2)}$	$\Theta^{(CASSCF+1+2)}$	$q_{zz}^{(CASSCF+1+2)}$
4.00	-0.676529	6.510713	-0.101622	-0.705215	7.121579	-0.118858	-0.705687	7.125007	-0.117823
4.20	-0.685641	7.006891	-0.080494	-0.714043	7.611135	-0.094839	-0.714521	7.616944	-0.093866
4.40	-0.693154	7.542574	-0.058710	-0.721296	8.106593	-0.070449	-0.721777	8.115253	-0.069549
4.60	-0.699302	8.095166	-0.038802	-0.727209	8.602022	-0.048222	-0.727691	8.613950	-0.047402
4.80	-0.704253	8.660105	-0.021778	-0.731950	9.091946	-0.029287	-0.732429	9.107491	-0.028549
5.00	-0.708149	9.218485	-0.008120	-0.735655	9.571238	-0.013908	-0.736128	9.590688	-0.013249
5.20	-0.711115	9.790702	0.002808	-0.738450	10.034975	-0.001873	-0.738914	10.058665	-0.001289
5.40	-0.713268	10.358778	0.011078	-0.740453	10.478329	0.007246	-0.740905	10.506571	0.007762
5.60	-0.714714	10.923459	0.017220	-0.741770	10.896492	0.013942	-0.742209	10.928895	0.014407
5.80	-0.715553	11.482864		-0.742505	11.284632		-0.742928	11.322316	
6.00	-0.715874	12.035201	0.024706	-0.742750	11.637890	0.021879	-0.743156	11.681202	0.022243
6.20	-0.715756	12.578909	0.026709	-0.742588	11.951400	0.023866	-0.742976	12.000658	0.024190
6.40	-0.715270	13.112595	0.027894	-0.742095	12.220335	0.024920	-0.742464	12.275809	0.025209
6.60	-0.714478	13.634998	0.028456	-0.741336	12.439987	0.025263	-0.741686	12.501862	0.025521
6.80	-0.713433	14.144966	0.028549	-0.740370	12.605868	0.025071	-0.740700	12.674224	0.025301
7.00	-0.712181	14.641457		-0.739246	12.713846		-0.739556	12.788626	
7.20	-0.710763	15.123539	0.027781	-0.738009	12.760304	0.023601	-0.738298	12.841298	0.023786
7.40	-0.709213	15.590401	0.027086	-0.736696	12.742321	0.022516	-0.736964	12.829156	0.022681
7.60	-0.707559	16.041376		-0.735341	12.657877		-0.735588	12.750004	
7.80	-0.705827	16.475935		-0.733970	12.506049		-0.734196	12.602742	
8.00	-0.704037	16.893663	0.024402	-0.732606	12.287213	0.018610	-0.732813	12.387563	0.018726
8.20	-0.702208	17.294197	0.023420	-0.731270	12.003201	0.017228	-0.731456	12.106138	0.017330
8.40	-0.700356	17.677181	0.022430	-0.729976	11.657416	0.015854	-0.730143	11.761701	0.015945
8.60	-0.698491	18.052354	0.021524	-0.728737	11.254866	0.014511	-0.728886	11.357011	0.014586
8.80	-0.696626	18.400495	0.020547	-0.727562	10.802076	0.013214	-0.727695	10.902680	0.013279
9.00	-0.694769	18.729552	0.019595	-0.726459	10.306885	0.011976	-0.726576	10.404438	0.012033
9.20	-0.692927	19.040392	0.018674	-0.725431	9.778127	0.010807	-0.725534	9.871023	0.010857
9.40	-0.691108	19.333005	0.017786	-0.724481	9.225181	0.009714	-0.724572	9.311737	0.009758
9.60	-0.689315	19.607279	0.016932	-0.723609	8.657511	0.008699	-0.723688	8.736019	0.008738
9.80	-0.687553	19.863139	0.016112	-0.722813	8.084203	0.007765	-0.722883	8.153747	0.007803

10.00	-0.685825	20.100570	0.015327	-0.722091	7.513588	0.006911	-0.722153	7.572013	0.006945
10.20	-0.684133	20.319621	0.014577	-0.721440	6.952990	0.006136	-0.721496	6.999671	0.006166
10.40	-0.682481	20.520403	0.013860	-0.720855	6.408582	0.005434	-0.720906	6.443132	0.005462
10.60	-0.680869	20.703081	0.013176	-0.720332	5.885339	0.004804	-0.720379	5.908522	0.004830
10.80	-0.679298	20.867868	0.012525	-0.719865	5.387060	0.004239	-0.719911	5.399738	0.004265
11.00	-0.677769	21.015020	0.011904	-0.719451	4.916441	0.003736	-0.719495	4.919801	0.003762
11.20	-0.676283	21.144827	0.011314	-0.719084	4.475179	0.003288	-0.719128	4.470612	0.003315
11.40	-0.674839	21.257610	0.010753	-0.718760	4.064112	0.002892	-0.718804	4.053100	0.002920
11.60	-0.673437	21.353714	0.010219	-0.718474	3.683350	0.002541	-0.718519	3.667374	0.002571
11.80	-0.672078	21.433508		-0.718223	3.332424		-0.718269	3.312894	
12.00	-0.670760	21.497376	0.009230	-0.718002	3.010410	0.001960	-0.718049	2.988615	0.001993
12.20	-0.669483	21.545718	0.008773	-0.717808	2.716057	0.001720	-0.717856	2.693131	0.001755
12.40	-0.668247	21.578947	0.008338	-0.717638	2.447881	0.001510	-0.717688	2.424791	0.001546
12.60	-0.667051	21.630102	0.007967	-0.717489	2.204257	0.001326	-0.717540	2.181797	0.001362
12.80	-0.665893	21.605432	0.007534	-0.717359	1.983485	0.001164	-0.717411	1.962288	0.001202
13.00	-0.664774	21.627420		-0.717245	1.783850		-0.717298	1.764404	
13.20	-0.663691	21.573202		-0.717145	1.603660		-0.717198	1.586334	
13.40	-0.662645	21.569939	0.006509	-0.717058	1.441274	0.000790	-0.717112	1.426411	0.000829
13.60	-0.661634	21.534641	0.006197	-0.716982	1.295135	0.000695	-0.717036	1.282845	0.000734
13.80	-0.660656	21.480158	0.005895	-0.716915	1.163762	0.000612	-0.716969	1.154208	0.000651
14.00	-0.659712	21.411388		-0.716857	1.045779		-0.716910	1.039086	
14.20	-0.658800	21.330455		-0.716806	0.939905		-0.716859	0.935960	
14.40	-0.657919	21.238474	0.005074	-0.716761	0.844957	0.000420	-0.716813	0.843735	0.000458
14.60	-0.657069	21.136176		-0.716722	0.759849		-0.716773	0.761236	
14.80	-0.656247	21.024138	0.004594	-0.716687	0.683587	0.000330	-0.716738	0.687395	0.000366
15.00	-0.655453	20.902876	0.004371	-0.716657	0.615266	0.000293	-0.716707	0.621546	0.000328
15.20	-0.654687	20.772879	0.004161	-0.716631	0.554060	0.000260	-0.716679	0.562632	0.000295
15.40	-0.653946	20.664626		-0.716607	0.499227		-0.716655	0.509895	
15.60	-0.653231	20.499817		-0.716587	0.450098		-0.716633	0.462655	
15.80	-0.652540	20.372120	0.003610	-0.716569	0.406068	0.000185	-0.716613	0.420305	0.000216
16.00	-0.651873	20.188778	0.003422	-0.716595	0.384745	0.000220	-0.716596	0.387886	0.000220

Table D-18. Na_2 ($^1\Sigma_g^+$) aug-cc-pvqz : Internuclear separation v.s. property, R increments of 0.05 a_0
Energy in atomic units plus 323.0

R	$E^{(SCF)}$	$\Theta^{(SCF)}$	$q_{zz}^{(SCF)}$	$E^{(CASSCF)}$	$\Theta^{(CASSCF)}$	$q_{zz}^{(CASSCF)}$	$E^{(CASSCF+1+2)}$	$\Theta^{(CASSCF+1+2)}$	$q_{zz}^{(CASSCF+1+2)}$
5.51970	-0.714212	10.707458	0.014911	-0.741317	10.731932	0.011514	-0.741761	10.762315	0.012001
5.56970	-0.714536	10.842838		-0.741610	10.834948		-0.742051	10.866584	
5.61970	-0.714822	10.981671	0.017689	-0.741867	10.936133	0.014489	-0.742304	10.969043	0.014948
5.66970	-0.715071	11.121156	0.018903	-0.742088	11.035412	0.015794	-0.742521	11.069618	0.016239
5.71970	-0.715283	11.260565		-0.742274	11.132709		-0.742703	11.168233	
5.76970	-0.715461	11.399678	0.021035	-0.742427	11.227948	0.018074	-0.742853	11.264812	0.018493
5.81970	-0.715606	11.538407		-0.742549	11.321053		-0.742971	11.359279	
5.86970	-0.715719	11.676709	0.022815	-0.742641	11.411948	0.019954	-0.743059	11.451558	0.020348
5.91970	-0.715802	11.814550	0.023586	-0.742705	11.500556	0.020759	-0.743118	11.541571	0.021141
5.96970	-0.715855	11.951905	0.024284	-0.742741	11.586803	0.021480	-0.743149	11.629244	0.021851
6.01970	-0.715881	12.088747	0.024914	-0.742751	11.670611	0.022123	-0.743155	11.714498	0.022484
6.06970	-0.715879	12.225055	0.025479	-0.742736	11.751904	0.022693	-0.743136	11.797258	0.023043
6.11970	-0.715851	12.360805	0.025984	-0.742697	11.830608	0.023194	-0.743092	11.877447	0.023534
6.16970	-0.715799	12.495976		-0.742636	11.906645		-0.743027	11.954988	
6.21970	-0.715724	12.630546	0.026829	-0.742553	11.979942	0.024007	-0.742940	12.029805	0.024327
6.26970	-0.715625	12.764495	0.027175	-0.742450	12.050422	0.024326	-0.742832	12.101824	0.024638
6.31970	-0.715505	12.897802	0.027476	-0.742328	12.118013	0.024593	-0.742706	12.170970	0.024896

CHAPTER 5

The Electronic Structure of ScLi, TiLi, VLi, CrLi, and CuLi and Their Positive Ions

A. Introduction

In an earlier study, Harrison[1] showed that those states of ScLi that dissociate to ground state Li and Sc in a $4s^23d$ configuration are characterized by a small (<0.27 eV) dissociation energy, while those states that correlate with Sc in a $4s3d^2$ configuration are strongly bound, relative to this configuration. This is understood as follows: As Sc and Li approach, the initial encounter is between the Sc $4s^2$ pair and the Li 2s orbital. This is a repulsive interaction, and a bond will not form until Sc has hybridized the 4s, 4p into two sp hybrids. This takes energy and the resulting bond energy reflects this cost of hybridization. The $4s3d^2$ configuration, however, can form a bond using the singly occupied 4s and does not suffer a hybridization[2] penalty. It does, however, suffer an exchange energy loss[3] (EEL) (since the 4s and 3d's are all high-spin coupled) in uncoupling the 4s electron from the two high-spin 3d's.

Generalizing these observations to the remaining early transition metal atoms, it is expected that the cost to hybridize the $4s^2$ pair to two sp hybrids will be related to the separation between the $4s^23d^n$ and $4s4p3d^n$ configurations. Since the lowest $4s4p3d^n$ states are ~ 2 eV above[4] the s^2d^n states for Sc, Ti, and V, we expect the hybridization cost will be approximately constant across this series, and the bond energies relative to the s^2d^n configuration will be similar and essentially independent of the number of 3d electrons. In contrast, because of EEL, the bond energy associated with the sd^{n+1} configuration will decrease, as the number of 3d electrons increases in going from Sc to Cr. Note that the exchange energy loss is a maximum for Cr and is zero for Cu, and we will study CuLi as an important reference. Of course, superimposed on these

considerations are orbital effects such as the variation of the size of the 4s orbital in going from Sc to Cu.

The variation of the experimental[4]/calculated s^2d^n - sd^{n+1} separation for the elements considered here is shown in Figure 1. The drop in this separation, as one goes from Sc to Cr, suggests that either Ti or V lithide might have ground states that correlate with the excited sd^{n+1} configurations. As we shall see, the ground state of TiLi is $^4\Phi$ and traces its lineage to the s^2d^2 configuration, while the ground state of VLi is $^5\Delta$ and traces its lineage to the sd^4 configuration.

Also presented in this work is a study of the mono-positive ions, MLi^+. Ionizing the lithides dramatically changes the nature of the bonding. The easiest way to see this is to note that lithium's ionization potential is smaller than that of the first-row transition elements, so the lowest energy asymptotic fragments are Li^+ and M in its ground state. The resulting molecular states retain this qualitative description and are bound, due primarily to the large polarizability of the transition element.

B. Technical Details and Wavefunction Construction

The basis sets used for the transition metal atoms consisted of a 14s9p5d primitive set of Wachters[5] augmented with two additional p functions and a diffuse d as recommended by Hay.[6] This set of functions was contracted to 5s4p3d, using the Raffenetti[7] contraction scheme. Two additional f functions were added to correlate the d electrons, and their exponents were determined variationally at the MCSCF+1+2 level. A

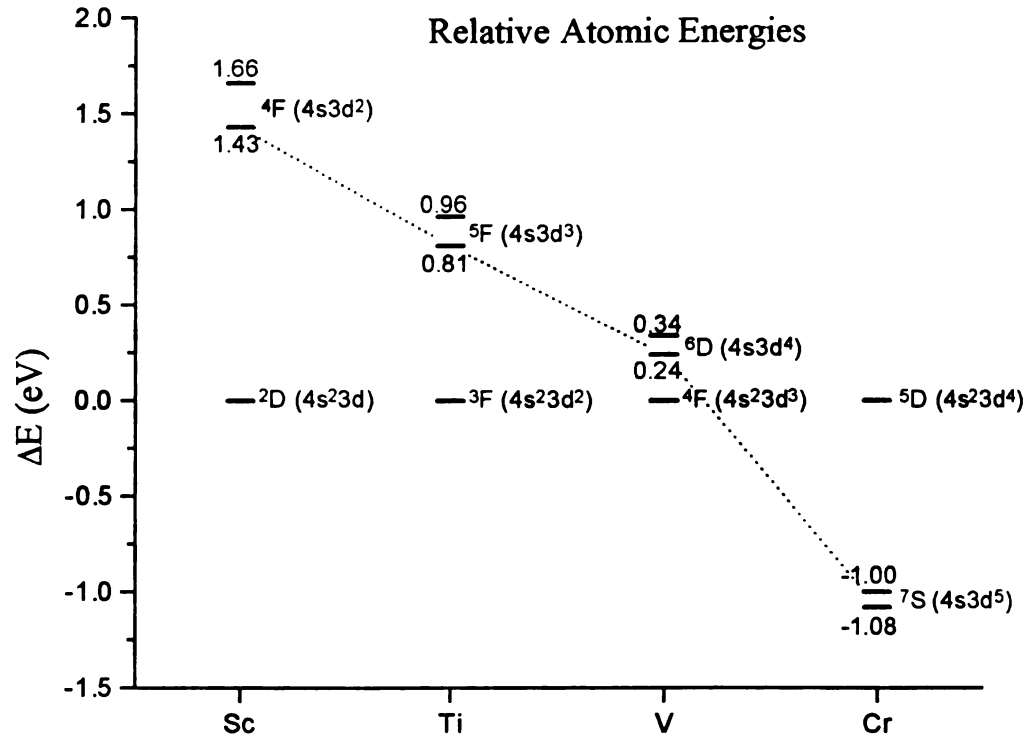

Figure 1. Energy separation between the lowest terms of the s^2d^n and sd^{n+1} configurations. Calculated(MRCI) and experimental separations are presented with the experimental results connected by a dotted line.

second f set of four primitive functions, contracted to 3, were taken from Langhoff and Bauschlicher[8] and were used in the CuLi calculations.

For the Lithium basis, a Williams and Streitwieser[9] 4p representation of the Li 2p orbital was added to a 12 *s* primitive set of van Duijneveldt.[10] The Lithium basis set was contracted to 3s2p and proves flexible enough to describe both the ground- and the low-lying excited ^2P state of Lithium.

All calculations were performed on Silicon Graphic Workstations, using the Columbus92[11] set of codes. Multiconfigurational Self-Consistent Field wavefunctions (MCSCF) were constructed, using two orbitals to describe the bonding electron pair and permitting the d electrons to occupy orbitals so that the angular momentum (electronic symmetry) was accurately described. For the Configuration Interaction wavefunction, all single and double excitations were calculated from the MCSCF wavefunction, MCSCF+1+2. Unlinked clusters were accounted for by an Averaged Coupled-Pair Functional[12] (ACPF) over the same MCSCF+1+2 CSF space. In what follows, we will refer to the MCSCF+1+2 as the multireference CI or MRCI. We show, in Figure 2, the basic form of the MCSCF wavefunction and, in Table 5-1, the number of configuration state functions (CSF's) used in the MCSCF and MRCI wavefunctions.

C. Neutral Lithides

We will consider, first, the states that result when a Li atom interacts with the ground state of the transition elements. This means we will consider the s^2d^n configurations for Sc, Ti, and V and the sd^{n+1} configuration of Cr and Cu. To orient the discussion, Figures 3 and 4 show the potential energy curves for the states of TiLi that

Ground State MCSCF WaveFunctions

Neutral Ions

ScLi $\Psi_{mcscf} = (core)\ (b\ b^*)^2\ \sigma\ 3d_{\delta+}^{\ 1}$ $^3\Delta$

TiLi $\Psi_{mcscf} = (core)\ (b\ b^*)^2\ \sigma\ [3d_{\pi x}\ 3d_{\delta+} - 3d_{\pi y}\ 3d_{\delta-}]^2$ $^4\Phi$

VLi $\Psi_{mcscf} = (core)\ (b\ b^*)^2\ 3d_{\sigma}^{\ 1}\ 3d_{\delta+}^{\ 1}\ 3d_{\pi x}^{\ 1}\ 3d_{\pi y}^{\ 1}$ $^5\Delta$

CrLi $\Psi_{mcscf} = (core)\ (b\ b^*)^2\ 3d_{\sigma}^{\ 1}\ 3d_{\delta-}^{\ 1}\ 3d_{\delta+}^{\ 1}\ 3d_{\pi x}^{\ 1}\ 3d_{\pi y}^{\ 1}$ $^6\Sigma^+$

CuLi $\Psi_{mcscf} = (core)\ (b\ b^*)^2\ 3d_{\sigma}^{\ 2}\ 3d_{\delta-}^{\ 2}\ 3d_{\delta+}^{\ 2}\ 3d_{\pi x}^{\ 2}\ 3d_{\pi y}^{\ 2}$ $^1\Sigma^+$

Positive Ions

$ScLi^+$ $\Psi_{mcscf} = (core)\ (b\ b^*)^2\ \ 3d_{\delta+}^{\ 1}$ $^2\Delta$

$TiLi^+$ $\Psi_{mcscf} = (core)\ (b\ b^*)^2\ \ [3d_{\pi x}\ 3d_{\delta+} - 3d_{\pi y}\ 3d_{\delta-}]^2$ $^3\Phi$

VLi^+ $\Psi_{mcscf} = (core)\ (b\ b^*)^2\ \ 3d_{\delta+}^{\ 1}\ 3d_{\pi x}^{\ 1}\ 3d_{\pi y}^{\ 1}$ $^4\Delta$

$CrLi^+$ $\Psi_{mcscf} = (core)\ \sigma\ 3d_{\sigma}^{\ 1}\ 3d_{\delta-}^{\ 1}\ 3d_{\delta+}^{\ 1}\ 3d_{\pi x}^{\ 1}\ 3d_{\pi y}^{\ 1}$ $^7\Sigma$

$CuLi^+$ $\Psi_{mcscf} = (core)\ \sigma\ 3d_{\sigma}^{\ 2}\ 3d_{\delta-}^{\ 2}\ 3d_{\delta+}^{\ 2}\ 3d_{\pi x}^{\ 2}\ 3d_{\pi y}^{\ 2}$ $^2\Sigma$

Figure 2. Orbitals involved in the MCSCF wavefunctions for the neutral and monopositive transition-metal lithides.

Table 5-1. Energy separation between the lowest terms of the s^2d^n and sd^{n+1} configurations. Calculated (MRCI) and experimental separations are presented with the experimental results connected by a dotted line.

Molecule	State	High-Spin Electron Configuration	CSF's	
			MCSCF	MRCI
ScLi	$^3\Delta$	σd_δ	5	4817
$ScLi^+$	$^2\Delta$	d_δ	4	1619
$ScLi^+$	$^4\Delta$	$\sigma\sigma^1 d_\delta$	1	721
TiLi	$^4\Phi$	$\sigma d_\pi d_\delta$	12	17723
TiLi	$^4\Delta$	$d_{\pi_x} d_{\pi_y} d_\delta$	6	9770
$TiLi^+$	$^3\Phi$	$d_\pi d_\delta$	5	4622
$TiLi^+$	$^5\Delta$	$\sigma\, d_{\pi_x} d_{\pi_y} d_\delta$	1	1293
VLi	$^5\Delta$	$\sigma\, d_{\pi_x} d_{\pi_y} d_\delta$	7	17641
VLi	$^5\Delta$	$d\sigma\, d_{\pi_x} d_{\pi_y} d_\delta$	7	17641
VLi^+	$^4\Delta$	$d_{\pi_x} d_{\pi_y} d_\delta$	6	9770
VLi^+	$^6\Sigma^+$	$\sigma\, d_{\pi_x} d_{\pi_y} d_{\delta_+}\, d_{\delta_-}$	1	2056
CrLi	$^6\Pi$	$\sigma\, d_\sigma d_{\pi_y} d_{\delta_+}\, d_{\delta_-}$	8	27338
CrLi	$^6\Sigma^+$	d^5	8	27338
$CrLi^+$	$^5\Sigma^+$	$d_{\pi_x} d_{\pi_y} d_{\delta_+}\, d_{\delta_-}$	7	16970
$CrLi^+$	$^7\Sigma^+$	σd^5	1	2833
CuLi	$^3\Delta$	σd_δ	5	98030
CuLi	$^1\Sigma^+$	—	3	24747
$CuLi^+$	$^2\Delta$	d_δ	4	49166
$CuLi^+$	$^2\Sigma^+$	σ	4	49166

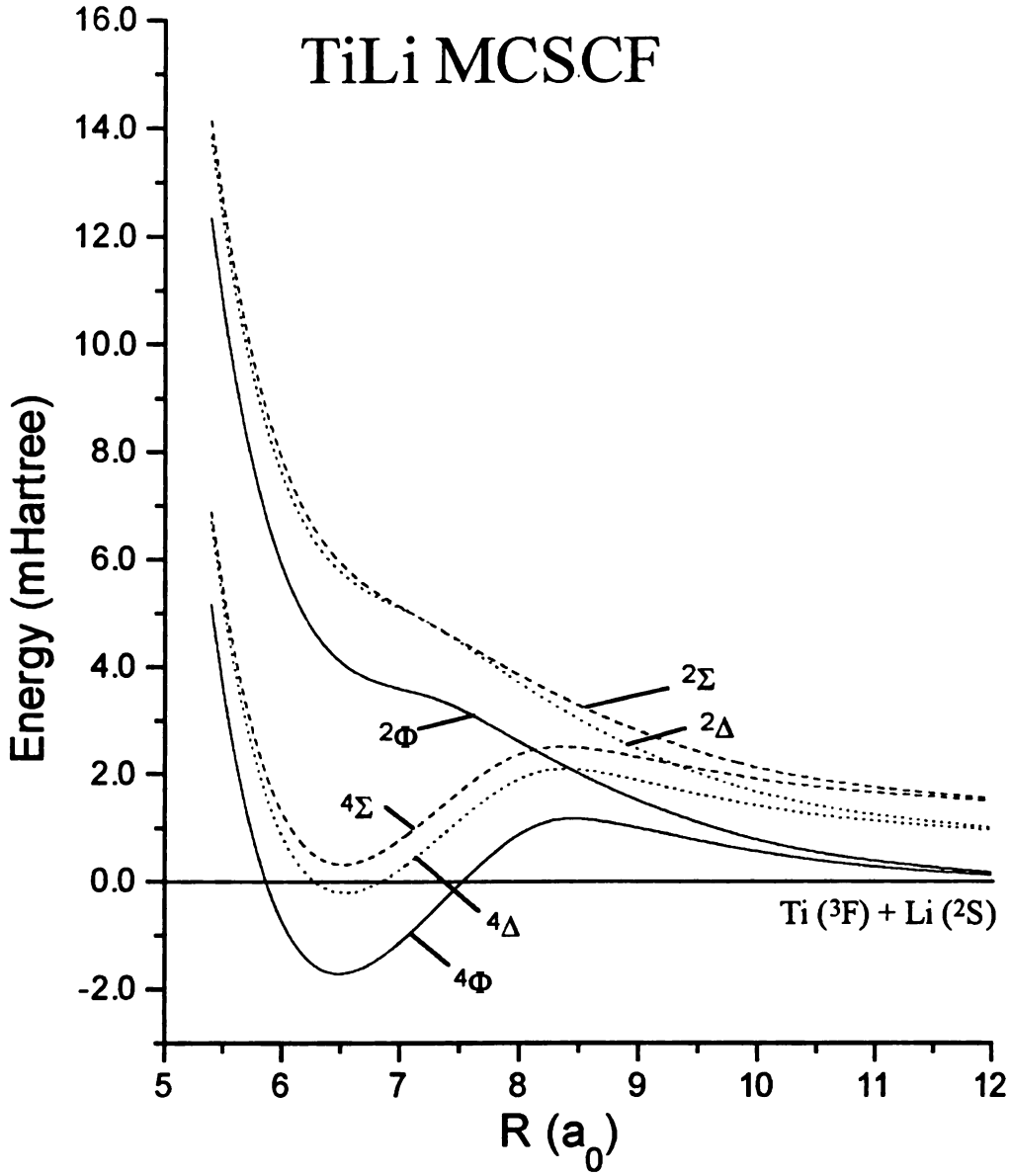

Figure 3. Calculated (MCSCF) potential energy curves for the lowest quartet and doublet states of TiLi that correlate with the ground-state products, $Ti(^3F) + Li(^2S)$.

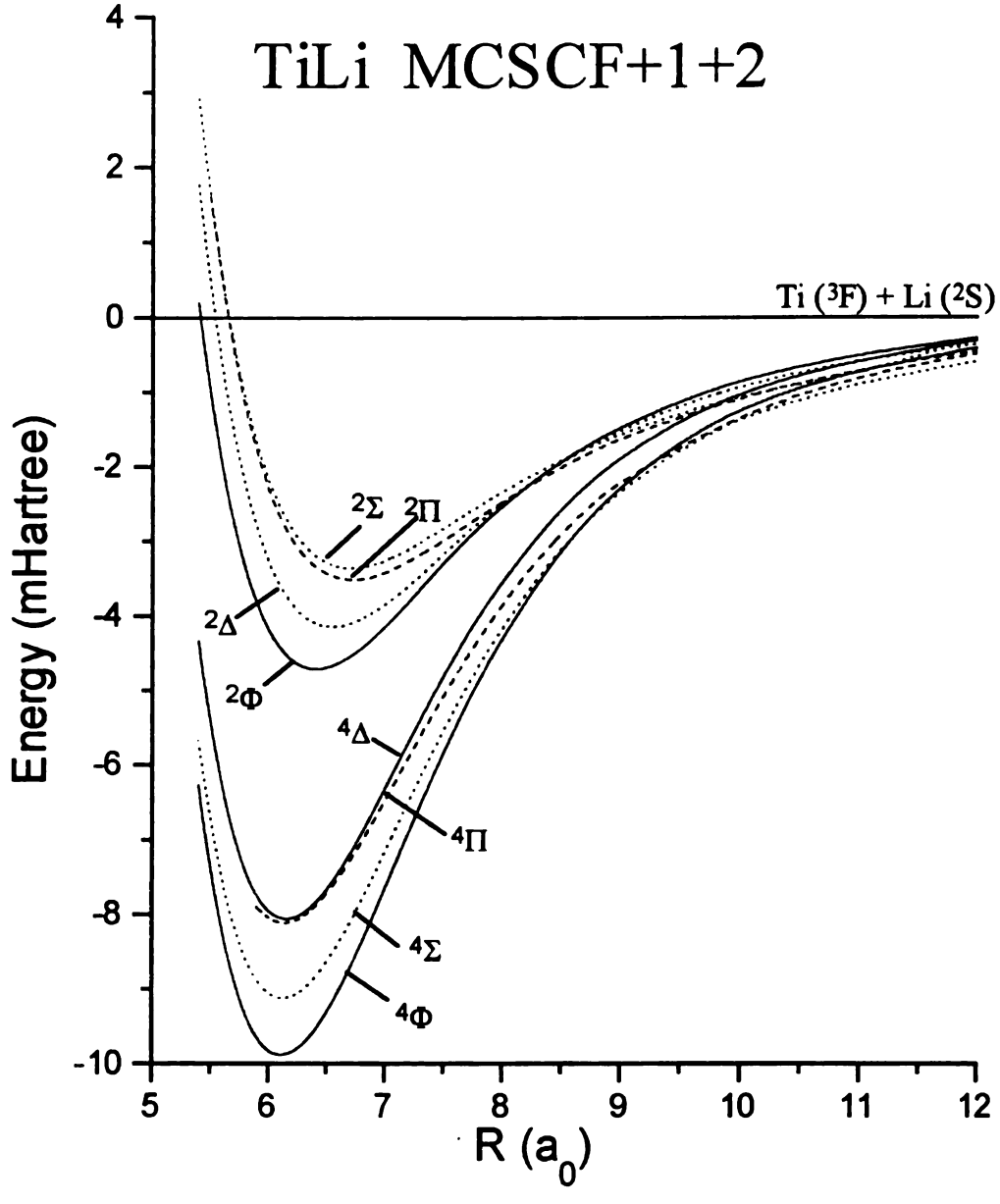

Figure 4. Calculated (MCSCF+1+2) potential energy curves for the lowest quartet and doublet states of TiLi that correlate with the ground-state products, Ti(^{3}F) + Li(^{2}S).

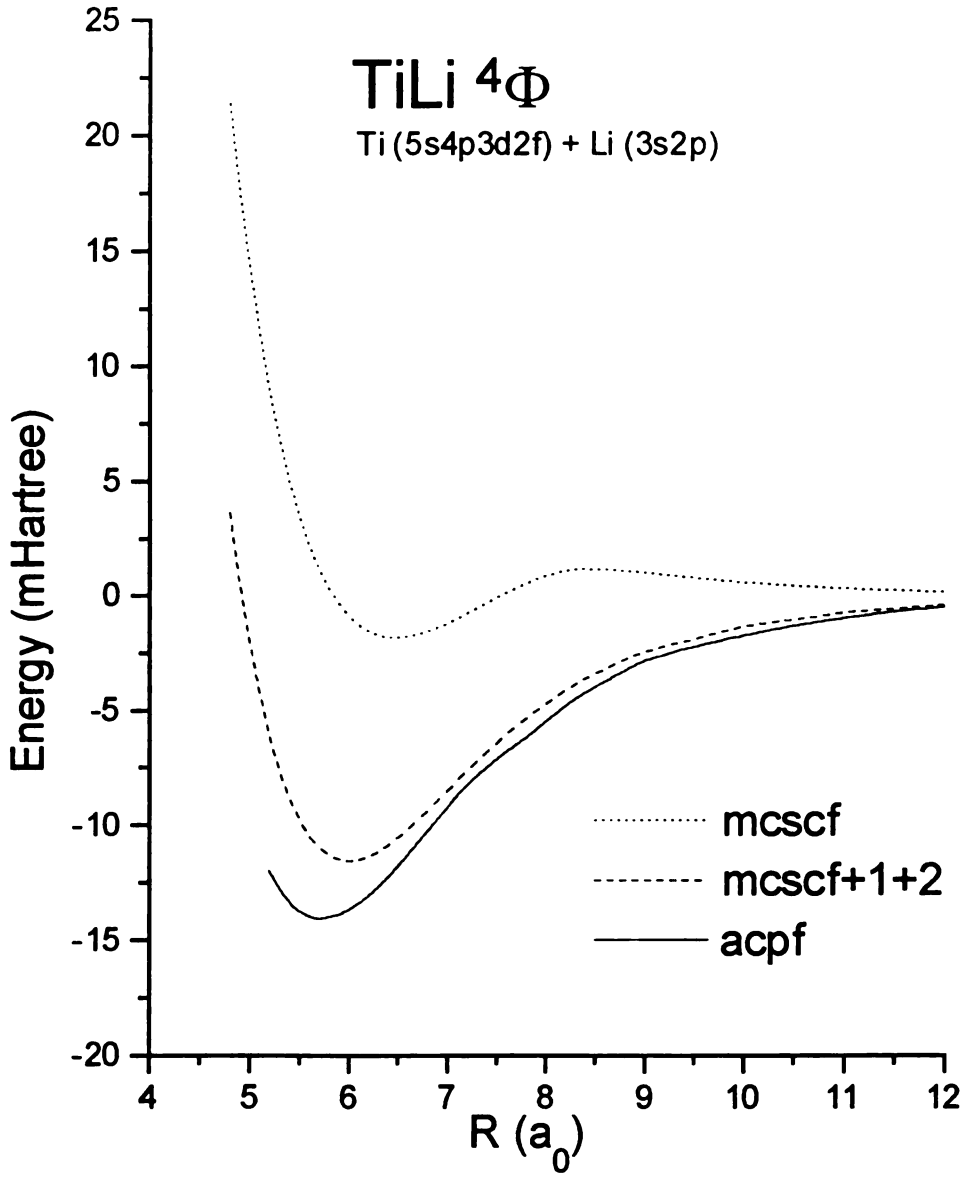

Figure 5. $^4\Phi$ ground-state potential curve of TiLi, calculated with the MCSCF, MCSCF+1+2, and ACPF techniques.

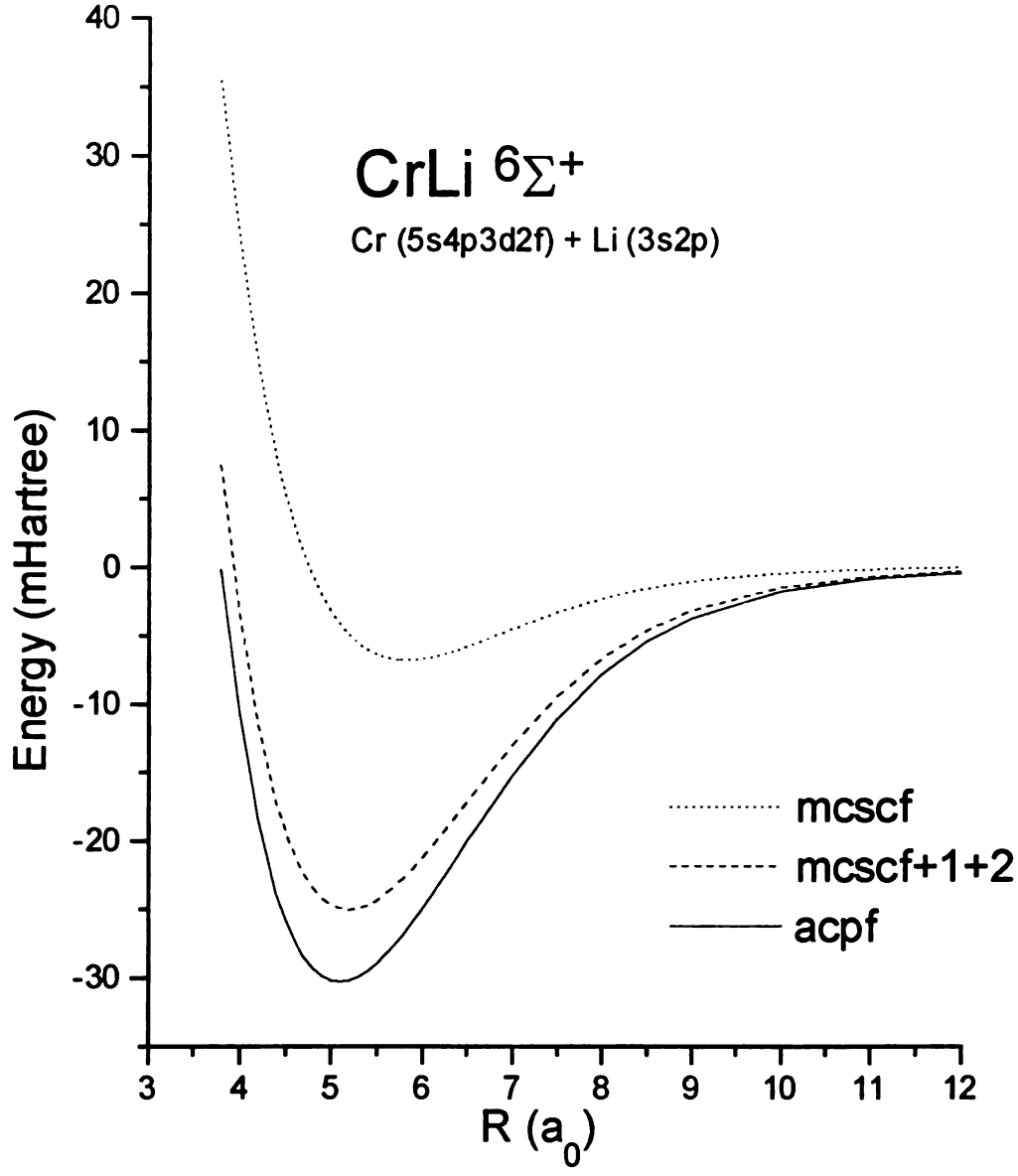

Figure 6. $^6\Sigma^+$ ground-state potential energy curves of CrLi, calculated with MCSCF, MCSCF+1+2, and ACPF techniques.

Table 5-2. Dissociation energy, bond length, and vibrational frequency for states of ScLi, TiLi, VLi, CrLi, and CuLi asymptotic to the transition metal $4s^23d^n$ and $4s3d^{n+1}$ atomic states.

		$4s^23d^n$					$4s3d^{n+1}$				
Molecule	Method	D_e (eV)	R_e (Å)	ω_e (cm^{-1})	State	Comment	D_e (eV)	R_e (Å)	ω_e (cm^{-1})	State	Comment
ScLi	MRCI	0.305	3.305	210	$^3\Delta$ $(\sigma\, d_\delta)$	Ground State	Not Converged			$^3\Sigma^-$ $(d_{\pi x} d_{\pi y})$	Excited State
	ACPF	0.335	3.282	216							
TiLi	MRCI	0.305	3.183	216	$^4\Phi$ $(\sigma\, d_\pi d_\delta)$	Ground State	0.890	2.787	276	$^4\Delta$ $(d_{\pi x} d_{\pi y} d_\delta)$	Excited State
	ACPF	0.389	3.028	198			1.102	2.698	319		
VLi	MRCI	0.264	3.116	209	$^5\Delta$ $(\sigma d_{\pi x} d_{\pi y} d_\delta)$	Excited State	0.868	2.702	287	$^5\Delta$ $(d_\sigma d_{\pi x} d_{\pi y} d_\delta)$	Ground State
	ACPF	Not Converged					1.042	2.644	306		
CrLi	MRCI	0.201	3.132	196	$^6\Pi$ $(\sigma d_\sigma d_{\pi y} d_{\delta+} d_{\delta-})$	Excited State	0.683	2.751	269	$^6\Sigma^+$ $(d_\sigma d_{\pi x} d_{\pi y} d_{\delta+} d_{\delta-})$	Ground State
	ACPF	0.239	3.094	205			0.824	2.697	288		
CuLi	MRCI	Not Converged			$^2\Delta$ $(\sigma d_\sigma^2 d_{\pi y}^2 d_{\delta+}^2 d_{\delta-}^2)$	Excited State	1.165	2.486	329	$^1\Sigma^+$ (d^{10})	Ground State
	ACPF						1.445	2.444	350		
	MRCI						1.616	2.428	356		"3f" basis

correlate with the ^3F ground state of Ti. The MCSCF results in Figure 3 suggest strongly that this level of theory is incapable of describing bond formation in this molecule. The MRCI results in Figure 4, however, are much improved and predict that TiLi is bound in all of the quartet and doublet states that derive from Ti(^3F) + Li(^2S). Note, also, the remarkably small binding energies and the large density of states predicted for this system. The ACPF[12] approximation corrects for unlinked cluster effects in the MRCI, and we compare, in Figure 5, the results of this technique with the MCSCF and MRCI prediction for the ground $^4\Phi$ state of TiLi. This figure illustrates a recurring theme when Li interacts with a transition metal atom in the s^2d^n configuration; i. e., most of the bond energy is correlation energy. Similar results obtain for ScLi ($^3\Delta$) and VLi ($^5\Delta$).

The ground-state terms of both Cr and Cu are derived from the sd^{n+1} configuration, and when Li interacts with these terms, we form $^6\Sigma^+$ and $^1\Sigma^+$ states, respectively. The potential energy curves for CrLi are shown for various levels of calculations in Figure 6. Note that, in this instance, the MCSCF seems qualitatively correct, although correlation effects are crucial to the accurate representation of these interactions. A similar result obtains for CuLi in the $^1\Sigma^+$ state. Summarized in Table 5-2, the dissociation energy, bond length, and vibrational frequency for these states and several others yet to be discussed.

The ground state of ScLi, TiLi, CrLi, and CuLi each correlate with the lowest term of the transition element. The ground state of VLi is not the $^5\Delta$ (s^2d^3) state described above but a second $^5\Delta$ state that correlates to the sd^4 configuration. These two

Table 5-3. Calculated (MCSCF) potential energy curves for the lowest quartet and doublet states of TiLi that correlate with the ground state products, $Ti(^3F) + Li(^2S)$.

Element	States	EEL (eV)	EEL (eV)/d Electron	D_e (eV)		D_e* (eV)	
				MRCI	ACPF	MRCI	ACPF
Sc	$^2F - ^4F$	0.212	0.106	—	—	—	—
Ti	$^3F - ^5F$	0.307	0.102	0.890	1.102	1.197	1.409
V	$^4D - ^6D$	0.391	0.098	0.868	1.042	1.259	1.433
Cr	$^5S - ^7S$	0.471	0.094	0.680	0.824	1.151	1.295
Cu	—	0	0	1.165	1.445 (1.616)+	1.165	1.445 (1.616)+

+using the "3f" basis described in text

states are shown in Figure 7. The MRCI binding energy for the $^5\Delta$ (sd^4) state is 0.868 eV, relative to the ^6D asymptote, while the binding energy of the $^5\Delta$ (s^2d^3) state is 0.264 eV, relative to the ^4F asymptote. Since our calculated s^2d^3-sd^4 splitting is 0.342 eV, the $^5\Delta$ (sd^4) is the ground state by 0.262 eV. This raises the question of how far above the ground states of the other transition metal lithides are the states that correlate with the excited state of the transition metal? To address this, wavefunctions were constructed for TiLi that trace their lineage to the ^5F (sd^3) configuration of Ti and for CrLi that traces their lineage to the ^5D (s^2d^4) of Cr. We were unsuccessful in constructing the corresponding multireference CI functions that correlate with the ^4F (sd^2) state of Sc or the ^2D (s^2d^9) state of Cu. The results are collected in Table 5-2. Figures 8-11, the summarized results of bonding to the s^2d^n or sd^{n+1} states, for all of the lithides except CuLi.

From Table 5-2, we see that those states that correlate with the s^2d^n configuration of the transition element have bond energies (at the MRCI level) between 0.2 and 0.3 eV; and further, the De's increase with increasing bond length. Also, the vibrational frequencies are all ~ 200 cm^{-1}. The states that correlate with the sd^{n+1} configurations have somewhat different characteristics. The bond strengths, relative to the adiabatic asymptote, are larger than those of the s^2d^n states, and the vibrational frequencies are also uniformly larger.

It is expected that, in order for Li to bond to a high-spin state of the sd^{n+1} configuration, the transition metal must uncouple the 4s spin from the remaining high-spin 3d electrons. The energy involved in this randomization of the 4s spin, the exchange

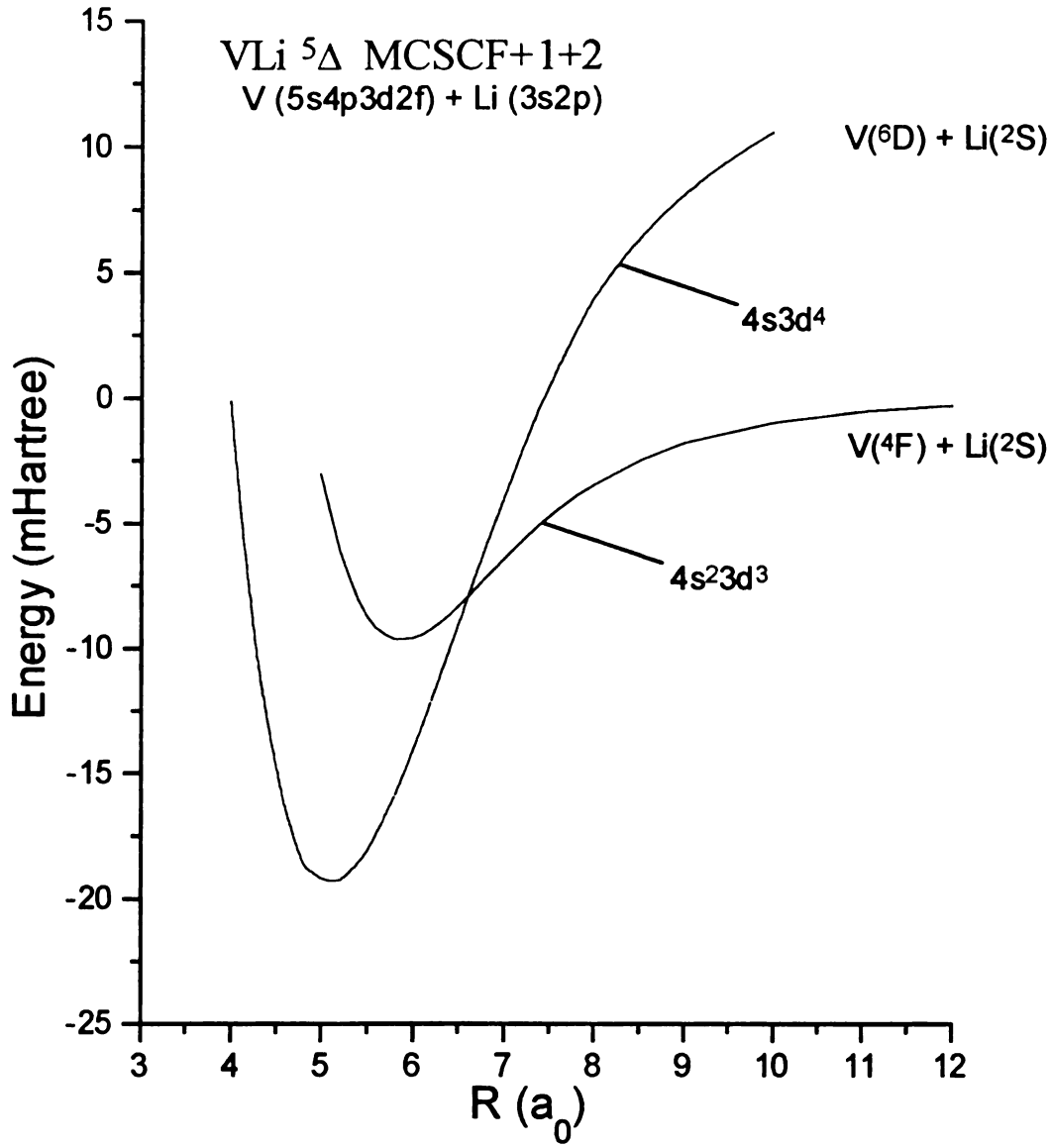

Figure 7. Two $^5\Delta$ states of VLi that correlate with the s^2d^3 and sd^4 asymptotes.

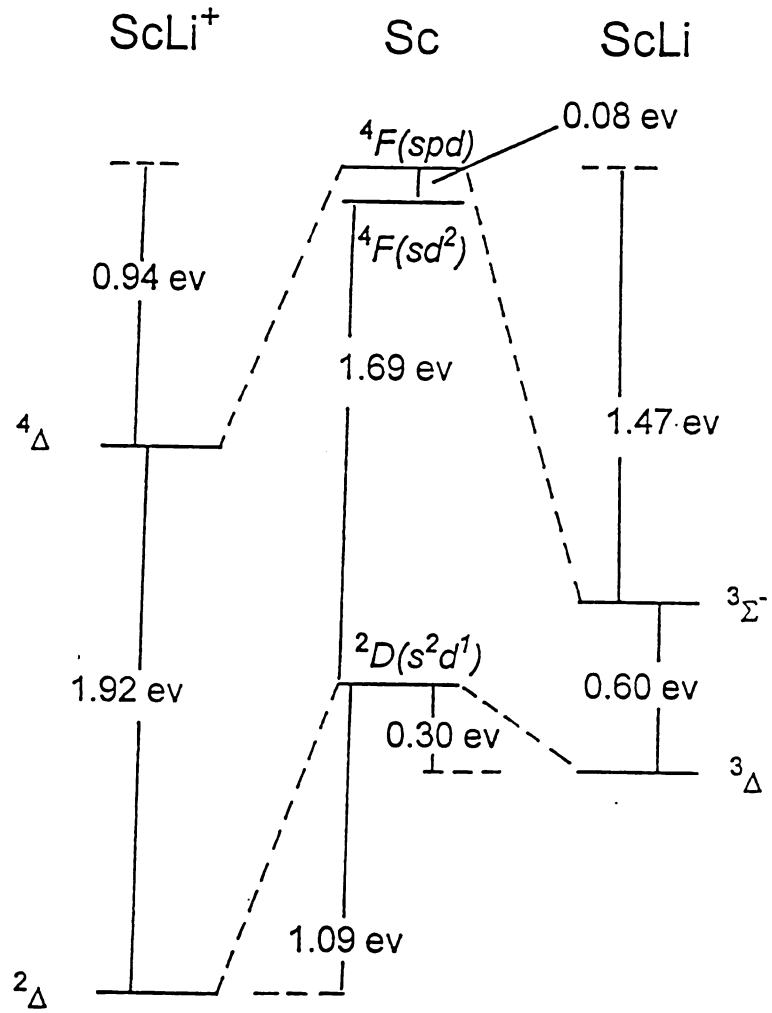

Figure 8. Comparison of the neutral and positive ion states of ScLi, calculated at the MRCI level.

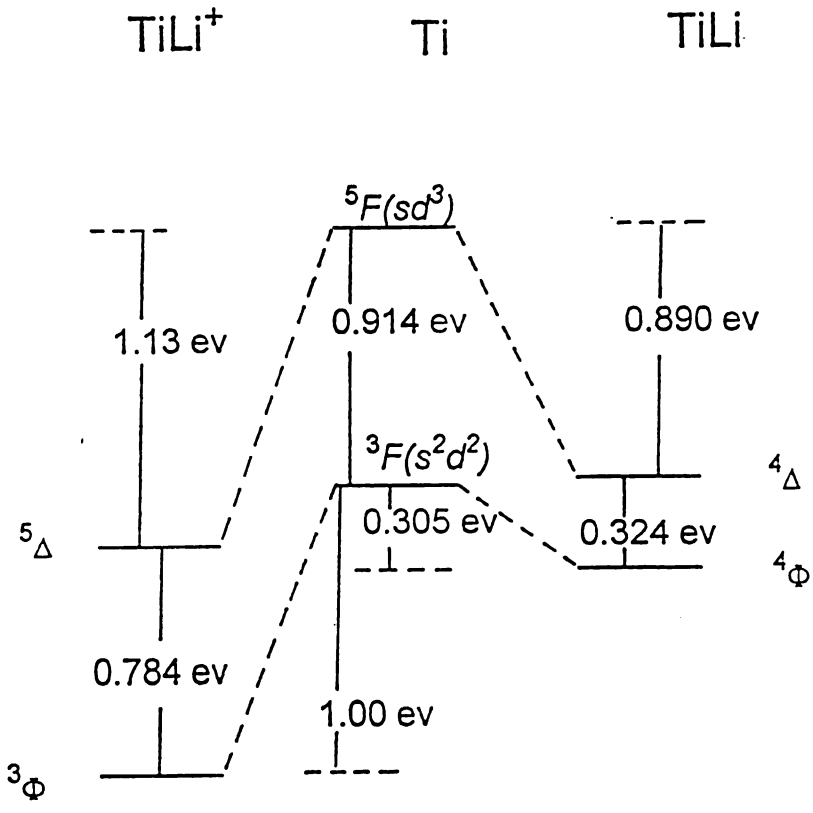

Figure 9. Comparison of the neutral and positive ion states of TiLi, calculated at the MRCI level.

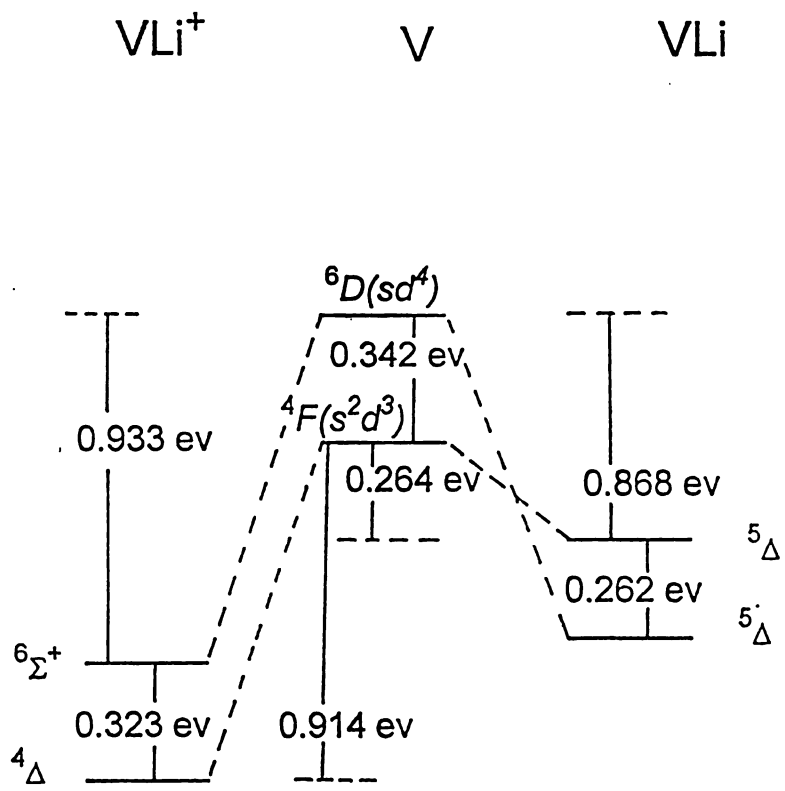

Figure 10. Comparison of the neutral and positive ion states of VLi, calculated at the MRCI level.

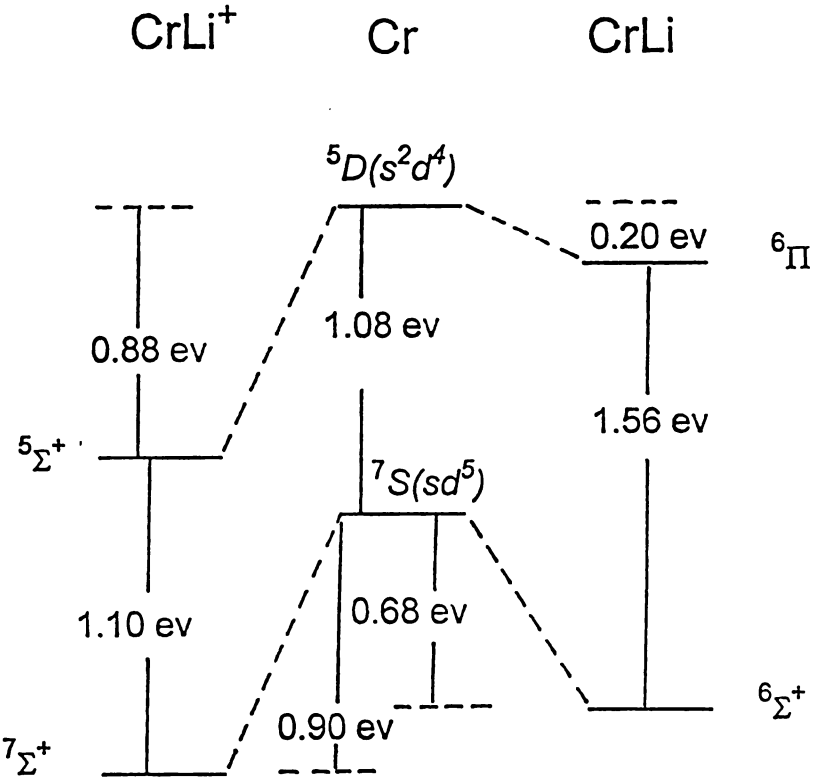

Figure 11. Comparison of the neutral and positive ion states of CrLi, calculated at the MRCI level.

energy loss,[3] is easily estimated as half of the difference between the state in which the 4s is high-spin coupled to the $3d^{n+1}$ system and in which it is low-spin coupled. For example, in Sc, the ^4F term corresponds to the 4s being high-spin coupled to the high-spin $3d^2$ core, while the lowest ^2F term corresponds to it being low-spin coupled to this same high-spin $3d^2$ core. This energy difference[4] is 0.424 eV and, therefore, the EEL is 0.212 eV. Continuing in this way, we construct Table 5-3 in which we tabulate the total EEL for Sc-Cr as well as the EEL per 3d electron. Note that this latter quantity decreases slightly in going from Sc-Cr, reflecting the contracting 3d shell. The calculated De(both the MRCI and ACPF values) was augmented with the experimental EEL to produce the tabulated "intrinsic" bond energies. These results suggest that the intrinsic bond strength of Li and a 4s transition element orbital is ~ 1.62 eV (ACPF result) or 1.40 eV (MRCI result). This allows us to estimate the as-yet-calculated De for the $^3\Sigma^-$ (sd^2) state of ScLi as 1.4 - 1.2 eV. Summarized in Figure 12 are the ground-state potential curves for these lithides.

D. Positive Lithides

The asymptotic products for $M\text{-}Li^+$ are $M + Li^+$, $M^+ + Li$, and $M^* + Li^+$, where M^* is an excited state of the transition metal. The relative experimental energies of these asymptotes are shown in Figure 13. The lowest asymptote for all transition elements is the ground-state M, interacting with Li^+, and we will consider this interaction first. Once again, there are two classes of interaction. With Sc, Ti, and V, the Li^+ ion encounters a s^2d^n configuration, while, for Cr and Cu, it is an sd^{n+1} configuration.

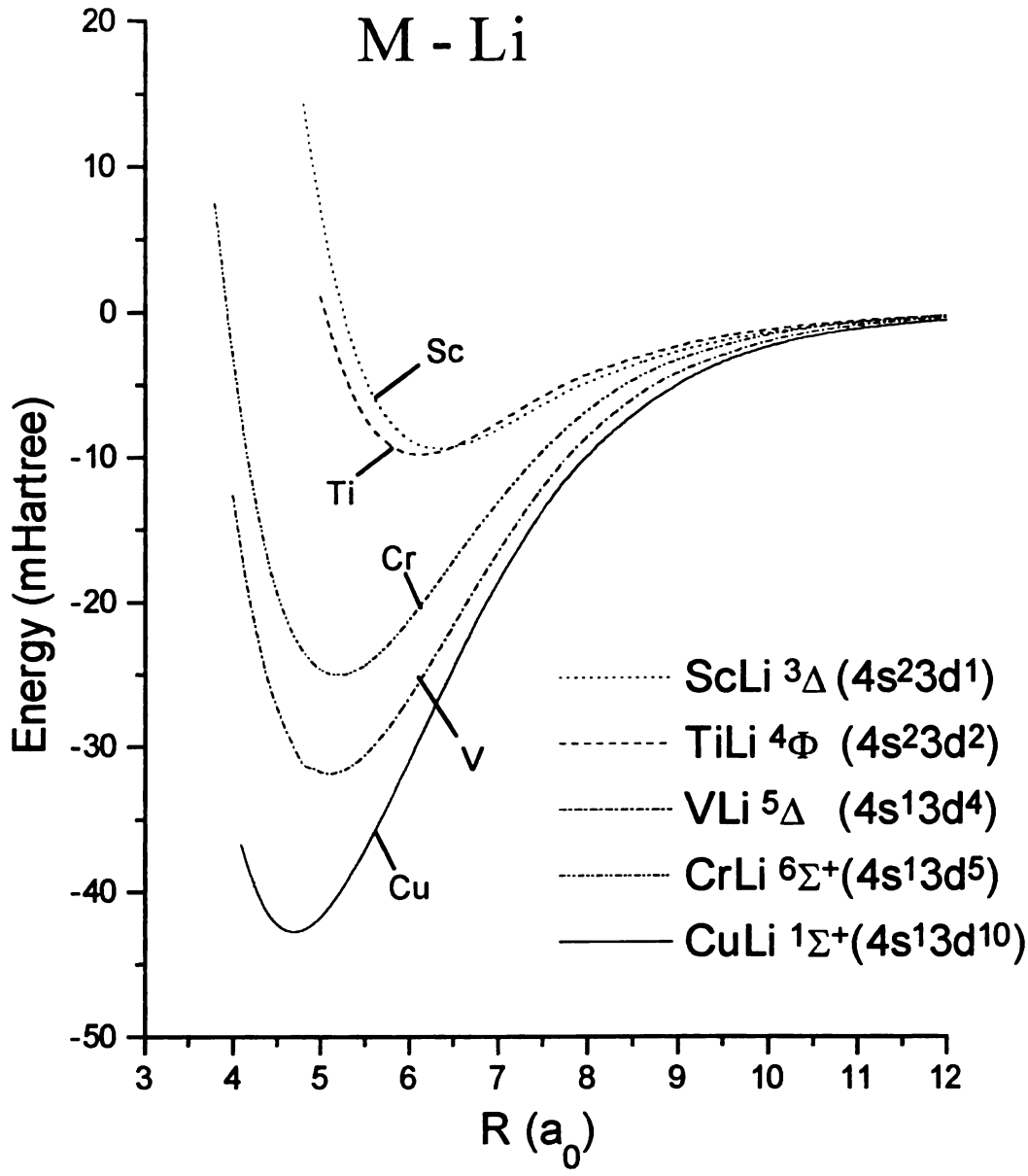

Figure 12. MRCI ground-state potential curves for the neutral lithides.

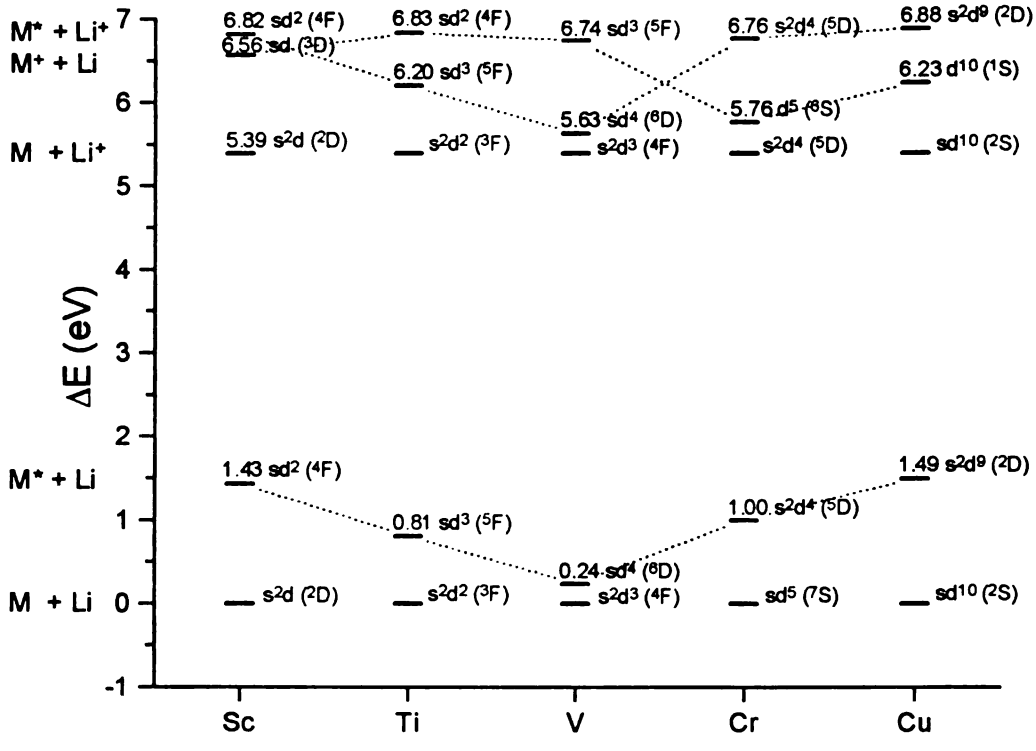

Figure 13. Experimental energy levels for the low-lying asymptotic products M + Li, M^+ + Li, M + Li^+, and M* + Li^+.

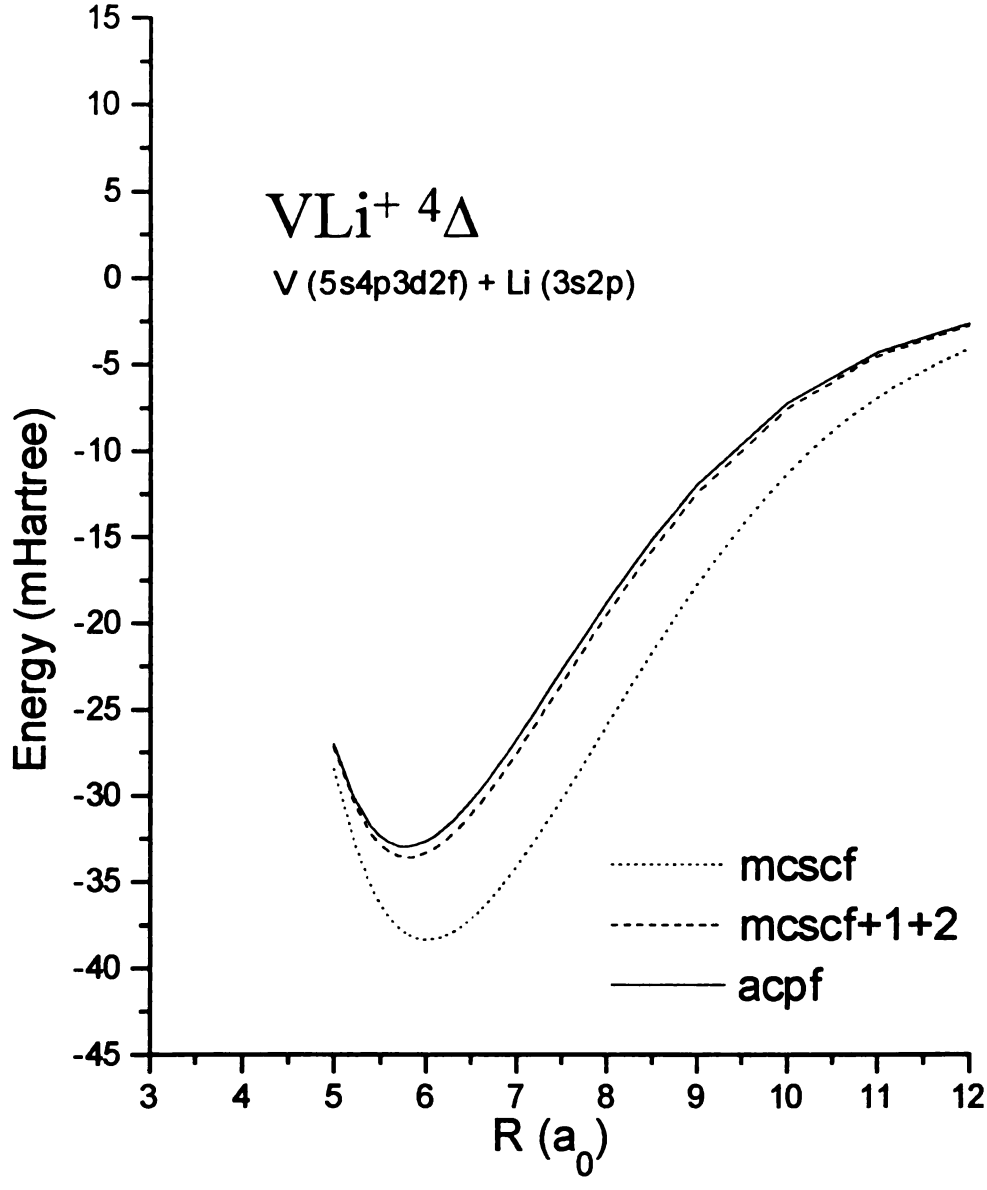

Figure 14. $^4\Delta$ ground-state potential curves of VLi^+, calculated with the MCSCF, MCSCF+1+2, and ACPF techniques.

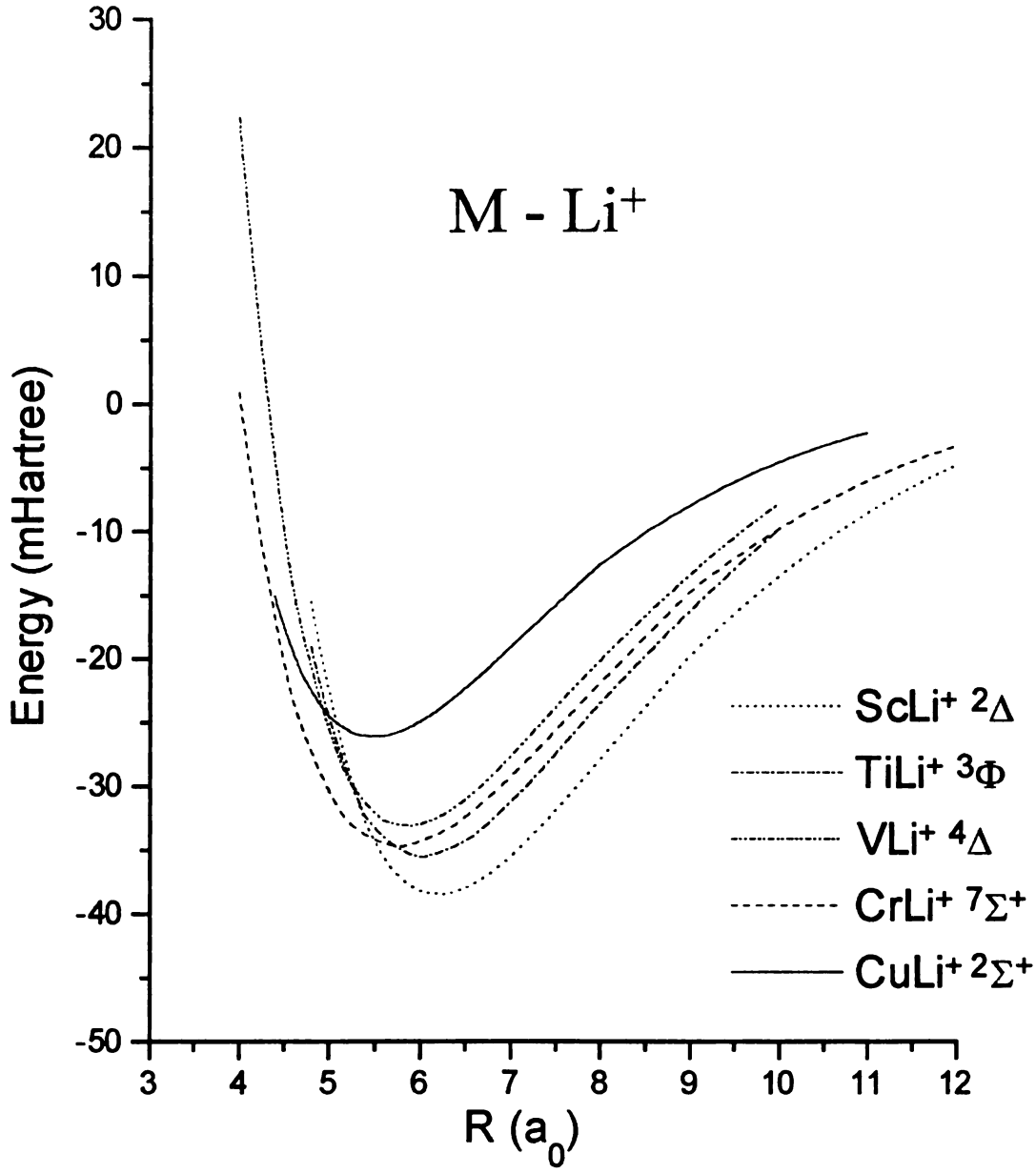

Figure 15. MRCI ground-state potential energy curves for the monopositive lithides.

Table 5-4. Calculated Characteristics of Various Transition-Metal Lithide Cations

	$4s^23d^n$					$4s3d^{n+1}$				
Molecule	D_e (eV)	R_e (Å)	ω_e (cm^{-1})	State	Comment	D_e (eV)	R_e (Å)	ω_e (cm^{-1})	State	Comment
$ScLi^+$	1.09	3.259	240	$^2\Delta$ ($\sigma^2 d_\delta$)	Ground State	0.94	3.641	181	$^4\Delta(\sigma\,\sigma' d_\delta)$	Excited State
$TiLi^+$	1.00	3.148	243	$^3\Phi$ ($\sigma^2 d_\pi d_\delta$)	Ground State	1.13	3.059	217	$^5\Delta$ ($\sigma\, d_{\pi_x} d_{\pi_y} d_\delta$)	Excited State
VLi^+	0.91	3.072	241	$^4\Delta$ ($\sigma^2\, d_{\pi_x} d_{\pi_y} d_\delta$)	Ground State	0.93	3.129	212	$^6\Sigma^+$ ($\sigma\, d_{\pi_x} d_{\pi_y} d_{\delta_+} d_{\delta_-}$)	Excited State
$CrLi^+$	0.90	3.006	247	$^5\Sigma^+$ ($\sigma^2\, d_{\pi_x} d_{\pi_y} d_{\delta_+} d_{\delta_-}$)	Excited State	0.88	3.021	214	$^7\Sigma^+$ (σd^5)	Ground State
$CuLi^+$	0.59	2.867	246	$^2\Delta$ $\left(\sigma^2 d_\sigma^2 d_\pi^4 d_\delta^3\right)$	Excited State	0.71	2.913	220	$^2\Sigma^+$ (σd^{10})	Ground State

In the presence of Li^+, the ^2D of Sc generates $^2\Sigma^+$, $^2\Pi$, and $^2\Delta$ symmetries; the ^3F of Ti generates $^3\Sigma^-$, $^3\Pi$, $^3\Delta$, and $^3\Phi$, and the ^4F of V generates $^4\Sigma^-$, $^4\Pi$, $^4\Delta$, and $^4\Phi$. We have considered the $^2\Delta$ of $ScLi^+$, the $^3\Phi$ of $TiLi^+$, and the $^4\Delta$ of VLi^+. The potential energy curves for each of these states were calculated at several theoretical levels, and representative curves for VLi^+ are shown in Figure 14. It is interesting that, relative to the more correlated techniques, the MCSCF level of theory overestimates the interaction energy between Li^+ and these transition metals in the s^2d^n configurations. Since this interaction energy will depend strongly on the *in-situ* charge on Li, we speculate that the MCSCF function does not permit as much charge transfer from M to Li^+ as the ACPF and MRCI calculations. Another viewpoint is that the CI techniques more accurately order the various mono-positive asymptotes shown in Figure 13. These results also indicate that, unlike the neutral lithides, these systems can be adequately described without significant electron correlation. The potential energy curves for these systems are compared in Figure 15, while the dissociation energies, bond lengths, and vibrational frequencies calculated at the MRCI level are collected in Table 5-4.

In each of these states, the transition element starts out with a s^2d^n configuration. If the interaction was purely ionic, the number of electrons on Li at the equilibrium separation in MLi^+ would be 2, the $1s^2$ pair. From the population analysis shown in Table 5-5, we see that Lithium has gained between 0.39 and 0.35 electrons, attesting to a significant covalent interaction. Cr and Cu are fundamentally different, in that their ground states have a sd^{n+1} configuration and the bare Li^+ interacts with a configuration without any singlet coupled electron pairs. When interacting with Li^+, the ^7S state of Cr generates a $^7\Sigma^+$ state, while the ^2S state of Cu generates a $^2\Sigma^+$ state. The potential

curves for these states are also shown in Figure 15, and their dissociation energies, bond length, and vibrational frequencies are collected in Table 5-4. The population analysis (Table 5-5) suggests that, in addition to the long-range electrostatic interaction, a small but significant amount of charge is transferred to Li^+, resulting in a one-electron, two-center bond.

The data in Table 5-4 show that the bond energies of the ground-state M-Li^+ ions increase with increasing bond length. The correlation is almost linear, as we can see in Figure 16. This is remarkable, considering that the bonding in the $ScLi^+$, $TiLi^+$, and VLi^+ is quite different from $CrLi^+$ and $CuLi^+$. To pursue this further, we constructed wavefunctions for the states derivable from the M* + Li^+ asymptote. For Cr and Cu, this means Li^+ will interact with the ^5D and ^2D (s^2d^n) asymptote, respectively, so, we studied the $^5\Sigma^+$ state of $CrLi^+$ and the $^2\Delta$ state of $CuLi^+$. These results are shown in Table 5-4 and the corresponding population analysis in Table 5-5. Note that the correlation between the bond length and bond energies is maintained. It is also noteworthy that, while the bond energies change by a factor of two and the bond lengths by 0.4 Å, the vibrational frequencies of all of the s^2d^n states changes by only 7 cm^{-1} in going from the lowest (240 cm^{-1}) to the highest (247 cm^{-1}).

States derivable from the M* + Li^+ asymptote for Sc, Ti, and V were also considered. For Ti and V, this means that Li^+ will interact with the ^5F (sd^3) and ^6D (sd^4) states, respectively, so also studied was the $^5\Delta$ state of $TiLi^+$ and the $^6\Sigma^+$ state of VLi^+. These results are collected in Tables 5-4 and 5-5. The $^5\Delta$ (sd^3) state of $TiLi^+$ is bound by

Table 5-5. Population analysis of M-Li^+.

Orbital	$ScLi^+$		$TiLi^+$		VLi^+		$CrLi^+$		$CuLi^+$	
	$^2\Delta$ (s^2d)	$^4\Delta$ (spd)	$^3\Phi$ (s^2d^2)	$^5\Delta$ (sd^3)	$^4\Delta$(s^2d^3)	$^6\Sigma^+$ (sd^4)	$^5\Sigma^+$ (s^2d^4)	$^7\Sigma^+$ (sd^5)	$^2\Delta$ (s^2d^9)	$^1\Sigma^+$(sd^{10})
M 4s	1.458	1.014	1.498	0.490	1.480	0.495	1.534	0.578	1.723	0.657
M $4p_\sigma$	0.112	0.436	0.112	0.150	0.093	0.142	0.114	0.122	0.094	0.109
M $3d_\sigma$	0.051	0.160	0.044	0.032	0.037	0.032	0.048	1.000	2.008	2.005
M $3d_{\delta+}$	1.000	1.000	0.500	0.000	0.000	1.000	1.000	1.000	2.000	2.000
Li 2s	0.257	0.291	0.228	0.231	0.250	0.228	0.190	0.203	0.101	0.153
Li $2p_\sigma$	0.123	0.091	0.118	0.097	0.140	0.102	0.114	0.099	0.074	0.075
M $4p_y$	0.	0.	0.	0.003	0.	0.000	0.000	0.001	0.000	0.
M $3d_{\pi y}$	0.	0.	0.500	0.993	1.000	1.000	1.000	0.998	2.000	2.000
Li $2p_y$	0.	0.	0.	0.000	0.	0.000	0.000	0.001	0.000	0.
M $4p_x$	0.	0.	0.	0.003	0.	0.000	0.000	0.001	0.000	0.
M $3d_{\pi x}$	0.	0.	0.500	0.993	1.000	1.000	1.000	0.998	2.000	2.000
Li $2p_x$	0.		0.	0.000	0.	0.000	0.000	0.001	0.000	0.
M $3d_{\delta-}$	0.	0.	0.500	1.000	1.000	1.000	1.000	1.000	1.000	2.000
Q (M)	+0.380	+0.382	+0.346	+0.328	+0.391	+0.330	+0.304	+0.303	+0.175	+0.229

1.13 eV, relative to its adiabatic asymptote, while the $^3\Phi$ (s^2d^2) state is bound by 1.00 eV. Since the s^2d^2-sd^3 separation is 0.96 eV, the $^5\Delta$ state is bound, relative to ground-state Ti and Li^+. A similar situation obtains for the $^6\Sigma^+$ state of VLi^+. The calculated s^2d^3-sd^4 separation in V is 0.34 eV and the $^6\Sigma^+$ state is bound by 0.93 eV, placing it well below the asymptote ground-state products, V (^{4}F) and Li^+. Scandium, once again, has been difficult to characterize. We attempted to calculate the interaction of the ^{4}F (sd^2) state of Sc with Li^+ and selected the $^4\Delta$ component of the term. Our results are summarized in Tables 5-4 and 5-5. We see that, instead of the desired 4s d_σ d_δ configuration, we have converged to a state with a large 4 p_σ component and very little $3d_\sigma$. This is, of course, the result of the ^{4}F (4s4p3d) term of Sc being only 0.07 eV (calculated) above the ^{4}F ($4s3d^2$) term and is the same problem we encountered in trying to determine the bond energy of $^3\Sigma^-$ ScLi.

These energetics are summarized, and compared with the neutral lithides, in Figures 8-11.

E. Previous Work

Very little is known about the transition-metal lithides. There are two published experimental studies. Neubert and Zmbov[13] have estimated the dissociation energy of CuLi to be 1.96 ± 0.09 eV, using a Knudsen effusion technique combined with analysis of the vapor composition. Van Zee, Braumann, and Weltner[14] have identified the ESR spectrum of CrLi ($^6\Sigma^+$) in an argon matrix at 4 K. They determined the g-tensor, hyperfine, and zero-field splitting parameters. There have been three previous

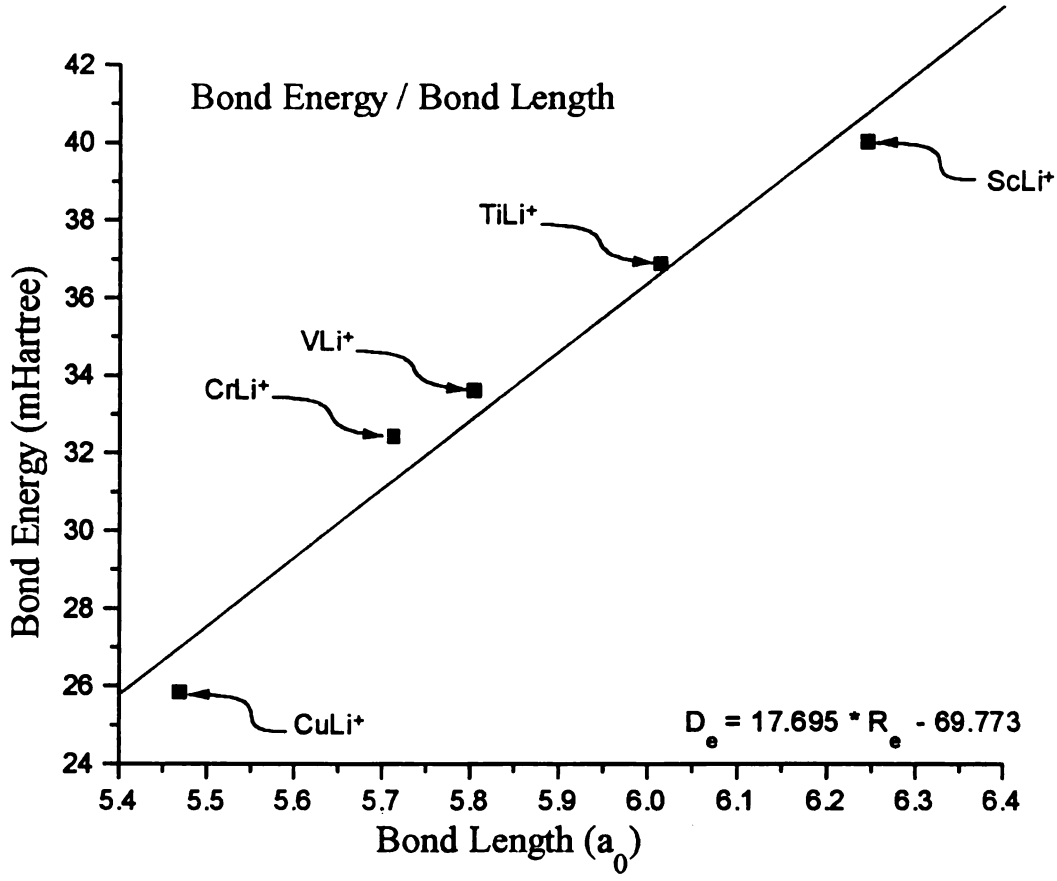

Figure 16. Variation of the calculated (MRCI) De's of monopositive lithides with equilibrium bond length.

Table 5-6. Comparison of Experimental and Theoretical Results

ScLi ($^3\Delta$)

Reference	D_e(eV)	R_e(Å)	Comments
Harrison[1]	0.27	3.28	MRCI
Beckmann[14] *et al.*	0.05	3.49	MRCI/pseudo potential
Lawson & Harrison	0.30/0.33	3.31/3.28	MRCI/ACPF

CuLi ($^1\Sigma^+$)

	D_e(eV)	R_e(Å)	ω_e(cm^{-1})	Comments
Beckmann[14] *et al.*	1.30	2.65	—	—
Bauschlicher[15] *et al.*	1.22/1.74	2.34/2.31	377/392	SDCI/CPF
Lawson and Harrison	1.30/1.62	2.47/2.43	332/356	MRCI/ACPF
Neubert and Zmbov[12]	1.96 ± 0.09	—	—	Exp

theoretical studies. The first, by Harrison[1] (a MRCI study), discussed the structure of ScLi and was followed by a study by Beckmann[15] *et al.* in which they examined the electronic structure of ScLi, CuLi, and PdLi. These authors employed a pseudo potential for the Sc and Cu, Argon cores and a MRCI for the remaining valence electrons. The last is by Bauschlicher[16] *et al.* in which various metal dimers and trimers, including CuLi, were studied. These authors used a large expansion basis and the SDCI and CPF techniques. The experimental and theoretical results are summarized in Table 5-6.

F. Conclusions

First, consider the neutral lithides. Our results demonstate:

- Bonding is primarily between transition metal 4s and Li 2s electrons.
- Significant 4s,4p hybridization in the ground states of ScLi and TiLi. These states trace their lineage to the lowest state of the $4s^2 3d^n$ transition metal configuration.
- Virtually no 4s,4p hybridization in the ground states of VLi, CrLi, or CuLi. These states trace their lineage to the lowest state of the $4s3d^{n+1}$ transition metal configuration.
- Bonding is extremely sensitive to electron correlation. Bond lengths decrease with electron correlation, while bond energies increase significantly.
- Bond strength increases significantly in going from ScLi (0.335 eV) to CuLi (1.62 eV), while bond length decreases from ScLi (3.305 Å) to CuLi (2.471 Å).

Now, the positive ions:

- Bonding is primarily ionic and to first order seems to be Li^+ interacting with the highly polarizable neutral transition metal atoms.
- The bond energies decrease as one goes from $ScLi^+$ (1.09 eV) to $CuLi^+$ (0.705 eV).
- The bond lengths decrease as one goes from $ScLi^+$ (3.259 Å.) to $CuLi^+$ (2.913 Å)
- Bonding is insensitive to electron correlation. The MCSCF, MRCI, and the ACPF methods all predict similar R_e, D_e, and ω_e's.

The behavior upon ionization varies considerably across the series. For example,

- $ScLi^+$ and $TiLi^+$ are more strongly bound than their neutral ground-state precursors

- VLi^+ has a bond strength comparable to its neutral precursor but has a much larger bond length.
- $CrLi^+$ ($^7\Sigma^+$) has a larger dissociation energy and a longer bond length than CrLi ($^6\Sigma^+$)
- $CuLi^+$ ($^2\Delta$) is more weakly bound and has a longer bond length than CuLi ($^1\Sigma^+$).

G. References

1. Harrison, J. F. J. Phys. Chem. **1983**, *87*, 1323.
2. Brewer, L.; Winn, J. S. Faraday Symp. Chem. Soc. **1980**, *14*, 126.
3. Alvarado-Swaisgood, A. E.; Harrison, J. F. J. Mol. Struct. **1988**, *169*, 155.
4. Moore, C. E. "Atomic Energy Levels," National Bureau of Standards, Washington, DC, 1949, *Natl. Bur. Stand. (U. S.), Circ. No. 467, Vol. 1 & 2.*
5. Wachters, A. J. H. J. Chem. Phys. **1970**, *52*, 1033.
6. Hay, P. J. J. Chem. Phys. **1977**, *66*, 4377.
7. Raffenetti, R. C. J. Chem. Phys. **1973**, *58*, 4452.
8. Langhoff, S. R.; Bauschlicher, Jr., C. W. Chem. Phys. Lett. **1986**, *124*, 241.
9. Williams, Jr., J. E.; Streitwieser, Jr., A. Chem. Phys. Lett. **1974**, *25*, 507.
10. van Duijneveldt, F. B. IBM Research Report No. RJ945, **1971**.
11. Shepard, R.; Shavitt, I.; Pitzer, R. M.; Comeau, D. C.; Pepper, M. T.; Lischka, H.; Szalay, P. G.; Ahlrichs, R.; Brown, F. B.; and Zhao, J. G. Internat. J. Quantum Chem. **1988**, *S22*, 149.
12. Gdanitz, R. J.; Ahlrichs, R. Chem. Phys. Lett. **1988**, *143*, 413.
13. Neubert, A.; Zmbov, K. F. Trans. Faraday Soc. **1974**, *70*, 2219.
14. Van Zee, R. J.; Baumann, C. A.; Weltner, Jr., W. Chem. Phys. Lett. **1985**, *113*, 524.
15. Beckmann, H.; Geanfranco, P.; Jeung, G. Chem. Phys. Lett. **1985**, *116*, 423.
16. Bauschlicher, Jr., C. W.; Langhoff, S. R.; Partridge, H.; Walch, S. P. J. Chem. Phys. **1987**, *86*, 5603.

CHAPTER 6

The Electronic Structure of LiAl and Its Positive Ions

A. Introduction

In a recent experimental study[1] of some spectroscopic states of AlLi, the ground state was determined to be $^1\Sigma^+$. Two other excited states where also detected, however, the symmetries of these states where not determined. Other theoretical work agrees with the $^1\Sigma^+$ as the ground state, however, the location and symmetry of the excited states are still indeterminate. This study evaluates the spectroscopic constants and potential energy curves of the AlLi molecule. A comparison is made between the electronic ground state of ScLi and AlLi.

B. Computational Methods

A Dunning correlation consistent polarized quadrupole zeta (cc-pvqz) basis was augmented with an additional 2s2p2d Double Rydberg Dunning Hay[2] basis giving 18s13p5d2f primitive functions on the Al atom. Adding the Rydberg Dunning Hay functions improved the flexibility of the Al basis enough to characterize the low lying atomic states of interest including the $3s^24s^1$ or ^2S configuration. This basis set was contracted to 8s7p5d2f providing a compact basis set with enough contractions to characterize various atomic as well as molecular excited states.

Lithium basis sets came from the van Duijenveldt[4] 11s8p primitive with the addition of 5d functions basis functions. The basis set was contracted to 6s5p4d and gave near Hartree-Fock limit energy for the ground state of the Li atom. The wavefunctions for various excited states of the Al and Li atoms were evaluated and their energies are summarized in Figure 1. As shown in the plot, these energies

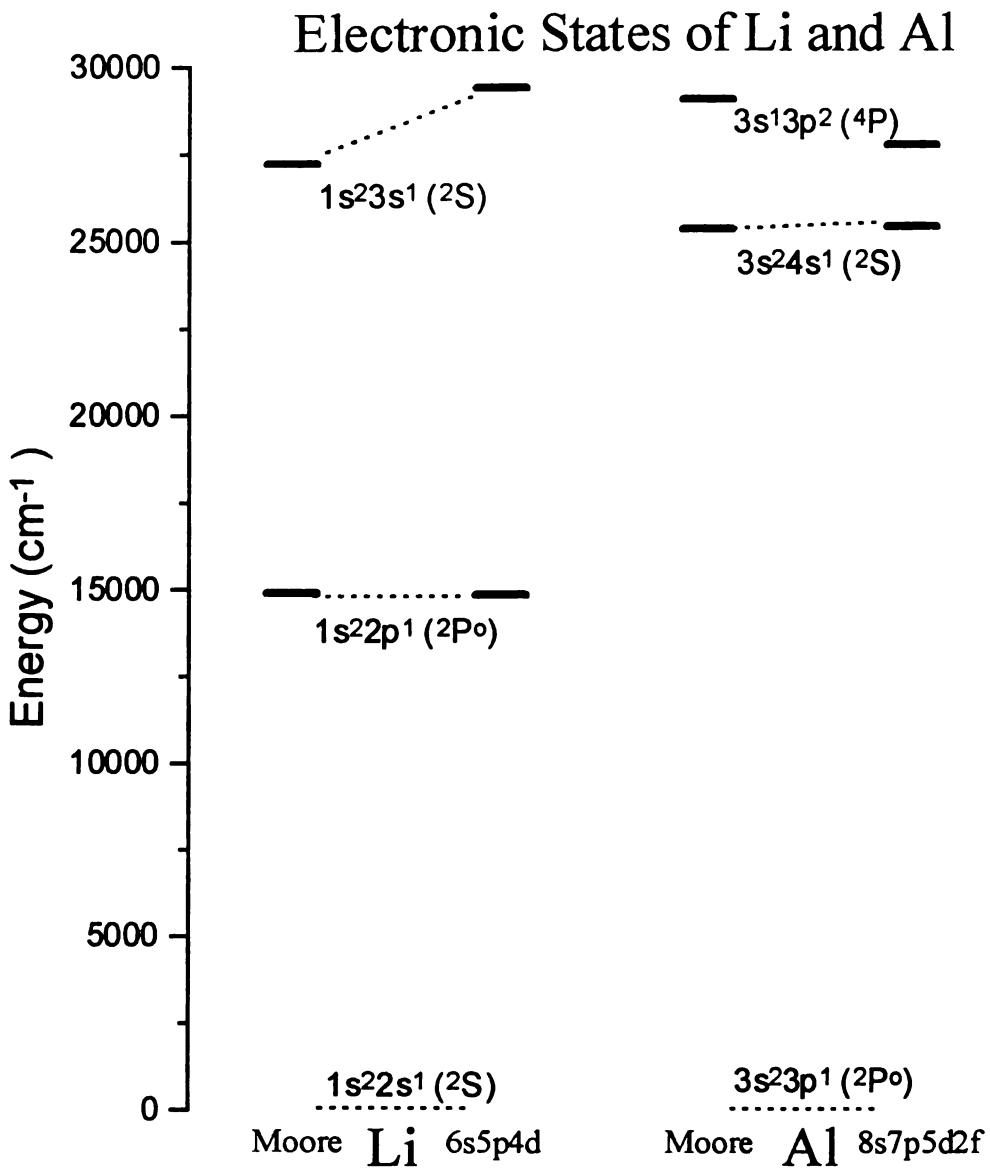

Figure 1. Low lying excited atom energies.

compare well with the transition energies in Moore's tables. The ionization potentials of Al and Li were determined to be 5.976 ev and 5.380 ev which compare well with the experimental values of 5.984 ev and 5.390 ev. The ionization potentials for each atom with various wavefunctions are summarized in Table 6-1.

Table 6-1. Adiabatic ionization potentials as $S \Rightarrow S^+ + e^-$

	MCSCF	MRCI	ACPF
Al	5.4281	5.9623	5.9755
Li	5.4320	5.3796	5.3804
AlLi	5.1354	6.5034	7.2461

Initially, Multireference-Self-Consitent-Field(MCSCF) wavefunctions were generated from the valance space consisting of Al $3s3p_z3p_x3p_y$ and the Li 2s space. Multireference-Configuration-Interaction(MRCI) wavefunctions were constructed from the MCSCF reference space. A larger set of MRCI active space calculations were derived from the same MCSCF reference space, in which, single and double excitations were also included out of Al $2s2p_x2p_y2p_z$ orbitals and from the Li 1s orbital. Averaged Coupled Pair Functional(ACPF) wavefunctions used the same MCSCF reference space both with and without the single and double excitations from the core electrons as in the MRCI calculations. All calculations were performed in C_{2v} symmetry using the Columbus suite of codes.

C. Results

Three MCSCF wavefunctions were considered to describe electronic states that dissociate to the ground state atoms and 2 MCSCF wavefunctions dissociate to the first excited state of Li. Table 6-2 shows the various spectroscopic properties and Figure 2 gives the relative potential energy surfaces of each electronic state. The ground state was determined by MCSCF to be the $^1\Sigma^+$ with a bond energy of De=0.959 ev relative to the ground state atoms and a vibrational frequency of ωe=319 cm^{-1} and a bond length of R_{opt}=5.379 a_0. Mulliken population analysis shows the bond to be from the atomic Al $3p_z$ orbital and a Li $2s2p_z$ hybrid orbital as expected. Four other states are also summarized by Table 6-2 and Figure 2.

The MRCI and ACPF results are also given in Table 6-1 along with results of the larger active space calculations. MRCI correlation increases the bond energy by +0.055 ev and decreases the bond length by -0.011 a_0. The relative populations of the 5 low lying states are provided in Table 6-3. The Al atom in the ground state acquires a charge of -0.206 and this state has the smallest charge on Al of any of the low lying states. The larger active space of the MRCI and ACPF wavefunctions increase the MCSCF bond energy of the ground state by 0.060 ev and 0.112 ev respectively. Both the MRCI and the ACPF gave the fundamental vibrational frequency as ωe=303 cm^{-1}. Though changing the total energy by as much as 21.1 Hartrees, these large active space calculations indicate the insignificance of correlation in bonding to the core orbitals.

Table 6-2. Characteristics of low lying states

State	Method	Total Energy	De (mH / eV)	R_{eq} (a_0)	μ(debye)	ω_e(cm^{-1})
$^1\Sigma^+$	MCSCF	-249.344441	35.229 / 0.9587	5.3787	3.752	319
	MRCI	-249.404096	40.034 / 1.0894	5.3800	3.083	318
		-249.444066	37.450 / 1.0191	5.3522	3.279	308
	ACPF	-249.431216	38.398 / 1.0449	5.3437		303
		-249.452287	39.340 / 1.0753	5.3107		308
expt.[1]			27.729 / 0.7545			318
Boldyrev, Gonzales, and Simons[5]			37.1 / 1.01			
$^1\Sigma^-$	MCSCF	-249.295088	28.273 / 0.7694	4.6222	4.236	391
	MRCI	-249.355194	52.347 / 1.4245	4.5537	4.226	419
		-249.393786	51.019 / 1.3883	4.4931	4.074	439
	ACPF	-249.361025	57.129 / 1.5546	4.6093		399
		-249.404229	58.432 / 1.5900	4.5583		407
$^3\Sigma^-$	MCSCF	-249.311093	44.279 / 1.2049	4.5359	4.033	412
	MRCI	-249.394522	69.896 / 1.9020	4.5041	4.056	428
		-249.412987	70.208 / 1.9150	4.4836	4.153	431
	ACPF	-249.398735	72.418 / 1.9706	4.5087		428
		-249.419624	74.918 / 2.0387	4.4854		432
$^1\Pi$	MCSCF	---.---	--.---- / --.----	-.----		---
	MRCI	-249.398901	6.641 / 0.1807	5.2181	5.007	242
		-249.416317	6.839 / 0.1861	5.2056	5.121	241
	ACPF	-249.402313	8.368 / 0.2277	5.1979		251
		-249.421863	9.524 / 0.2592	5.1689		255
$^3\Pi$	MCSCF	-249.343916	9.433 / 0.2567	5.0684	5.485	317
	MRCI	-249.420417	28.158 / 0.7662	4.9769	5.260	341
		-249.437743	28.737 / 0.7820	4.9680	5.276	382
	ACPF	-249.423809	29.864 / 0.8126	4.9443		367
		-249.443119	32.614 / 0.8875	4.9390		374

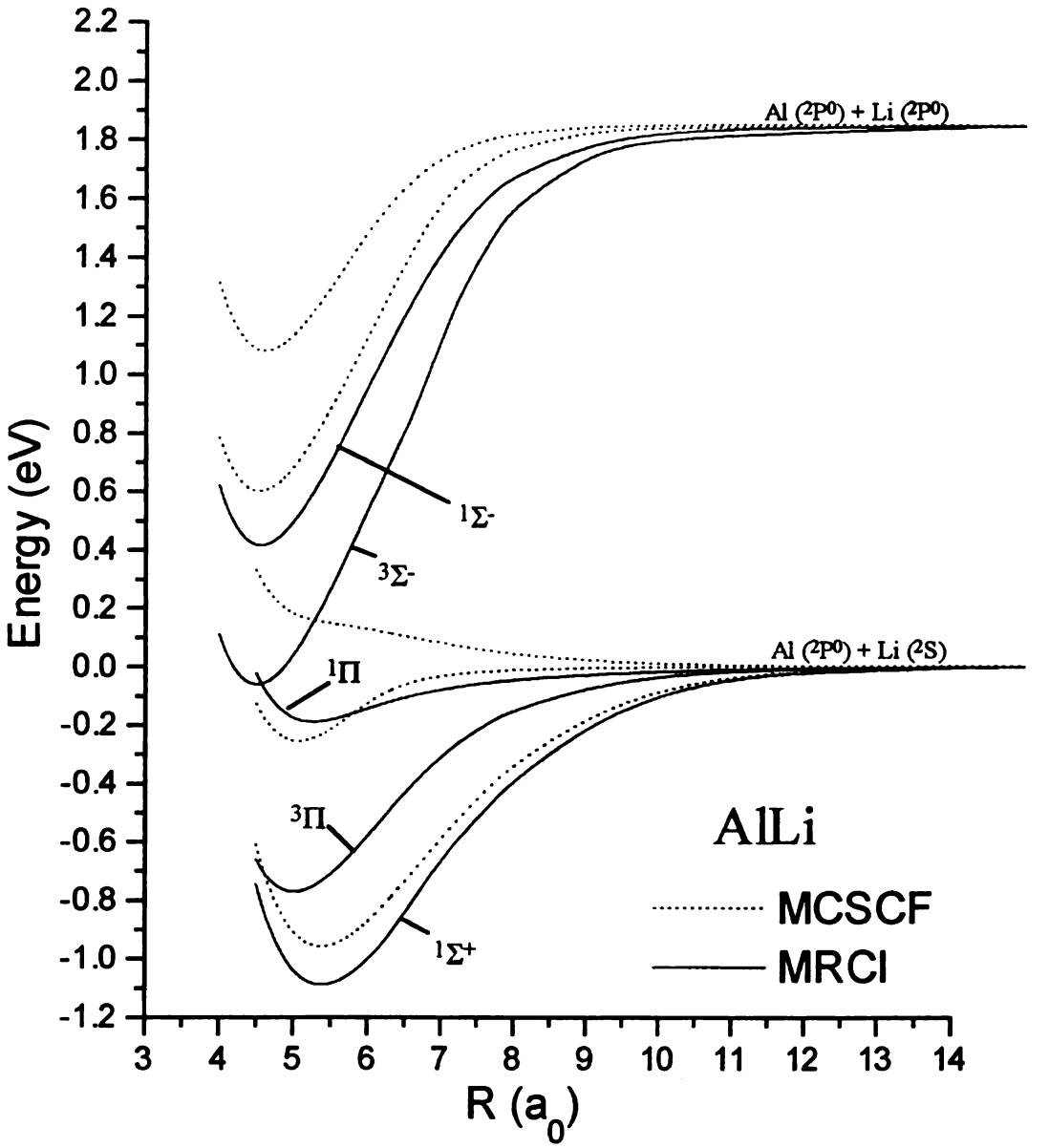

Figure 2. Potential energy curves of the low lying electronic states of AlLi using MCSCF and MRCI.

Table 6-3. Population analysis of low lying states of AlLi

	$I^1\Sigma^+$	$I^1\Sigma^-$	$I^3\Sigma^-$	$I^1\Pi$	$I^3\Pi$
Al 3s	1.9370	1.8112	1.7467	1.8319	1.8469
Al $3p_z$	1.1673	0.0823	0.0824	0.4983	0.5997
Al $3p_y$	0.0187	0.7902	0.8259	0.9757	0.8398
Al $3p_x$	0.0187	0.7902	0.8259	0.0339	0.0373
Li 2s	0.7082	0.0505	0.0625	0.5348	0.4048
Li $2p_z$	0.0530	0.0454	0.0601	0.0602	0.0833
Li $2p_y$	0.0148	0.1835	0.1780	0.0102	0.1292
Li $2p_x$	0.0148	0.1835	0.1780	0.0002	0.0000
Q(M)	+0.2092	+0.5049	+0.5214	+0.3944	+0.3825

The bond dissociation energy is inconsistent with the experimental value of Duncan and co-workers (0.755 ev, 6089 cm^{-1}) and a previous theoretical value of Rosenkrantz (De=0.793 ev). However, it is consistent with Boldyrev and co-workers (De=1.01 ev). Duncan regards his value as an estimate since it is based on a fit of four vibrational hotband energy levels to a Morse potential. Based on initial calculations of the excited states Al atom, a large diffuse basis set is required to characterize the electronic states with any degree of accuracy.

D. Excited States

A variety of other excited states of AlLi have been characterized by optimizing the higher roots from the MRCI wave. Figure 3 gives the potential energy curves of all states computed by MRCI. The asymptotes of the potential energy curves are ordered according to the energies of the corresponding atomic products. The ground state is labeled $I\ ^1\Sigma^+$ and higher roots of the same multiplicity and electronic symmetry

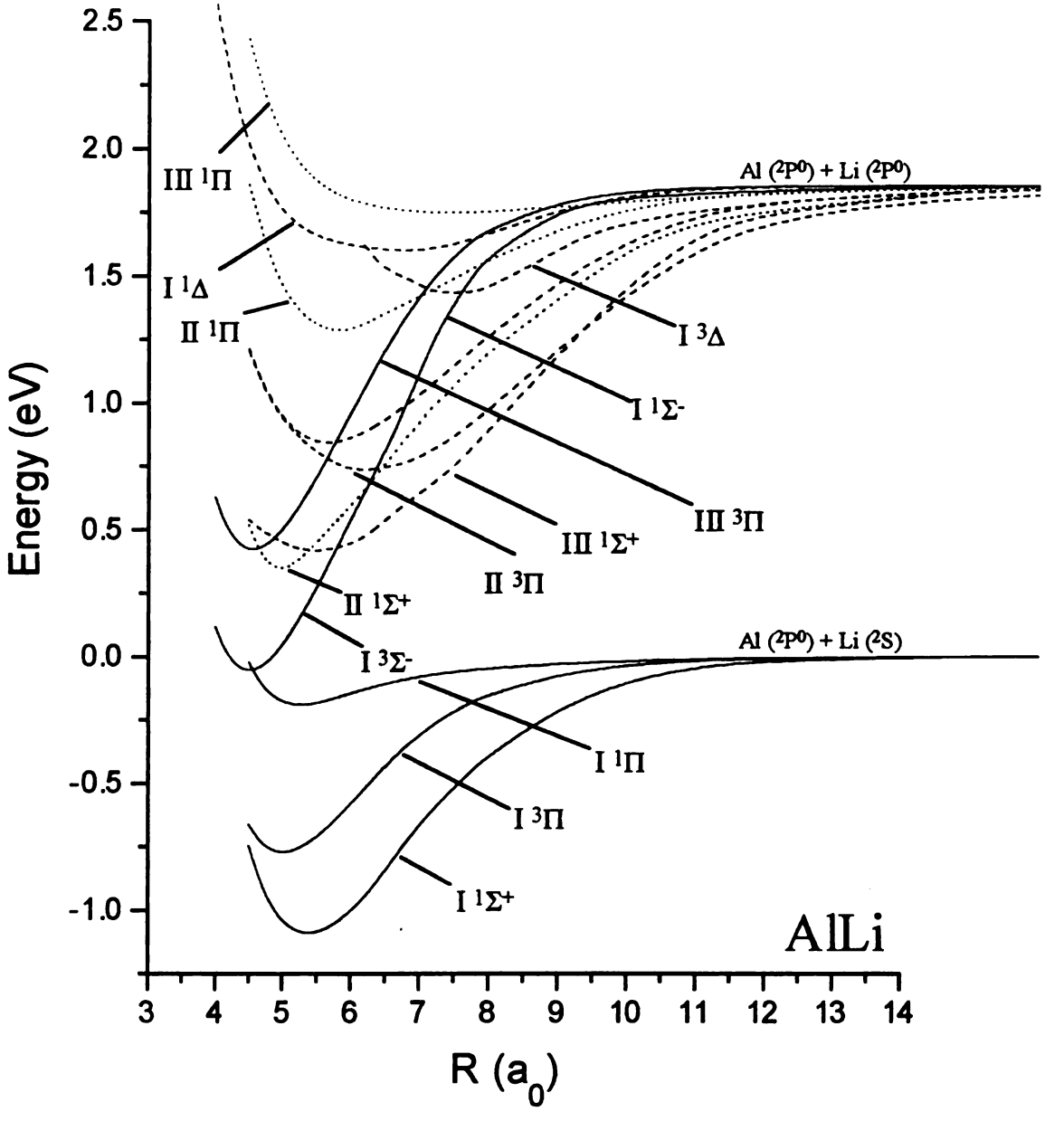

Figure 3. Potential energy curves of the low lying electronic states of AlLi using MRCI.

are labeled II, III,... in order of increasing energy. Both of the Δ states come from the second roots of the singlet and triplet A_2 wavefunction.

Table 6-4 provides the total energies of the roots corresponding to each electronic state.

Table 6-4. Calculated characteristics of MRCI roots

State	MRCI	Total Energy	TE(eV)	De (mH / eV)	R_{eq} (a_0)	ω_e(cm^{-1})
$I^1\Sigma^+$	ROOT 1	-249.404096	0.0	40.034 / 1.089	5.3800	317
$II^1\Sigma^+$	ROOT 2	-249.318327	2.3372	52.602 / 1.431	5.4734	206
$III^1\Sigma^+$	ROOT 3	-249.308791	2.6620	55.188 / 1.502	4.9678	457
$I^1\Sigma^-$	ROOT 1	-249.355194	1.5504	52.347 / 1.424	4.5538	419
$I^1\Delta$	ROOT 2	-249.284764	3.2966	9.985 / 0.272	6.7297	130
$I^3\Sigma^-$	ROOT 1	-249.394522	0.5172	69.884 / 1.902	4.5041	428
$I^3\Delta$	ROOT 2	-249.290997	3.2610	16.203 / 0.441	7.5073	355
$I^1\Pi$	ROOT 1	-249.377533	0.7233	7.010 / 0.191	5.2638	238
$II^1\Pi$	ROOT 2	-249.317899	2.3633	36.965 / 1.006	5.6686	254
$III^1\Pi$	ROOT 3	-249.284391	3.4157	3.771 / 0.1026	7.4928	73
$I^3\Pi$	ROOT 1	-249.398905	0.1751	28.362 / 0.772	5.0056	337
$II^3\Pi$	ROOT 2	-249.321009	2.3598	40.915 / 1.113	6.1799	222
$III^3\Pi$	ROOT 3	-249.299366	3.9665	20.677 / 0.563	5.8474	254

The adiabatic transition energy, optimized separation, and vibrational frequency are also provided. All of the computed transition energies are within 4 ev of the ground state. The potential energy curves of the first three electronic state are asymptotic to the ground state atoms. The next 10 excited states dissociate to a ground state Al atom and the first excited state of the Li atom. The remaining 3 electronic states

dissociate to products of a ground state Li atom and various electronic configurations of the Al atom.

E. Positive Ion

The MCSCF first adiabatic ionization potential of AlLi was 5.1354 ev. MRCI and ACPF give an ionization potential of 6.5034 ev and 7.2461 ev respectively. The ground state of $AlLi^+$ was determined to be the $^2\Sigma^+$ state. The positive ion was bound at the MCSCF level by De=1.1837 ev. MRCI and ACPF both increased the bonding by less than 6 mev. The positive charge in the system reduces the bonding to an electrostatic interaction of a positive Li ion and a neutral polarizable Al atom. Thus correlation offers little change in the bonding energy. The correlation difference between the MCSCF and MRCI ionization potential is attributed to the increase in total energy of the neutral system with correlation.

Two other states, $^2\Pi$ and $^4\Pi$, also obtained minima in their potential energy curves. As shown in Figure 4, the $^2\Pi$ dissociates to a ground state Al atom and a Li^+, while the asymptotic limit of the $^4\Pi$ is an Al atom with a $3s3p^2$ configuration and a positive Li atom. Populations for all bound states are given in Table 6-6.

F. AlLi AND ScLi

The ground state orbital configuration of the Sc atom is $4s^23d^1$ while the Al atom has a similar ground state of $3s^23p^1$. Similarities between the bonding of ScLi and AlLi ground states might be expected, however, the two molecules have

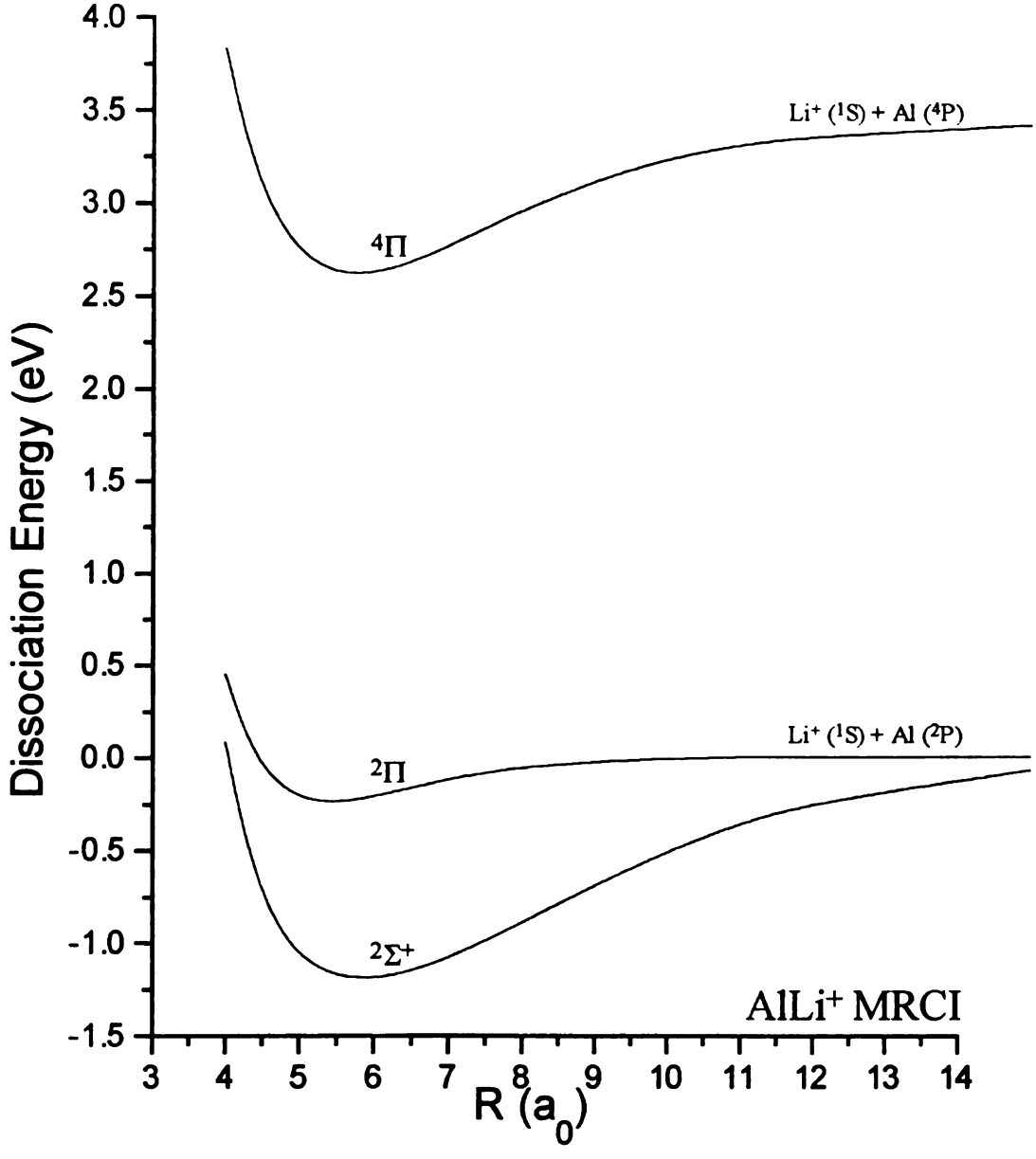

Figure 4. Potential energy curves of the low lying electronic states of $AlLi^+$ using MRCI.

Table 6-5. Characteristics of Low Lying States of the Positive Ion

State	Method	Total Energy	De (mH / eV)	R_{eq} (a_0)	ω_e(cm^{-1})
$^2\Sigma^+$	MCSCF	-249.156876	43.499 / 1.1837	5.3824	206
	MRCI	-249.166473	43.717 / 1.1896	5.8449	663
	ACPF	-249.166382	43.620 / 1.1869	5.9138	321
Boldyrev, Gonzales, and Simons[5]			37.131 / 1.0104	5.6786	242
$^2\Pi$	MCSCF	-249.010094	26.567 / 0.7229	5.3799	269
	MRCI	-249.180183	8.599 / 0.2340	5.4433	208
	ACPF	-249.199630	9.751 / 0.2653	5.3419	228
Boldyrev, Gonzales, and Simons[5]				5.3309	205
$^4\Pi$	MCSCF	-249.059376	30.198 / 0.8217	5.8064	232
	MRCI	-249.077067	30.192 / 0.8216	5.7890	235
	ACPF	-249.077286	30.194 / 0.8216	5.7897	234

Table 6-6. Population anaylsis of $AlLi^+$

	$^2\Sigma^+$	$^2\Sigma^-$	$^4\Pi$
Al 3s	1.9894	1.2591	0.9983
Al $3p_z$	0.7323	0.0306	0.8093
Al $3p_y$	0.0003	0.6266	0.9478
Al $3p_x$	0.0003	0.6266	0.0040
Li 2s	0.2555	0.0089	0.1467
Li $2p_z$	0.0002	0.0114	0.0162
Li $2p_y$	0.0000	0.0272	0.0225
Li $2p_x$	0.0000	0.0272	0.0001
Q(M)	+0.2555	+0.1097	+0.1785

significantly different chemistry. As stated in Chapter 5, there is a repulsive interaction between the Sc $4s^2$ and the Li 2s orbitals and remains repulsive until the Sc hybridizes. The singly occupied Sc 3d is unable to bond with the Li 2s due to its compact nature, or rather the diffuse nature of the Li 2s orbital prevents it from passing the Sc 3s. The energy required for hybridization of the Sc 3s leaves an optimal bonding configuration for the ground state of ScLi as a Sc atom with $4s^13d^2$ configuration and the Li $2s^1$ atomic configuration. For an Al atom the $3s^2$ orbital is also repulsive to an approaching Li 2s, however, the single occupied 2p orbital extends well beyond the Al 3s. There is no energy loss required for hybridization and the Li 2s orbital readily forms a bond with the Al 3p orbital. It is also of interest to point out that the energy need for an Sc atom to go from a $4s^23d^1$ state to a $4s^13d^2$ state is 1.427 ev while the energy needed for an Al atom to go from $3s^23p^1$ configuration to a $3s^13p^2$ configuration is 3.605 ev.

G. Conclusion

In this study we computed the spectroscopic properties (re, we, Te, and De) of 16 electronic states of AlLi using MCSCF followed by MRCI and ACPF. The ground state of the AlLi was determined to be $^1\Sigma^+$ state with a bond length of R_{opt}=5.311 a_0 (2.8103 Angstroms), a vibrational frequency of ωe=308 cm^{-1} and a dissociation energy of De=1.071 ev relative to the ground state asymptotes.

H. References

1. L. R. Brock, J.S. Pilgrim, M.A. Duncan, Chem. Phys. Lett. **1994**, 230, 93

2. M.E. Rosenkrantz, University of Dayton Interim Report No. PL-TR-3088, Phillips Laboratory, Edwards Air Force Base, CA(**1992**)

3. A.I. Boldyrev, J. Simons and P. Von Schleyer, J.Chem.Phys., **1993**, 99, 8793

4. H.P. Cheng, R.N. Barnett and U. Landman, Phys. Rev. B, **1993**, 48, 1820

5. A.I. Boldyrev, N. Gonzales, and J. Simons, J. Phys. Chem., **1994**, 98, 2098

6. C.E. Moore, Atomic Energy Levels, NSRDS-NBS, Circular No. 35 (US GPO, Washington, **1971**)

7. van Duijneveldt, F. B., IBM Research Report No. RJ945, **1971**.

8. Basis sets were obtained from the Extensible Computational Chemistry Environment Basis Set Database, Version 1.0, as developed and distributed by the Molecular Science Computing Facility, Environmental and Molecular Sciences Laboratory which is part of the Pacific Northwest Laboratory, P.O. Box 999, Richland, Washington 99352, US, and funded by the U.S. Department of Energy. The Pacific Northwest Laboratory is a multi-program laboratory operated by Battelle Memorial Institue for the U.S. Department of Energy under contract DE-AC06-76RLO 1830. Contact David Feller, Karen Schuchardt, or Don Jones for further information.

9. Shepard, R.; Shavitt, I.; Pitzer, R. M.; Comeau, D. C.; Pepper, M. T.; Lischka, H.; Szalay, P. G.; Ahlrichs, R.; Brown, F. B.; and Zhao, J. G. Internat. J. Quantum Chem. **1988**, *S22*, 149.